Spontaneity to Serendipity: From an Enediyne Core Biosynthetic Hypothesis to the Hexadehydro-Diels–Alder Reaction

A DISSERTATION
SUBMITTED TO THE FACULTY OF THE GRADUATE SCHOOL
OF THE UNIVERSITY OF MINNESOTA BY

Brian Patrick Woods

IN PARTIAL FULFILLMENT OF THE REQUIREMENTS
FOR THE DEGREE OF
DOCTOR OF PHILOSOPHY

Thomas R. Hoye, Adviser

August 2014

Acknowledgements

While my name is on the first page of this thesis, countless family, friends, and colleagues contributed their knowledge, support, and love to help make this document a reality. First and foremost, I need to thank my family. I owe everything to my parents, Steve and Diane, who were my first teachers and have been and continue to be inspiring examples of how a life of constant learning and exploration never gets old. They instilled in me their value in the benefits of education and the doors it opens for those willing to knock. For both my siblings and I, they always encouraged us to pursue our dreams and desires—from CSI investigator, to Broadway actor, to NASA scientist—and provided us with the guidance and support to reach them. To my sister and brother, Shannon and Tyler, I thank them for their innate ability to keep me grounded and their unwavering confidence in me. To each of them, along with their partners Braxton and Esther, and my nephew Harrison, I thank them for being a constant reminder that there's nothing more important than family. For their continual love I would also like to thank my extended family of aunts, uncles, and cousins—and more specifically my grandparents Patrick and Virginia Woods. Additionally, for their friendship throughout my time at Minnesota and help in maintaining the requisite levity and sanity in my life, I thank Antonio Campos, Ryan Knutson, Jeff Vervacke, and especially my roommates Jeremy Bedard and Drew Thompson.

From a more professional standpoint, I first need to give the utmost thanks to my adviser, Thomas R. Hoye. Tom has been a phenomenal adviser, going above and beyond what I expected when I arrived at graduate school. He has a passion for chemistry and particularly teaching that is contagious. Both a brilliant scientist and incredibly effective mentor, Tom has an appreciation for the beauty and intricacies of organic chemistry that shapes the tone of his group. His commitment and loyalty to his students is especially commendable. From every stage of graduate school he has always readily offered useful guidance and insight, related to course schedules in the first year to career advice in the fifth year. I thank him for taking a chance on an eager new student from a small

undergraduate college five years ago and allowing me to join his research group. I would not be anywhere near the teacher, researcher, writer, or overall scientist I am today without his mentorship.

I also need to thank the rest of the outstanding faculty at the University of Minnesota who have had a hand in shaping my growth as a teacher and scientist. In particular, I thank Jane Wissinger. Jane guided me through my first year as a Teaching Assistant and helped show me the gratification and fulfillment that comes from effectively taking a group of students through a semester of Organic Chemistry. Working closely with Jane for three years as the Head Organic TA she became like a second adviser to me. I learned innumerable leadership, motivational, and educational skills from her for which I will always be appreciative. In the same context I would like to thank Michael Wentzel for allowing me to attend and guest-lecture in his Organic Chemistry class at Augsburg College. Mike was my graduate student contact at Minnesota for my first visit, and has been an inspirational mentor and friend ever since. Next, I would like to thank my committee members Steve Kass, Christopher Douglas, and Carston Wagner. They have been patient, flexible and supportive as I progressed through the written and oral preliminary exam and on to the final thesis submission and oral defense. For their generosity and help with the use of their DSC instrument, I am grateful to Marc Hillmyer and his group. To my professors Christopher Cramer, Andrew Harned, Valerie Pierre, and again Tom, Chris Douglas, and Steve Kass, I give thanks for their valuable coursework. I would also like to thank Letitia Yao for her admirable work maintaining the essential NMR facilities, and Laura J. Clouston, Victor G. Young, and the X-Ray Crystallographic Laboratory for their determination of the crystallographic data presented in this Thesis.

Throughout my studies at Minnesota, I have benefited immensely from being surrounded by an exceptionally talented group of colleagues. The majority of my work was done in collaboration with Beeru Baire, Dawen Niu, and Patrick Willoughby, or “Team Benzyne” as we came to call ourselves. Being involved in the early stages of the HDDA project with these three creative, driven, and genuinely good-natured colleagues

made coming to work every day exciting, rewarding, and enjoyable. The project would not have been nearly as productive without such a cordial and spirited collaboration. Specifically, I am forever indebted to my senior graduate students Patrick and Dawen for the prolific advice and guidance I gained on a daily basis simply from observing how they handle themselves as scientists.

For early encouragement from my time as an overwhelmed and naïve new graduate student, I thank Mandy Bialke and Susie Emond for welcoming me to my lab in Smith 413. They were the first to introduce me to the ways of the Hoye lab and, more importantly, the mechanics of the MPLC setup. I thank my current Smith 413 tenants Vedamayee Pogula, Xiao Xiao, Moriana Haj, Quang Luu Nguyen, and Andrew Mullins for maintaining the friendly atmosphere that Mandy and Susie established. Matthew Jansma was my first mentor from a research standpoint, and I benefited immensely from witnessing his work ethic, preparation, and bench skills on a day-to-day basis, not to mention his role in teaching me everything I needed to know to operate and maintain the group GC-MS. I thank Joshua Marell and Xiangyun Lei from the group of Chris Cramer for their extensive computational analysis in what turned into an enjoyable and fruitful collaboration. For their friendship and helpful subgroup meetings I thank former group members Adam Wohl, Susan Brown, Julian Lo, and Eric Buck. The current group members have also contributed greatly to the state of the HDDA project with vigor and enthusiasm; the project has continued to thrive thanks to the brilliant work of Junhua Chen, Tao Wang, and Sean Ross. I have had the opportunity to work with two terrific undergraduates during my time as a graduate student, Moriana and Quang, who I thank for their patience, assistance, and outstanding work. I need to give particular thanks to my colleague Andrew Michel for the monumental task of maintaining (for the most part) the group LC-MS, for his friendship, and for constructive and essential pre-group meetings. I am also very thankful to Moriana, Sean, Junhua, and Andrew for critically reviewing portions of this thesis.

To my Parents

My lifelong teachers and role models

Abstract

Enediyne containing natural products have promising potential as cancer therapeutics due to their unique molecular architecture. The (*Z*)-1,5-diyn-3-ene subunit in the enediyne core can undergo cycloaromatization to yield a diradical capable of scission of the DNA double helix. While the biological mechanism of action is well established, almost nothing is known about the biosynthesis of the enediyne core. Specifically, researchers have been unable to identify a cyclase enzyme capable of ring-closing acyclic precursors. In the case of 9-membered enediynes, we propose that the bicyclic enediyne core is formed biosynthetically via *spontaneous* (i.e. non-enzymatic) cyclization from an acyclic precursor. In the course of examining this hypothesis, we serendipitously encountered a [4+2] cyclization between a diyne and an alkyne. The product of such a cycloaddition is one of the oldest and most interesting reactive intermediates in organic chemistry, *o*-benzyne. This process, which we have termed a hexadehydro-Diels–Alder (HDDA) reaction, has remained almost entirely unexploited until now. The strategy unites an entirely atom-economical, thermal generation of arynes with their in situ elaboration into a diverse set of polysubstituted benzenoids. HDDA precursor triynes cycloisomerize in a very exergonic fashion to produce complex benzyne intermediates, which are trapped with a variety of inter- and intra-molecular functionalities in an efficient and selective manner. The byproduct-free environment in which the benzynes are generated allows for new trapping reactions to be discovered and for mechanistic pathways to be interrogated and elucidated.

Table of Contents

Supplementary Information for Chapters 2–6

List of Figures

List of Tables

List of Abbreviations

Ac_2O	Acetic anhydride
ACP	Acyl carrier protein
AT	Acyl transferase
Bn	Benzyl
BRSM	Based on recovered starting material
Bz	Benzoyl
CoA	Coenzyme A
DBU	1,8-Diazabicyclo[5.4.0]undec-7-ene
DCC	Dicyclohexylcarbodiimide
DCM	Dichloromethane
DCE	1,2-Dichloroethane
DFT	Density functional theory
DH	Dehydratase
DMAP	*N*,*N*-4-Dimethylaminopyridine
DMF	*N*,*N*-Dimethylformamide
DMSO	Dimethyl sulfoxide
DNA	Deoxyribonucleic acid
DSC	Differential scanning calorimetry
EDCI	*N*-(3-Dimethylaminopropyl)-*N'*-ethylcarbodiimide hydrochloride
ee	Enantiomeric excess
epi	Epimer
EtOAc	Ethyl acetate
Et_3N	Triethylamine
Et_2O	Diethyl ether
GC-MS	Gas chromatography-mass spectrometry
HR ESI-MS	High resolution electrospray ionization-mass spectrometry
IR	Infrared
KHMDS	Potassium *bis*(trimethylsilyl)amide

KR	Ketoreductase
KS	Ketoacyl synthase
LC-MS	Liquid chromatography-mass spectrometry
LDA	Lithium diisopropylamide
LUMO	Lowest unoccupied molecular orbital
MeCN	Acetonitrile
Ms	Methanesulfonyl
MS	Molecular sieve
mp	Melting point
NADPH	Nicotinamide adenine dinucleotide phosphate
NBS	*N*-Bromosuccinimide
NMP	*N*-Methyl-2-pyrrolidone
NMR	Nuclear magnetic resonance
PCP	Peptidyl carrier protein
$PhCH_3$	Toluene
PhH	Benzene
PKS	Polyketide synthase
PKSE	Enediyne polyketide synthase
PPh_3	Triphenylphosphine
Py	Pyridine
SMD	Universal solvation model
TBAF	Tetra-*n*-butylammonium fluoride
TBAI	Tetra-*n*-butylammonium iodide
TBS	*t*-Butyldimethylsilyl
TD	Terminal domain
TES	Triethylsilyl
Tf	Trifluoromethanesulfonyl
TFA	Trifluoroacetic acid
TIPS	Triisopropylsilyl

THF	Tetrahydrofuran
TLC	Thin layer chromatography
TMEDA	Tetramethylethylenediamine
TMS	Trimethylsilyl
Tol	4-Methylphenyl
Ts	*p*-Toluenesulfonyl

Part I

Investigation of a Spontaneous Cyclization in the Biosynthesis of Nine-Membered Enediyne Natural Products

Chapter 1. Background and Biosynthetic Hypothesis

1.1. Introduction to the Enediyne Natural Products

The enediynes represent a family of structurally unique natural products that exhibit remarkably potent biological activity. Calicheamicin[1] **1002-B** and esperamicin[2] **1002-A**, the first enediyne-containing natural products, were isolated in 1987 and since their discoveries the enediyne family of natural products has grown to include 13 total members (Figure 1). Many of these structures exhibit antibiotic and antitumor activities comparable to or greater than any known microbial metabolite.[3] For example, C-1027 **1001-B** (Figure 1A) shows potent cytotoxicity against KB carcinoma cells *in vitro* (IC_{50} =

Figure 1 | Representative members of (A) nine-membered and (B) ten-membered enediyne natural products.

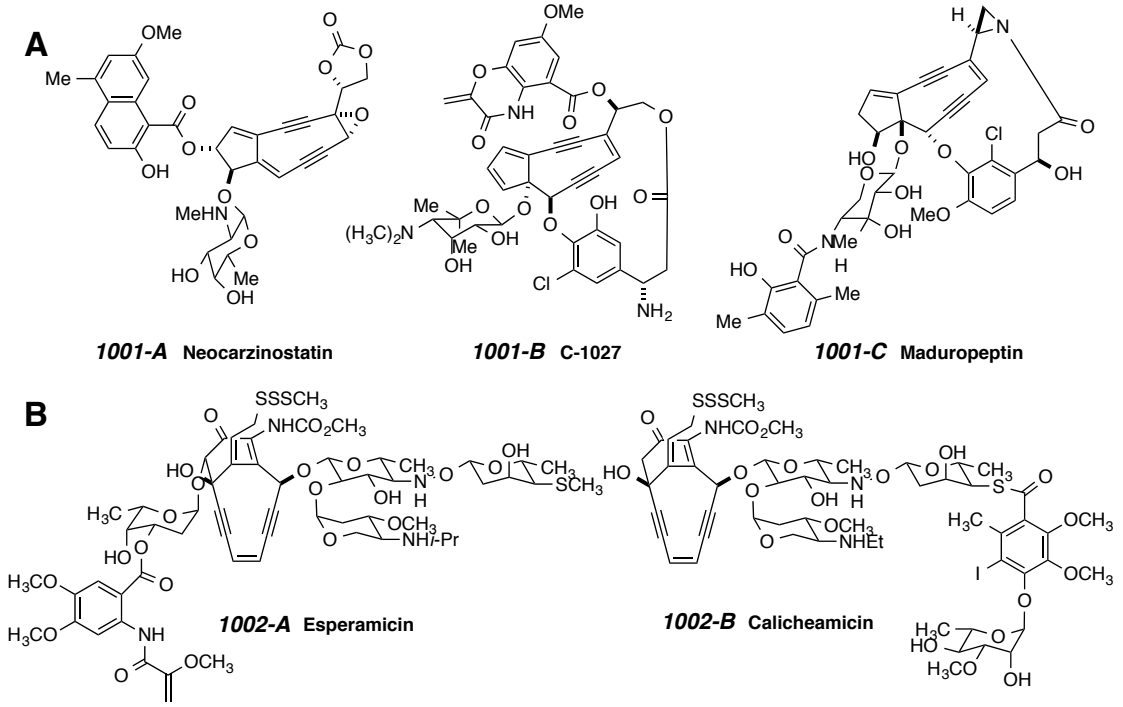

[1] Lee, M.; Dunne, T.; Chang, C.; Siegel, M. Calicheamicins, a novel family of antitumor antibiotics. 4. Structure elucidation of calicheamicins β_1^{Br}, Υ_1^{Br}, α_2^I, α_3^I, β_1^I, Υ_1^I, and δ_1^I. *J. Am. Chem. Soc.* **1992**, 11*4*, 985–997.

[2] Golik, J.; Dubay, G.; Groenewold, G.; Kawaguchi, H.; Konishi, M.; Krishnan, B.; Ohkuma, H.; Saitoh, K.; Doyle, T. Esperamicins, a novel class of potent antitumor antibiotics. 3. Structures of Esperamicins A1, A2, and A1b. *J. Am. Chem. Soc.* **1987,** *109* , 3462–3464

[3] Wang, X.; Xie, H. C-1027. *Drugs of the Future* **1999,** *24*, 847–852.

0.1 ng/mL).[4] A common core structural motif among the enediynes is either a nine (Figure 1A, cf. **1001-A-C**) or ten-membered (Figure 1B, cf. **2001-A** and **-B**) carbocycle containing a (*Z*)-1,5-diyn-3-ene unit (Figure 2, **1003**) that is capable of undergoing a Bergman cycloaromatization to yield a benzenoid diradical (Figure 2, **1004**). This diradical abstracts two hydrogen atoms from the sugar phosphate backbone of adjacent DNA strands, resulting in the aromatic ring **1005** and cell death from DNA scission (Figure 2). The exceptional biological activity paired with the challenging molecular architecture of the enediynes has generated considerable interest from the synthesis community to produce the natural enediynes and analogues thereof. Concurrent with these studies, scientists in the fields of biochemistry, medicinal chemistry, and nucleic acid chemistry have devoted significant efforts to better understand the biological mechanism and consequences of enediyne induced DNA cellular damage. However, our interest in the enediyne family hinges on the biosynthetic route that nature utilizes to produce these intriguing natural products.

Figure 2 | Bergman cyclization and subsequent DNA cleavage of the enediyne core.

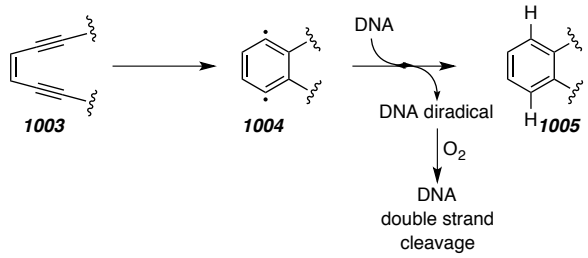

In 2002, Shen and co-workers established that the biosynthesis of the enediynes proceeds via an iterative type 1 polyketide pathway distinct from all known polyketide synthases.[5] Further investigations regarding these biosynthetic pathways have addressed aspects of the front-end assembly of acyclic precursors and aromatic or carbohydrate subunits. However, gene fragments that encode for a cyclase enzyme to close an acyclic precursor have not been identified. Retrobiosynthetically, all nine-membered enediynes can be envisioned to arise in nature from a common bicyclic core. We propose that the

[4] Sugimoto, Y.; Otani, T.; Oie, S.; Wierzba, K.; Yamada, Y. Mechanism of action of a new macromolecular antitumor antibiotic, C-1027. *The Journal of Antibiotics* **1990**, *43*, 417–421.
[5] Liu, W.; Christenson, S.; Standage, S.; Shen, B. Biosynthesis of the enediyne antitumor antibiotic C-1027. *Science* **2002**; *297*, 1170–1173.

enediyne core is formed biosynthetically via *spontaneous* (i.e. non-enzymatic) cyclization from an acyclic precursor **1007** (cf. **1007** → **1006**, Scheme 1). After formation of the achiral bicyclic core (i.e., **1006**), enantioselective action of epoxidases followed by ring opening and acylation/glycosidation would complete the enediyne biosynthesis.

A positive outcome of our hypothesis could have far-reaching impact on the study of polyketide biosynthesis and on understanding of natural product formation in general. With one modified enediyne already in clinical use in Japan[6] and several antibody-enediyne conjugates currently being evaluated for clinical significance as anticancer drugs,[7] there is an increasing desire to be able to harness and manipulate these powerful antibiotics. Along the way to testing our hypothesis, advanced synthetic strategies will be employed to construct the necessary complex intermediates. Elucidation of the biosynthetic pathway leading to the enediyne core may provide scientists with the ability to generate novel enediyne analogs that could potentially be developed into anticancer drugs.

1.2. Biosynthetic Hypothesis for 9-Membered Enediyne Core

The bicyclic core **1006** common to the nine-membered enediynes is shown in Scheme 1. The two acetylenic groups in conjugation with the double bond are in close proximity, oriented to undergo the cycloaromatization necessary for biological activity. The remaining elements of the bicyclic core serve as handles for additional aromatic and carbohydrate moieties that distinguish each natural product. We propose that **1006** is formed through dehydrative cyclization of the highly unsaturated primary alcohol **1007** (Scheme 1). In aqueous buffer, the s-*cis* conformer about the C6-C7 σ-bond should minimize the hydrophobic surface area of **1007**. Furthermore, this conformation would facilitate an electrocyclic elimination of hydroxide to form the highly delocalized bicyclic

Scheme 1| Proposed biosynthetic pathway to the enediyne core **1006**.

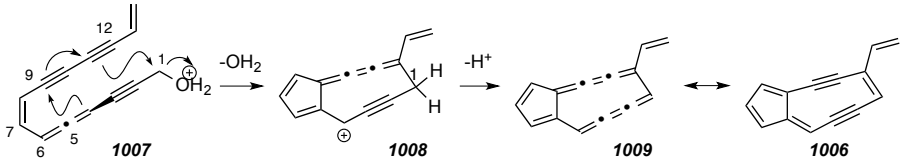

[6] Maeda, H. Enediyne Antibiotics as Antitumor Agents. New York, 1995.
[7] Brukner, I. Curr. Opin. Oncol. Endocr. Met. Invest. Drugs **2000,** 2, 344.

carbenium ion **1008**. The nature of the oxygen leaving group is only a matter of experimentation and has no effect on the cyclization. The leaving group could be hydroxide or water (as shown) following protonation, or perhaps a carboxylate, phosphate, or sulfate. Deprotonation at C1 of the cumulene carbenium **1008** produces the bis-cumulene **1009**, which is a resonance structure of the nine-membered enediyne core **1006**.

This biosynthetic hypothesis hinges on the ability of nature to produce our proposed enediyne precursor **1007** or a phosphorylated or sulfonated derivative. While its highly unsaturated system represents a unique molecular framework, searches of previously isolated natural products offer support for the possible biosynthetic production of **1007** by existing classes of biosynthetic transformations (Figure 3). Many natural lipids possess a 1,3-disubstituted allene in conjugation with an alkyne or alkene (cf. **1011**) and there are numerous examples with primary propargylic alcohols (cf. **1010**). Additionally, hundreds of examples can be found of natural products containing acyclic alkynes in conjugation with a Z-1,2-disubstituted alkene, even including a few acyclic enediynes (cf. **1012**).[8]

Figure 3 | Isolated natural products containing substructure elements of **1007**.

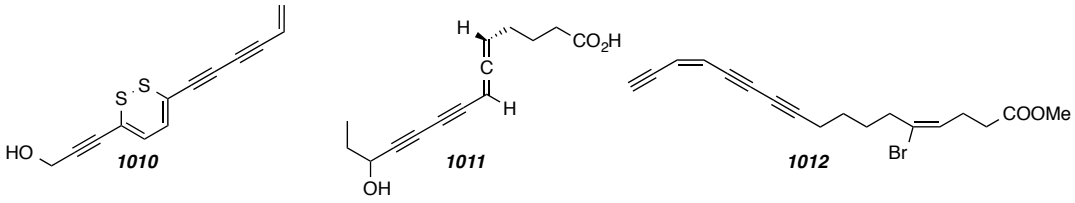

1.3. Previous Synthetic Studies Relevant to 9-Membered Enediynes

1.3.1. Sondheimer Chemistry

The spontaneous cyclization of eneyne **1007** to the bicyclic core of the enediynes is not unprecedented for a compound with such a highly unsaturated framework. A series of communications by Sondheimer and co-workers from the late 1950s and early 1960s report base-induced eliminations to form highly unsaturated macrocyclic compounds. Initial studies focused on oxidative coupling of unfunctionalized terminal acetylenes

[8] Rezanka, T.; Dembitsky, V. Novel brominated lipidic compounds from lichens of Central Asia. *Phytochemistry* **1999**, *51*, 963-968.

(Scheme 2). High-dilution oxidation of 1,5-hexadiyne **1013** with cupric acetate gave its linear dimer along with a series of cyclic poly-acetylenes, notably the C_{18}-hexa-yne **1014**, albeit in low yield.[9] Treatment of **1014** with potassium *t*-butoxide initiated prototropic rearrangement to afford the hexa-ene-tri-yne **1015** (Scheme 2).[10] The proposed mechanism involves rearrangement of each 1,5-diyne to a 1,3-diene-3-yne unit to provide a fully conjugated aromatic system **1016**.

Scheme 2 | Preparation and hydrogenation of macrocyclic polyynes (adapted from ref 9).

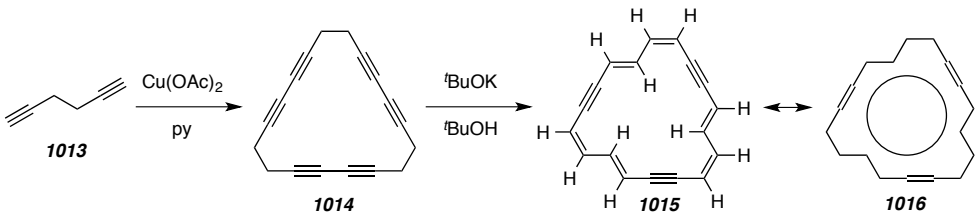

This aromatic macrocycle was observed again via an alternative route of reduction and dehydration from the corresponding 1,5-hexadiyn-3-ol **1017** (Scheme 3). Oxidative coupling proceeded with comparable yields to give the macrocycle **1018**, which was partially hydrogenated with $LiAlH_4$ and dehydrated to give the aromatic macrocycle **1016**.[11]

Scheme 3 | Preparation, hydrogenation and dehydration of macrocyclic polyynes (adapted from ref 10).

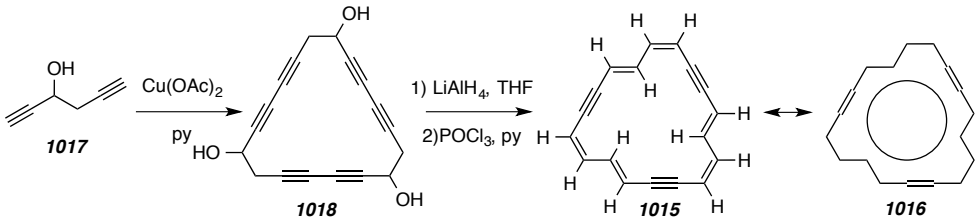

While these transformations might be easily predicted in such a system, Sondheimer observed an unexpected bicyclic product from another highly unsaturated

[9] Sondheimer, F.; Amiel, Y.; Wolovsky, R. Unsaturated macrocyclic compounds. V. 1 large ring poly-acetylenes. *J. Am. Chem. Soc.* **1957**, *79*, 4247–4248.
[10] Sondheimer, F.; Wolovsky, R. Unsaturated macrocyclic compounds. VI. The synthesis of cyclo-octadeca-1, 3, 7, 9, 13, 15-hexane-5, 11, 17-triyne, a completely conjugated eighteen-membered ring cyclic system. *J. Am. Chem. Soc.* **1959**, *81*, 1771.
[11] Sondheimer, F.; Amiel, Y.; Gaoni, Y. Unsaturated macrocyclic compounds. VII. 1 Synthesis of cyclooctadeca-1, 3, 7, 9, 13, 15-hexaene-5, 11, 17-triyne from 1, 5-hexadiyn-3-ol. *J. Am. Chem. Soc.* **1959**, *81*, 1771–1772.

macrocycle (Scheme 4). Exposure of tetrayne **1019** to methanolic KOH formed the bicycle **1024** in 15-20% yield at room temperature.[12] The structural similarity of **1024** with the nine-membered enediyne core **1006** makes Sondheimer's observation particularly relevant to our proposed biosynthetic hypothesis. A mechanism was not offered by Sondheimer, but one possibility would involve mesylate elimination from **1019** to give diene **1020** (Scheme 4). Base-induced [1,3]-prototropic shift would give rise to isomeric allene **1021**. Another deprotonation by base would give carbanion **1022**,

Scheme 4 | Suggested mechanism for the transformation of **1019** to **1024**.

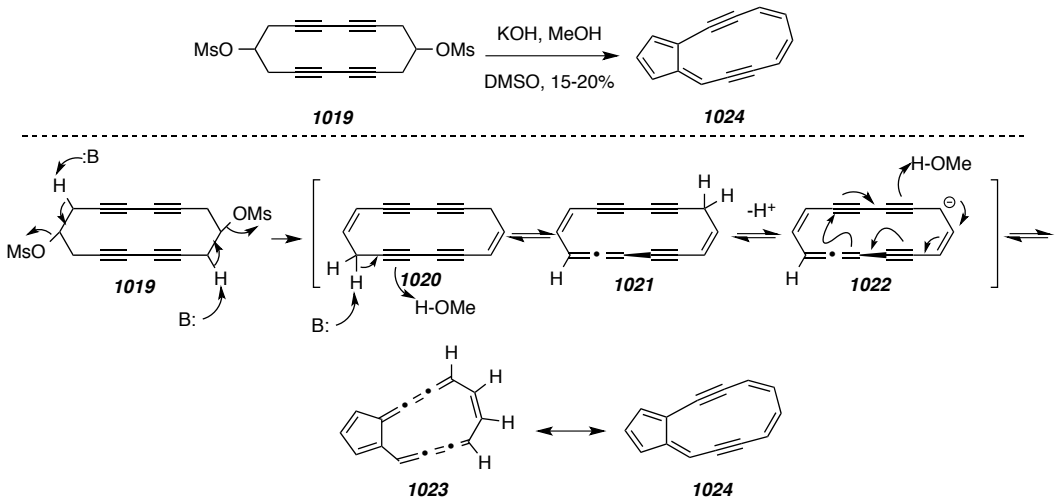

which could undergo a transannular rearrangement with concomitant reprotonation via solvent. A slight change in geometry accompanies the formal [1,2]-prototropic shift to produce the bis-cumulene **1023**, which is merely a resonance form of **1024**.

The similarity of this proposed mechanism to our hypothesized cyclization to form the nine-membered enediyne core (ref. Scheme 1, Sec. 1.2) is striking. In each case the final prototropic shift results in the formation of a bis-cumulene bicycle, which is a resonance form of the final (hypothesized) bicyclic product. For Sondheimer to observe such a rearrangement to the bicyclic system of **1024** is encouraging for the potential cyclization of acyclic precursor **1007**.

[12] Mayer, J.; Sondheimer, F. 1, 5, 9-Tridehydro [14] annulene and bicyclo [9.3. 0] tetradeca-1, 5, 7, 11, 13-pentaene-3, 9-diyne, an acetylenic homolog of azulene containing fused five- and eleven-membered rings. *J. Am. Chem. Soc.* **1966**, *88*, 602–603.

1.3.2. Enediyne Core Stability and Reactivity

Each of the isolated nine-membered enediyne natural products exists as a chromoprotein complex consisting of the enediyne chromophore bound to what is known as an apo-protein. It was originally speculated that the apo-protein stabilized the enediyne core and prevented cycloaromatization prior to contact with cellular DNA. Later studies on the apo-protein showed that it also directs transport and interaction of the chromophore with target DNA.[13] Nicolaou and co-workers[14] investigated the propensity of enediyne cores to undergo the cycloaromatization involved in their biological mode of action. The key factors determining the rate of rearrangement are ring strain and the distance between the ends of the 1,5-diyn-3-ene system. In the biological activation of calicheamicin (**1002-B**), for example, a nucleophile attacks the trisulfide, forming the thiol **1025** (Figure 4). This triggers an intramolecular addition of the thiol to the α,β-unsaturated ketone of the enediyne core to give **1026**, converting a trigonal bridgehead position to a tetrahedral center. This conversion induces a change in geometry that results in closer proximity of the two termini of the enediyne unit in **1026** while introducing considerable strain into the ten-membered ring. Strain is released by subsequent cycloaromatization to produce the benzenoid diradical **1027**. The diradical

Figure 4 | Mechanism for DNA cleavage by calicheamicin **1002-B** (adapted from ref 13).

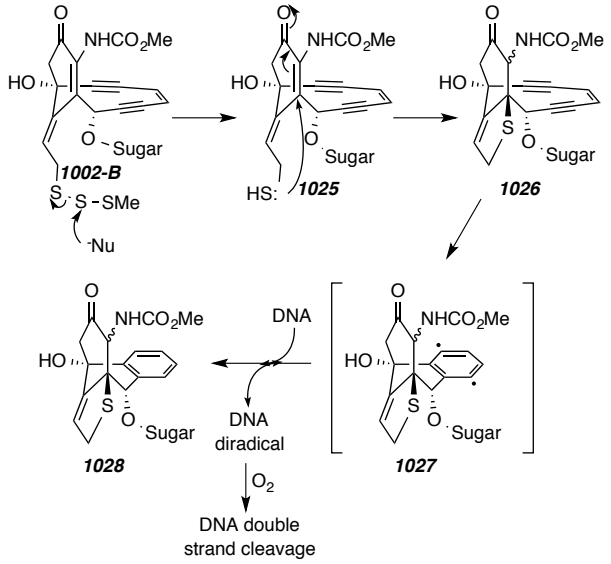

[13] Thorson, J.; Shen, B.; Whitwam, R.; Liu, W.; Li, Y.; Ahlert, J. Enediyne biosynthesis and self-resistance: a progress report. *Bioorg. Chem.* **1999,** *27*, 172–188.
[14] Smith, A.; Nicolaou, K. C. The enediyne antibiotics. *J. Med. Chem.* **1996**, *39*, 2103–2117.

abstracts hydrogen atoms from DNA leading to strand cleavage and the aromatic product **1028**.

Nicolaou and co-workers synthesized a series of monocyclic enediynes of varying size (**1029**, n = 1-8, Scheme 5) and studied their cyclization.[15] The nine- membered enediynes (**1029**, n = 1) were found to be extremely susceptible to the electronic rearrangement. In fact, attempted syntheses of these compounds failed and only aromatic products (**1030**, n=1) derived from the Bergman reaction were identified. The ten-membered ring **1029** (n = 2) cyclized at room temperature ($t_{1/2}$ = 18 h) while larger enediyne rings (**1029** n = 3-8) were found to be stable. As expected, a clear trend between the *c-d* distance of the enediyne termini and an increased tendency to cyclize was observed. Nicolaou and co-workers set a critical upper limit for the *c-d* distance

Scheme 5 | Cycloaromatization of synthesized monocyclic enediynes.

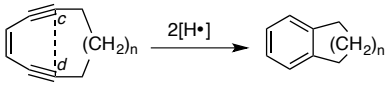

1029 **1030**

of these monocyclic compounds to be between 3.2-3.3 Å for the Bergman reaction to occur at a measurable rate at ambient temperature. Additional computational and kinetic studies by Snyder have determined the relative strain energies of the ground and transition states to be the crucial factor in determining cycloaromatization.[16] With their increased stability, the ten-membered enediyne natural products do not require any apo-proteins and have been isolated as discrete small molecules. Nicolaou went on to design analogues of the ten-membered monocyclic enediyne ring that successfully caused DNA cleavage at low concentrations and at biological temperatures with no additives.[17]

1.3.3. Previous Syntheses of the Enediyne Core

The instability of the nine-membered enediynes complicated efforts toward their total synthesis, and so early attempts focused instead on ten-membered enediyne natural

[15] Nicolaou, K.; Zuccarello, G.; Riemer, C.; Estevez, V.; Dai, W. Design, synthesis, and study of simple monocyclic conjugated enediynes. The 10-membered ring enediyne moiety of the enediyne anticancer antibiotics. *J. Am. Chem. Soc.* **1992,** *114*, 7360–7371.
[16] Snyder, J. Monocyclic enediyne collapse to 1, 4-diyl biradicals: a pathway under strain control. *J. Am. Chem. Soc.* **1990,** *112*, 5367–5369.
[17] Nicolaou, K.; Sorensen, E.; Discordia, R.; Hwang, C.; Bergman, R.; Minto, R.; Bharucha, K. Ten-membered ring enediynes with remarkable chemical and biological profiles. *Angew. Chem., Int. Ed.* **1992,** *31*, 1044–1046.

products. The first total synthesis of an enediyne natural product was the ten-membered calicheamicin (**1002-B**) completed by Nicolaou and co-workers in 1993.[18] Danishefsky and co-workers published their synthesis of **1002-B** one year later,[19] and Myers and co-workers followed with a total synthesis of the ten-membered enediyne dynemicin A in 1995.[20] It wasn't until years later that a chromophore from a nine-membered enediyne complex was successfully synthesized. Myers and co-workers[21] published their total synthesis of neocarzinostatin (**1001-A**) in 1998 after years of extensive studies and syntheses of nine-membered enediyne core model systems.[22]

Myers' first successful construction of the nine-membered enediyne core came in 1991 with the formation of the epoxy diyne core of neocarzinostatin (Scheme 6).[23] A convergent synthesis focused on stepwise inter- and intra-molecular coupling of terminal acetylenes to carbonyl functional groups. The diyne **1031** resulted from a series of transformations starting with Sonogashira coupling of (trimethylsilyl)acetylene to (Z)-

Scheme 6 | Preparation of epoxy-diyne core of neocarzinostatin (adapted from ref 23).

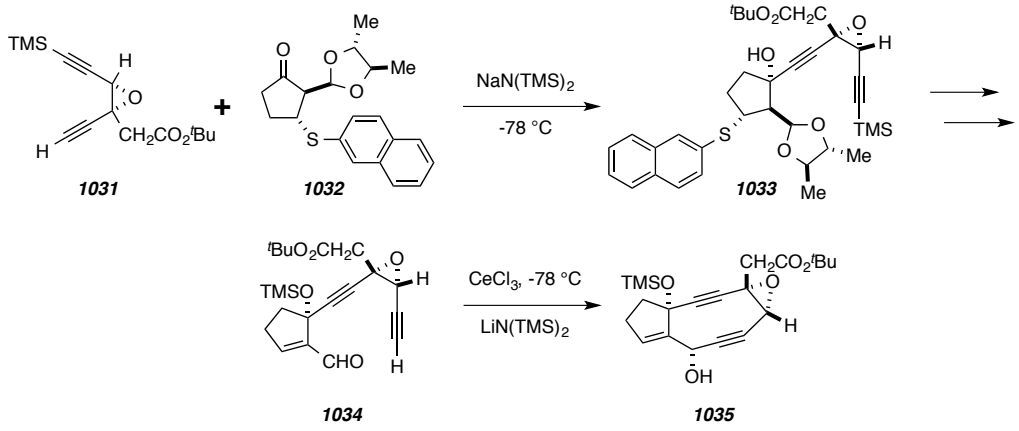

[18] Nicolaou, K.; Hummel, C.; Nakada, M.; Shibayama, K.; Pitsinos, E.; Saimoto, H.; Mizuno, Y.; Baldenius, K.; Smith, A. Total synthesis of calicheamicin. gamma. 1I. 3. The final stages. *J. Am. Chem. Soc.* **1993,** *115* , 7625–7635.

[19] Danishefsky, S.; Shair, M. Observations in the chemistry and biology of cyclic enediyne antibiotics: Total syntheses of calicheamicin [gamma] 1I and dynemicin A. *J. Org. Chem* **1996,** *61*, 16–44.

[20] Myers, A.; Fraley, M.; Tom, N.; Cohen, S.; Madar, D. Synthesis of (+)-dynemicin A and analogs of wide structural variability: establishment of the absolute configuration of natural dynemicin A. *Chem. Biol.* **1995**, *2*, 33–43.

[21] Myers, A.; Liang, J.; Hammond, M.; Harrington, P.; Wu, Y.; Kuo, E. Total synthesis of (+)-neocarzinostatin chromophore. *J. Am. Chem. Soc.* **1998,** *120*, 5319–5320.

[22] Myers, A.; Hammond, M.; Wu, Y.; Xiang, J.; Harrington, P.; Kuo, E. Enantioselective synthesis of neocarzinostatin chromophore aglycon. *J. Am. Chem. Soc* **1996,** *118*, 10006–10007.

[23] Myers, A.; Harrington, P.; Kuo, E. Enantioselective synthesis of the epoxy diyne core of neocarzinostatin chromophore. *J. Am. Chem. Soc.* **1991,** *113*, 694–695.

ethyl 2,3-dibromopropenoate to afford the (*Z*)-enediyne. The coupling partner **1032** was produced from a series of functionalizations of the parent cyclopentanone. Metalation of epoxy acetylene **1031** followed by addition of ketone **1032** produced an 18:1 mixture of the coupling product **1033** and the ß-hydroxy epimer. Modifications of the cyclopentane substituents along with protecting group manipulations afforded aldehyde **1034**.

Myers' ring-closing strategy drew inspiration from an intramolecular acetylide addition implemented by Danishefsky and coworkers in their syntheses of models of the ten-membered enediyne natural products calicheamicin (**1002-B**) and esperamicin (**1002-A**).[24] By treating a slurry of **1034** and anhydrous $CeCl_3$ in THF at -78 °C with excess $LiN(TMS)_2$ for one hour and quenching with a pH 7 phosphate buffer solution, the cyclic epoxy diyne **1035** was obtained as a single diastereomer. The stereochemical outcome of the ring-closing step results from acetylide attack on the *s*-trans aldehyde rotamer of **1034**, an outcome previously observed in studies by Danishefsky and co-workers.[24] Hirama and co-workers also employed this protocol in the late stages of their synthesis of the nine-membered enediyne C-1027 chromophore framework in 2004.[25] Samples of **1035** had to be stored in solution at -20 °C because decomposition was problematic, exemplifying the highly strained nature of the cyclononadiyne ring.

1.3.4. Enediyne Core Formation via Transannular Cyclization

In 2007, the Myers laboratory followed up the first total synthesis of neocarzinostatin with an ambitious synthesis of the nine-membered enediyne chromophore kedarcidin, which provided evidence for a stereochemical revision of its structure.[26] Instead of opting to continue with the well-established acetylide addition method to close the enediyne ring, Myers employed a transannular cyclization. Sondheimer's transformation from 1966 (Scheme 4 Sec. 1.3.1) served as the motivation for attempting to form the bicyclic enediyne core from a cyclic polyacetylene precursor. Using an oxidative Glaser[27] coupling similar to the conditions Sondheimer used to prepare his fourteen-carbon tetrayne **1019**, Myers successfully prepared the twelve-

[24] Danishefsky, S.; Mantlo, N.; Yamashita, D.; Schulte, G. A concise route to the calicheamicin−esperamicin series: the crystal structure of a core subunit. *J. Am. Chem. Soc.* **1988,** *110*, 6890–6891.
[25] Inoue, M.; Sasaki, T.; Hatano, S.; Hirama, M. Synthesis of the C-1027 chromophore framework through atropselective macrolactonization. *Angew. Chem., Int. Ed.* **2004,** *43*, 6500–6505.
[26] Ren, F.; Hogan, P.; Anderson, A.; Myers, A. Kedarcidin chromophore: Synthesis of its proposed structure and evidence for a stereochemical revision. *J. Am. Chem. Soc.* **2007,** *129*, 5381–5383.
[27] Glaser, C. Contribution to the Chemistry of Phenylacetylenes. *Ber.* **1869**, *2*, 422–424.

carbon tetrayne **1036**.[28] While Sondheimer observed his transformation in basic methanol, Myers used an aluminum reducing agent in combination with potassium bis(trimethylsilyl)amide (KHMDS) to initiate the transannular cyclization to produce the

Scheme 7 | Reductive transannular cyclization to enediyne core (adapted from ref 28).

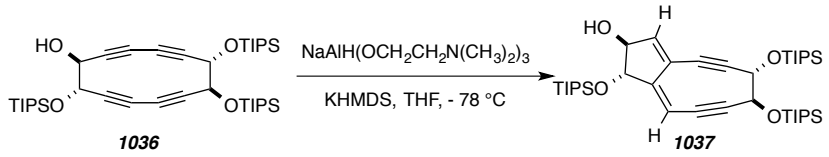

1036 *1037*

bicyclic core **1037**. This protocol to reach the tetrayne precursor would have to be modified, however, to accommodate the more highly functionalized substrate necessary for the total synthesis of kedarcidin. Specifically, requirement of the free hydroxyl to direct hydride addition meant that the introduction of the pyridyl ether functionality present in the natural product must occur after the formation of the strained, highly reactive bicyclic core.

An alternative route was envisioned that generated the tetrayne system using a vinyl halide precursor (Scheme 8).[29] Lithium halogen exchange with the vinyl halide could set the stage for a vinyl-metal intermediate capable of initiating the transannular ring closure. This route was tested with the model compound **1041**. Sonogashira coupling of dibromoolefin **1039** and diyne **1038** resulted in exclusive formation of the (*Z*)-vinyl bromide **1040**. This selectivity is presumably a result of the oxidative addition of Pd^0 into the less-hindered carbon-bromine bond. The bulky *tert*-butyldimethylsilyl (TBS) group on the terminal acetylene also would direct towards (*Z*)-olefin formation. Cleavage of the silyl protecting groups with tetrabutylammonium fluoride (TBAF), however, was complicated by concurrent elimination of hydrogen bromide to prematurely form the tetrayne. Eventually, optimal conditions were developed that involved the addition of TBAF to a solution of **1040** and 2-nitrophenol in THF at 0 °C, which cleanly formed the desilylated product. Anticipating the inherent instability of the

[28] Myers, A.; Goldberg, S. Concise synthesis of the bicyclic core of the chromoprotein antibiotics kedarcidin and neocarzinostatin by transannular reductive cyclization of a tetrayne precursor. *Tetrahedron Lett.* **1998**, *39*, 9633–9636.
[29] Myers, A.; Goldberg, S. Synthesis of the kedarcidin core structure by a transannular cyclization pathway. *Angew. Chem., Int. Ed.* **2000,** *112*, 2844–2847.

Scheme 8 | Preparation of kedarcidin core (adapted from ref 29).

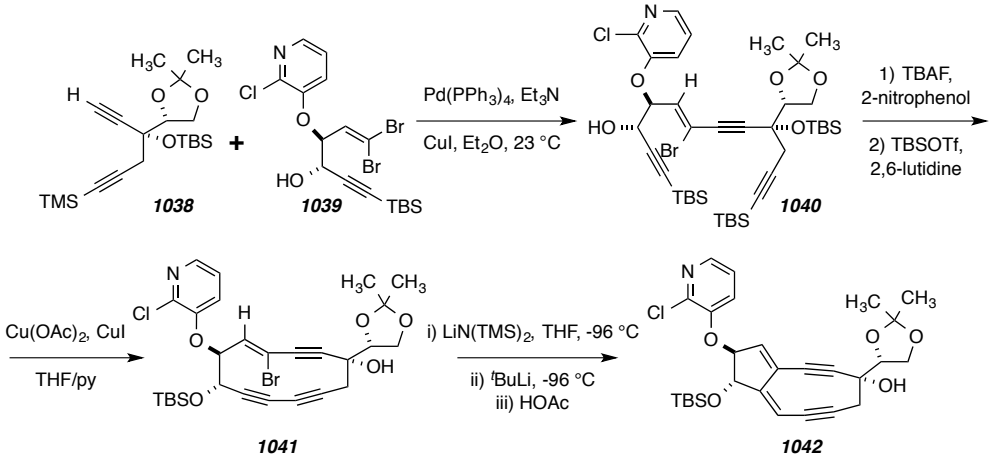

tetrayne, the secondary hydroxyl group was silylated with TBSOTf prior to ring formation. Initial attempts at oxidative acetylenic coupling to form the conjugated diyne unit under standard Glaser or Eglinton[30] conditions failed to achieve the transformation. Eventually, a procedure using a mixture of copper (II) acetate and copper (I) iodide successfully closed the macrocycle to form **1041**, leaving the vinyl bromide intact. To prepare the substrate for the key synthetic step, a solution of **1041** was treated with lithium bis(trimethylsilyl)amide (LHMDS) with subsequent addition of *t*-butyllithium to ensure that lithium-halogen exchange of the vinyl bromide would not be compromised by the tertiary alcohol. Quenching with acetic acid immediately after *t*-butyl lithium addition afforded the bicyclic product **1042**, with a small amount of the product from protonation of a vinyllithium intermediate also isolated. Delaying the acid quench did not diminish this side product, supporting the hypothesis that it arises from proton transfer with hexamethyldisilazane, which is formed stoichiometrically in the reaction. Observation of the side product also demonstrates the rate at which the cyclization must occur to be able to compete with such a process. This successful transannular cyclization illustrates an impressive route to synthesize the nine-membered enediyne core. Myers and co-workers would utilize this strategy in their total synthesis of the kedarcidin chromophore-the first of its kind-seven years later.[26]

[30] Eglinton, G.; Galbraith, A. Macrocyclic acetylenic compounds. Part I. Cyclotetradeca-1: 3-diyne and related compounds. *Journal of the Chemical Society (Resumed)* **1959**, *27*, 3320–3321.

1.4. Previous Biosynthetic Studies of Enediynes

1.4.1. Enediyne Biosynthetic Progress

While the research and strategies for the construction of both nine and ten-membered enediynes represent impressive total syntheses, all of the reported routes leave much to be desired. For this reason, recent studies and attempts at the synthesis of the enediynes have slowed substantially compared to the fervent interest these natural products sparked in the 1980s. Focus has shifted to the biosynthetic processes by which the enediynes are assembled in nature. Research in this field has increased considerably in the last decade with advances in gene cloning and characterization. Uncovering the gene clusters and enzymes used in enediyne biosynthesis could pave the way to engineer new enediynes with a combination of antitumor potency and cytotoxicity necessary for use as anticancer agents. Initial studies in the early 1990's on the enediyne core involved isotope-labeling experiments on neocarzinostatin, dynemicin and esperamicin.[31] The results indicated that the core originates from a minimum of eight head-to-tail acetate units, but it did not establish whether enediyne core biosynthesis acts by degradation of fatty acids or *de novo* synthesis with a fatty acid or polyketide synthase. A decade later, advances in gene recognition allowed the cloning and characterization of the gene cluster of five different enediynes,[32] setting the stage for extensive investigation into enediyne biosynthesis.

---

[31] (a) Hensens, O.; Giner, J.; Goldberg, I. Biosynthesis of NCS chrom A, the chromophore of the antitumor antibiotic neocarzinostatin. *J. Am. Chem. Soc.* **1989**, *111*, 3295–3299; (b) Tokiwa, Y.; Miyoshi-Saitoh, M.; Kobayashi, H.; Sunaga, R.; Konishi, M.; Oki, T.; Iwasaki, S. Biosynthesis of dynemicin A, a 3-ene-1, 5-diyne antitumor antibiotic. *J. Am. Chem. Soc.* **1992,** *114*, 4107–4110; (c) Lam, K.; Veitch, J.; Golik, J.; Krishnan, B. Biosynthesis of esperamicin A1, an enediyne antitumor antibiotic. *J. Am. Chem. Soc.* **1993**, *115*, 12340–12345.

[32] (a) Liu, W.; Christenson, S.; Standage, S.; Shen, B. Biosynthesis of the enediyne antitumor antibiotic C-1027. *Science (Washington, DC, U.S.)* **2002,** *297*, 1170; (b) Liu, W.; Nonaka, K.; Nie, L.; Zhang, J.; Christenson, S. The neocarzinostatin biosynthetic gene cluster from Streptomyces carzinostaticus ATCC 15944 involving two iterative type I polyketide synthases. *Chem. Biol.* **2005**, *12*, 293–302; (c) Lomovskaya, N.; Whitwam, R.; Thorson, J.; Czisny, A. The Calicheamicin Gene Cluster and Its Iterative Type I Enediyne PKS. *Science (Washington, DC, U.S.)* **2002**, *297*, 1173–1176; (d) Liu, W.; Ahlert, J.; Gao, Q.; Wendt-Pienkowski, E.; Shen, B.; Thorson, J. Rapid PCR amplification of minimal enediyne polyketide synthase cassettes leads to a predictive familial classification model. *Proc. Natl. Acad. Sci. U.S.A.* **2003,** *100*, 11959; (e) Zazopoulos, E.; Huang, K.; Staffa, A.; Liu, W.; Bachmann, B.; Nonaka, K.; Ahlert, J.; Thorson, J.; Shen, B.; Farnet, C. A genomics-guided approach for discovering and expressing cryptic metabolic pathways. *Nat. Biotechnol.* **2003,** *21*, 187–190; (f) Van Lanen, S.; Oh, T.; Liu, W.; Wendt-Pienkowski, E., Shen, B. Characterization of the maduropeptin biosynthetic gene cluster from Actinomadura madurae ATCC 39144 supporting a unifying paradigm for enediyne biosynthesis. *J. Am. Chem. Soc.* **2007**, *129*, 13082–13094.

1.4.2. Enediyne Biosynthesis: An Iterative Type I PKS

The unique structure of the enediyne core makes it impossible to predict what type of polyketide synthase (PKS) is responsible for the biosynthesis of nine-membered enediyne natural products. Work by Shen and co-workers[32a] showed the nine-membered enediyne C-1027 (**1001-B**) cluster included thirteen genes encoding the enediyne core, only one of which, sgcE, contains a PKS. This enediyne polyketide synthase (PKSE) consists of four domains that are characteristic of PKSs: ketoacyl synthase (KS), acyltransferase (AT), ketoreductase (KR), and dehydratase (DH). A fifth terminal domain (TD) was identified at the terminal region and it is unique to the enediyne PKSs. Additionally, Shen speculated that the region between the AT and KR domains contains a putative acyl carrier protein (ACP) domain (Figure 5). Shen and co-workers hypothesized that this scgE gene is responsible for the assembly of a linear polyunsaturated intermediate, that after the action of other enzymes, would cyclize to afford the enediyne core. When the sgcE gene was replaced with a mutant copy where the KS domain was knocked out, C-1027 was not produced, indicating that the C-1027 enediyne core biosynthesis proceeds via an iterative type I polyketide pathway. Simultaneously, Thorson and co-workers[32c] had characterized the gene cluster of the ten-membered calicheamicin and isolated the only PKS-containing gene, calE8. Subsequent

Figure 5 | Domain organization and comparison between 9- (SgcE) and ten-membered (CalE8) enediynes. aa, amino acid. (adapted from ref 33).

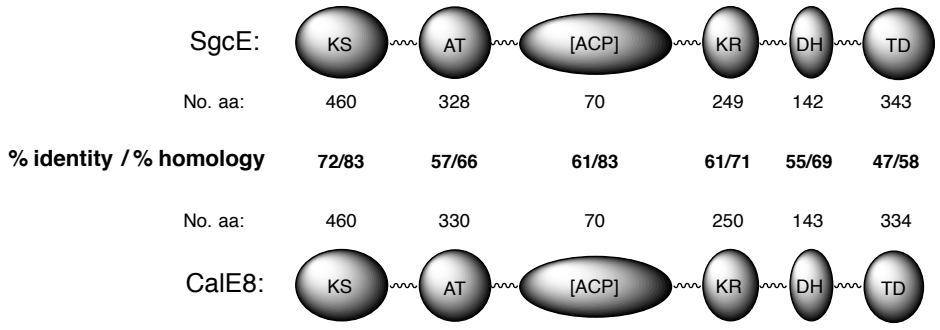

knockout studies verified that the biosynthesis of calicheamicin also proceeded iteratively with a type I PKS. Incredibly, comparison of this calE8 PKSE to the sgcE PKSE of C-1027 revealed a head-to-tail sequence homology (67% similarity) and an identical domain organization. The two PKSs showed that the KS, AT, KR and DH domains are

highly conserved while divergence occurs at the enediyne-specific TD (Figure 5).[33] The cloned gene sequences of these enediynes proved that despite differences between the gene clusters, nine and ten-membered enediynes share a common biosynthetic scheme involving an iterative type I PKS. This conclusion was contrary to the hypothesis proposed by Hensens and co-workers[31a] based on their isotope labeling studies that identified that the nine-membered neocarzinostatin (**1001-A**) enediyne had originated from a fatty acid precursor different than that for the ten-membered enediynes. While various type I PKSs that synthesize polyunsaturated polyketides iteratively from acetyl and malonyl starting units have been reported, the enediyne PKS family is unique in structure and mechanism from any PKS known to date.

1.4.3. A Complete Enediyne Biosynthetic Gene Cluster

In their analysis of the C-1027 chromoprotein, Shen and co-workers were able to identify and localize the entire gene cluster. The C-1027 chromophore can be deconstructed into four biosynthetic building blocks consisting of the endiyne core, a β-amino acid, a deoxy aminosugar, and a benzoxazolinate moiety (Figure 6). Along with the thirteen genes responsible for enediyne core biosynthesis previously discussed, the gene sequences for the peripheral moieties of the chromophore were established. Six genes, SgcC to sgcC5, were found to encode the β-amino acid biosynthesis, which originates from L-α-tyrosine. This pathway uncovered an unprecedented aminomutase gene, SgcC4, responsible for the first step of converting the L-α-tyrosine to L-β-tyrosine. The tyrosine is then capable of interacting with the SgcC1 gene, a gene known to load only β-tyrosine and other β-analogs to a free-standing peptidyl carrier protein SgcC2. The final of the five steps incorporate the β-amino acid into the endiyne core with a type II condensation enzyme, SgcC5. Whether or not this coupling occurs before or after full functionalization of the moiety is not yet known. For the deoxy aminosugar portion of C-1027, seven genes, SgcA to SgcA6, were identified. Characterization of the recombinant enzyme SgcA1 confirmed that this moiety originates from glucose-1-phosphate. A glycosyl transferase enzyme responsible for addition of the aminosugar to the enediyne core was also observed. The final building block of C-1027, the benzoxazolinate moiety,

[33] Ben, S.; Wen, L.; Koichi, N. Enediyne natural products: biosynthesis and prospect towards engineering novel antitumor agents. *Curr. Med. Chem.* **2003,** *10*, 2317–2325.

Figure 6 | Convergent biosynthesis of the enediyne C-1027 (adapted from ref 33).

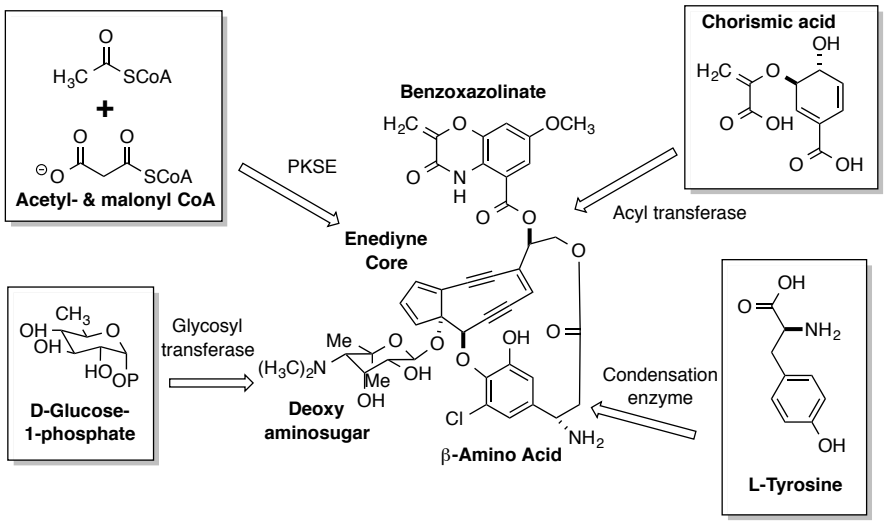

is an uncommon structural component of natural products. Seven genes, SgcD to SgcD6, encode its biosynthesis, and these genes are similar to other enzymes responsible for anthranilate biosynthesis. This suggests the pathway begins from chorismate, proceeds via the conversion to anthranilate, and ends with a covalent attachment to the enediyne core by an acyl transferase.

Sequencing and characterization of the isolated gene clusters for the three peripheral moieties of C-1027 uncovered a few novel biosynthetic pathways, but overall the construction and incorporation of the components into the enediyne core can be easily rationalized. However, the thirteen genes identified to encode the formation of the enediyne core have little in common with any known biosynthetic genomes. Three of the genes show homology with oxidoreductases, yet a family of seven isolated genes exhibit no sequence homology to any proteins of known function. Understanding the enzymatic steps responsible for assembling and cyclizing the highly unsaturated core appears to be on hold. For now, these enzymes are candidates for processing a linear polyunsaturated compound produced by the PKSE into an enediyne core intermediate. Identification of such a PKSE-produced intermediate is now the center of research efforts for further exploration of the activity and mechanism of enediyne core biosynthesis.

1.4.4. Isolation of a Biosynthetic Intermediate

In 2008, Shen and co-workers[34] found evidence for an ACP domain and a phosphopantetheinyl transferase (PPTase) domain in the PKSE. The presence of a terminal PPTase domain that phosphopantetheinylates the preceeding ACP domain in the C-1027 and neocarzinostatin core biosynthesis implies that each domain should initiate natural product formation when introduced in a heterologous host. However, initial attempts to isolate an intermediate from either protein failed, and an alternative approach was developed. Gene cluster characterization revealed a putative thioesterase (TE) immediately downstream of all PKSEs, and it was hypothesized that this TE could hydrolyze a polyketide intermediate produced from PKSE to be isolated. The PKSE genes were then coexpressed *in vitro* with their corresponding TE from *E. coli* as well as *Streptomyces albus* and *Streptomyces lividans*, all combinations of which produced an intermediate that was isolated and characterized as the heptaene compound **1044**.

Shen and co-workers envisioned enediyne core biosynthesis initiating with seven rounds of Claisen condensation with concomitant ketoreduction and dehydration in an iterative manner to yield an ACP-tethered 3-hydroxy-hexadecahexaene product (Figure 7). The thioester linkage could be hydrolyzed by the TE to generate the linear polyene **1043** that finally undergoes decarboxylation and dehydration to afford the fully conjugated **1044**. This represents the first isolated intermediate for enediyne core biosynthesis and shows that the PKSE is interchangeable within the nine-membered family of enediynes.

At the same time Shen and co-workers were isolating the nine-membered enediyne intermediate, the Liang group in Singapore was performing similar *in vitro* studies on the CalE8 PKS-containing gene of the ten-membered enediyne calicheamicin (**1002-B**).[35] Coexpression of the PKSE gene along with its TE led to the isolation of a unique linear intermediate, which Liang and co-workers found to be the carbonyl-conjugated polyene **1049** (Scheme 9). These results, in combination with those published

---

[34] Zhang, J.; Van Lanen, S.; Ju, J.; Liu, W.; Dorrestein, P.; Li, W.; Kelleher, N.; Shen, B. A phosphopantetheinylating polyketide synthase producing a linear polyene to initiate enediyne antitumor antibiotic biosynthesis. *Proc. Natl. Acad. Sci. U.S.A.* **2008,** *105*, 1460–1465.

[35] Kong, R.; Goh, L.; Liew, C.; Ho, Q.; Murugan, E.; Li, B.; Tang, K.; Liang, Z. Characterization of a carbonyl-conjugated polyene precursor in 10-membered enediyne biosynthesis. *J. Am. Chem. Soc.* **2008,** *130* , 8142–8143.

Figure 7 | Tandem reactions catalyzed by PKSE/TE to produce linear heptaene **1044** (adapted from ref 34).

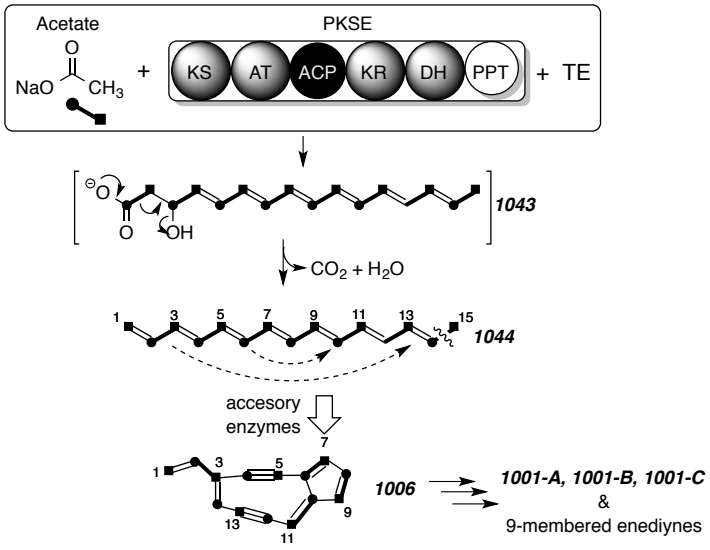

by the Shen laboratory, suggest that divergence of the biosynthetic pathways for nine and ten-membered enediynes originates at the PKS stage. However, one year later Townsend and co-workers at Johns Hopkins University published contradictory results regarding their *in vitro* experimentation with the calicheamicin PKSE.[36] After coexpression of the CalE8 gene along with its TE, multiple intermediates were isolated. Townsend observed the same methyl ketone **1049** as Liang, as well as the anticipated precursor acid **1047** from extracts of the same reaction. This labile compound undergoes decarboxylation over time, measurable by HPLC, to ketone **1049**. The contradiction arises from the fact that Townsend also isolated heptaene **1044**, the same proposed intermediate for the nine-membered enediynes seen by Shen. Townsend proposed (Scheme 9) that the PKSE would produce the CalE8-bound intermediate **1045**, which the thioesterase activity of CalE7 could release directly from CalE8 to give the β- keto acid **1047** and methyl ketone **1049** after decarboxylation. Alternatively, if CalE8 were to execute one more reduction via the KR domain, the β-hydroxythioester **1046** would form before release by CalE7 to the free acid **1048**. Finally, dehydration and decarboxylation of **1048** would lead to the

[36] Belecki, K.; Crawford, J. M.; Townsend, C. A. Production of octaketide polyenes by the calicheamicin polyketide synthase CalE8: Implications for the biosynthesis of enediyne core structures. *J. Am. Chem. Soc.* **2009,** *131*, 12564–12566.

Scheme 9 | Proposed biosynthetic intermediates by Townsend (adapted from ref 36).

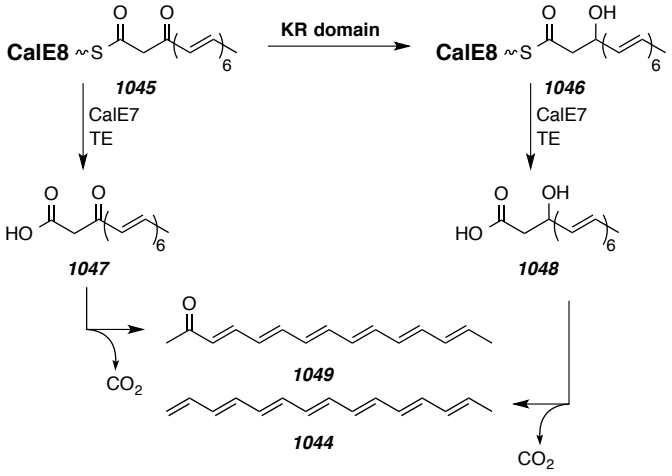

observed heptaene **1044**. The heptaene was found to be extremely unstable and Townsend notes that Liang and co-workers' use of a trifluoroacetic acid quench in their reactions may be to blame for their inability to observe this product. Townsend concludes that neither the methyl ketone **1049** nor heptaene **1044** serve as the branchpoint to nine and ten-membered enediyne biosynthesis. He reasons that the polyenes **1044**, **1049** and **1047** isolated from the calicheamicin biosynthesis may simply be an instance of errant PKS behavior in the absence of required auxiliary enzymes and contends that divergence to nine or ten-membered enediynes results from the action of accessory enzymes acting in concert with the enediyne PKS.

Addressing Townsend's claim, the Liang group reevaluated their calicheamicin experimentation without a trifluoroacetic acid quench and found that the polyene **1044** becomes the single dominant product under mild assay conditions.[37] The ketone **1049** was still observed in some cases, and it was found that product ratios varied considerably with substrate concentration and assay conditions. Coexpression of the C-1027 PKSE with its TE also showed both ketone and polyene products in a ratio that favored **1044** under biologically relevant conditions, but in a run with the ten-membered enediyne dynemicin, the ketone **1049** was never observed as a major product. This suggests that the nine and ten-membered PKSEs contain subtle differences and Liang concludes, in

[37] Sun, H.; Kong, R.; Zhu, D.; Lu, M.; Ji, Q.; Liew, C.; Lescar, J.; Zhong, G.; Liang, Z. Products of the iterative polyketide synthases in 9-and 10-membered enediyne biosynthesis. *Chem. Commun. (Cambridge, U.K.)* **2009,** *47*, 7399–7401.

opposition to Townsend, that the polyene **1044** can in fact be a biologically relevant intermediate.

1.4.5. Biosynthetic Divergence of Nine and Ten-Membered Enediynes

In 2010 the Guo group performed additional studies on the biosynthesis of the nine-membered C-1027.[38] Expression of the PKSE-containing gene SgcE with its thioesterase SgcE10 in *E. coli* produced the heptaene **1044**, identical to observations from the other labs. However, expression of SgcE alone without SgcE10 showed no production of 1044, and instead a nonaketide product characterized as **1051** was observed. These results were reproduced in the presence of SgcE10 at concentrations up to 2 μM, but above that threshold, yields of **1051** decreased in conjunction with increasing amounts of heptaene **1044** and a second product characterized as ketone **1052**.

Biosynthetically, the heptaene **1044** and ketone **1052** products can be formed from hydrolysis of SgcE-bound intermediates **1049** and **1050** by the SgcE10 TE and subsequent decarboxylation of the β-keto-carboxylates (Scheme 10). Without the presence of SgcE10, the PKS intermediate **1050** can undergo a thermodynamically

Scheme 10 | Proposed biosynthetic intermediates isolated by Guo and co-workers (adapted from ref 38).

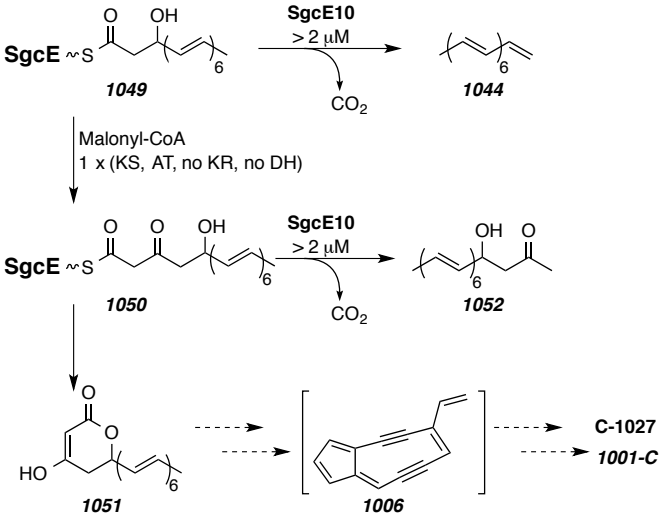

[38] Chen, X. G., P. Lai; Sze, K.; Guo, Z. Identification of a nonaketide product for the iterative polyketide synthase in biosynthesis of the nine-membered enediyne C-1027. *Angew. Chem., Int. Ed.* **2010,** *49*, 7926–7928.

favorable ∂-lactonization to produce the observed nonaketide product **1051**. Guo suggests that the lack of observation of **1051** and **1052** in previous studies may be because of their degradation by host enzymes or simply a failure to detect them in previous HPLC analysis due to a 400 nm setting of the UV/Vis detector, a wavelength at which neither of these products shows absorption. The nonaketide **1051** appears to be a new potential enediyne biosynthetic precursor for C-1027, analogous to the nine-membered enediyne cores in general.

Recognizing the apparent condition-dependent product profiles in these systems, Shen and co-workers reexamined the origin of biosynthetic divergence with studies comparing the products from three nine-membered (C-1027, neocarzinostatin, maduropeptin) and two ten-membered (calicheamicin, dynemicin) PKSE-TE systems.[39] While all previous studies used *in vitro* methods, the Shen group elected to use an *in vivo* system in hopes of more faithfully reproducing true biosynthetic conditions. All five PKSE-TE pairs in *E. coli* produced heptaene **1044** as the only major product. PKSE constructs for C-1027 and calicheamicin were also expressed in *S. lividans*, yielding identical results. Shen also examined fermentation products of four different native enediyne producers (C-1027, neocarzinostatin, calicheamicin and esperamicin) and all strains tested produced **1044**, providing further evidence that nine vs. ten-membered enediyne pathway divergence occurs outside the PKSE. Additionally, tests in which the five PKSE and TE genes were constructed in each of twenty different combinations also yielded **1044** in every case in both *E. coli* and *S. lividans* hosts. This PKSE-TE interchangeability offers more support for a unified view of PKSE catalysis. In accumulating these substantial results, Shen reiterates his previous hypothesis that accessory enzymes modify a universal PKSE intermediate en route to formation of the nine- or ten-membered enediyne core structures.

1.4.6. A Possible Mechanism for Enediyne Biosynthetic Divergence

To summarize Shen's work from 2008 and 2010, he found that the TEs are interchangeable across all classes of enediyne PKSs and that the heptaene **1044** is a major product from all combinations. He also found that PKSs from enediynes of the same 9- or

[39] Chen, Y.; Thorson, J.; Shen, B. Polyketide synthase chemistry does not direct biosynthetic divergence between 9-and 10-membered enediynes. *Proc. Natl. Acad. Sci. U.S.A.* **2010**, *107*, 11331–11335.

10-membered class effectively substitute for the native synthase and continue natural product production. However, the 9- and 10-membered PKSs are not interchangeable in this sense. Enediyne core-specific protein-protein interactions between the PKSE and these corresponding accessory enzymes could explain these results, and still be consistent with the hypothesis of enediyne divergence coming after the PKS pathway.[34]

Townsend suggests that collectively, these results imply that heptaene **1044** is not actually a precursor to the enediynes, but a shunt product. To probe this question, Townsend and co-workers set out to observe the products of calicheamicin PKS CalE8 in vivo, in the absence of its TE.[40] The conditions for cell expression had a significant impact on products isolated. With cultures protected from ambient light, they were able to isolate the ß-hydroxy acid **1048** for the first time (Scheme 11). This is the same intermediate they had proposed in the biosynthetic route to the heptaene **1044** (Scheme 9, page 20). The acid **1048** represents the first definitive example of programmed control of polyketide processing by CalE8, as it is the full chain length expected for the calicheamicin core structure. In an impressive report the following year, the Townsend group developed a method for accessing intermediates while they are still bound to their respective carrier proteins.[41] Utilization of this method resulted in the first characterization of enzyme-bound polyketides from enediyne systems when they isolated the ß-hydroxy thioester **1053**. Their data support a biosynthetic model that includes the ß-hydroxy thioester **1053** as a key intermediate en route to calicheamicin. Also, **1053** is the presumed precursor to the heptaene **1044**, which is prevalent in both 9- and 10-membered enediyne PKSs, indicating that **1053** is efficiently produced by each enediyne subclass. Townsend and co-workers believe thioester **1053** represents the last common intermediate in enediyne biosynthesis, and thus the point of divergence between 9- and 10-membered enediynes. Their hypothesis relies on tailoring enzymes specific to each subclass to interact directly with **1053** and direct the divergence. A radical pathway is

[40] Belecki, K.; Townsend, C. A. Environmental Control of the Calicheamicin Polyketide Synthase Leads to Detection of a Programmed Octaketide and a Proposal for Enediyne Biosynthesis. *Angew. Chem. Int. Ed.* **2012**, *51*, 11316–11319.

[41] (1) Belecki, K.; Townsend, C. A. Biochemical Determination of Enzyme-Bound Metabolites: Preferential Accumulation of a Programmed Octaketide on the Enediyne Polyketide Synthase CalE8. *J. Am. Chem. Soc* **2013**, *135*, 14339–14348.

Scheme 11 | A proposed biosynthetic mechanism for enediyne biosynthetic divergence (adapted from ref 40).

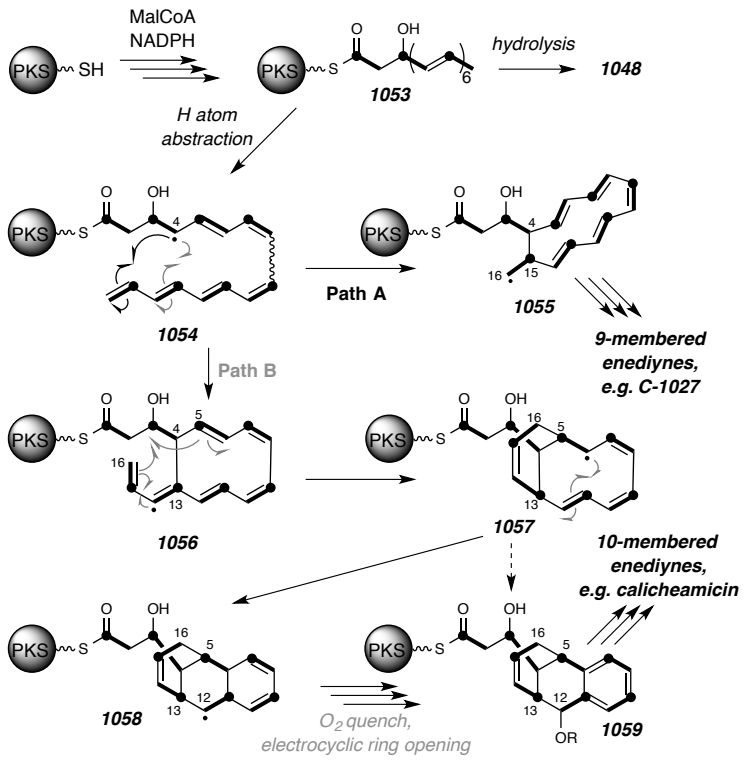

suggested in the mechanism proposed in Scheme 11, but cationic and electrocyclic mechanisms can be envisioned as well. This most recent work by Townsend represents the most complete picture of enediyne core biosynthesis to date, but it remains to be seen what roles tailoring enzymes may or may not play in taking the PKS-bound intermediate **1053** on to the final enediyne core structures.

Chapter 2. Synthetic Approaches to Sondheimer Substrates and Enediyne Core Precursor

2.1. Re-examination of Sondheimer Chemistry

In conjunction with exploring our enediyne core hypothesis, we first set out to replicate Sondheimer's preparation of tetrayne macrocycles that were shown to participate in intriguing electrocyclic rearrangements analogous to our hypothesized cyclization (cf. Scheme 4). Sondheimer isolated **1024** after subjecting **1019** to basic conditions in methanol (Scheme 12). The macrocycle tetrayne was the product of a Glaser coupling of the diynol **2001**. The diynol resulted from a double Grignard addition of metalated propargyl bromide to ethyl formate.

Scheme 12 | Retrosynthetic analysis of **1024**.

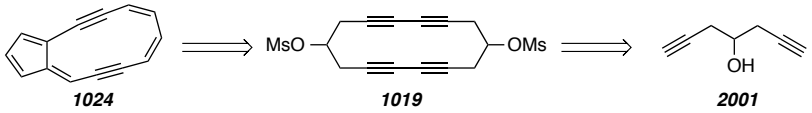

Our attempts at replicating this synthesis are detailed below. Mixing of propargyl bromide with magnesium turnings formed the Grignard reagent, and drop-wise addition of ethyl formate gave crude hepta-1,6-diyn-4-ol **2001**. Purification by flash chromatography provided a good yield of the pure diyne, which was stable at room temperature but did undergo decomposition upon prolonged heating. The method employed by Sondheimer in the preparation of the macrocycle **2003** used Glaser conditions for oxidative coupling of terminal acetylenes. Standard Glaser conditions use catalytic amounts of a copper(I)-salt in aqueous ammonia. Sondheimer used two equivalents of copper(I) chloride in his procedure, and isolated the macrocycle **2003** from a complex mixture of products after in situ acetylation of diol **2002** and recrystallization in 1.4% yield (Scheme 13). These typical Glaser conditions have drawbacks of being

Scheme 13 | Glaser coupling of diyne **2001** as performed by Sondheimer.

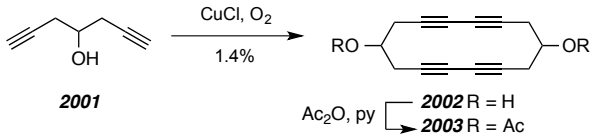

heterogeneous, slow, and low yielding, especially in Sondheimer's case. Initial attempts at replicating this reaction on considerably smaller scale failed to produce any detectable sign (via GC, LC-MS or NMR) of macrocycle formation, so we investigated alternative protocols for oxidative acetylenic coupling. A modified Glaser-type coupling using a combination of copper(I) iodide, *N*-bromosuccinimide (NBS), and Hünig's base was reported by Zhang[42] as an efficient and mild procedure for alkyne coupling. Treatment of **2001** with a full equivalent of both copper iodide and NBS along with two equivalents of Hünigs base provided a mixture of products. LC-MS showed that a mixture of linear polyynes was produced (Scheme 14) from successful oxidative acetylenic coupling, but the desired macrocycle was not observed. Separation of the products by flash chromatography led to characterization of the homocoupled diol **2004**, the trimer **2005** and tetramer **2006**. The extent of polymerization for each product is easily identified by comparison of relative ^{1}H NMR integration values for the distinct terminal alkyne protons with either the methylene or carbinol protons. The use of copper(I) iodide in

Scheme 14 | Oxidative acetylenic coupling of **2001**.

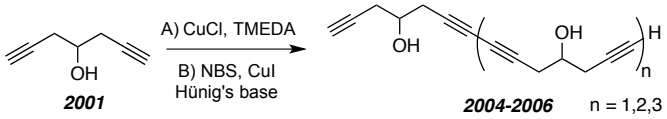

Zhang's procedure complicated the workup, so a different protocol utilizing Hay's catalyst[43] was adopted. Premixing copper(I) chloride with the complexing agent TMEDA (tetramethylethylenediamine) in acetone followed by decanting away from solid particulates before addition of the supernatant to the alkyne gives a homogeneous reaction mixture and a clean workup. Product distribution was analogous to the copper(I) iodide system, with a mixture of oligomers isolated and no evidence for any macrocycle formation. Decreasing the reaction time increased dimer and trimer formation relative to other byproducts, as did decreasing the alkyne concentration. Varying the concentration of Hay's catalyst only produced a slight rate enhancement and no detectable variation in product mixtures.

[42] Li, L.; Wang, J.; Zhang, G.; Liu, Q. A mild copper-mediated Glaser-type coupling reaction under the novel CuI/NBS/DIPEA promoting system. *Tetrahedron Lett.* **2009**, *50*, 4033–4036.
[43] Hay, A. Oxidative Coupling of Acetylenes. II1. *J. Org. Chem.* **1962**, *27*, 3320–3321.

2.2. Ring-Closing Attempts

With standard Glaser coupling conditions failing to close the macrocycle, we pursued alternative methods for cyclization using an oxidative acetylenic coupling. Eglinton and Galbraith developed a protocol for diyne formation using an excess of copper(II) acetate in pyridine.[30] The pyridine-copper complex is readily solvated by methanol or ether and was found to make the process homogeneous and faster. More importantly, when run at low concentrations, macrocyclic diynes could be formed in low to moderate yields for some substrates in which the conventional copper chloride coupling procedure only gave linear products.

Isolating the linear diynes from the product mixture of Glaser coupling of **2001** provided a starting material to examine Eglinton coupling conditions. The diol **2004** and bis-acetate **2007** were subjected to Eglinton conditions in high dilution (0.5 mM) with addition of a fresh five equivalents of copper(II) acetate every 12 h over 48 h. No macrocycle formation was evident as workup and isolation yielded only starting material

Scheme 15 | Eglinton conditions for acetylenic coupling.

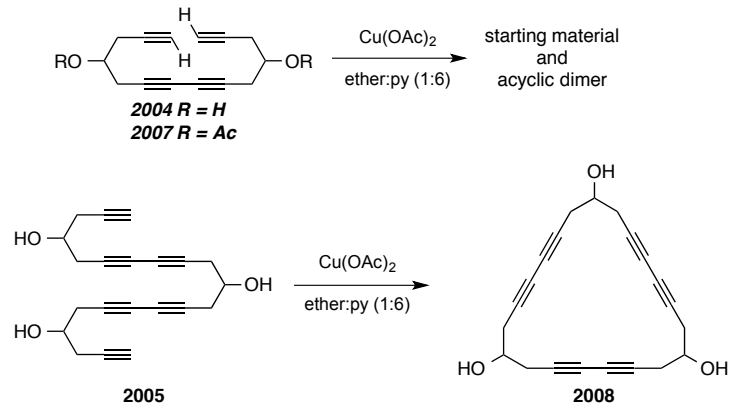

and the dimers. In an attempt to observe any macrocycle formation whatsoever, a few milligrams of isolated linear triol **2005** were subjected to high dilution Eglinton conditions (Scheme 15). After 72 h, analysis by LC-MS showed predominantly starting material, but also a trace of a new product peak at a lower retention time with a mass corresponding to that of the cyclized triol **2008**. The retention time of this cyclic product can be rationalized relative to its acyclic precursor. In the reverse-phase, we would expect the retention time of any cyclized compounds to decrease significantly due to the

forced outward orientation of the polar hydroxyl groups. If nothing else, this product observation and LC-MS data offer insight into the possible chromatography characteristics of the ultimately desired tetrayne macrocycle.

The ability of the trimer **2005** to cyclize where the dimer has failed reveals an important factor that is working against macrocycle formation of the tetrayne **2002**. The linear geometry of our starting material and the inherent strain of having two pairs of conjugated alkynes is energetically unfavorable for fourteen-membered ring formation. After the first oxidative coupling event, the diol **2004** has numerous degrees of freedom which all need to arrange in a very low-populated conformation for the next oxidative coupling to close the ring. The trimer **2005** has similar issues, but its cyclized product **2008** is not as strained as the corresponding fourteen-membered macrocycle.

2.3. Examining Glaser and Cadiot-Chodkiewicz Coupling Conditions

The Glaser conditions for acetylenic coupling are notoriously irreproducible, especially when attempting to form large ring systems.[29,44] Experimental studies have shown that such reactions are highly dependent on the reaction conditions. Also, the reaction mechanism is still not fully understood, although it is generally believed to proceed through dimeric copper(II) acetylide complexes.[45] There are many reported instances when slight modifications of precedented procedures had to be developed for synthesizing bisacetylenes. One example is that of Breslow and co-workers' work in synthesizing cage-like structures.[44] When standard Glaser and Eglinton conditions failed, Breslow used a combination of 100 equivalents of anhydrous copper(I) chloride and twelve equivalents of anhydrous copper(II) chloride to successfully form the conjugated di-ynes.

Myers and Goldberg encountered similar obstacles in their synthesis of the kedarcidin enediyne core (Scheme 8, Sec. 1.3.4).[28] Standard Glaser and Eglinton procedures did not form their desired macrocycle, and neither did Breslow's conditions described above. Myers and Goldberg settled on yet another unique adaptation of Glaser conditions using thirty equivalents of copper(II) acetate and five equivalents of copper(I)

---

[44] Denmeade, S.; Chiang, M.; Breslow, R. Efficient triple coupling reaction to produce a self-adjusting molecular cage. *J. Am. Chem. Soc.* **1985**, *107*, 5544–5545.

[45] Klebanskii, A. L. G., I. V.; Kuznetsova, O. M. Reaction of formation of diacetylenic compounds, from monosubstituted derivatives of acetylene. *Zh. Obshch. Khim.* **1957,** *27*, 2977–2983.

iodide in a pyridine/THF solvent pair with heating to 60 °C under an inert atmosphere, which formed the macrocycle in an impressive 74-86% yield. It was also found that the mixture of copper salts had to be prepared in an exacting procedure; simply co-mixing the solid reagents gave significantly lower yield of products.

We attempted both the Breslow and Myers modifications in hopes that their circumstantial success would be amenable to tetrayne **2002** (Scheme 16). Unfortunately, replication of substrate concentration as well as copper salt preparation and stoichiometry did not result in any detectable macrocycle formation.

Scheme 16 | Unsuccessful cyclization reactions with modified Glaser coupling conditions.

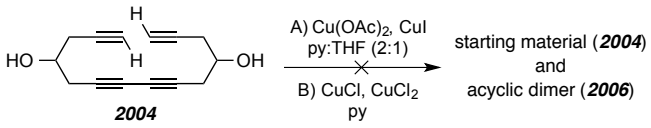

In our next attempt, we investigated the Cadiot-Chodkiewicz [46] reaction. Developed as a heterocoupling alternative to the Glaser reaction, the Cadiot-Chodkiewicz reaction combines a terminal alkyne with a haloalkyne in the presence of a copper(I) salt and an amine base. To ensure the presence of the required copper(I) salt, hydroxylamine hydrochloride was added to a premixed solution of copper(I) chloride and ethylamine in methanol until the reaction mixture changed from light blue to colorless. The brominated compound **2010** and terminal alkyne **2001** were added at 0 °C and TLC analysis showed

Scheme 17 | Macrocycle formation via Cadiot-Chodkiewicz coupling.

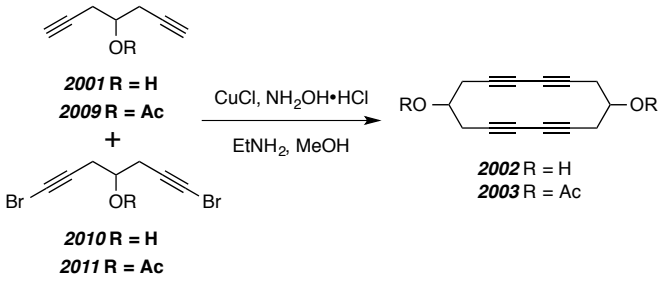

starting material consumption in 20-40 minutes depending on the concentration (Scheme 17). Analysis of the crude product mixture by LC-MS after workup revealed a

[46] Chodkiewicz, W. *Chemistry of Acetylenes*. Dekker: New York, 1957.

previously unobserved peak, albeit of low intensity, with an observed mass corresponding to that of the closed cyclic diol **2002**. The retention time of this peak falls in line with the value that we would expect in reference to those observed for similar products. The cyclized product **2002** would have a shorter retention time than its acyclic precursor **2004**, but their difference would not be as drastic as that for the acyclic triol **2005** when it cyclizes to **2008**. The acetylated starting materials **2009** and **2011** were synthesized in an attempt to improve yields and gain more chromatographic data for these types of compounds. Evidence for the formation of the macrocycle **2003** was observed with a retention time of 11.59 minutes with the appropriate mass. In each of these coupling reactions branched acyclic oligomers constitute a vast majority of the product mixture, and at this point purification and isolation of the macrocycles remained unsuccessful.

2.4. Macrocycle Formation and Isolation

With evidence for macrocycle formation in hand, the challenge now lay in isolation of the cyclic tetraynes. Since the desired products were identified with the Cadiot-Chodkiewicz reaction, those coupling conditions were replicated on a larger scale. The extremely polar nature anticipated for the cyclic diol **2002** and verified by the LC-MS retention time suggested that isolation of such a polar product would be difficult. For this reason, the alcohol coupling partner **2001** was modified to the phenylamide **2011** and coupled with the already synthesized dibromo alcohol **2010**. Under Cadiot-Chodkiewicz conditions, the LC-MS chromatogram of the crude product mixture contained the same peak which we had previously correlated to the cyclic diol **2002**. This indicated either that loss of the amide group back to the alcohol was occurring under these coupling conditions, or that we were observing homocoupling of the alcohol **2001**. Regardless of the process, when this crude product mixture was purified via HPLC, a peak was isolated and confirmed via ^{1}H NMR and high-resolution mass spectrometry analysis to be that of the cyclic diol **2002** (Scheme 18). Only a trace amount (<1 mg, ca. 1%) was isolated from the reaction mixture. We envisioned taking advantage of the Thorpe-Ingold effect to favor cyclization with the preparation of the *tert*-butyl malonate **2014** and its brominated coupling partner **2013**. Presumably, the steric buttressing of the bulky *tert*-butyl esters would result in a greater population of the reactive conformer, leading to productive

alkyne coupling and macrocycle formation. The malonate macrocycle **2015** was isolated after HPLC purification, however in only a slightly increased yield (2%).

Scheme 18 | Isolation of tetrayne macrocycles **2002** and **2014**.

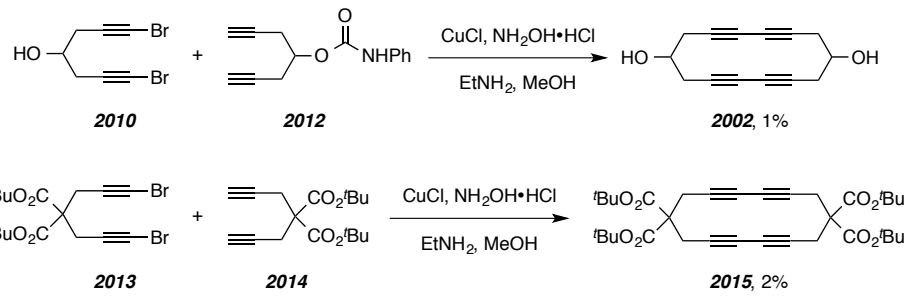

The isolation of a macrocycle via HPLC gave us a blueprint to follow for future isolation of these types of products. We decided to return to the Hay's catalyst conditions of copper (I) chloride and TMEDA for alkyne coupling, hoping to eliminate the bromination step necessary in Cadiot-Chodkiewicz coupling. Gratifyingly, when the acetate diyne **2009** was subjected to high dilution in acetone with the presence of the premixed Hay's catalyst, we were able to separate a small sample of our desired macrocycle via HPLC. Sondheimer observed his unique cyclization in the dimesylate tetrayne **1019** (Scheme 12, Sec. 2.1) via base-induced elimination. The diacetate **2003** proved easier to isolate compared to the more polar diol **2003**, so we planned to arrive at the mesylate without having to purify and isolate the troublesome diol. This was realized by deacetylation with potassium carbonate in methanol followed by mesylation of the crude mixture of diol **2003**, which gave the desired macrocycle **1019** after more HPLC purification (Scheme 19).

Scheme 19 | Alternative approach to macrocycle formation.

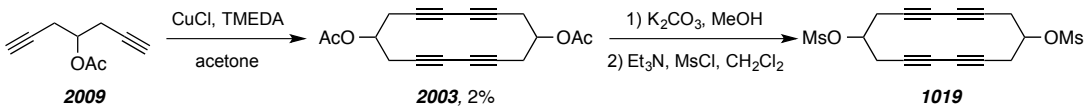

Grateful to have even a few milligrams of tetrayne macrocycles in hand, we cautiously proceeded to examine potential electrocyclizations of these compounds. While Sondheimer used methanolic potassium hydroxide to initiate his cyclization, we initially turned to the organic amidine base 1,8-diazabicycloundec-7-ene (DBU). To an NMR tube

of the tetrayne **1019** in 600 μL $CDCl_3$ was added 10 μL of DBU and the reaction followed via ^1H NMR. Unfortunately, there was no sign of any cyclized or rearranged product, only the rapid decomposition of starting mesylate was observed (Scheme 20). After 1 h at room temperature there was no remaining mesylate **1019** and no identifiable products. In contrast, the diacetate was not nearly as labile in the presence of DBU. In the same experiment with DBU and the diacetate macrocycle **2003**, there was no sign of loss of starting material, even after 24 h at room temperature. The dearth of starting material certainly frustrated attempts to replicate and examine Sondheimer's interesting cyclization. Valuable insights could be obtained in relation to our enediyne core biosynthetic hypothesis, the viability of which we were concomitantly pursuing.

Scheme 20 | Base-induced elimination attempts.

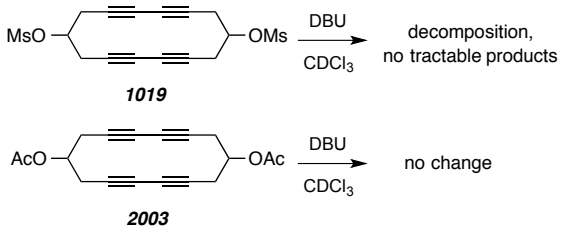

2.5. Retrosynthetic Analysis of Hypothesized Acyclic Enediyne Core Precursor

Our proposed strategy for synthesizing the key acyclic intermediate **1007** is shown below (Scheme 21). We envisioned a convergent approach involving a late-stage Stille coupling[47] of vinyl halide **2016** and stannane **2017**. The vinyl halide could originate from a sila-Sonagashira coupling of *Z*-dichloroethene **2018** with the conjugated

Scheme 21 | Retrosynthetic analysis of acyclic precursor **1007**.

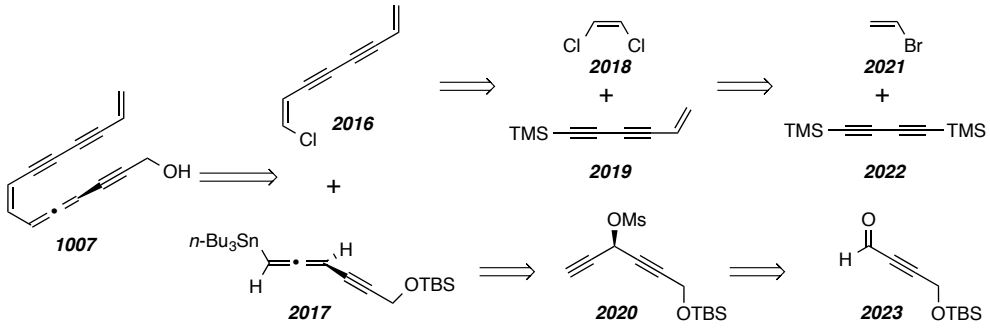

[47] Stille, J. The palladium-catalyzed cross-coupling reactions of organotin reagents with organic electrophiles [new synthetic methods (58)]. Angew. Chem., Int. Ed. 1986, 25, 508–524.

enediyne **2019**.[48] A Sonagashira coupling of bromoethene **2021** with the mono-silylated lithium salt of the commercially available bis(trimethylsilyl)butadiyne **2022** would furnish **2019**. For the organotin Stille coupling partner, tributyltin lithium addition to enantiopure propargylic mesylates (cf. **2020**) has been shown to produce enantiopure allenylstannanes (cf. **2017**).[49] Alkynyl Grignard addition to a protected ynal (cf. **2023**) with in situ mesylate trapping of the intermediate alkoxide should provide alkynyl mesylates (cf. **2020**).[50]

We had hoped to access our key acyclic precursor and probe the conditions for its proposed cyclization. However, en route to **1007**, an unanticipated side reaction occurred. This isolation, characterization, and subsequent identification of mechanism of this reaction opened up a previously unexplored area of chemistry. This quickly became the primary research focus for the author of this Thesis and comprises the remainder of the work presented herein.

[48] (a) Mio, M. J.; Kopel, L. C.; Braun, J. B.; Gadzikwa, T. L.; Hull, K. L.; Brisbois, R. G.; Markworth, C. J.; Grieco, P. A. One-pot synthesis of symmetrical and unsymmetrical bisarylethynes by a modification of the sonogashira coupling reaction. *Org. Lett.* **2002,** *4*, 3199–202; (b) Kende, A.; Smith, C. A mild synthesis of 1, 3-Diynes. *J. Org. Chem.* **1988**, *53*, 2655–2657.

[49] Marshall, J.; Wang, X. Synthesis of enantioenriched homopropargylic alcohols through diastereoselective SE'additions of chiral allenylstannanes to aldehydes. *J. Org. Chem.* **1992**, *57*, 1242–1252.

[50] Saccavini, C.; Tedeschi, C.; Maurette, L. Functional [6] pericyclynes: Synthesis through [14+ 4] and [8+ 10] cyclization strategies. *Chem.-Eur. J.* **2007**, *13*, 5378–5387.

◊ Part II ◊

The Hexadehydro-Diels–Alder (HDDA) Reaction

Chapter 3. HDDA Generality and Intramolecular Trapping

3.1. A Serendipitous Finding

The studies presented in this section, and sporadically throughout the rest of Part II have been recently disclosed in Nature.[51] *In order to tell a complete story, portions of the published story have been included even though the author of this Thesis did not personally carry out the experiments. Only data for the experiments performed by the author of this Thesis have been included in the experimental.*

In the course of exploring our enediyne core hypothesis, Dr. Beeru Baire set out to synthesize the acyclic precursor **1007**. One strategy involved installation of the allene moiety of **1007** through a propargylic transposition of alcohol **3001** (Scheme 22). However, when attempting to oxidize **3001**, no amount of **3002** was isolated in a reaction mixture that contained a tractable major product in 53% yield. After extensive one- and two-dimensional NMR, IR, and mass analysis, the isolated product was identified as benzenoid **3003**. Three characteristics of this product immediately stood out: 1) the presumed intermediate ketone, acyclic **3002**, had undergone a tricycloisomerization; 2)

Scheme 22 | Serendipitous finding that **3002** undergoes cycloisomerization to benzenoid **3003** via the aryne intermediate **3004**/**3005**.

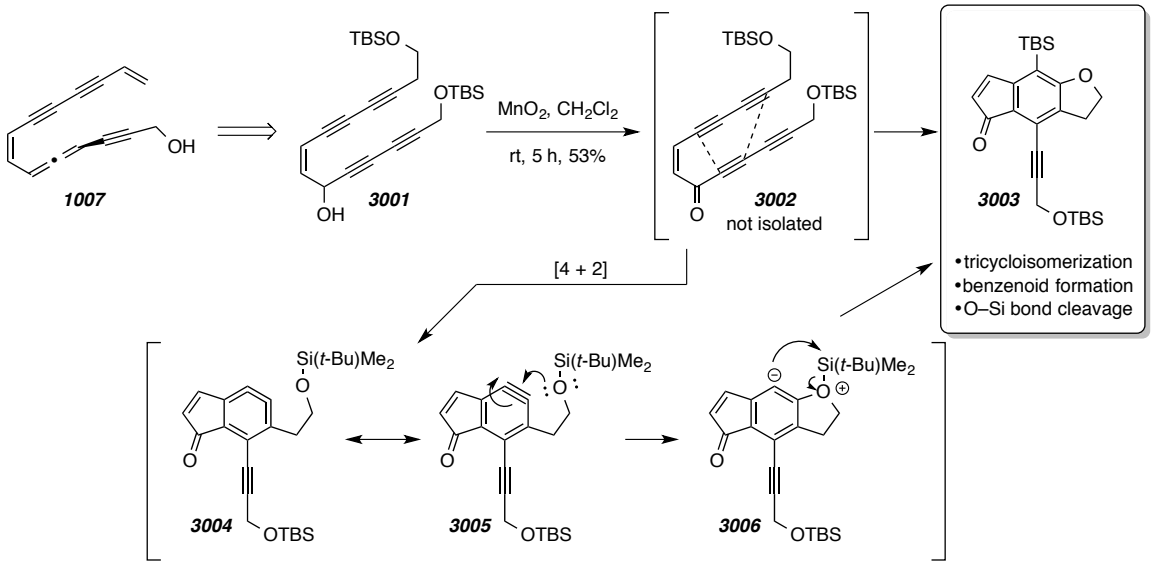

[51] a) Hoye, T. R.; Baire, B.; Niu, D.; Willoughby, P. H.; Woods, B. P. The hexadehydro-Diels–Alder reaction. *Nature* **2012**, *490*, 208–212. b) Niu, D.; Willoughby, P. H.; Woods, B. P.; Baire, B.; Hoye, T. R. Alkane desaturation via concerted double hydrogen atom transfer to benzyne. *Nature* **2013**, *501*, 531–534.

the product contained an aromatized benzene core, while only one of the four initial alkynes from the starting material remained; and 3) one of the oxygen-silicon bonds present in the starting material had been cleaved and added across adjacent carbons of the benzene ring. Collectively, these observations led us to envision the mechanism proposed along the bottom of Scheme 22. We presumed that the MnO_2 oxidation was taking place as expected to arrive at the *cis*-enone **3002**. The three alkynes that eventually comprise the benzene core of the product then undergo a [4+2] cyclization (dashed lines on **3002**), which results in the strained cumulene bicycle **3004**. This cumulene is simply an additional, but much less encountered, resonance form of the common reactive intermediate *o*-benzyne **3005**. The pendant silyl ether is conveniently positioned five-atoms away from the reactive benzyne, and the oxygen lone pair can trap the benzyne to result in the zwitterion **3006**. This zwitterion undergoes silyl migration from oxygen to the aryl carbon to arrive at the isolated benzenoid **3003** in a process reminiscent to a retro-Brook[52] rearrangement (arrows shown in Scheme 22).

Scheme 23 | Alternate, and unproductive, mode of [4+2] cyclization of ketone **3002**.

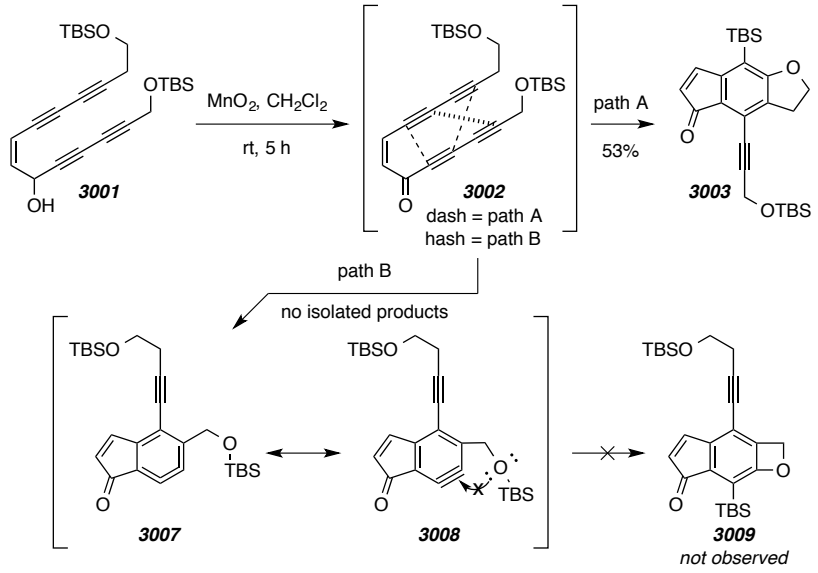

[52] Bailey, W. F.; Jiang, X. Stereochemistry of the cyclization of 4-(*t*-butyldimethyl)siloxy-5-hexenyllithium: *cis*-Selective ring-closure accompanied by retro-[1,4]-Brook rearrangement. *ARKIVOK* **2005**, *6*, 25–32.

We were fortunate in multiple different ways, many of which were not fully realized until much later, in our finding of this tetrayne-to-benzenoid reaction. One piece of luck that was recognized shortly after our mechanistic proposal was the benefit of the fortuitously placed silyl ether that serves to trap the highly reactive benzyne intermediate. However, the key [4+2] cyclization only requires reaction of three alkyne units, meaning that our tetrayne starting material contained an available alternative pathway for cyclization (Scheme 23). If the reacting diyne is now in conjugation with the ketone (hashed lines from **3002**), the [4+2] reaction results in the benzyne intermediate **3007**/**3008**. The silyl ether moiety in this case is now only four-atoms away from the reactive benzyne, and is unable to trap to form the strained four-membered ring in **3009**. This led us to wonder how efficiently the reaction would proceed if this unproductive path were eliminated. To examine that question we prepared the triyne **3014**, which has only one available mode of [4+2] cyclization. Sonagashira coupling of diyne **3011** with the bromoaldehyde **3010** gave the diyne **3012** in good yield. Addition of the lithium acetylide of trimethylsilylacetylene followed by oxidation of the corresponding propargyl alcohol **3013** gave the triynone **3014** efficiently in short order. Remarkably, the triyne

Scheme 24 | Preparation of triyne **3014** and its clean cyclization to benzenoid **3015**.

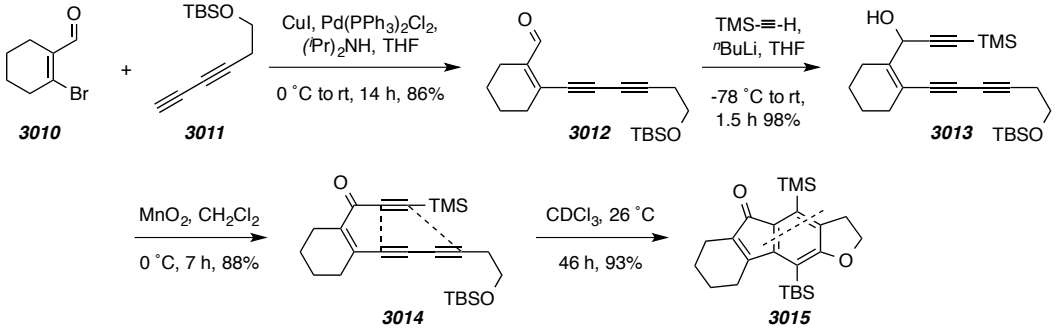

3014 cyclized to the benzenoid **3015** cleanly at room temperature in 93% yield! At this point it became clear that "the game is on."[53]

The cleanliness and high yield of our observed triyne cycloisomerization was surprising. So we turned to computational analysis in order to gain a better understanding

[53] a) Heine, H. W. Personal communication. *Bucknell University* **1969**; b) Hoye, T. R. Personal communication. *University of Minnesota* **2011**.

of the key thermodynamic features of the transformation. Specifically, we were curious as to the energetics of conversion of a triyne to an *o*-benzyne. Experimentally, we found that the ester-containing simple triyne **3016** was capable of cycloisomerization (120 °C, 40 h) to benzyne **3017** where subsequent intermolecular trapping with *t*-butanol resulted in the 5-*t*-butoxyphthalide **3018**. DFT calculations of this system concluded that the benzyne-forming reaction is exoergic by 51 kcal·mol^{-1}! It is particularly remarkable that such a highly reactive intermediate like benzyne can be accessed by a purely thermal process that is so exoergic. This is a testament to the considerable amount of potential energy contained within an alkyne functional group. This point is emphasized by the fact that the overall reaction to the final phthalide is exoergic by >120 kcal·mol^{-1}.

Scheme 25 | Computed free energy changes for an HDDA cascade.

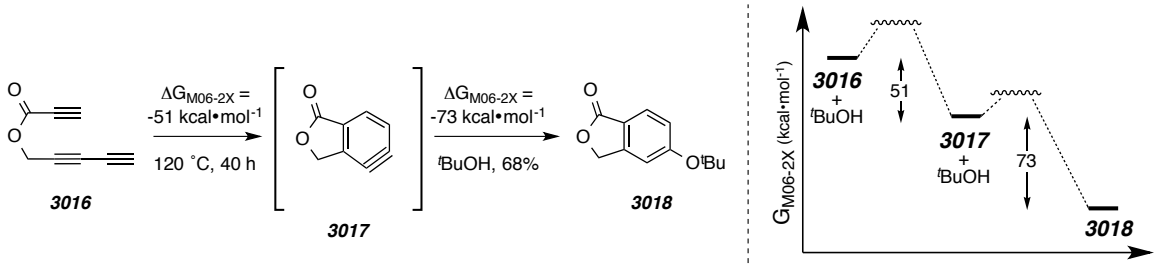

3.2. HDDA Background and Precedence

The alkyne-plus-diyne [4+2] cyclization that we serendipitously observed represents an additional mode of Diels–Alder[54] reaction. The prototypical event is reaction of 1,3-butadiene (**3020**) as the 4π-component with ethylene as the 2π-component (**3019**) to give cylcohexene (**3021**, Panel A, Figure 8). If acetylene (**3022**) is substituted in place of ethylene, then the analogous [4+2] cyclization results in cyclohexadiene (**3023**). We have proposed that this be deemed a didehydro-Diels–Alder reaction (Panel B). The next-most highly oxidized variant can involve a 1,3-enyne (**3024**) as the 4π-component reacting with an alkyne (Panel C). The [4+2] cyclization of these partners

[54] Diels, O.; Alder, K. Syntheses in the hydroaromatic series [in German]. *Justus Liebigs Ann. Chem.* **1928**, *460*, 98–122.

Figure 8 | Diels–Alder reactions of varying oxidation states; A) prototypical Diels–Alder reaction, B) the didehydro-Diels–Alder reaction, C) the tetradehydro-Diels–Alder (TDDA) reaction, D) the hexadehydro-Diels–Alder (HDDA) reaction.

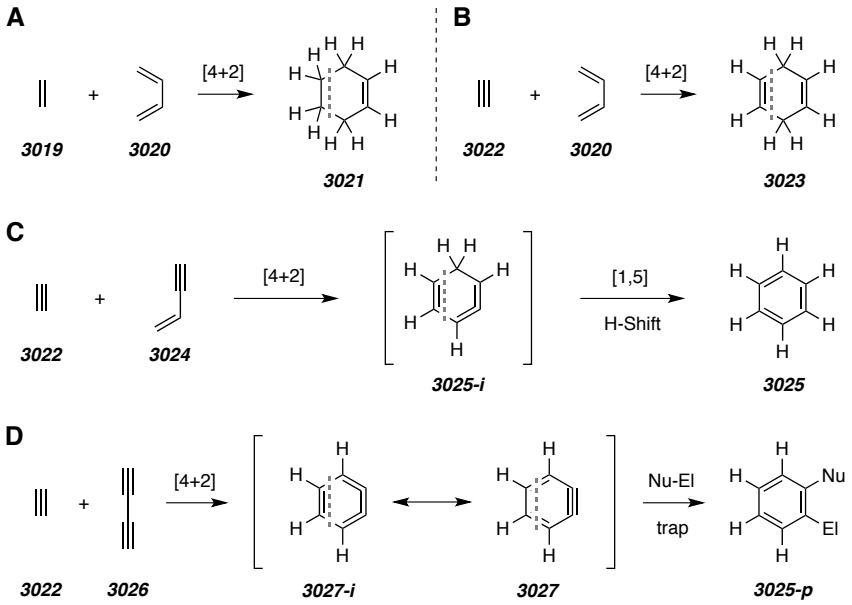

produces the cyclic allene **3025-i** intermediate that rapidly rearranges via a [1,5] hydrogen atom shift, resulting in benzene **3025**. We have suggested this variant be named the tetradehydro-Diels–Alder cyclization. Surprisingly, the first tetradehydro-Diels–Alder reaction was observed with the thermal dimerization of phenylpropiolic acid[55] 30 years prior to the initial report of Diels and Alder.[54] This brings us to the final, most highly oxidized, variant: addition between a 1,3-diyne (**3026**) with an alkyne in a hexadehydro-Diels–Alder (HDDA) reaction (Panel D). This cyclization results in the reactive intermediate *o*-benzyne (**3027**), which must be subsequently trapped to arrive at an *ortho*-functionalized benzenoid (**3025-p**). In stark contrast to the extensive research on the prototypical Diels–Alder reaction and its other variants, at the time of our initial observation (cf. Scheme 22) the HDDA reaction had been almost entirely unexploited. One rationale for this lies in the way *o*-benzyne is most commonly drawn, as the strained alkyne **3027**. This depiction makes retrosynthetic analysis via a [4+2] cyclization

[55] Michael, A.; Bucher, J. E. Über die Einwirkung von Eissigsäureanhydrid auf Phenylpropiolsäure. *Chem. Zentrblt*. **1898**, 731–733.

unattainable—it is only through the much less commonly encountered Kekulé depiction of *o*-benzyne **3027-i** that this cycloaddition assembly strategy becomes evident.

Other factors that worked against any previous development of the HDDA reaction lay in the conditions used and mechanistic rationale presented in the first reported examples of this type of transformation. In 1997 the labs of both R. P. Johnson and Ikuo Ueda reported the first cases of polyyne systems capable of cyclization to aromatic hydrocarbons. Johnson proposed a diyne-plus-alkyne Diels–Alder cyclization as a logical extension of the other, known, dehydro-Diels–Alder reactions. In a flash-vacuum-pyrolysis experiment, 1,3,8-nonatriyne (**3028**) was heated to 600 °C at 0.01 Torr and the products indane **3030** and indene **3031** were isolated, accounting for >95% of the products, along with some 'soot' (Scheme 26).[56] The intermediacy of benzyne **3029** was verified through cyclization of a deuterated analog of **3028**, ruling out an alternative vinylidene mechanism. The production of indene **3031** was confirmed to be a secondary product of indane dehydrogenation by pyrolysis of indane under the same conditions. The source of hydrogen being added to the benzyne is unknown, but the authors note there is precedence for reduction of benzynes under similar pyrolytic conditions.[57]

Scheme 26 | Thermal cyclization of triyne **3028** via benzyne **3029** (adapted from ref 55).

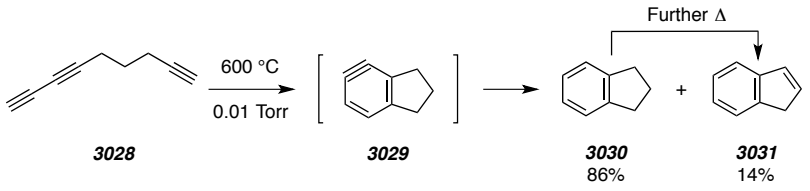

Later that same year came the first in a series of publications from the Ueda group detailing the production of benzenoids from polyyne systems. Their seminal report[58] showed that tetrayne **3032** cyclizes spontaneously at room temperature to produce the

[56] Bradley, A.; Johnson, R. Thermolysis of 1,3,8-nonatriyne: Evidence for intramolecular [2+4] cycloaromatization to a benzyne intermediate. *J. Am. Chem. Soc.* **1997**, *119*, 9917–9918.
[57] Brown, R. F.; Coulston, K. J.; Eastwood, F. W. Formation of biphenylene by elimination of C_2 from 9, 10-didehydrophenanthrene at 1100 ºC. *Tetrahedron Lett.* **1996**, *37*, 6819–6820.
[58] Miyawaki, K.; Suzuki, R.; Kawano, T.; Ueda, I. Cycloaromatization of a non-conjugated polyenyne system: Synthesis of 5H-benzo[d]fluoreno[3,2-b]pyrans via diradicals generated from 1-[2-{4-(2-alkoxymethylphenyl)butan-1,3-diynyl}]phenylpentan-2,4-diyn-1-ols and trapping evidence for the 1,2-didehydrobenzene diradical. *Tetrahedron Lett.* **1997**, *38*, 3943–3946.

benzenoid isomers **3033** and **3034** (Scheme 27). Their mechanistic proposal is shown on the bottom of Scheme 27 and includes exclusively radical intermediates. First, the two

Scheme 27 | Thermal cyclization of tetrayne **3032** and mechanistic hypothesis from Ueda and coworkers (adapted from ref 58).

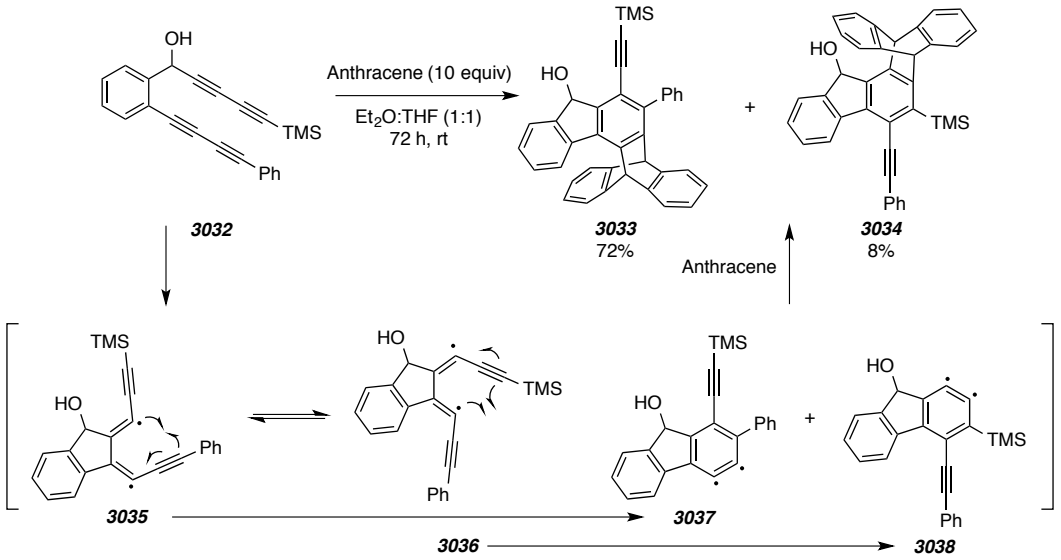

proximal alkynes cyclize to a rapidly equilibrating mixture of configurational isomers **3035** and **3036**. Each of these diradical intermediates cyclizes again to give the two 1,2-didehydroarene diradicals **3037** or **3038** which are then trapped by an anthracene molecule. Over the next decade Ueda would produce a series of reports of similar cyclizations, with all mechanistic proposals containing step-wise, diradical intermediates.[59] A diradical depiction of dehydroarenes such as **3037** and **3038** is

[59] a) Miyawaki, K.; Kawano, T.; Ueda, I. Multiple cycloaromatization of novel aromatic enediynes bearing a triggering device on the terminal acetylene carbon. *Tetrahedron Lett.* **1998**, *39*, 6923–6926. b) Ueda, I.; Sakurai, Y.; Kawano, T.; Wada, Y.; Futai, M. An unprecedented arylcarbene formation in thermal reaction of non-conjugated aromatic enetetraynes and DNA strand cleavage. *Tetrahedron Lett.* **1999**, *40*, 319–322. c) Miyawaki, K.; Kawano, T.; Ueda, I. Domino thermal radical cycloaromatization of non-conjugated aromatic hexa- and heptaynes: Synthesis of fluoranthene and benzo[*a*]rubicene skeletons. *Tetrahedron Lett.* **2000**, *41*, 1447–1451. d) Kawano, T.; Inai, H.; Miyawaki, K.; Ueda, I. Synthesis of indenothiophenone derivatives by cycloaromatization of non-conjugated thienyl tetraynes. *Tetrahedron Lett.* **2005**, *46*, 1233–1236. e) Kawano, T.; Inai, H.; Miyawaki, K.; Ueda, I. Effect of water molecules on the cycloaromatization of non-conjugated aromatic tetraynes. *Bull. Chem. Soc. Jpn.* **2006**, *79*, 944–949. f) Kawano, T.; Suehiro, M.; Ueda, I. Synthesis and inclusion properties of 6,6′-Bi(benzo[*b*]fluoren-5-ol) derivative by cycloaromatization. *Chem. Lett.* **2006**, *35*, 58–59. g) Kimura, H.; Torikai, K.; Miyawaki, K.; Ueda, I. Scope of the thermal cyclization of nonconjugated ene–yne–nitrile system: A facile synthesis of cyanofluorenol derivatives. *Chem. Lett.* **2008**, *37*, 662–663. h) Torikai, K.; Otsuka, Y.; Nishimura, M.; Sumida, M.; Kawai,

interesting in that it is simply another resonance form of classical *o*-benzyne, yet there is no mention of benzyne in any of Ueda's reports.

The only other account of an HDDA cyclization in the literature comes more recently from Sterenberg in 2009.[60] The bis-diyne-bridged dinuclear metal complex **3039** was found to cyclize in a [4+2] fashion at room temperature to generate the aryne intermediate **3040** (Scheme 28). The choice of metal was crucial in influencing the reactivity of the two metal-templated diynes. The longer W–P bond lengths maintain the two diynes far enough apart for the complex to be stable, yet the shorter Pt–P bond brings the diynes within what Sterenberg defines as the 'threshold' distance of 3.2 Å to react. They were able to trap the aryne intermediate with furan via a Diels–Alder process or, more unconventionally, with dihydrogen via tetrahydrofuran (THF). It was verified that the hydrogen atoms originated from the THF by performing the reaction in THF-d_8 and observing the dideuterium labeled product.

Scheme 28 | Metal-templated HDDA cyclization of **3039** (adapted from ref 60).

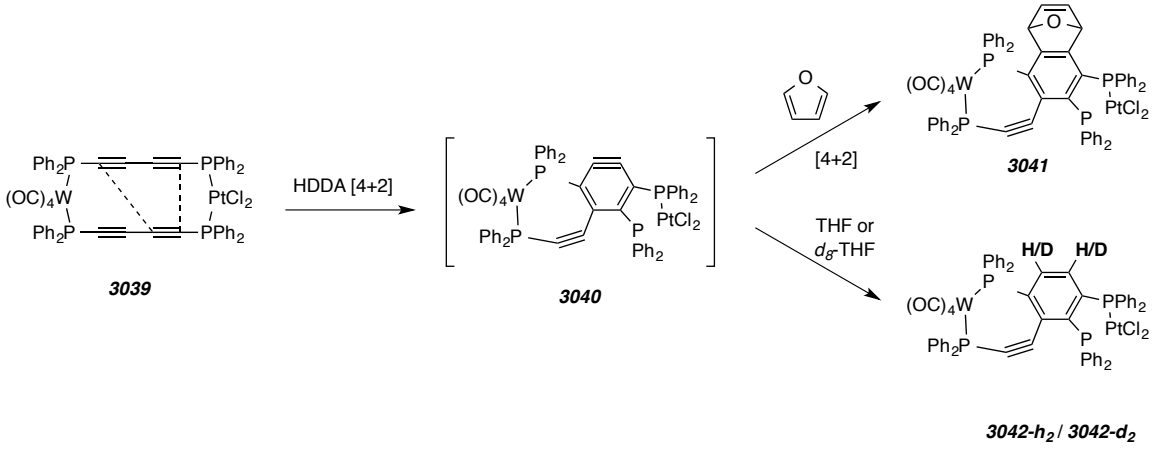

Looking back at these limited examples of HDDA cyclizations in the literature, it is not far-fetched to surmise that perhaps the only way the generality and utility of the process be fully explored would be through a serendipitous observation such as ours. Had

T.; Sekiguchi, K.; Ueda, I. Synthesis and DNA cleaving activity of water-soluble non-conjugated thienyl tetraynes. *Bioorgan. Med. Chem.* **2008**, *16*, 5441–5451.

[60] Tsui, J. A.; Sterenberg, B. T. A Metal-Templated 4 + 2 Cycloaddition Reaction of an Alkyne and a Diyne To Form a 1,2-Aryne. *Organometallics* **2009**, *28*, 4906–4908.

we first scoured the literature for these reports, our conclusions might have been something to the effect of 1) the HDDA is too energetically unfavorable because it requires either temperatures near 600 °C or the coordinating effect of tungsten or platinum metals, or 2) the process contains numerous diradicals within the mechanism and would not be manageable for practical use. These factors coupled with the previously discussed predilection of the scientific community for the classical alkyne-containing benzyne resonance structure makes our serendipitous HDDA findings all the more significant.

3.3. A Brief History of Aryne[61] Chemistry

o-Benzyne, or 1,2-dehydrobenzene, has fascinated the scientific community for over a century.[62] The first reported evidence for an aryne intermediate, in hindsight, was reported in 1902.[63] Not until the 1950s did clever isotope labeling and trapping experiments sufficiently prove the intermediacy of benzyne.[64] With the symmetrical structure and interesting reactivity of benzyne established, aryne chemistry flourished in the following decades, a startlingly rapid growth collected in a 1967 monograph by Hoffman containing hundreds of examples.[65] Figure 9 shows the classical methods for benzyne **(3027**) generation.[66] Aryl halides (cf. **3048**, **3050**) can be treated with strong bases to generate benzyne, or *o*-dihalides can be treated with Mg(0) or *n*-BuLi (cf. **3049**,

---

[61] For the purposes of this Thesis, i) an aryne (or *o*-aryne) will refer to any aromatic ring containing an adjacent pair of sp-hybridized carbon atoms (this includes any of the subfamilies of, for example, benzynes, pyridynes, naphthalynes, or indolynes); ii) *o*-benzyne will refer to the parent 1,2-dehydrobenzene; iii) a benzyne derivative (collectively, "benzynes") refers to any substituted *o*-benzyne analog; this may or may not be fused to an additional, non-aromatic ring.

[62] Wenk, H. H.; Winkler, M.; Sander, W. One century of aryne chemistry. *Angew. Chem. Int. Ed.* **2003**, *42*, 502–528.

[63] Stoermer, R; Kahlert, B. Ueber das 1- und 2-brom-cumaron. *Ber. Dtsch. Chem. Ges.* **1902**, *35*, 1633–1640.

[64] Roberts, J.D.; Simmons, H.E.; Carlsmith, L.A.; Vaughan, C.W. Rearrangement in the reaction of chlorobenzene-1-C^{14} with potassium amide. *J. Am. Chem. Soc.* **1953**, *75*, 3290–3291. b) Huisgen, R.; Rist, H. Über Umlagerungen bei nucleophilen Substitutionen in der aromatischen Reihe und ihre Deutung. *Naturwissenschaften* **1954**, *41*, 358–359. c) Wittig, G.; Pohmer, L. Intermediäre Bildung von Dehydrobenzol (Cyclohexadienin). *Angew. Chem.* **1955**, *67*, 348.

[65] Hoffmann, R.W. Dehydrobenzone and Cycloalkynes. *Organic Chemistry, a Series of Monographs*, 11; Academic Press, 1967.

[66] Tadross, P. M.; Stoltz, B. M. A comprehensive history of arynes in natural product total synthesis. *Chem. Rev.* **2012**, *112*, 3550–3577.

3051, **3052**) to undergo elimination at lower temperatures. An even milder approach utilizes Pb(IV)-mediated oxidation of aminobenzotriazoles such as **3045**. Stiles and

Figure 9 | Classical methods for generation of benzyne (adapted from ref 66).

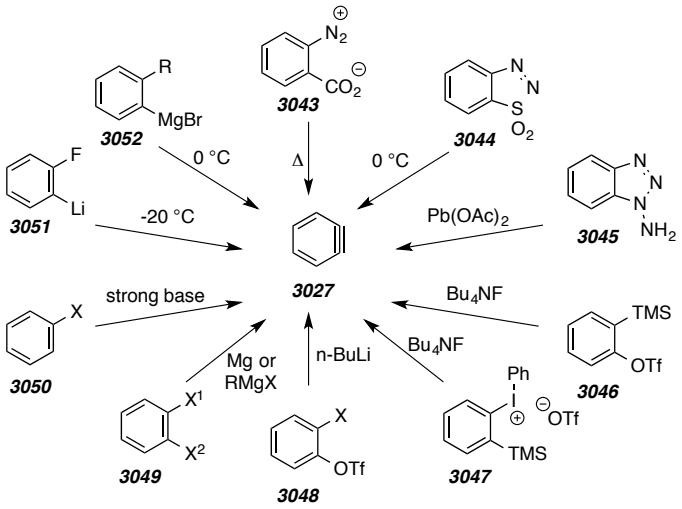

Miller found that the *o*-benzendiazonium carboxylate **3043** decomposes at ca. 50 °C to generate benzyne without the use of strong bases or metal oxidizing agents.[67] Shortly thereafter, Wittig and Hoffman demonstrated that the diazosulfonamide **3044** undergoes a similar decomposition, but at lower temperatures of ca. 10 °C.[68] Today, the most widely used method for benzyne generation is fluoride-induced elimination of 2-(trimethylsilyl)phenyl trifluoromethanesulfonate **3046** developed by Kobayashi three decades ago.[69] Kitamura demonstrated that the iodonium triflate **3047** is also capable of generating benzyne in the presence of a mild fluoride source[70], but the synthesis of Kobayashi's reagent has since been optimized[71] and is now commercially available from Aldrich.

[67] Stiles, M.; Miller, R. G.; Burckhardt, U. Reactions of benzyne intermediates in non-basic media. *J. Am. Chem. Soc.* **1963**, *85*, 1792–1797.
[68] Wittig, G.; Hoffmann, R. W. 1,2,3-Benzothiadiazole 1,1-dioxide. *Org. Syn.* **1967**, *47*, 4–9.
[69] Himeshima, Y.; Sonoda, T.; Kobayashi, H. Fluoride-induced 1, 2-elimination of *o*-trimethylsilylphenyl triflate to benzyne under mild conditions. *Chem. Lett.* **1983**, 1211–1214.
[70] Kitamura, T.; Yamane, M. (Phenyl)[*o*-(trimethylsilyl)phenyl]iodonium triflate. A new and efficient precursor of benzyne. *Chem. Commun.* **1995**, 983–984.
[71] Bronner, S. M.; Garg, N. K. Efficient synthesis of 2-(trimethylsilyl)phenyl trifluoromethanesulfonate: A versatile precursor to *o*-benzyne. *J. Org. Chem.* **2009**, *74*, 8842–8843.

These especially mild conditions for benzyne generation (TBAF, room temperature) along with the availability of **3046** have ignited a renaissance of aryne chemistry. A plethora of new benzyne trapping reactions have been developed[72] and significant progress has been made in utilizing benzynes as a strategy for rapidly assembling complex scaffolds in natural product synthesis.[66,73] However, the generation and use of benzynes still has its pitfalls. As Figure 9 makes clear, all current benzyne generation techniques originate from an aromatic precursor and consist of, essentially, an elimination event followed by addition to the benzyne resulting in a net substitution reaction. The conditions to initiate this elimination have been consistently improved upon and are generally mild. However, the necessity of reagents to induce elimination and the byproducts of that elimination complicate mechanistic investigations as well as limit the list of potential trapping agents. Our rediscovery of benzyne generation via an HDDA process avoids these drawbacks. The HDDA cascade of thermal generation of benzyne from triyne precursors and subsequent benzyne trapping (either intra- or intermolecularly) is completely atom economical and produces the benzyne in a pristine environment in the absence of any complicating byproducts.

3.4. Substrate Scope of Intramolecular Trapping of HDDA Benzynes with Alcohols and Silyl Ethers

After the successful cyclization of our first triyne substrate (cf. Scheme 22), we quickly investigated the potential scope of the HDDA cascade. A collection of an initial set of triynes synthesized is shown in Scheme 27. Each contains the same intramolecular silyl ether that was serendipitously found to efficiently trap the intermediate benzyne. As evident by the variety of heteroatoms and functionalities present in the triynes above, the substrate scope is remarkably broad. The acetate analog **3053** of our initial cyclohexenone substrate (**3014**, Scheme 22) cyclizes with equal efficiency to the corresponding benzenoid **3054**, but requires significantly higher temperatures to do so

---

[72] a) Bhunia, A.; Yetra, S. R.; Biju, A. T. Recent advances in transition-metal-free carbon-carbon and carbon-heteroatom bond-forming reactions using arynes. *Chem. Soc. Rev.* **2012**, *41*, 3140–3152. b) Yoshida, H.; Takaki, K. Aryne insertion reactions into carbon-carbon σ-bonds. *Synlett.* **2012**, *23*, 1725–1732.

[73] Gampe, C. M.; Carreira, E. M. Arynes and cyclohexyne in natural product synthesis. *Angew. Chem. Int. Ed.* **2012**, *51*, 3766–3778.

(110 °C vs. ambient temperature). Nitrogen (**3057**) and oxygen (**3061**) heteroatoms are tolerated in the triyne precursors, allowing for the construction of isobenzofuran (**3058**)

Scheme 27 | Initial substrate scope for triyne HDDA cyclization with silyl ether trapping.

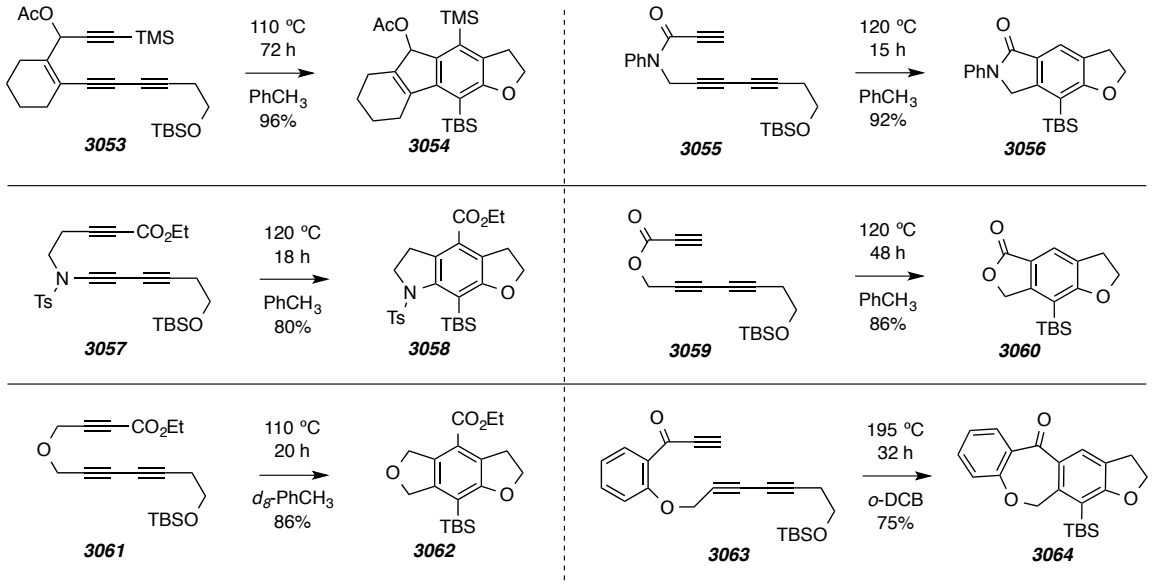

and indoline (**3062**) heterocyclic cores via HDDA cascades. Amides (**3055**) cyclize to isoindolinones (**3056**) at a slightly faster rate than the analogous esters (**3059**) react to form isobenzofuranones (**3060**). Additionally, triynes containing five atoms that tether the reacting alkyne and 1,3-diyne (**3063**) are capable of cyclization to form seven-membered benzenoids (**3064**), albeit at very high temperatures (195 °C).

We quickly found that alcohols are also effective intramolecular trapping agents, with the O–H bond adding across the benzyne carbons analogous to silyl ether trapping. Also, we found symmetrical tetraynes (where each of the two possible modes of HDDA are degenerate) undergo clean HDDA cyclization. Examples of tetrayne HDDA cascades are shown in Scheme 28. Symmetrical ethers (**3071**) and tosylamides (**3067**) readily form their corresponding benzenoids (**3072** and **3068**). Tetraynes with all-carbon linkers (**3065**, **3069**) also cyclize at slightly higher temperatures to form indane cores (**3066**, **3070**). Substrates **3065** and **3069** also show alcohol traps are not limited to the resulting benzofurans, but benzopyrans are also viable. Lee and coworkers have worked with these

tetrayne systems in HDDA processes and shown the pendant alkyne of the benzenoid product can serve as a functional group handle for subsequent manipulation.[74]

Scheme 28 | Initial substrate scope for tetrayne HDDA cyclization with intramolecular trapping.

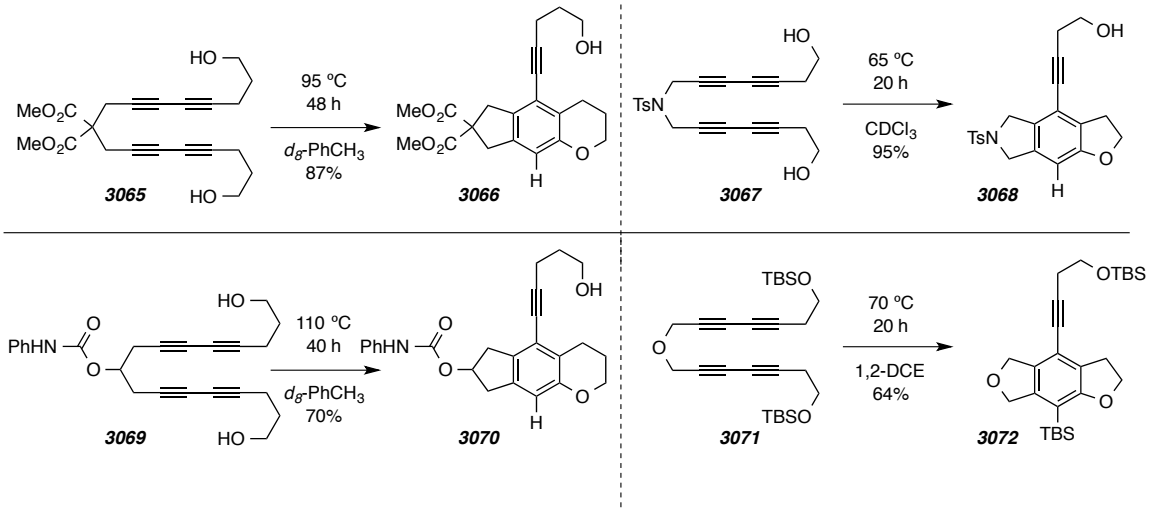

3.5. Tertiary Alcohol Trapping en Route to Salfredin Core

The substantial substrate scope exhibited in the previous section allows for the rapid construction of polycyclic compounds with diverse composition. One particular group of natural products shown in Figure 10, the Salfredins, contains a tricyclic core easily amenable to construction via our HDDA cascade. Isolated in 1994 from the fermentation broth of the fungi RF-3817, the Salfredins show potential as aldose reductase inhibitors, which could have applications in treating diabetes.[75] Having already established the ability of primary alcohols to trap HDDA-generated benzynes, we were interested in the potential of tertiary alcohols as intramolecular traps. If successful, the tricylic core of Salfredin B_{11} could be synthesized in just a few steps.

[74] Wang, K.-P.; Yun, S. Y.; Mamidipalli, P.; Lee, D. Silver-mediated fluorination, trifluoromethylation, and trifluoromethylthiolation of arynes. *Chem. Sci.* **2013**, *4*, 3205–3211.
[75] Matsumoto, K.; Nagashima, K.; Kamigauchi, T.; Kawamura, Y.; Yasuda, Y.; Ishii, K.; Uotani, N.; Sato, T.; Nakai, H.; Terui, Y. Salfredins, new aldose reductase inhibitors produced by Crucibulum sp. RF-3817. I. Fermentation, isolation and structures of salfredins. *J. Antiobiot.* **1995**, *48*, 439–446.

Figure 10 | Selected members of the Salfredin family of natural products.

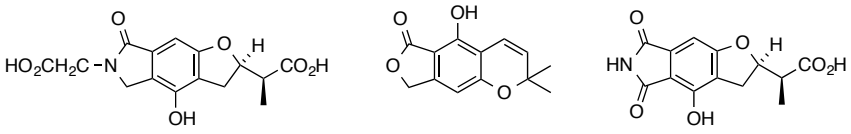

Our synthesis, shown in Scheme 29, hinged on the HDDA cyclization of the triyne **3078** with tertiary alcohol trapping to generate the Salfredin B_{11} core. Starting with the tertiary alcohol **3076**, a Cadiot-Chodkiewicz coupling with bromopropargyl alcohol resulted in the diyne **3077**. DCC coupling with 3-(trimethylsilyl)propynoic acid gave the triyne ester **3078**. To our delight, the triyne cleanly underwent HDDA cyclization with trapping by the tertiary alcohol to give benzenoid **3079**. The final element of unsaturation of the Salfredin core was installed via a two-step benzylic bromination and DBU-induced elimination to arrive at the **3080**. Conversion of the aryl trimethylsilyl group of **3080** to the free phenol would result in the Salfredin B_{11} natural product, but all attempts at this oxidation were unsuccessful. Nonetheless, the synthesis of the tricyclic core of the natural product in five steps and a 14% overall yield displays the exciting potential for application of the HDDA cascade in total synthesis.

Scheme 29 | Five-step synthesis of the tricyclic core of Salfredin B_{11}.

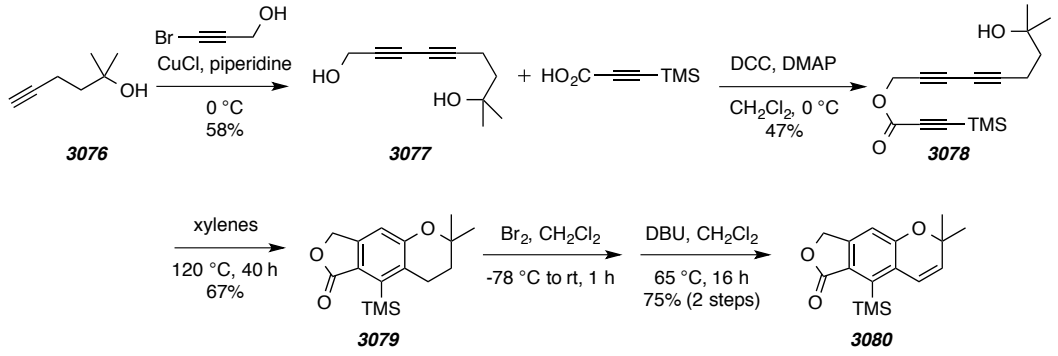

3.6. Additional Silyl Ether Traps and Intramolecular Dihydrogen Transfer

Our initial silyl ether trapping was limited to the transfer of a TBS group, so we set out to establish an expanded scope of intramolecular silyl trapping agents. In order to expedite the process of examining various traps, we developed a gram-scale synthesis of

an HDDA precursor amenable to easy incorporation of such traps (Scheme 30). Starting with commercially available bromobenzaldehyde **3081**, a Sonogashira coupling with trimethylsilylacetylene gave **3082**, which was desilylated with potassium carbonate in methanol to give the terminal alkyne **3083**. Preparation of the lithium acetylide of trimethylsilylacetylene with *n*-BuLi and addition to the aldehyde gave the key diyne precursor **3084**. With the terminal alkyne available for Cadiot-Chodkiewicz coupling, **3084** is a valuable substrate to have in hand for quick synthesis of desired triyne HDDA

Scheme 30 | Synthesis of HDDA-precursor building block **3084**.

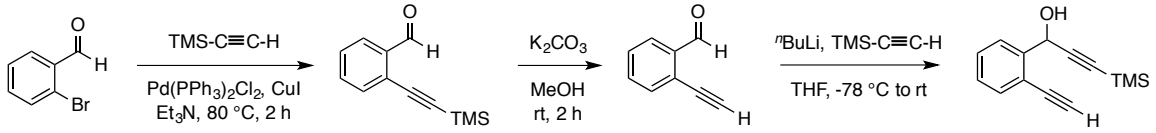

precursors. The entire sequence can be performed on gram-scale with good yields of 70-75% easily reproducible.

With **3084** as a convenient point of divergence, we quickly generated a set of triyne precursors with either an alcohol or various silyl ethers poised for intramolecular trapping. The brominated butynol derivatives **3085-3089** were synthesized, which included the parent alcohol as well as the TMS, TBS, triethoxy- and tri(t*ert*-butoxy)-silyl ether compounds. Cadiot-Chodkiewicz coupling followed by MnO_2 oxidation gave the triynones **3090a–e**. When heated at 85 °C for 20 h, each triyne cyclized cleanly to the fluorenone products **3091a–e**. Our group would go on to show via extensive cross-over experiments and computational results that the silyl ether intramolecular trapping process is unimolecular in nature.[76] The alcohol of **3090-a** trapped as expected in good yield, and was a useful standard to verify the presence of any desilylated products in the reactions of **3090b-e**. There was evidence of minor amounts of desilylated products in the cyclization of the most labile trimethylsilyl containing **3090-b**, as well as in the extremely water-

[76] Hoye, T. R.; Baire, B.; Wang, T. Tactics for probing aryne reactivity: mechanistic studies of silicon–oxygen bond cleavage during the trapping of (HDDA-generated) benzynes by silyl ethers. *Chem. Sci.* **2013**, *5*, 545.

sensitive silylethers **3090-d** and **3090-e**. When the compound is not at high risk of desilylation, as in the TBS silyl ether **3090-c**, very high yields are attainable. The trapping of the trisiloxy compound in **3090-d** to generate **3091-d** opens up the potential for further manipulation of the fluorenone via Fleming-Tamao oxidation[77] of the resulting arylsilane. Also of note, each of the arylsilanes **3091-b** and **3091-c** undergoes protodesilylation (at the silicon *meta* to the carbonyl) when subjected to an acidic environment (TFA, AcOH) to yield **3091-a**, with the trimethylsilyl *ortho* to the carbonyl remaining intact.

Scheme 31 | Silyl ether trapping to generate fluorenones **3090a–d**.

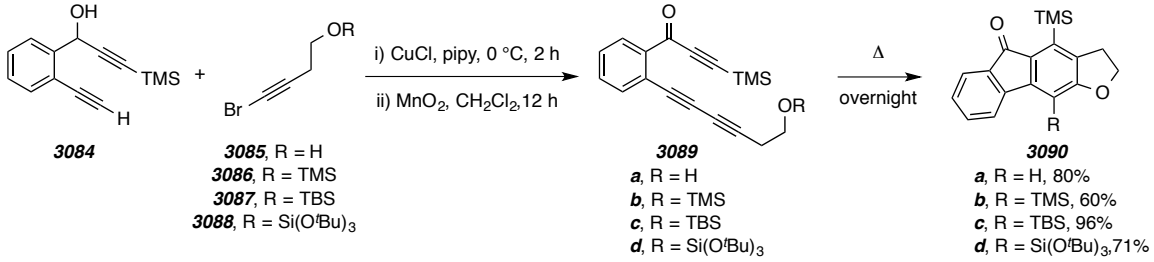

3084

3085, R = H
3086, R = TMS
3087, R = TBS
3088, R = Si(O^{t}Bu)$_3$

3089
a, R = H
b, R = TMS
c, R = TBS
d, R = Si(O^{t}Bu)$_3$

3090
a, R = H, 80%
b, R = TMS, 60%
c, R = TBS, 96%
d, R = Si(O^{t}Bu)$_3$,71%

A triisopropylsilyl (TIPS) variant is not present in **3090a–d** because of an usual byproduct observed with that silyl ether in another study. In the course of examining the viability of an ester triyne cyclization towards the Salfredin B_{11} core, the model substrate **3091** was prepared (Scheme 32). After heating in toluene for two days, the expected HDDA product was isolated, in 68% yield, along with a small amount of an unknown byproduct. It was immediately apparent that a dihydrogen addition across the benzyne was occurring, based on the presence of aromatic (7.3–7.5 ppm) ^{1}H NMR resonances of the compound and their diagnostic *ortho*-coupling. It then became clear that an additional element of unsaturation was incorporated into this product, as evident by the olefin (5.3–5.8 ppm) ^{1}H NMR resonances. High-resolution mass spectrometry verified that the compound was a constitutional isomer of the starting triyne, and extensive ^{1}H and ^{13}C NMR spectroscopic analysis lead us to characterize the product as **3093**. It appears the

[77] Tamao, K.; Ishida, N.; Tanaka, T.; Kumada, M. Silafunctional compounds in organic synthesis. Part 20. Hydrogen peroxide oxidation of the silicon-carbon bond in organoalkoxysilanes. *Organometallics* **1983**, *2*, 1694–1696.

benzyne formed after HDDA reaction (**3094** in Scheme 32) is either being trapped by the silyl ether as expected or, competitively, abstracting two hydrogens from adjacent carbons of an isopropyl group from the TIPS ether in a net redox process.

Scheme 32 | Discovery of intramolecular dihydrogen transfer via the TIPS ether.

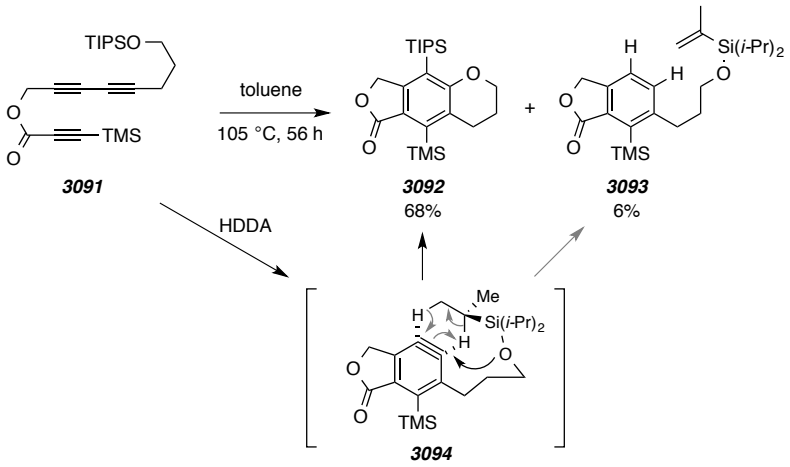

To probe the practicality of this transformation, two triyne substrates were synthesized in which the O–Si atom transfer pathway was prohibited and only intramolecular dihydrogen transfer viable. Both the ester- and benzene-tethered triynes **3095** and **3097** contain propargyl TIPS ethers in which the oxygen is unable to trap the benzyne (Scheme 33). Each was heated at high temperature in either 1,2-dichlorobenzene (*o*-DCB) or dioxane. Now, in both cases, the intramolecular hydrogen transfer products **3096** and **3098** are the major product isolated[78], in moderate yield. The ability of the TIPS group to facilitate the hydrogen transfer led us to predict that a triethylsilyl (TES)

Scheme 33 | Intramolecular dihydrogen transfer via the TIPS ether.

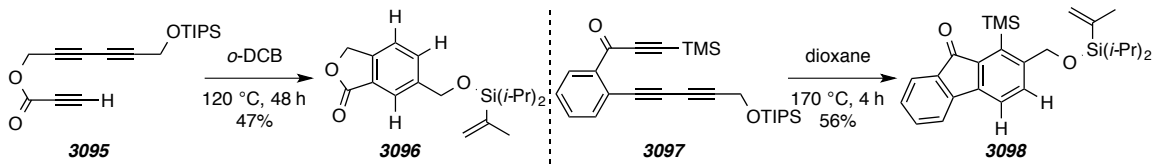

[78] The product mixture of the reaction of **3095** also contained a minor (~20%) amount of the *o*-DCB-trapped product, as evidenced by GC-MS and crude ^{1}H-NMR.

group should also be effective. To this end, the TES ether triyne **3099** was synthesized but surprisingly we saw no intramolecular hydrogen transfer product when run in identical conditions to the TIPS substrate **3097** (Scheme 34). When the TES ether triyne was heated at high temperature in *o*-DCB, the only isolable product was that in which a solvent *o*-DCB molecule participates in an intermolecular [4+2] Diels–Alder reaction with the benzyne. This [4+2] intermolecular addition product was also present with the TIPS substrate **3095** in minor amounts, but generally o-DCB serves as a helpful high-boiling solvent in HDDA reactions requiring high temperatures because of its disinclination for intermolecular benzyne trapping. Typically, when the HDDA reaction is run in the absence of an effective trapping agent, we observe the formation of intractable, dark-colored mixtures, which we speculate to be oligomeric substances. When the TES ether **3099** is heated in a completely nonparticipating solvent such as dioxane (Scheme 34), we observe exactly that: a dark, intractable product mixture with

Scheme 34 | Failed intramolecular dihydrogen transfer with TES ether.

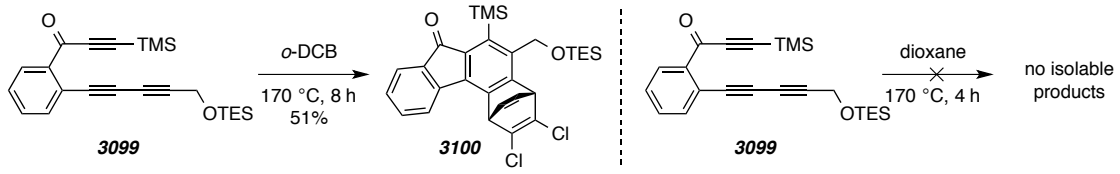

no evidence of any intramolecular dihydrogen transfer. This drastic discrepancy between the TES and TIPS ethers ability to undergo the net redox process is puzzling. We later found that intermolecular dihydrogen transfer processes like this one are concerted in nature[51b], requiring the six reacting atoms involved in bond-breaking and –making events be coplanar. More specifically, a concerted transition state for this particular intramolecular dihydrogen transfer from a TIPS group was also found.[76] We propose the significantly larger steric bulk of three isopropyl groups (vs. three ethyl groups) is enough to force a high enough population of the reactive conformation where one isopropyl is positioned within close enough proximity, with coplanar orientation, to the benzyne for productive reaction to occur.

3.7. Intercepting Intramolecular Oxygen Trapping

In the course of examining the potential for other intramolecular traps, the allyl ether **3106** was synthesized (Scheme 35). Ether formation from 4-pentyn-1-ol and allyl bromide gave the diyne ether **3103**, which was brominated to generate the coupling partner **3104**. Standard Cadiot-Chodkiewicz coupling with our diyne building block **3084** gave the alcohol **3105**, which after MnO_2 mediated oxidation gave the HDDA precursor

Scheme 35 | Synthesis and proposed cyclization of ether **3106**.

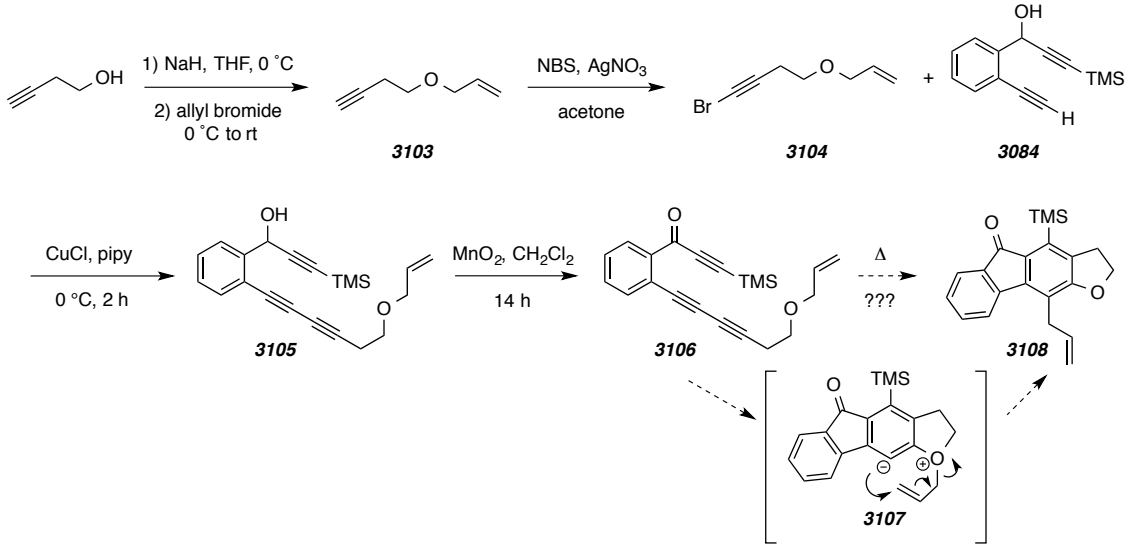

keto-triyne **3106**. We hypothesized that after heating and benzyne formation, the ether oxygen would trap to generate the zwitterion **3107** in a similar fashion to that of the silyl ether intramolecular traps we previously observed. The zwitterion might be able to quench itself via allyl-group transfer (arrows shown in Scheme 35) to generate compound **3108**. This allyl transfer would show that the mechanistic analysis seen with the unimolecular silyl transfer might be applicable for many more functional group transfers. Also, installation of the allyl group on the benzenoid serves as another functional handle for potential further manipulations.

However, when we heated triyne **3106** to initiate HDDA cascade, we did not observe or isolate any of the allyl transfer product **3108**. Instead, the major isolated

product was the benzenoid **3109**, the result of formal addition of the ether oxygen and hydrogen across the benzyne with loss of the allyl group. This led us to question the origin of the hydrogen being added to the benzyne as well as the ultimate fate of the lost allyl group. The reaction was next run in deuterated chloroform that had been washed extensively with D_2O to remove any residual water in the chloroform. Heating under

Scheme 36 | Cyclization of ether **3106** and deuterium incorporation study.

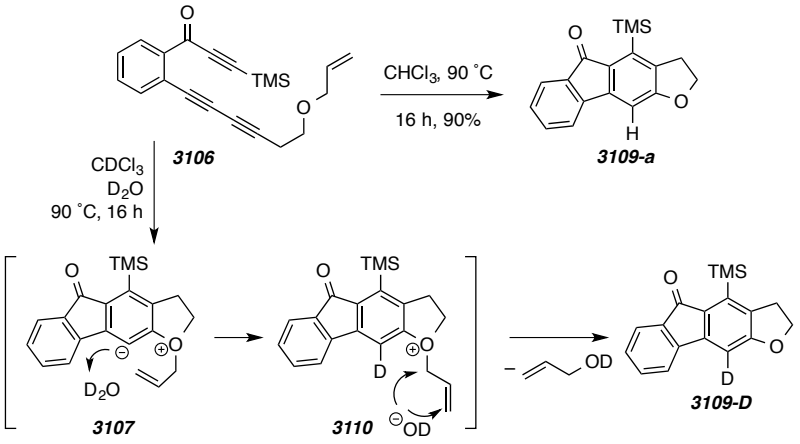

these conditions resulted in product **3109-D** with deuterium incorporation (64%). It appears that residual water was responsible for the source of hydrogen to trap the aryl anion of the transient zwitterion intermediate **3107**. In this bimolecular trapping route, it is reasonable to view the resulting hydroxide anion as responsible for initiating the loss of the allyl group in either an S_N2 or S_N2' mechanism (cf. **3110** in Scheme 36) to give the observed product **3109-D**.

This bifurcation between the acting mechanisms of unimolecular, concerted, silyl ether trapping vs. bimolecular benzyne trapping with ethers is intriguing. It led us to question the mechanism of free alcohol trapping that we had previously seen. If this process is also occurring bimolecularly, then perhaps the transient zwitterion intermediate could be intercepted by an electrophile other than hydrogen from residual water. To probe this possibility, we reexamined cyclization of our triyne alcohol **3090-a**. When heated in ethyl acetate overnight at 95 °C, the triyne cleanly cyclized to give two products. The major product, **3091-a**, is the previously isolated benzenoid resulting from alcohol

addition across the benzyne. The minor product (2:1 ratio after product isolation) was identified as benzenoid **3111**, in which we have intercepted the zwitterionic intermediate through trapping with the acetate carbonyl of ethyl acetate, resulting in acyl transfer to the benzyne. The same product distribution was isolated in a reaction ran in ethyl propionate, with the corresponding propionated benzenoid **3112** as the minor product.

Scheme 37 | Interrupted intramolecular oxygen trapping studies.

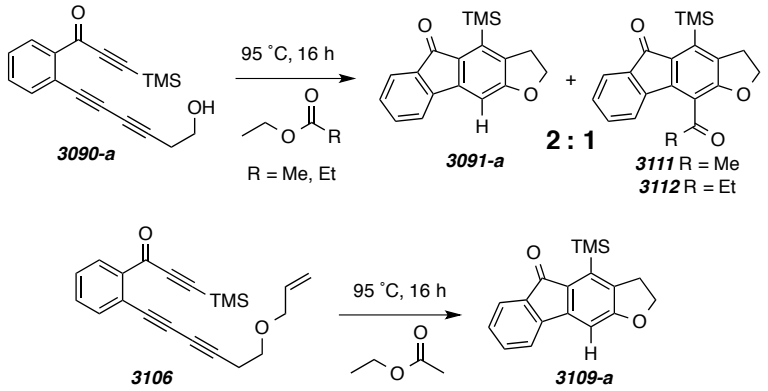

Having successfully interrupted the intramolecular alcohol addition across the benzyne with an ester nucleophile, we surmised that perhaps the allyl ether **3106** would produce the acyl-incorporated product **3111** as the sole product. However, when heated in identical conditions as the experiment that produced acyl incorporation, the only compound isolated was the **3109-a** product of alcohol addition. It is possible that residual water intercepted the zwitterion to result in **3019-a**. Yet the same source of (dried) ethyl acetate was used for both experiments, so one would expect to be able to detect at least a trace of the acyl transfer product in the allyl ether experiment, which was not the case. Alternatively, the zwitterion from allyl ether cyclization could be abstracting a proton from the α-carbon of the ester, making the enolate of ethyl acetate.

In order to determine the ultimate fate of the lost allyl group in the HDDA cyclizations of allyl ether **3106** to benzenoid **3109-a**, the triyne was heated in the presence of phenol. The alcohol product **3109-a** was isolated as anticipated. Gratifyingly, in this experiment we were able to observe the presence of a byproduct. Judging by ^{1}H NMR and GC-MS (total mass and fragmentation pattern), the benzoxyallyl ether **3114**

was being formed. As hypothesized, the phenol is able to donate its phenolic hydrogen to the benzyne and the resulting phenoxide capable of displacing the allyl group to quench the oxonium **3113** and produce the detected ally ether product. This is strong evidence for an intermolecularly initiated loss of the allyl group in the transformations of Schemes 36-38. The factors that determine the discrepancy of the phenyl anion **3107** to abstract a proton (Scheme 38) or initiate nucleophilic attack (Scheme 37) remain to be determined.

Scheme 38 | Reaction of allyl ether **3106** with phenol trapping.

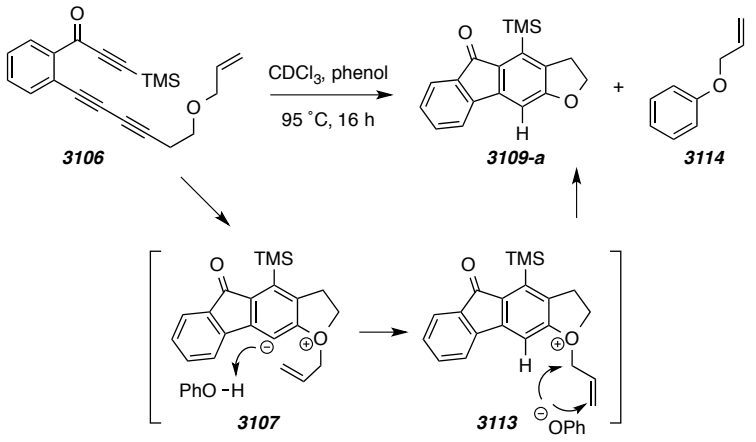

Overall, the studies of this Chapter highlight both the generality and scope of the HDDA reaction. We have already found a wide array of triynes and tetraynes capable of participating in the HDDA cycloisomerization to generate a diverse set of molecular scaffolds. The purely thermal, reagent free conditions of the HDDA reaction make the transformation an especially valuable process. The [4+2] ring-forming reaction between alkynes is a powerful extension of the venerable Diels–Alder reaction, and the generation of a byproduct-free benzyne allows for myriad different trapping possibilities. With over a century of benzyne history already documented, the applications of this new method are boundless.

Chapter 4. Intermolecular Traps for HDDA-Generated Benzynes

4.1. Intermolecular Trapping of HDDA-Generated Benzynes

The HDDA cycloisomerization of triynes to benzynes is capable of forming a variety of useful and interesting heterocycles. Chapter 3 highlighted the diversity of products capable of being synthesized through variation of the atoms and functionalities that connect the reacting diyne and alkyne (diynophile). With the intramolecular traps covered in Chapter 3 (alcohols, silyl ethers, ethers), the resulting benzenoid is either entirely or almost entirely functionalized, resulting in a class of compounds particularly difficult to synthesize by conventional means. The ability to further modify the groups that decorate the resulting benzenoid core is a particularly valuable extension of this HDDA chemistry. This is most easily achievable through intermolecular trapping of the HDDA-generated benzynes. When an intramolecular trap is not built into the triyne substrate, the benzyne is free to react with an external reagent in the reaction mixture.

We first encountered this intermolecular benzyne trapping with the acetate **4001**. When we prepared **4001**, we initially anticipated an intramolecular acyl transfer to occur (cf. Scheme 37, Sec. 3.7). Yet the acetate functional group was unable to trap, and the starting material simply decomposed when heated in chloroform at high enough temperature to effect HDDA cyclization. Thus, the acetate triyne was a useful substrate to begin investigating intermolecular trapping. When **4001** was heated in benzene a new fluorenone **4004** was isolated in high yield (Scheme 39). A benzene solvent molecule had participated in a [4+2] Diels–Alder reaction with the resulting benzyne, our first example of an intermolecularly trapped HDDA cascade. While this process has already been documented[67], aromatics have rarely been trapped by benzyne in such high yields due to their low reactivity. This result also shows that this intermolecular trapping by solvent is considerably slower compared to many of the intramolecular traps shown in Chapter 3; many of the high-yielding intramolecular trapping experiments were conducted in aromatic solvents with no evidence of a byproduct.

Scheme 39 | Intermolecular trapping of acetate **4001**.

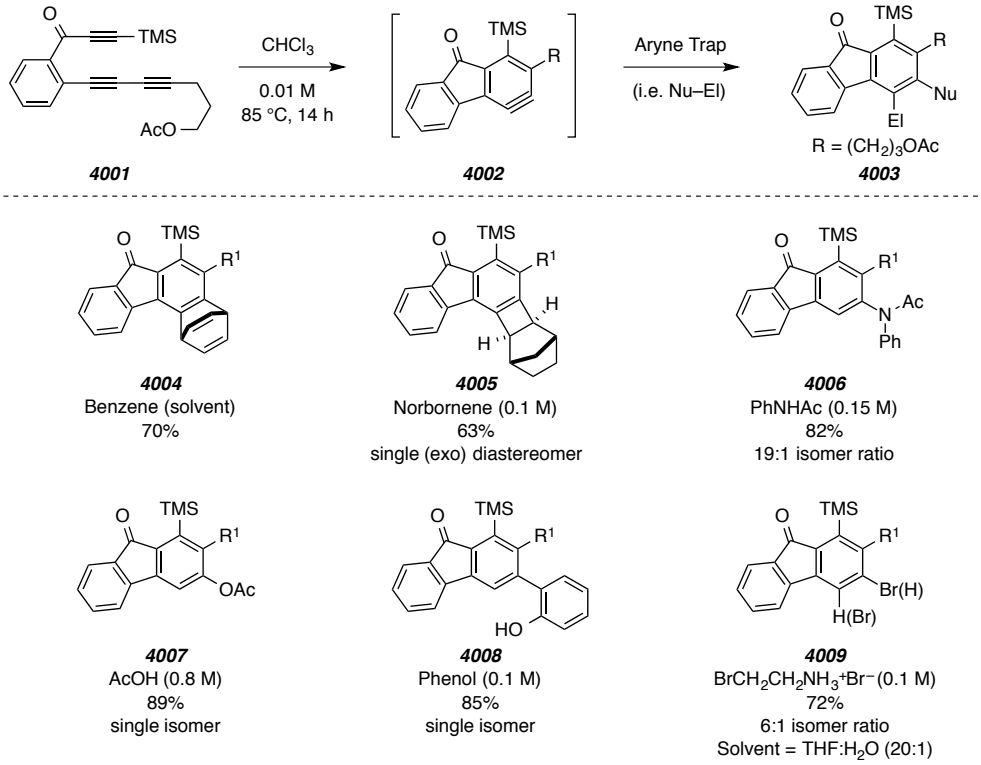

The triyne acetate **4001** presented us with the opportunity to examine the viability of other groups to act as intermolecular traps. These results are shown in Scheme 39. Norbornene traps the benzyne **4002** in a [2+2] fashion to produce **4005** in a higher yield than previously attained via conventional benzyne trapping.[65] *N*-phenylacetamide traps efficiently with the nitrogen atom to give **4006**, displaying a convenient synthesis of aniline derivatives. Both acetic acid and phenol cleanly trap the benzyne, giving **4007** and **4008**, in similar processes that can be viewed as hydroxy proton transfer in a concerted fashion with nucleophilic attack at the benzyne. This new mode of phenol addition to benzyne is unique and complementary to the previously observed process with conventionally generated (Kobayashi[69] method) benzynes.[79,80] Lastly, the net addition of

[79] Liu, Z.; Larock, R. C. Facile O-Arylation of Phenols and Carboxylic Acids. *Org. Lett.* **2004**, *6*, 99–102.
[80] Cheong, P. H.-Y.; Paton, R. S.; Bronner, S. M.; Im, G.-Y. J.; Garg, N. K.; Houk, K. N. Indolyne and aryne distortions and nucleophilic regioselectivites. *J. Am. Chem. Soc.* **2010**, *132*, 1267–1269.

hydrogen bromide across the benzyne to give **4009** is achieved through the use of $Br(CH_2)_2NH_2$•HBr in a THF/H_2O (20:1) solvent mixture.[81]

The regioselectivities of the various intermolecular traps in Scheme 39 vary slightly, but all favor the products shown with nucleophilic addition occurring *para* to the benzyne carbonyl. Suzuki and co-workers examined the origin of this benzyne regioselectivity in 2003, when they found that the ring strain of an additional carbocycle bound to the benzyne directs addition.[82] The bridgehead carbon bound to the strained carbocycle is known to rehybridize to use orbitals of a higher p character.[83] With the p character of the orbitals tied up balancing the ring strain, the remaining bond to the proximal benzyne carbon has higher s character. The higher electronegativity in this s orbital renders the distal sp-hybridized benzyne carbon the most nucleophilic, and the preferred site for intermolecular addition. Computational analysis verified the higher values of natural atomic charge at these distal benzyne carbons.

More recently, individual reports by Cramer/Buszek[84] and Garg/Houk[85] detail a protocol for computing the geometry of an aryne intermediate to deduce the regioselective preference for addition to the aryne. Unsymmetrical arynes (of which all of our HDDA-generated benzynes are) have, by definition, a distorted aryne and two non-equivalent sp-hybridized carbons. By computing the geometry of an unsymmetrical aryne, the difference in bond angles at these two carbons can be determined. Garg/Houk and Cramer/Buszek found that the relative difference between the more acute and more

---

[81] Zhang, H.; Hu, Q.; Li, L.; Hu, Y.; Zhou, P.; Zhang, X.; Xie, H.; Yin, F.; Hu, Y.; Wang, S. Convenient one-step construction of yne-functionalized aryl halides through domino cyclization from tetraynes. *Chem. Commun.* **2014**, *50*, 3335.

[82] Hamura, T.; Ibusuki, Y.; Sato, K.; Matsumoto, T.; Osamura, Y.; Suzuki, K. Strain-Induced Regioselectivities in Reactions of Benzyne Possessing a Fused Four-Membered Ring. *Org. Lett.* **2003**, *5*, 3551–3554.

[83] a) Finnegan, R. A. Organometallic Chemistry. IX. The Metalation of Benzocyclobutene with Sodium and Potassium Alkyls1, 2. *J. Org. Chem.* **1965**, *30*, 1333–1335. b) Streitwieser, A., Jr; Ziegler, G. R.; Mowery, P. C.; Lewis, A.; Lawler, R. G. Some generalizations concerning the reactivity of aryl positions adjacent to fused strained rings. *J. Am. Chem. Soc.* **1968**, *90*, 1357–1358.

[84] Garr, A. N.; Luo, D.; Brown, N.; Cramer, C. J.; Buszek, K. R.; VanderVelde, D. Experimental and Theoretical Investigations into the Unusual Regioselectivity of 4,5-, 5,6-, and 6,7-Indole Aryne Cycloadditions. *Org. Lett.* **2010**, *12*, 96–99.

[85] Im, G.-Y. J.; Bronner, S. M.; Goetz, A. E.; Paton, R. S.; Cheong, P. H.-Y.; Houk, K. N.; Garg, N. K. Indolyne Experimental and Computational Studies: Synthetic Applications and Origins of Selectivities of Nucleophilic Additions. *J. Am. Chem. Soc.* **2010**, *132*, 17933–17944.

obtuse angles at the aryne carbons dictated the preferred site of nucleophilic attack. Using similar rationale that Suzuki used to reach his conclusions, the more obtuse angle contains more p-character and is thus more electrophilic (shown in **4002-I** and **3017-i** in Scheme 40). This computational analysis holds for our HDDA-generated benzynes as

Scheme 40 | Computed geometry of intermediate benzyne **4002** and **3017**.

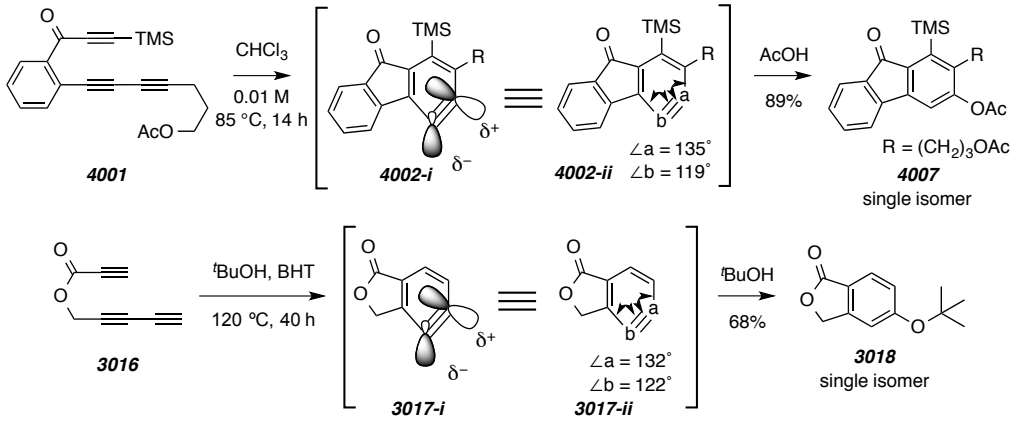

well. Scheme 40 shows the computed (DFT [M06-2X/6-31+G(d,p)]) bond angles for fluorenyne **4002** and phthalidyne **3017**. The bond angles of **4002-ii** are computed to be 135° and 119°. The more obtuse bond angle at carbon a is the preferred site of nucleophilic intermolecular trapping in all the examples in Scheme 39, and is the exclusive product for acetic acid trapping to produce **4007**, shown again in Scheme 40. For the ester triyne **3016**, which we first used to compute the thermodynamics of the HDDA cascade (cf. Scheme 23, Sec. 3.1), the bond angles are computed to be 132° and 122°, with the more obtuse angle resulting in the site of nucleophilic trapping of *tert*-butanol to give exclusively the phthalide **3018**.

This section illustrates the potential that intermolecular trapping of HDDA-generated benzynes has in greatly expanding the scope of available products. The reagent-free conditions of HDDA-generated benzynes allow for the generation of a benzyne in a pristine environment, where previously incompatible reagents can be introduced as traps in new and exciting ways. Aside from synthesizing interesting and useful products, the thermal generation of benzynes in this unique environment also permits the mechanistic details of these benzyne reactions to be observed and

investigated like never before. The rest of Chapter 4 introduces some of the new intermolecular benzyne traps and mechanistic insights we have uncovered via the HDDA cascade.

4.2. Alkane Desaturation by Concerted Double Hydrogen Atom Transfer to Benzyne[51b]

In presenting the precedence for HDDA alkyne-plus-diyne reactions in Section 3.2, Sterenberg's 2009 report[60] of a bis-diyne-bridged dinuclear metal complex [4+2] cyclization to an aryne intermediate was discussed. One observation made by Sterenberg and co-workers from that report was particularly interesting to us. Their [4+2] cyclization resulted in the addition of two hydrogen atoms when run in THF. A complimentary experiment in THF-d_8 produced the di-deuterated product. While this did verify that the hydrogens/deuteriums originated from the THF solvent, the authors did not address the question of whether each hydrogen/deuterium originated from the same THF molecule or not. After digesting this information, we were curious as to two ideas: 1) would our HDDA-generated benzynes add two hydrogen atoms across the benzyne in a similar fashion, and 2) what was the origin of the hydrogen atoms.

Scheme 41 | Crossover experiment of THF 2H or 2D transfer to benzyne **4002**.

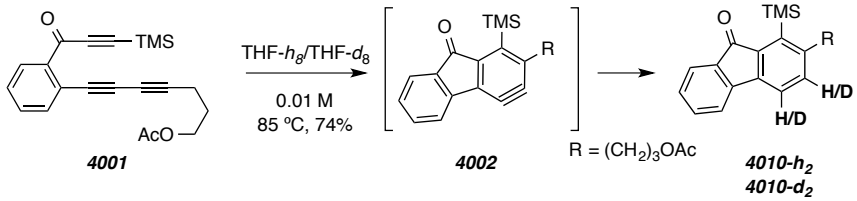

solvent	(4010-h_2 : 4010-d_2)
THF-h_8	100 : 0
THF-d_8	0 : 100
THF-h_8/THF-d_8 (1:1)	6 : 1
THF-h_8/THF-d_8 (1:6)	1 : 1

No Crossover (***4010-hd***)
Product Observed!

Our results are shown in Scheme 41. We heated the same triyne **4001** used for our other intermolecular trapping experiments in THF and observed surprisingly clean dihydrogen addition across the benzyne to give **4010-h$_2$**. Consistent with Sterenberg's work, when we switched to THF-d_8 we isolated the product **4010-d$_2$** with complete

deuterium incorporation. We then performed the necessary crossover experiment to deduce the origin of the atoms transferred. In a 1:1 mixture of THF-h_8 and THF-d_8 we isolated a mixture of **4010-h$_2$** and **4010-d$_2$** in a 6:1 ratio, with no evidence for any of the mono-H/mono-D analog (**4010-hd**). The 6:1 product ratio shows a significant primary H/D kinetic isotope effect for this transformation. The complimentary experiment in a 1:6 ratio of THF-h_8:THF-d_8 gave a nearly 1:1 product mixture. The complete lack of any detectable monodeuterated product provides clear, strong support that the hydrogens are transferring from the same THF molecule, in what could be rationalized by a concerted transfer via the transition structure **4011** (Figure 11). This sort of 6-atom transition state for concerted hydrogen transfer is unique, but not unprecedented. The classical diimide reduction of alkenes is typically viewed in a similar fashion[86,87], as well as the class of intramolecular dihydrogen transfers known as dyotropic reactions.[88,89] In 2013 Bertozzi reported cases of hydrogen transfer from THF to a strained cycloalkyne.[90] The strained cycloalkyne was generated via irradiation of a cyclopropenone precursor. In the absence of a suitable trap with THF solvent, they "unexpectedly" observed the alkene product. Analogous to Sterenberg's observations, when run in THF-d_8, the dideuterium alkene was produced. In order to verify that our dihydrogen transfer reaction was not being effected by any irradiation via light, we repeated our initial observations by heating an

Figure 11 | Proposed transition state structure **4011** and known analogous examples.

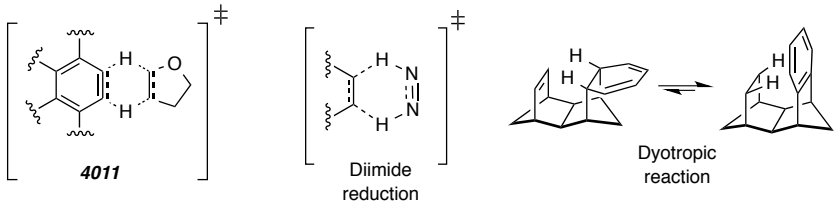

[86] Hunig, S.; Muller, H.; Thier, W. Reduktionen mit diimide. *Tetrahedron Lett.* **1961**, *2*, 353–357.
[87] Corey, E. J.; Pasto, D. J.; Mock, W. L. Chemistry of diimide. II. Stereochemistry of hydrogen transfer to carbon-carbon multiple bonds. *J. Am. Chem. Soc.* **1961**, *83*, 2957–2958.
[88] Fernández, I.; Cossío, F. P.; Sierra, M. A. Dyotropic Reactions: Mechanisms and Synthetic Applications. *Chem. Rev. (Washington, DC, U.S.)* **2013**, *109*, 6687–6711.
[89] Fernández, I.; Sierra, M. A.; Cossío, F. P. In-Plane Aromaticity in Double Group Transfer Reactions. *J. Org. Chem.* **2007**, *72*, 1488–1491.
[90] de Almeida, G.; Townsend, L. C.; Bertozzi, C. R. Synthesis and reactivity of dibenzoselenacycloheptynes. *Org. Lett.* **2013**, *15*, 3038–3041.

HDDA substrate in the dark in THF. The same dihydrogen product was observed, with no noticeable anomalies compared to experiments run under lab light.

Next we set out to examine other potential hydrogen donors. In the transition structure depicted as **4011** in Figure 10, the hydrogens from the 2 and 3 positions of THF are transferred to the benzyne. In the initial THF experiments we were unable to unambiguously identify the byproducts in the ^{1}H NMR spectra. Another possibility (not drawn) would be hydrogen transfer from the 3 and 4 positions of THF. The THF ether oxygen weakens the neighboring C–H bonds, which might be enough to influence their abstraction by benzyne. With a 74% yield of the dihydrogen transfer product using THF, we assumed 1,4-dioxane would offer a similar result. Additionally, the symmetry of 1,4-dioxane would produce only one byproduct for potential detection. However, when we heated the same triyne **4001** in 1,4-dioxane none of the fluorenone **4010** was produced. This suggested the ether oxygen of THF was not crucial in allowing for dihydrogen transfer. We proceeded to test a series of cyclic hydrocarbons and their ability to donate dihydrogen to the benzyne. These results are shown in Scheme 42. These experiments were run on substrate **4012**, where a methyl group is appended to the diyne. To our surprise, the first hydrocarbon we tried, cyclooctane, was able to undergo dihydrogen transfer to benzyne **4013** to produce **4014** in 97% yield. The rest of the hydrocarbons screened are shown in the table to the right of Scheme 42. Cycloheptane, cylcopentane, and even norbornane all readily participate in the reaction, in only slightly lower yield. Cyclohexane and the straight chain hydrocarbon *n*-heptane, on the other hand, are significantly poorer dihydrogen donors to the benzyne. In general, when an HDDA cyclization is performed in the absence of a suitable trapping agent, we observe the formation of intractable, dark-colored mixtures presumed to be oligomeric material. Without an efficient trap, we speculate the benzyne engages another molecule of starting triyne, most likely at the diyne moiety, to initiate oligomer formation. For this reason, we view the isolated yield of fluorenone **4014** as a meaningful reflection of the dihydrogen transfer rate from each solvent. When the concentration of triyne **4012** was decreased tenfold in the presence of cyclohexane and *n*-heptane, the isolated yields increased from

20% to 53% and 30% to 73%, respectively, consistent with our assumption that decomposition results from benzyne-triyne oligomerization.

Scheme 42 | Summary of hydrocarbons screened in dihydrogen transfer to benzyne **4013**.

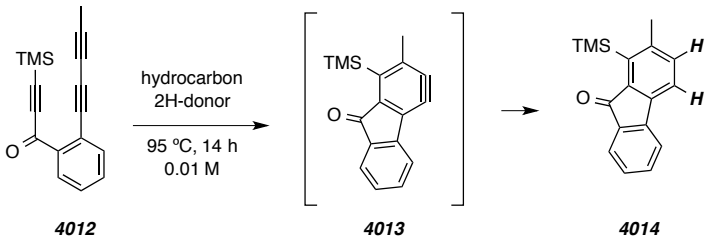

4012 ***4013*** ***4014***

2H-donor	% yield	k_{rel}	$^{a}G^{‡}$
cyclooctane	97%	2.6	17.6
cycloheptane	94%	2.3	17.7
cyclopentane	84%	1.0	18.7
cyclohexane	20%	0.01	24.1
norbornane	66%	0.60	18.5
THF	60%	0.4	19.2
1,4-dioxane	0%	—	27.1
n-heptane	30%	–	–

a M06-2X/6-311+G(d,p) kcal•mol^{-1}

The results of these various cyclic hydrocarbons dihydrogen donation to the benzyne presented us with the opportunity to observe the presumed cycloalkene byproducts. For this analysis, we turned to no-deuterium proton NMR (No-D NMR) spectroscopy. Following the reactions via this method, we were able to observe norbornene, cyclopentene, cycloheptene, and cyclooctene byproducts in a 1:1 ratio to the reduced benzyne product. Additionally, with this strategy we could compete two different dihydrogen donors easily, and extract a relative reducing power based on the ratios of the cycloalkene products. Those k_{rel} values are shown in the table in Scheme 42. These relative rates correlate exceptionally well with computational analysis. DFT calculations for the free energy of activation ($\Delta G^{‡}$) of the various hydrocarbons dihydrogen transfer to *o*-benzyne are shown in Scheme 42 (rightmost column of table). The transition-state structures for this transformation are analogous to the concerted, planar structure depicted as **4011** in Figure 11. For this planar, concerted six-atom transition state to be achieved, the two hydrogens from the donor molecular must reach an eclipsed geometry. This explains the inability of dioxane to act as a dihydrogen donor, due to its chair-like geometry (shown in Figure 12) where all vicinal hydrogens have a 60° dihedral angle ($\Delta G^{‡}$ = 27.1 kcal/mol). Cyclooctane exists in a boat-like conformation which allows pairs of vicinal hydrogens a 0° dihedral angle and is the most effective dihydrogen donor we examined ($\Delta G^{‡}$ = 17.6 kcal/mol). Cyclopentane, also a competent dihydrogen donor,

exists in an envelope-like conformation, with hydrogens at an eclipsed conformation and an activation energy of 17.7 kcal/mol. Not coincidentally, the energy difference between chair and boat conformations of cyclohexane (approximately 6 kcal/mol) is very similar to the difference in computed activation energies for cyclopentane and cyclohexane.

Figure 12 | Examples of geometries of dihydrogen donors.

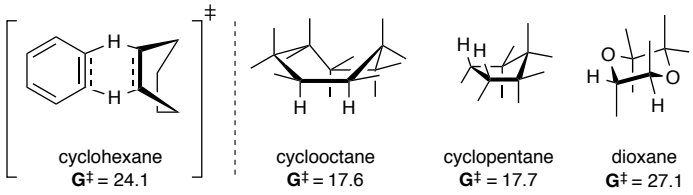

This dihydrogen transfer reaction could have practical synthetic utility as well. Scheme 43 shows the scope of HDDA-generated benzynes capable being reduced by cyclooctane to produce the diversely functionalized benzenoids. Each product was isolated after heating in the corresponding triyne precursor in neat cyclooctane at the indicated temperatures and times. A variety of functional groups are tolerant of the benign reducing conditions. The cyclohexene triyne precursor to **4015** shows the dihydrogen transfer is feasible at ambient temperatures. Tetraynes do not conflict with the process, as **4016** and **4019** illustrate. The benzenoid products are either 1,2,3,4-tetrasubstituted or 1,2,4-trisubstituted (**4017** and **4018**), patterns that are difficult to access by traditional aromatic synthesis strategies. Halogen-containing fluorenones were also synthesized (**4020**) and the reaction is not limited by scale, as evident by the gram-scale synthesis of **4021**.

Scheme 43 | Scheme of benzenoids synthesized via reduction by cyclooctane.

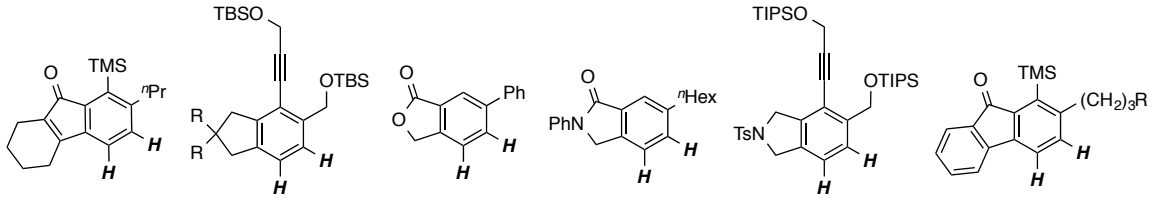

4015 rt, 48 h, 64%

4016, R = CO_2Me 110 °C, 14 h, 61%

4017 120 °C, 40 h, 53%

4018 120 °C, 20 h, 58%

4019 110 °C, 14 h, 74%

4020 R = Cl 100 °C, 14 h, 60%
4021 R = H, gram scale 85 ºC, 18 h, 67%

This double hydrogen transfer to benzyne is interesting in its capacity to synthesis new benzenoid products, but the real novelty of the process lies in the mechanism itself. We have shown substantial evidence that both hydrogens originate from the same donor molecule, and that the process has a substantial dependence on the dihedral angle of the donor. Donors having a greater population of conformers with eclipsed vicinal hydrogens are more reactive. These observations are consistent with a pathway in which both hydrogens are transferred simultaneously to the benzyne. This removal of vicinal hydrogen atoms from an alkane has been a particular challenge for synthetic chemists. Nature has the luxury of desaturases and acetylenases to achieve these essential oxidations in biosynthesis[91], but in the laboratory these transformations almost always involve one or more chemical intermediates. That makes this dihydrogen transfer desaturation of simple, unactivated alkanes a mechanistically unique process, one that could be viewed as a metal-free double C–H activation event.[92]

4.3. Dichlorination of HDDA-Generated Benzynes[93]

One intermolecular trapping result from our earliest studies involved the formal addition of HBr to produce monobromoarenes **4009a** and **4009b** (Scheme 44). With the triethylammonium bromide in chloroform, the two regioisomers were isolated in an approximate 13:1 ratio favoring **4009a**, consistent with computational models. Subsequent experiments showed that treatment with various ammonium chlorides gave a similar outcome, forming monochlorides **4022a** and **4022b** in a 6:1 regioisomeric ratio. Attempts at iodination of HDDA-generated benzynes were not as successful. These types of monohaloarenes are valuable synthons, capable of subsequent modification via

---

[91] a) Buist, P. H. Fatty acid desaturases: selecting the dehydrogenation channel. *Nat.Prod. Rep*. **2004**, *21*, 249–262. b) Bhattacharya, A. et al. Characterization of the fungal gibberellin desaturase as a 2-oxoglutarate-dependent dioxygenase and its utilization for enhancing plantgrowth. *Plant Physiol.* **2012**, *160*, 837–845. c) Moran, N. A.; Jarvik, T. Lateral transfer of genes from fungi underlies carotenoid production in aphids. *Science* **2010**, *328*, 624–627.

[92] Davies, H. M. L.; Du Bois, J.; Yu, J.-Q. C–H functionalization in organic synthesis. *Chem. Soc. Rev*. **2011**, *40*, 1855–1856.

[93] Niu, D.; Wang, T.; Woods, B. P.; Hoye, T. R. Dichlorination of (Hexadehydro-Diels–Alder Generated) Benzynes and a Protocol for Interrogating the Kinetic Order of Bimolecular Aryne Trapping Reactions. *Org. Lett.* **2014**, *16*, 254–257.

palladium-catalyzed chemistry.[94] Additionally, aryl chlorides specifically are commonly encountered molecules in agrochemicals, pharmaceuticals, natural products, and photonic

Scheme 44 | Monohaloarene formation through net hydrogen halide addition.

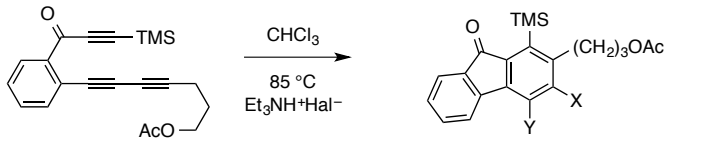

4001

4009a X = Br, Y = H ***4022a*** X = Cl, Y = H
4009b X = H, Y = Br ***4022b*** X = H, Y = Cl

materials. Monochloroarenes are typically prepared via the Sandmeyer reaction or electrophilic aromatic substitution. This HDDA-enabled method for monochlorination is a viable alternative.

1,2-Dichlorobenzene derivatives are even more challenging to prepare. In fact, dihalogenation of arynes has only been reported on a very limited basis. Diiodination[95] and dibrominations[95a] of arynes has been achieved, but proceed much less effectively for any benzynes more elaborate than the parent *o*-benzyne. Lee recently reported the only other example of dihalogenation of arynes and co-workers with the silver(I)-promoted mixed fluorohalogenation of HDDA-generated benzynes using FCl, FBr, or FI.[74] In the course of examining potential halogenation reactions of our HDDA-generated benzynes, we developed an efficient and mild strategy for preparing 1,2-dichlorinated arenes. These products also serve as valuable target compounds (Figure 13). Agrylin is a platelet reducing agent for treatment of thrombocytosis, indacrinone is a diuretic developed for treatment of gout and hypertension, the kutzerides are a class of antimicrobial peptides, and the tetracycle shown on the right of Figure 13 has organoelectronic applications.

[94] Noyori, S.; Nishihara, Y. Recent Advances in Cross-Coupling Reactions with Aryl Chlorides, Tosylates, and Mesylates. Applied Cross-Coupling Reactions; *Springer: Berlin Heidelberg*, **2013**; pp 177−202.
[95] (a) Friedman, L.; Logullo, F. M. Substitution reactions with photochemically produced acyl radicals. *Angew. Chem., Int. Ed. Engl*. **1965**, *4*, 239−240. (b) Birkett, M. A.; Knight, D. W.; Little, P. B.; Mitchell, M. B. A new approach to dihydrobenzofurans and dihydrobenzopyrans (chromans) based on the intramolecular trapping by alcohols of benzynes generated from 7-substituted-1-aminobenzotriazoles *Tetrahedron* **2000**, *56*, 1013. (c) Perry, R. J.; Turner, S. R. Preparation of N-substituted phthalimides by the palladium-catalyzed carbonylation and coupling of o-dihalo aromatics and primary amines. *J. Org. Chem.* **1991**, *56*, 6573. (d) Rodríguez-Lojo, D.; Cobas, A.; Peña, D.; Pérez, D.; Guitián, E. Aryne Insertion into I–I σ-Bonds. *Org. Lett*. **2012**, *14*, 1363−1365. (e) For a related haloamination reaction see: Hendrick, C. E.; McDonald, S. L.; Wan, Q. Insertion of arynes into *N*-halo bonds: A direct approach to *o*-haloaminoarenes. *Org. Lett*. **2013**, *15*, 3444−3447.

Our first attempts at dihalogenation of benzynes utilized simply I_2 or Br_2. These were unsurprisingly unsuccessful. One of the hallmarks of using HDDA-generated benzynes is the lack of external reagents needed to generate the reactive intermediate.

Figure 13 | Examples of 1,2-dichlorinated target compounds.

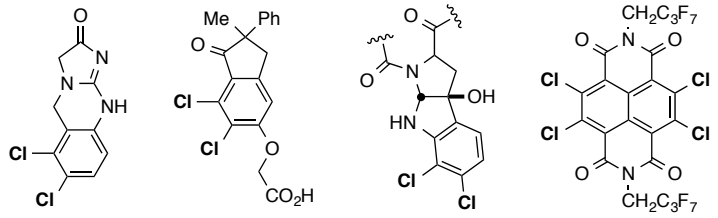

This allows for a more diverse set of potential traps to be investigated. However, the trapping reagents do still need to be compatible with the starting triyne substrate. Addition of Cl_2 and Br_2 to alkynes is a relatively fast process, so we did not expect them to be compatible with our HDDA substrates. However, it is known that certain metal halides can act as milder dihalogen surrogates for dihalogen addition reactions.[96] To study these metal-halogen complexes, we used the tetrayne **4023** shown in Scheme 45. This tosylamide-tethered symmetrical tetrayne is easily prepared and has relatively high

Scheme 45 | Dichlorination of tetrayne **4023** with various chloride sources to give **4024**.

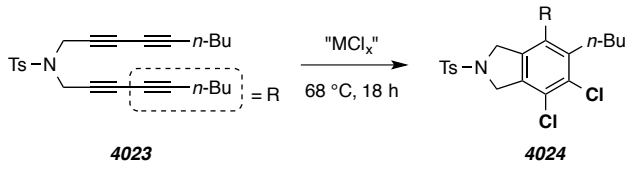

4023 ***4024***

entry	MCl_x	solvent	yield
1	$FeCl_3$	CH_3CN	0%
2	$CuCl_2$	CH_3CN	67%
3	Li_2CuCl_4	CH_3CN	67%
4	**Li_2CuCl_4**	**THF**	**85%**
5	Li_2CuCl_4	dioxane	trace

[96] (a) Rodebaugh, R.; Debenham, J. S.; Fraser-Reid, B.; Snyder, J. P. *J. Org. Chem.* **1999**, *64*, 1758−1761. (b) Uemura, S.; Sasaki, O.; Okano, M. *J. Chem. Soc. D* **1971**, 1064−1065. (c) Uemura, S.; Onoe, A.; Okano, M. Bull. *Chem. Soc. Jpn*. **1974**, *47*, 692−697. See also: (d) Kovacic, P.; Brace, N. O. *J. Am. Chem. Soc.* **1954**, *76*, 5491−5494. (e) Yang, L.; Lu, Z.; Stahl, S. S. *Chem. Commun*. **2009**, 6460−6462.

reactivity as an HDDA substrate. Our first attempt with iron (III) chloride as the dihalogenating agent failed to produce any of the desired product **4024**. Copper (II) chloride in acetonitrile gave our first indication of successful dichlorination. Lithium tetrachlorocuprate, formed in situ by mixing $CuCl_2$ with LiCl, gave a similar result in acetonitrile. The Li_2CuCl_4 is only sparingly soluble in dioxane but readily soluble in THF, and the yields (0% and 85%, respectively) seem to reflect that. Under these conditions, we never observed any noticeable dehydrogenation products (via THF, cf. Sec. 4.2) or monochlorination products in the mixture.

With the conditions and dihalogenating agent settled, we interrogated the scope of this process. Scheme 46 shows the set of dichlorinated arenes we have synthesized, in moderate to high yields, with this protocol. For each reaction, the corresponding tri- or tetrayne HDDA precursor was heated to the indicated temperature in the presence of ten equivalents of the Li_2CuCl_4 in THF (0.03M in substrate) for the indiated time. The benzenoids **4025–4029** encompass dichlorinated isoindoline, isoindolone, isobenzofuran, indane, and fluorenone skeletons. Myriad functional groups appear tolerant of the

Scheme 46 | Dichlorination of tetrayne **4023** with various chloride sources to give **4024**.

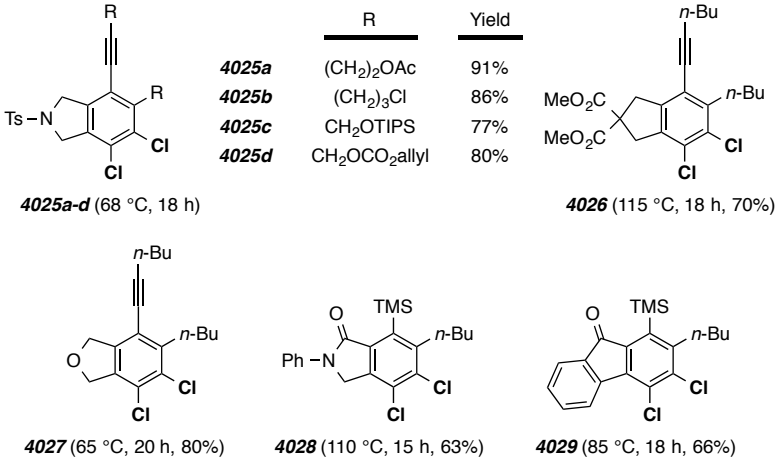

conditions, including a(n) toluenesulfonamide, ester, ether, amide, ketone, alkyl or aryl chloride, silyl ether, silyl alkyne, alkene, and aromatic ring. We have found that terminal alkynes and free alcohols are not compatible with the reaction conditions. The efficient transformations under mild and accommodating conditions make this Li_2CuCl_4 reaction

an exciting new method for synthesizing dichloroarenes. A protocol developed in our group for determining the kinetic order of aryne trapping reactions[93] found the process to be first order with respect to the Li_2CuCl_4, but currently the full mechanism has not been elucidated.

4.4. [2+2] Trapping of HDDA-Generated Benzynes

4.4.1 DMF and Acrylate [2+2] Trapping

We have shown that benzynes are reactive enough to engage in [4+2] reactions with benzene. Benzenes are especially resistant to participating as dienes in Diels–Alder reactions because of the accompanied loss of aromaticity. However, the high reactivity of benzyne overcomes this reluctance, even in the case of more substituted derivatives such as 1,2-dichlorobenzene (cf. Scheme 34, Sec. 3.6). Additionally, we have covered the [2+2] cycloaddition of benzynes with the highly strained olefin of norbornene (Scheme 39, Sec. 4.1). Having already observed a few of these intermolecular cycloaddition examples, we were curious as to other cycloaddition manifolds we could enter. We first looked at some cases of formal [2+2] cycloadditions with C=C π-bond of acrylates and the C=O π-bond of amides.

Studies have shown that benzyne reacts with the carbonyl π-bond of *N*,*N*-dimethylformamide (DMF) to produce, at least transiently, formal [2+2] adducts. Generally, the [2+2] adduct is hydrolyzed to result in a salicylaldehyde-like benzenoid.[97] The Yoshida[98] and Miyabe labs have capitalized reactivity of the carbonyl-benzyne adduct intermediates with synthetically useful sequential transformations with dialkylzincs[99] and other multicomponent coupling strategies.[100] We have observed an example of intermolecular trapping of an HDDA-generated benzyne with DMF followed

---

[97] Yaroslavsky, S. Reaction of aryldiazonium salts with dimethylformamide. Tetrahedron Lett. 1965, 6, 1503.

[98] Yoshida, H.; Watanabe, M.; Fukushima, H.; Ohshita, J.; Kunai, A. A 2:1 couling reaction of arynes with aldehydes via *o*-quinone methides Straightforward synthesis of 9-arylxanthenes. Org. Lett. 2004, 6, 4049

[99] Yoshioka, E.; Kohtani, S.; Miyabe, H. Sequential reactions of arynes via insertion into the π-bond of amides and trapping reaction with dialkylzincs. Org. Lett. 2010, 12, 1956.

[100] Yoshioka, E.; Kohtani, S.; Miyabe, H. A multicomponent coupling reaction induced by insertion of arynes into the C=O bond of formamide. Angew. Chem., Int. Ed. 2011, 50, 6638.

by an intramolecular ring-closing halide displacement (Scheme 47). When we heated triyne **4030** to induce HDDA cyclization in the presence of DMF (20 equiv), the only isolated product was the tetracycle **4031**. The proposed mechanism is suggested in the bottom of the scheme. The first few steps are analogous to previously reported trapping of benzynes by the aldehyde of DMF. The benzyne **4032** is susceptible to nucleophilic attack by the oxygen of DMF in the same regioselectivity as we observed with other nucleophiles. The iminium cation of zwitterion **4033** is in close proximity for intramolecular trapping by the benzyl anion to arrive at the formal [2+2] adduct **4034**. Hydrolysis from this point would arrive at the salicylaldehyde-like product, however the chloropropyl chain in the *ortho*-position of our substrate results in displacement by the phenoxide anion **4035** with loss of chloride to form the dihydropyran ring of the product. The final tetracyclic product is reminiscent of the product of intramolecular ether trapping in the presence of ethyl acetate or ethyl propionate (Scheme 37 Sec. 3.7).

Scheme 47 | Addition of DMF to HDDA-Generated benzyne from triyne **4030**.

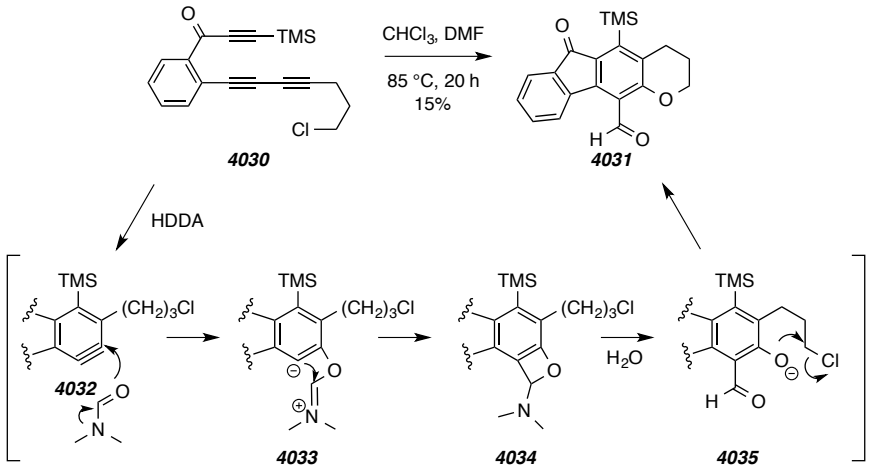

However, those cases resulted in aliphatic benzyl ketones while this DMF intermolecular trapping route allows access to simple formylation to benzynes. A modification to the propyl chloride group—different leaving groups or perhaps different nucleophiles to react with the phenoxide intermediate—opens up other potential synthetic applications for this unique pairing of intermolecular DMF trapping and intramolecular ring closure.

Olefins react with benzyne in a variety of ways.[101] Aside from [4+2] reactions with benzyne as the dienophile, olefins with allylic hydrogens participate in ene reactions with benzyne.[102] We have shown that HDDA-generated benzynes are capable of intramolecular ene reactions.[51a] In our preliminary example, the propargyl ether **4036** undergoes an efficient ene reaction to give the terminal alkene-containing benzenoid **4037** (Scheme 48). The Lee group has gone on to elaborate the scope of this transformation, showing that the ene reaction can construct large ring systems and allenes.[103] Olefins lacking allylic hydrogens are capable of [2+2] reactions to generate benzocyclobutanes. Unlike the stereospecific [4+2] cycloaddition with benzyne, the [2+2] variant has been shown to be a nonconcerted, stepwise process.[104] In one example, ketene silyl acetals cycloadd to benzyne, a useful route to benzocyclobutanones.[105] Our observation of an olefin participating in a [2+2] reaction occurred when the ester triyne

Scheme 48 | Reactions of olefins with HDDA-generated benzynes.

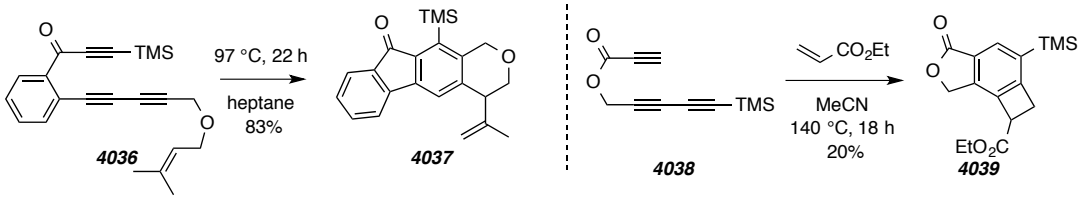

4038 was heated in the presence of ethyl acrylate (20 equiv) and the benzocyclobutane **4039** was isolated as the only regioisomer. The low isolated yield of this product suggests that this particular olefin cycloaddition to benzyne is not efficient, or that other competitive trapping events are present that proceed to decomposition rather than clean

[101] Crews, P.; Beard, J. Cycloadditions of benzyne with cyclic olefins. Competition between 2+ 4, ene, and 2+ 2 reaction pathways. *J. Org. Chem.* **2001**, *38*, 522–528.
[102] Tabushi, I.; Okazaki, K.; Oda, R. Relative reactivities of substituted olefins toward benzyne. *Tetrahedron* **1969**, *25*, 4401–4407.
[103] Karmakar, R.; Mamidipalli, P.; Yun, S. Y.; Lee, D. Alder-Ene Reactions of Arynes. *Org. Lett.* **2013**, *15*, 1938–1941.
[104] a) Jones, M., Jr; Levin, R. H. Stereochemistry of the 2+ 2 and 2+ 4 cycloadditions of benzyne. *J. Am. Chem. Soc* **1969**, *91*, 6411–6415. b) Gassman, P. G.; Benecke, H. P. Evidence for the formation of diradical intermediates in the 2+2 addition of benzyne to olefins. *Tet. Lett.* **1969**, *14*, 1089–1092.
[105] Hamura, T.; Ibusuki, Y.; Sato, K.; Matsumoto, T.; Osamura, Y.; Suzuki, K. Strain-induced regioselectivities in reactions of benzyne possessing a fused four-membered ring. *Org. Lett.* **2003**, *5*, 3551–3554.

products. Because HDDA-generation of this substrate required elevated heating, the benzocyclobutane could undergo [2+2] opening to *o*-quinodimethane intermediate, which is shown to be a reactive diene for subsequent Diels–Alder cycloadditions to produce tetrayhydronaphthalenes.[106]

4.4.2 Alkyne + Benzyne [2+2] Trapping Reaction en Route to Naphthalenes

In contrast to the ability of olefin π-bonds to undergo stepwise [2+2] addition to benzynes, alkynes are less reactive in this regard. Terminal alkynes can undergo C-H insertion to benzyne, and alkynes with propargylic hydrogens participate in ene reactions with benzyne.[107] Panel A of Scheme 49 shows the proposed mechanism for a three-component coupling of benzyne with THF and bromoalkynes.[108] If the ether of THF were to trap the benzyne to form zwitterion **4040**, a bromoalkyne such as **4041** is capable of ring-opening of the cyclic ether while halogenating the benzyne to form **4042**. A direct alkynylation of benzyne has been reported with terminal alkynes through in-situ formation of copper acetylides.[109] Panel B shows that copper acetylides **4043** can undergo insertion to benzyne (**3027**) in a formal C(sp)–H bond insertion after acidic workup of the benzo-cuprate species **4044** to provide phenylacetylenes **4045**. No π-bond addition/insertion products were reported as byproducts in either of these reports. In fact, all literature reports of benzyne trapping with C(sp)-C(sp) π-bonds require transition metals to coordinate and direct bond formation. Typically, nickel and palladium are used, as shown in Panels C and D of Scheme 49. In Panel C, palladium coordinates with the benzyne and directs carbopalladation of the alkyne **4046** to generate the palladacycle intermediate **4047**. This can go on to react with another benzyne molecule to generate

---

[106] Kraus, G. A.; Wu, T. A three-component reaction between benzynes, the enolate of acetaldehyde, and unsaturated esters and dihydroisoquinolines. *Tetrahedron* **2010**, *66*, 569–572.
[107] Jayanth, T. T.; Jeganmohan, M.; Cheng, M.-J.; Chu, S.-Y.; Cheng, C.-H. Ene reaction of arynes with alkynes. *J. Am. Chem. Soc.* **2006**, *128*, 2232–2233.
[108] Yoshida, H.; Asatsu, Y.; Mimura, Y.; Ito, Y.; Ohshita, J.; Takaki, K. Three-component coupling of arynes and organic bromides. *Angew. Chem. Int. Ed. Engl.* **2011**, *50*, 9676–9679.
[109] a) Xie, C.; Liu, L.; Zhang, Y.; Xu, P. Copper-catalyzed alkyne−aryne and alkyne−alkene−aryne coupling reactions. *Org. Lett.* **2008**, *10*, 2393–2396. b) Yoshida, H.; Morishita, T.; Nakata, H.; Ohshita, J. Copper-catalyzed 2:1 coupling reaction of arynes with alkynes. *Org. Lett*. **2009**, *11*, 373–376. c) Berti, F.; Crotti, P.; Cassano, G.; Pineschi, M. Copper-catalyzed arylation of alkenyl aziridines via three-component coupling reaction involving alkynes and benzyne. *Synlett* **2012**, *23*, 2463–2468.

phenanthrene derivatives **4048**.[110] Nickel complexes of benzyne such as **4049** can be isolated and, as shown in Panel D, react with acetylenes **4050** in a similar fashion as palladium to generate nickel metallacycles **4051**. With incorporation of another acetylene, substituted naphthalene derivatives **4052** can be produced.[111]

Scheme 49 | Reactions of alkynes with benzyne.

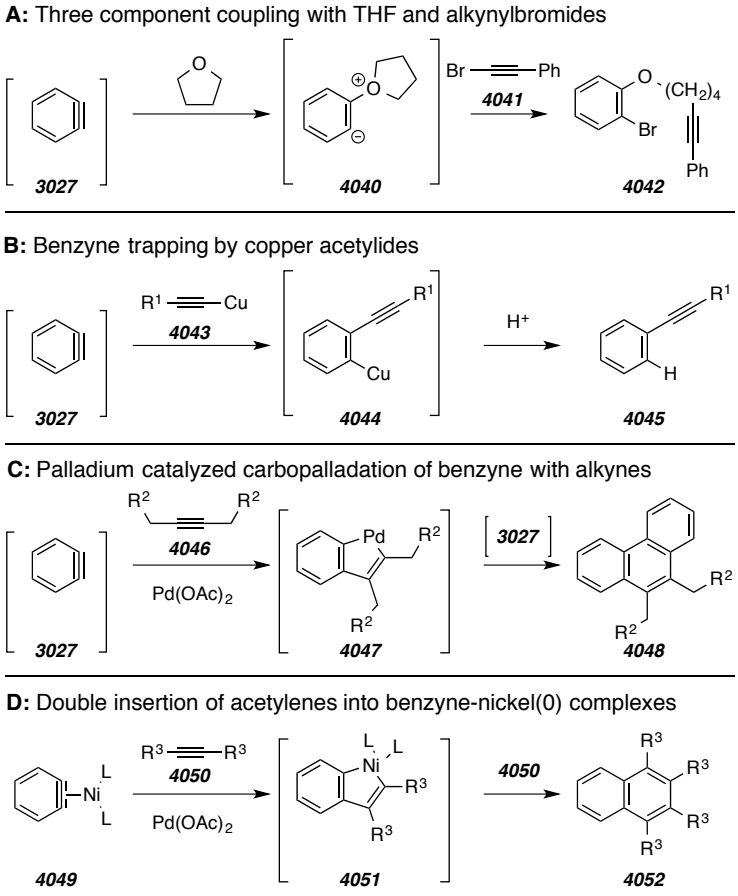

It should be noted that the reaction in Panel D works equally well with unsymmetrical alkynes as well as terminal alkynes. Also, 1,3-diynes will engage in the

[110] a) Yoshikawa, E.; Radhakrishnan, K. V.; Yamamoto, Y. Palladium-catalyzed controlled carbopalladation of benzyne. *J. Am. Chem. Soc.* **2000**, *122*, 7280–7286. b) Yoshikawa, E.; Yamamoto, Y. Palladium-catalyzed intermolecular controlled insertion of benzyne-benzyne-alkene and benzyne-alkyne-alkene-synthesis of phenanthrene and naphthalene derivatives. *Angew. Chem. Int. Ed. Engl.* **2000**, *39*, 173–175.

[111] a) Bennett, M. A.; Wenger, E. Insertion reactions of benzyne-nickel (0) complexes with acetylenes. *Organometallics* **1995**, *14*, 1267–1277. b) Bennett, M. A.; Wenger, E. Further observations on the formation of naphthalenes by double insertion of acetylenes into benzyne-nickel(0) complexes. *Organometallics* **1996**, *15*, 5536–5541.

same Ni(0) coordinated manifold to form dialkynyl naphthalenes in competition with previously reported [2+2+2] trimerization to form trialkynyl benzene products.[112] This is particularly intriguing, because throughout our studies of intermolecular trapping of HDDA-generated benzynes, we have been continually interested in how 1,3-diynes might react. Insight into these pathways would help explain the pathways of decomposition we observe when HDDA-triynes are heated in the absence of an effective trap. Nominally, there are two possibilities for benzyne trapping with a 1,3-diyne: that of a [4+2] or [2+2] stepwise or concerted addition.[113] The [4+2] cycloaddition between benzyne and a 1,3-diyne reaction would result in another subsequent benzyne, which could trigger a cascade to oligomerization and decomposition. The [2+2] reaction of benzyne and a 1,3-diyne addition forms a highly strained and highly reactive benzocyclobutadiene, which could also result in ensuing side reactions and decomposition.

In the course of examining the rate of cyclization of triyne substrates (rates to be covered extensively in Chapter 5 of this thesis), we have now observed for the first time evidence of a [2+2] reaction pathway between HDDA-generated benzynes and 1,3-diynes. When we heated **4053** in the presence of acetic acid, a highly efficient and rapid trapping agent, we observed the expected product **4054**, but also trace amounts of a second product **4055** in the ^{1}H NMR spectrum of the crude product mixture(Scheme 50). Low-resolution mass spectroscopy indicated the byproduct to be a dimer of the triyne ester. In an attempt to isolate the byproduct, the triyne was heated without the external acetic acid trap in the non-trapping solvent acetonitrile. After separation from the brown, oligomeric

Scheme 50 | First observation of dimerization of triyne **4053**.

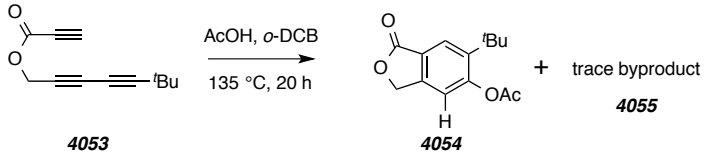

4053 ***4054*** ***4055***

[112] Deaton, K. R.; Gin, M. S. Regioselective [2 + 2 + 2] Cycloaddition of a Nickel−Benzyne Complex with 1,3-Diynes. *Org. Lett* **2003**, *5*, 2477–2480.

[113] Yang, T.; Zhao, X.; Nagase, S. Cycloaddition of Benzyne to Armchair Single-Walled Carbon Nanotubes: [2 + 2] or [4 + 2]? *Org. Lett* **2013**, *15*, 5960–5963.

mixture and purification, a white solid was isolated (45% mass recovery). High-resolution mass spectroscopy verified the dimeric nature of the product, and the ^{1}H-NMR spectrum corroborated that two *tert*-butyl groups, two methylene (CH_2) groups, and two aromatic protons were present. It was odd that each of these ^{1}H NMR signals was an isolated singlet, indicative of a non-symmetrical dimer structure. Both aromatic singlets were downfield at ca. 8.3 ppm. Particularly puzzling was the high downfield shift for one of the *tert*-butyl groups, at 1.8 ppm.

We were able to grow a crystal for X-ray analysis, and the structure of dimer **4055** is shown in Figure 14. Five of the six alkynes from two molecules of starting triyne have reacted to form a naphthalene core, while the remaining alkyne remains intact as a substituent on the naphthalene. The large downfield shift for one *tert*-butyl group can be

Figure 14 | X-ray structure of **4055**.

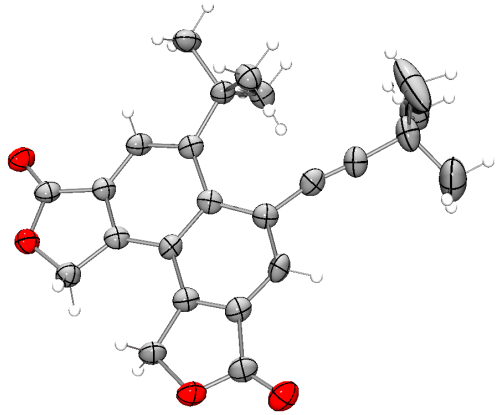

assigned to that on the naphthalene ring and juxtaposed to the alkyne, providing additional deshielding. Our proposed mechanism for this transformation is shown in Scheme 51. We surmise that the initial HDDA reaction first produces benzyne **4056**. This could undergo a (stepwise) [2+2] addition with an alkyne of the 1,3-diyne moiety in a second molecule of **4053** to produce the strained benzocyclobutene **4057**. This reactive species has another alkyne positioned four atoms away through the ester tether, which

could do an additional [2+2] cycloaddition to the 5-6-4-4-5 pentacycle **4058**. This also highly strained ring system can do a 4π electrocyclic ring opening, which results in the naphthalene core of **4055**. The first step of dimerization to form **4057** has two possible regioisomeric outcomes, but only the one shown was observed. This can be rationalized by the need for the minimally bulky alkyne to be on the side of the bulky *tert*-butyl benzyne substituent in order for the two reacting components to get in close enough proximity for the initial [2+2] reaction. Embedded within the bizarre pentacyclic framework of **4058** is a bicycle[2.2.0]hexa-2,5-diene, or Dewar benzene. In our case, it is attached to a benzene ring, making it a Dewar naphthalene. The interesting Dewar

Scheme 51 | Proposed mechanism of formation of naphthalene **5055**.

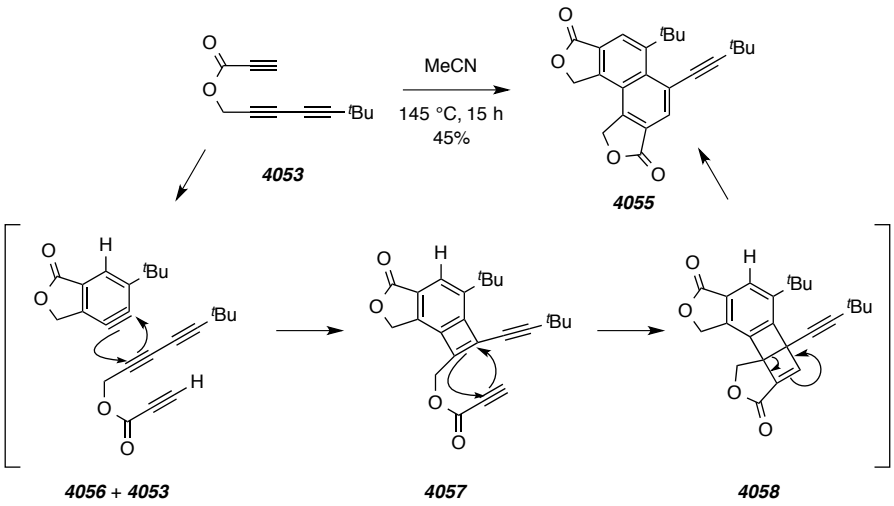

isomers of benzene,[114] naphthalene,[115] and anthracene[116] have all been prepared and their conversion to the Kekulé structures studied. The naphthalene formed in our dimerization after electrocyclic opening is highly substituted, and some forms of this type of Dewar-

[114] Van Tamelen, E. E.; Pappas, S. P.; Kirk, K. L. Valence bond isomers of aromatic systems. Bicyclo [2.2. 0] hexa-2, 5-dienes (Dewar benzenes). *J. Am. Chem. Soc.* **1971**, *93*, 6092–6101.
[115] Miki, S.; Katayama, T.; Yoshida, Z. Novel naphthalene derivatives undergoing thermal valence isomerization to hemi-Dewar-naphthalene. *Chem Lett.* **1992**, 41–44.
[116] Schottelius, M. J.; Chen, P. 9,10-Dehydroanthracene: p-Benzyne-type biradicals abstract hydrogen unusually slowly. *J. Am. Chem. Soc.* **1996**, *118*, 4896–4903.

naphthalene are stable and have been isolated.[117] The higher temperatures (130–140°C) needed to initiate the HDDA cyclization of this substrate most likely thwarts any opportunity to isolate **4058**.

Curious as to the thermodynamic realities to this proposed mechanism, we examined the intermediates with computational analysis (Scheme 52). To ease the computational burden, the *tert*-butyl group was omitted and the triyne **3016** was used, the

Scheme 52 | Computed free energy changes for the dimerization of triyne **4053** (M06-2X/6-311+G(d,p).

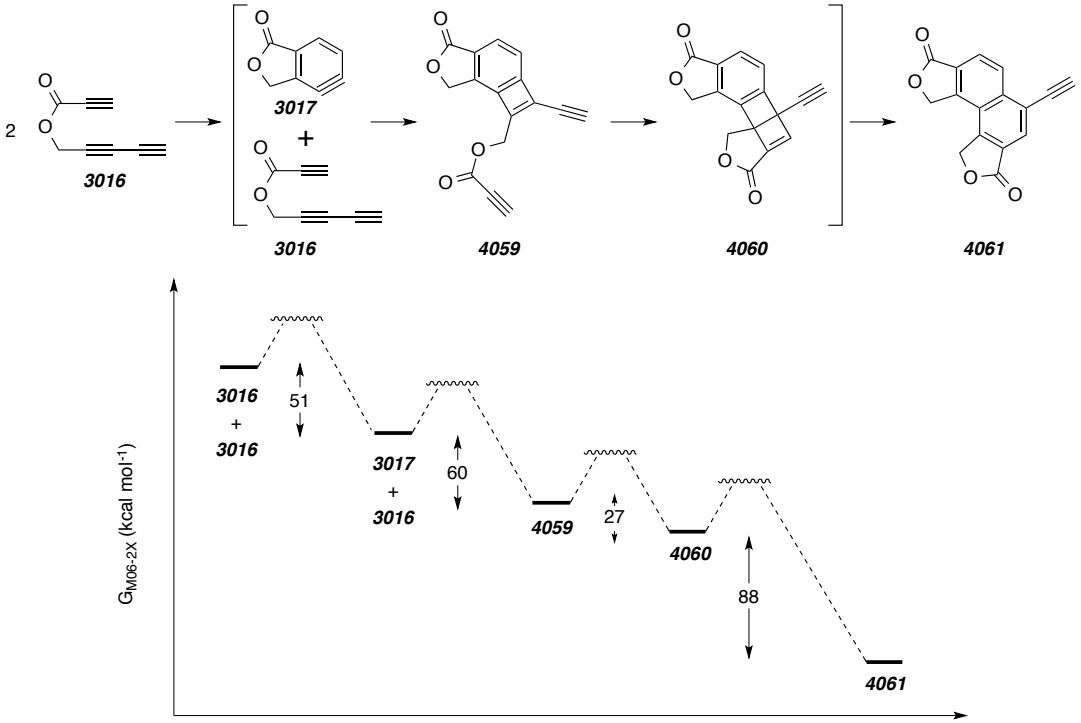

same substrate for our initial HDDA energetic calculations (Scheme 25, Sec. 3.1).[51a] In that previous analysis, we computed the initial benzyne formation to be exoergic by 51 kcal·mol^{-1}. The initial [2+2] reaction between benzyne **3017** and another molecule of **3016** is computed to be even more exoergic, a 60 kcal·mol^{-1} downhill step to form the benzocyclobutadiene **4059**. The second, now intramolecular, [2+2] reaction is only 27

[117] Miki, S.; Ema, T.; Shimizu, R.; Nakatsuji, H.; Yoshida, Z.-I. Synthesis and photoreaction of 1,2,3,4-tetra-*t*-butylnaphthalene: a highly crowded naphthalene derivative and its valence isomers. *Tetrahedron Lett.* **1992**, *33*, 1619–1620.

kcal·mol^{-1} downhill to **4060**, but the resulting opening of the two fused cyclobutenes to the naphthalene is the most exoergic step, at 88 kcal·mol^{-1} to form the product **4061**. Overall the process is computed to be 226 kcal·mol^{-1} downhill, a value that is in line with our previous HDDA calculations. In that study, we found the overall process of formation of benzyne **3017** followed by capture with *t*-BuOH was 124 kcal·mol^{-1} downhill. In this case we have five alkyne units reacting to produce the ten carbons of the aromatic naphthalene, in a process that is computed to be roughly twice as exoergic as that of our HDDA trapping.

This dimerization of a triyne via tandem [2+2]/[2+2] addition to an HDDA-generated benzyne is interesting from both a mechanistic as well as synthetic standpoint for its novel construction of substituted naphthalene cores. Future work will focus on the scope and optimized conditions for this unique transformation. Not unlike the first examination of the HDDA reaction, it is surprising how exoergic the entire process is. Also, this is another example where the ability to generate the reactive benzyne via the purely thermal conditions of the HDDA reaction open up new and potentially exciting manifolds for examination of new traps and re-examination of those previously studied. We have already seen multiple cases where the HDDA conditions allow for new trapping reactions to be discovered and mechanisms elucidated. There is vast literature precedence of myriad trapping reactions observed for traditionally generated benzynes upon which the new HDDA strategy can elaborate.

Chapter 5. Comparing Rates of HDDA Cyclizations

5.1. Strategy for Studying and Comparing Rates of HDDA Cyclizations

From our earliest studies and with re-examination of Ueda and Johnson's HDDA precedence it was clear that triynes have an extremely wide range of activation barriers for the initial cycloisomerization event. Johnson's earliest report of cyclization of nonatriyne occurred under flash-vacuum-pyrolysis conditions at 600 °C[56], while Ueda's early reactions of aromatic tetraynes proceeded at room temperature[58] (cf. Schemes 24 and 25, Sec. 3.2). While there have been numerous studies detailing the structural features that influence relative reactivity of classical [4+2] Diels–Alder reactions, the novelty of the HDDA reaction has not yet led to any analogous comprehensive studies of its relative rates. With our group's reports on the generality of HDDA cyclizations, we possessed the largest collection to date of examples of this reaction. We set out to identify and delineate the various structural and electronic features of triyne substrates that affect the rate of [4+2] HDDA cyclization. HDDA cascades consist of a two-stage process, with stage one constituting the [4+2] cyclization to generate the benzyne and stage II the intra- or intermolecular trapping of the benzyne (Figure 15). Because the Stage II trapping event is much faster, measuring the conversion of starting triyne to product benzenoid is an effective measure of the rate of [4+2] HDDA cyclization.

Figure 15 | The two stages of the HDDA cascade.

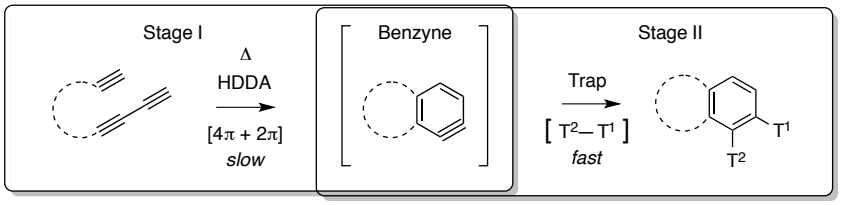

Our reported HDDA cyclizations are run in a variety of solvents. Often, the general cleanliness of the cyclization allows for product characterization without purification, so a low-boiling solvent is convenient for quick product isolation after solvent removal. Many times the reactions are heated to a temperature above the boiling point of the solvent, in vials sealed with Teflon-lined caps to avoid any loss of solvent. In

order to obtain valuable rate comparisons between HDDA substrates we first needed to establish whether the solvents were having any effect on the rate. The fluorenone precursor **3090c** was heated for 4 hours at 90 °C in one of three different deuterated solvents, and the percent conversion to **3091c** was measured by ^{1}H NMR spectroscopy. Cyclization of triynes with silyl ether intramolecular traps is generally clean (for this substrate, 96% isolated yield, Scheme 31, Sec. 3.6), making ^{1}H NMR an effective tool for measuring the conversion. Of the three deuterated solvents chosen, acetonitrile was the slowest at 43%, followed by chloroform and benzene at 60% and 69% respectively (Scheme 47). The percent conversion correlates with the dielectric constant Ɛ, or permittivity, of the solvent: the more nonpolar the solvent, the higher the conversion. This observation suggested the use of a constant solvent for all rates studies thereafter. We chose 1,2-dichlorobenzene (*o*-DCB) for all of our rate studies. Its high boiling point (180 °C) makes it ideal for use with high-activation barrier substrates without the worry of pressure buildup in the sealed vessel.

Scheme 47 | Solvent effects on rates of HDDA cyclization.

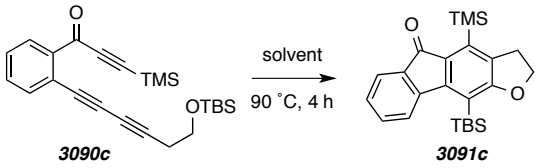

3090c ***3091c***

solvent	conversion	ε
C_6D_6	69%	2.27
$CDCl_3$	60%	4.81
CD_3CN	43%	37.5

Half-lives of reaction can be determined in short order for any cleanly-cyclizing substrate. In each experiment a 0.1 M solution of the HDDA substrate in *o*-DCB was placed in a closed vessel and held at an indicated temperature. Aliquots (~15 μL) taken at various time-points were diluted in $CDCl_3$ (600 μL) and analyzed directly via ^{1}H NMR spectroscopy (500 MHz). By monitoring the percent conversion it was relatively straightforward to deduce the half-life value and associated unimolecular rate constant [$k = \ln(2) / t_{1/2}$] at the reaction temperature used for that substrate. Given the wide range of reactivity differences across the various groups of substrates, it was not feasible to measure the experimental half-life at the same temperature for each triyne. In order to compare the approximate relative reactivities (k_{rel}s) among different substrates, the rate

constant can be adjusted to a common temperature via the Arrhenius equation (shown in Figure 16). To obtain a representative Arrhenius factor for performing the rate constant adjustments, an Arrhenius plot was developed for the substrate **3090c**. The half-life of

Figure 16 | Arrhenius value determination for representative substrate **3090c**.

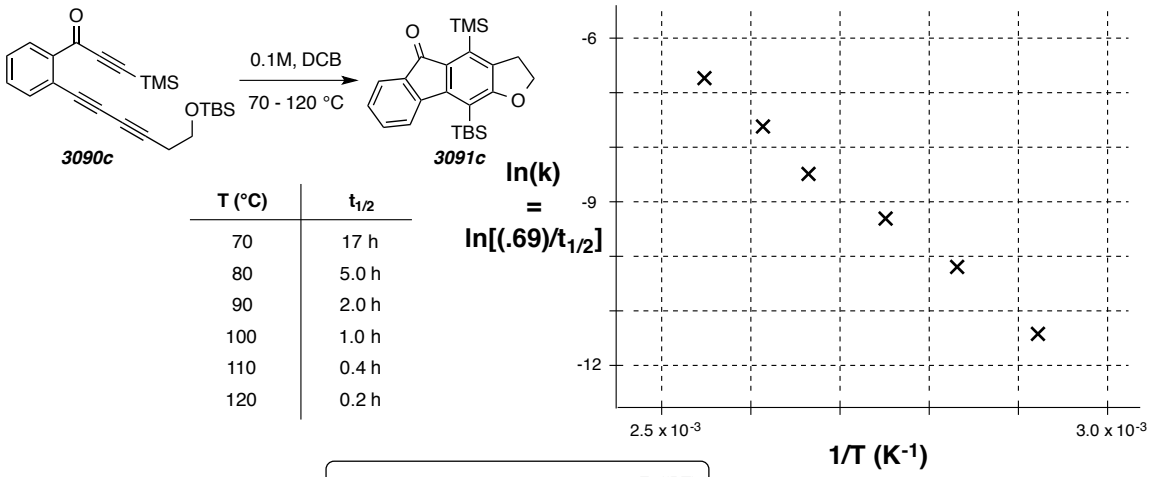

T (°C)	$t_{1/2}$
70	17 h
80	5.0 h
90	2.0 h
100	1.0 h
110	0.4 h
120	0.2 h

Arrhenius Equation: $k = Ae^{-Ea/(RT)}$

$\ln(k) = -E_a/R(1/T) + \ln(A)$

from the linear correlation (trendline): **y = -11884x + 23.38** with an $R^2 = 0.996$

$A = 1.42 \times 10^{10}\ s^{-1}$

cyclization at temperatures ranging from 70–120 °C varied from 11 min to 17 h (Figure 14). Plotting the natural log of these measured rate constants against the inverse temperature gives a trendline whose slope and y-intercept values can be used to obtain both the Arrhenius factor (A), and the energy of activation (E_a). With an experimentally derived Arrhenius factor in hand, the half-lives measured at any temperature can be scaled and the k_{rel}s determined. An example of this temperature adjustment is shown in

Figure 17 | Example rate constant adjustment to room temperature (298 K).

	A	B	C	D	E	F
1	**Substrate**	$t_{1/2}$ (h at T_{exp})	T_{exp} (K)	k_{Texp} (s^{-1})	E_a (kcal mol^{-1})	k_{298K} (s^{-1})
2	**3090c**	5	353	3.85×10^{-5}	23.5	7.89×10^{-8}

Cell D2 input: =LN(2)/(**B2***60*60)

Cell E2 input: =–(0.00198***C2**)*LN(**D2**/(1.42E10)) R = 0.00198 kcal•K^{-1}•mol^{-1}

Cell F2 input: =1.42E10*EXP(–**E2**/(0.00198*298)) A = 1.42×10^{10} (s^{-1})

Figure 17 as an excerpt from a spreadsheet. The half-life for substrate **3090c**, measured to be 5 h at 80 °C, gives a rate constant of 3.85×10^{-5} s^{-1}. When adjusted to room temperature (298 K) via the Arrhenius equation, the rate constant becomes 7.89×10^{-8} s^{-1}.

5.2. Impact of Linker Structure on Rates of HDDA Cyclizations

With a strategy in place for measuring HDDA substrate half-lives and comparing the relative rates of cyclization across various substrates, we first studied structural effects on intramolecular HDDA cyclization rates. We examined the reactivities of several sets of related HDDA substrates, all of which share the common generic structure **5001** (Scheme 48). All substrates differ primarily, but in a complementary fashion, in the nature of the "XYZ" atoms that serve to link the diyne to diynophile. The half-life for the Stage 1 cyclization, the rate-limiting step for all of these unimolecular isomerizations, was measured for each substrate and compared via relative reactivities (k_{rel}s) determined

Scheme 48| Generic substrates whose rates of HDDA cyclization were studied.

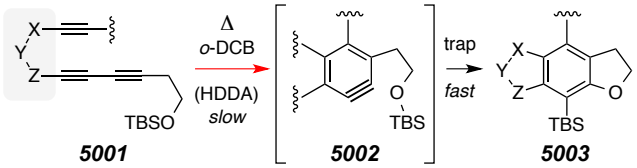

as described in Section 5.1. For the sake of consistency, the same β-(*t*-butyldimethylsilyloxy)ethyl moiety was used as the internal trapping group (cf. **5002** to **5003**) for each substrate. However, because the intramolecular Stage II trapping event is much faster than the Stage I HDDA reaction, it is safe to presume that the exact choice of the nature of this benzyne trap is not particularly relevant. Reactivities of intramolecular variants of classical Diels–Alder reactions have been extensively studied in similar fashion[118], but this represents the first systematic study of HDDA cyclization rates.

[118] (a) Juhl, M.; Tanner, D. Recent applications of intramolecular Diels–Alder reactions to natural product synthesis. *Chem. Soc. Rev.* **2009**, *38*, 2983–2992. (b) Takao, K.; Munakata, R.; Tadano, K. Recent advances in natural product synthesis by using intrmolecular Diels–Alder reactions. *Chem. Rev.* **2005**, *105*, 4779–4807. And references therein to numerous earlier reviews.

5.2.1. Comparison of Cyclization Rates of Triyne and Tetrayne HDDA Substrates

The first set of triyne substrates is shown in Table 1 (**5004**–**5006**); each cleanly gave the expected product (**5007**–**5009**, respectively) upon heating. These triynes differ only in the nature of the carbonyl functional group that is innate to the three-atom tether in each. The reaction temperatures and times for the observed half-lives are given in the

Table 1| HDDA cycloisomerization rates of triynes **5004**–**6**, which differ in the type of carbonyl-containing functional group embedded in the tether.

substrate	$t_{1/2}$ @temp	product (yield)	ca. k_{rel}
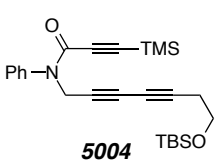 ***5004***	5 h, 90 ˚C	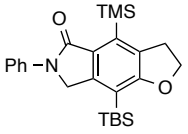 ***5007*** (76%)	**30,000**
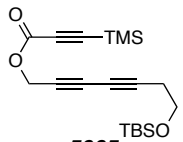 ***5005***	5 h, 110 ˚C	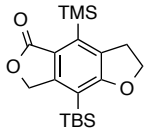 ***5008*** (95%)	**3000**
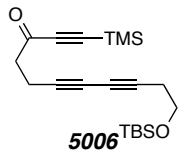 ***5006***	6 h, 180 ˚C	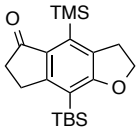 ***5009*** (80%)	**1**

second column. The approximate relative rates (rightmost column) for the unimolecular HDDA cyclization (the rate-determining step) span more than four orders of magnitude. The reactivity sequence is amide **5004** > ester **5005** >> ketone **5006**. These carbonyl functional groups affect both the electronic character of the diynophile (in this series, the monoyne) and the population of the reactive conformation[119] (cf. reactive rotamer effect[120]), which is the structure depicted for each of **5004**–**5006**. Intramolecular Diels–Alder (IMDA) reactions have been reported for analogous pairs of classical triene

[119] Martin, S. F.; Williamson, S. A.; Gist, R. P.; Smith, K. M. Aspects of the intramolecular Diels-Alder reactions of some 1,3,9-trienic amides, amines, and esters. An approach to the pentacyclic skeleton of the yohimboid alkaloids *J. Org. Chem.* **1983**, *48*, 5170-5180.

[120] Jung, M. E.; Kiankarimi, M. Substituent Effects in the Intramolecular Diels−Alder Reaction of 6-Furylhexenoates. *J. Org. Chem.* **1998**, *63*, 2968-2974.

substrates in which the only difference was the presence of an amide vs. an ester[119] or of an ester vs. a ketone[120] functionality within the tether. Those cases also showed greater reactivity of the amide over the ester and of the ester over the ketone, respectively, which is similar to what we have observed for this series of HDDA reactions.

Table 2| HDDA cycloisomerization rates of substrates having no conjugation or p-type electron withdrawing groups within their 3-atom tethers.

substrate	$t_{1/2}$@temp	product (yield)	ca. k_{rel}
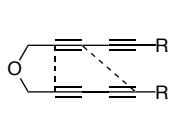 ***3071***	5 h, 65 °C	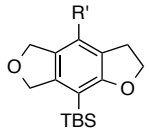 ***3072*** (64%)	210
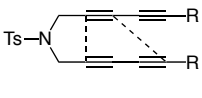 ***5010***	6 h, 65 °C	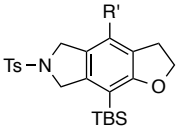 ***5012*** (88%)	170
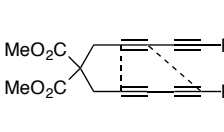 ***5011***	4 h, 115 °C	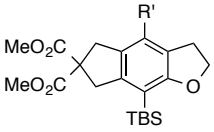 ***5013*** (75%)	1

R = CH_2CH_2OTBS R' =

Tetraynes we have studied are shown in Table 2. Each of the analogously symmetrical tetraynes **3071**, **5010**, and **5011** smoothly undergoes an HDDA cascade to give essentially a single product, **3072**, **5012**, and **5013**, respectively (Table 2). The only structural difference among the tetrayne substrates is the nature of the central atom within the three-atom linker joining the two identical 1,3-diyne moieties. The most reactive substrate is the ether-linked tetrayne **3071** and the least is the malonate **5011**. These three span a relative rate ratio of ca. 200, with the sulfonamide **5010** being nearly as reactive as the ether **3071**. The more reactive ether and sulfonamide tetraynes have, perforce, a more electronegative substituent on each of their propargylic carbons as well as a slightly shorter carbon-to-heteroatom bond length compared to the all-carbon linker.

The tetraynes in Table 2 have considerably lower activation barriers (cyclization at 65–115°C) than the triynes of Table 1 (cyclization at 90–180 °C). This trend of greater reactivity for tetraynes is evident even in the early reports of these types of cycloisomerizations. However, there is no basis for assessing the extent to which an additional alkyne substituent lowers the activation barrier for [4+2] cyclization. With the goal of quantifying the rate enhancement of a tetrayne with a directly analogous triyne, we prepared the triynes **5014a-c** (Scheme 49), each having a linker identical to that in one of the tetraynes in Table 2. Each of these triynes proved to be much less reactive than the analogous tetrayne. When finally heated to temperatures where starting material disappeared,[121] decomposition to dark-colored, intractable material was observed without any clear evidence for formation of the product of an HDDA cascade. We were successful, however, in determining the rate of reaction of tetrayne **5015** (Scheme 49).

In **5015** two modes of HDDA cyclization are now possible. These differ in whether the 1,3-diyne bearing the carbonyl substituent functions as the 2π or the 4π HDDA component—that is, the diynophile or the diyne, respectively. The first, which gives product **5016**, we call the 'normal' mode and the second, leading to **5017**, is the 'abnormal.' The normal mode of cyclization is favored over the abnormal, although only by a factor of ca. 2, as judged from the **5016**/**5017** product ratio.[122] For comparison we prepared the tetrayne **5018**, in which the tether comprises three methylene groups and, therefore, lacks the ketone carbonyl. It proved to be noticeably less reactive, ultimately decomposing at higher temperatures to mixtures that showed no evidence of formation of the expected HDDA product **5018'**.[123] Thus, the ketone carbonyl group in tetrayne **5015** has a definite activating effect on both the normal and abnormal pathways.

---

[121] Consumption of triyne to the extent of ca. 50% (^{1}H NMR analysis) was observed at 165 °C after 1 h for **5014a**, at 150 °C after 1 h for **5014b**, at 200 °C after 1 h for **5014c**.

[122] To guide assignment of the structure of the products **5016** and **5017**, we also studied two close structural analogs of the ketotetrayne **5015** in which one of the two siloxyethyl substituents was replaced by a siloxypropyl group on the top and bottom diyne. As expected, each reacted with essentially the same rate to give essentially the same ratio of normal to abnormal products, now with one containing a benzopyran and the other a benzofuran ring in each instance. See Experimental Section for details.

[123] When heated at 165 °C for one hour, only a few percent of **5018** remained, and no definitive evidence for any HDDA-derived product was observed by either ^{1}H NMR or GC-MS analysis. From the ^{1}H NMR spectrum, the coloration, and the tlc behavior of the crude reaction mixture, we judged that a substantial amount of oligomerization of **5018** was occurring.

With **5015** in hand, we were finally able to determine the extent of increased reactivity gained with tetrayne compared to triyne substrates. Both **5015** and **5006** (Table 1) contain a three-carbon ketone linker. The former (tetrayne) reacted nearly five orders

Scheme 49| Attempts to correlate tetrayne to triyne reactivity.

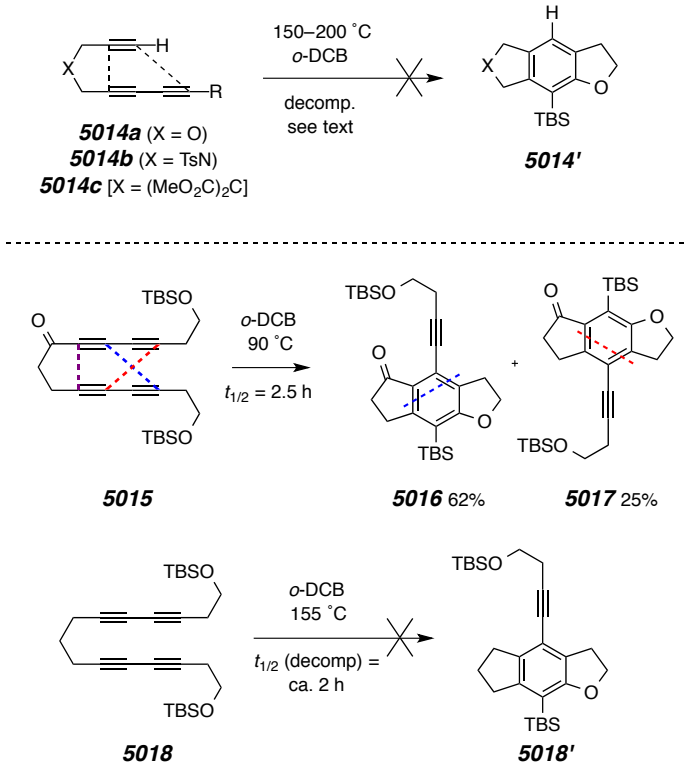

of magnitude faster than the latter (triyne) [$k_{rel(\mathbf{5015}\ vs.\ \mathbf{5006})}$ = 8x10^4]. While it might be tempting to assign a significant portion of this difference to a steric effect imposed by the trimethylsilyl group in **5006** that becomes more pronounced as the transition structure geometry is approached, the lack of reactivity of **5014a-c** suggests that this is not a dominant factor. Together, these observations further emphasize the fact that an alkyne substituent enhances the diynophilicity of the 2π-participant in HDDA cyclizations.

The similarities of **5018** and the malonate tetrayne **5011** (Table 2) also offer the opportunity for an additional rate comparison. Specifically, the rate enhancement from the reactive rotamer/Thorpe-Ingold effect imposed by the malonate substituents in **5011** apparently is sufficient to overcome the reluctance of **5018** to undergo HDDA cyclization.

However, the inability of **5018** to cyclize before decomposition thwarted chances of quantifying this effect. This was quickly probed by revisiting cyclization of the terminal alkyne ester **3059** to phthalide **3060** (Scheme 27, Sec. 3.4). The ester analogue with a tertiary carbon (in place of a methylene) within the tether, **3059-Me**, was prepared. It cleanly cyclized to **3060-Me** at 130 °C, but with a half-life much shorter than the

Table 3| Effect of increased steric buttressing on ester cyclizations.

substrate	$t_{1/2}$ @temp	product (yield)	ca. k_{rel}
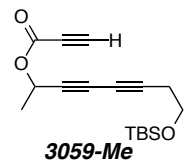 ***3059-Me***	0.5 h, 130 °C	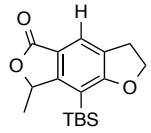 ***3060-Me*** (83%)	**11**
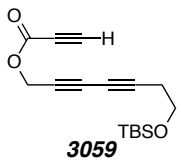 ***3059***	3 h, 130 °C	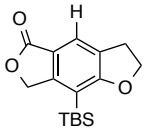 ***3060*** (86%)	**1**

methylene **3059** (Table 3). Comparing the relative rates shows that simple addition of the methyl group with the ester tether produces a rate enhancement of approximately an order of magnitude.

5.2.2. Effect of Tether Ring Size on Relative Rates

We next examined the influence of the size and/or the nature of the carbocycle upon which the diyne and diynophile are templated. The series of five triyne substrates **3014**, **3089c**, and **5019–5021** was studied and their reactivities are shown in Table 4. Varying the carbocycle embedded within the diyne-to-ynone linker results in HDDA-cyclization rates that, remarkably, span ca. seven orders of magnitude. The most reactive of all HDDA substrates we have studied to date is the cycloheptene-containing triyne **5019**, which cyclizes within hours at 0 °C. In contrast the cyclopentene substrate **5021** requires heating at 150 °C to achieve 50% conversion in four hours.

Comparison of the reactivity of the two closely related triynes **3014** vs. **3089c** (Table 4) is instructive. These differ only in the nature of the six-membered ring embedded in the tether. The cyclohexene compound **3014** was the first triyne we synthesized after our initial observation of the HDDA reaction (cf. Scheme 22, Sec. 3.1). At the time we were certainly surprised by its cyclization at room temperature, but did not realize how unique its low barrier for cyclization truly was. To date, it is one of only three substrates capable of cyclization at room temperature. Conversely, the benzene compound **3089c** (cf. Scheme 31, Sec. 3.6) requires heating to 80 °C to reach a comparable half-life. The cyclohexene compound **3014** reacts 500 times faster than its

Table 4| HDDA cycloisomerization rates of substrates with carbocycles of differing size and/or nature embedded in the linker. R = CH_2CH_2OTBS

substrate	$t_{1/2}$@temp	product (yield)	ca. k_{rel}
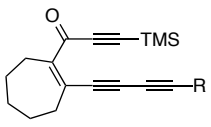 ***5019***	3 h, 3 °C	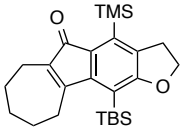 ***5022*** (72%)	20
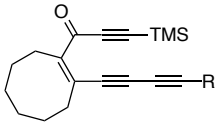 ***5020***	1 h, 24 °C	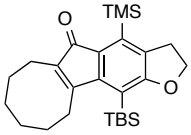 ***5023*** (90%)	6
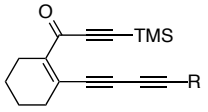 ***3014***	7 h, 23 °C	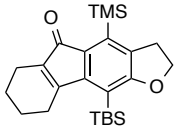 ***3015*** (93%)	1
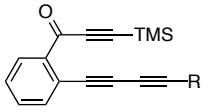 ***3089c***	5 h, 80 °C	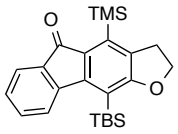 ***3090c*** (96%)	2×10^{-3}
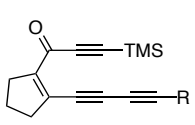 ***5021***	4 h, 150 °C	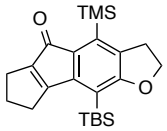 ***5024*** (53%)	1×10^{-6}

analogous benzene derivative **3089c**. We first surmised that the decreased bond distance associated with the higher bond order in the cyclohexene (ca. 1.33[124] Å) vs. benzene (ca. 1.38 Å) ring might be contributing in a significant way to this rate acceleration. However, this factor alone seemingly cannot explain the differences observed among the aliphatic cycloalkene members of this series, where the alkene bond lengths are, no doubt, all quite similar. That is, all of **5019**, **5020**, **3014**, and **5021** share essentially the same bond order and distances within their tethers, yet the relative rates of cyclization vary by $>10^7$! This

Table 5 | Relationship between the observed relative rates of reaction among **3014**, **3089c**, and **5019–5021** and the computed (DFT) geometries of their analogs.

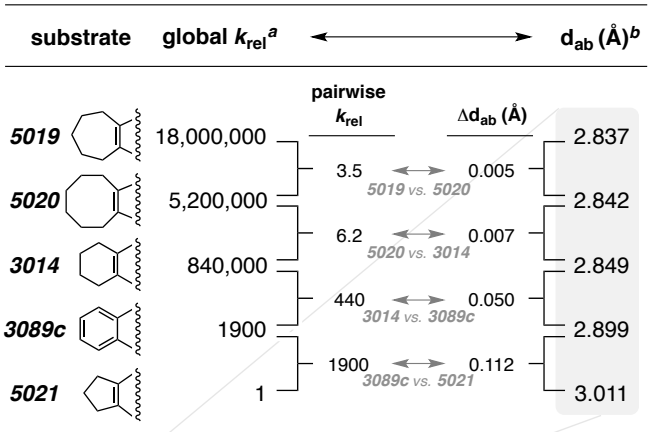

DFT Geometries

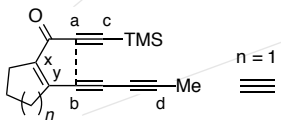

	n	∠x	∠y
5019'	3	124.8	125.7
5020'	4	125.1	124.8
3014'	2	125.1	125.4
3089c'	[benzo]	125.8	124.9
5021'	1	129.3	129.4

n = 1

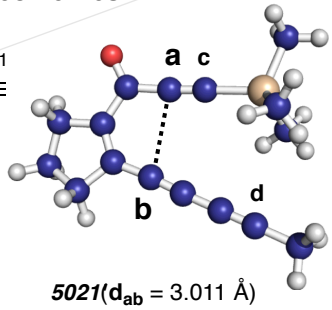

5021(d_{ab} = 3.011 Å)

[a] The global k_{rel} values here are normalized to the cyclopentene derivative **5021**, the least reactive of the series; they represent the same k_{rel} data given in Table 4. [b] Computed [DFT, M06-2X/6-31G(d,p)] values of the distance between atoms "a" and "b" (cf. **5021'**) when the "cabd" dihedral angle was constrained to be 0°.

[124] Allen, F. H.; Kennard, O.; Watson, D. G.; Brammer, L.; Orpen, A. G.; Taylor, R. Tables of bond lengths determined by X-ray and neutron diffraction. Part 1. Bond lengths in organic compounds. *J. Chem. Soc. Perkin Trans. II* **1987**, S1–S19.

suggested to us that internal bond angles within the tether might also be impacting the reactivity in an important way. We decided to probe some of these subtle geometric differences more specifically through computation.

Geometry optimization using density functional theory (DFT) was performed on a truncated analog of each of the substrates in Table 4. The $TBSO(CH_2)_2$ moiety was replaced by a simple methyl group. We constrained the four terminal sp-hybridized alkyne carbon atoms to be coplanar in order to approximate the reactive conformation (cf. carbons "a/b/c/d" in **1'** and **24'–27'** at the bottom of Table 5). This revealed a strong correlation of the experimentally observed reaction rates for these triynes (cf. "global k_{rel}s") vs. the computed distance between the nearest pair of alkyne carbons ("a" and "b") in the structure of each reactant—namely, d_{ab} (Table 5, rightmost column). The subtle yet convincing nature of this correlation is perhaps better seen through pairwise comparison of the changes in reactivity and distance upon progressing from the most to least reactive substrate. That is, the "pairwise k_{rel}s" change in concert with the change in "a–b" distance (Δd_{ab}) for each of the various pairs of reactants (middle of Table 5). The structural basis for the differences in d_{ab} values for the cycloalkenyl substrates can be associated with the internal bond angles "∠x" and "∠y", the computed values of which are shown for **3014'**, **3089c'** and **5019'–5021'**. It is impressive that a change of less than two-tenths of an angstrom difference in the d_{ab} values that span this entire set of reactants [$(\Delta d_{ab})_{\mathbf{5019'/5021'}}$ = 0.174 Å] accounts for such a dramatic difference in the measured relative rate of HDDA cyclization [$(k_{rel} > 10^7)_{\mathbf{5019/5021}}$]. This acute sensitivity to small geometric changes is reminiscent of observations made for Bergman (enediynes[15,125]) and Hopf (dienyne[126]) electrocyclizations. The following guideline is likely general: substrates having a structure that imposes greater proximity on the most proximal pair of sp-hybridized carbon atoms in the triyne are likely to have enhanced HDDA reactivity, all other things being equal.

---

[125] K. C. Nicolaou, Y. Ogawa, G. Zuccarello, E. J. Schweiger, T. Kumazawa, Cyclic conjugated enediynes related to calicheamicins and esperamicins: calculations, synthesis, and properties. *J. Am. Chem. Soc.* **1988**, *110*, 4866–4868.

[126] M. Prall, A. Kruger, P. R. Schreiner, H. Hopf, The cyclization of parent and cyclic hexa-1,3-dien-5-ynes–A combined theoretical and experimental study. *Chem.-Eur. J.* **2001**, *7*, 4386–4394.

5.2.3. Rate Effects of Altering the Electron-Withdrawing Group

Similar to our attempts at quantifying the effect of a tetrayne vs. a triyne, we also wished to more closely examine the effect of carbonyl activation on HDDA rates. To this end, we examined the effect of (i) reversing the relative orientation of the enone in a set of otherwise identical substrates [cf. the left column vs. the middle column in Table 6] as well as (ii) interrupting the contiguous conjugation by replacement of the ketone carbonyl with a reduced carbinol derivative (cf. the left column vs. the right column in Table 6). The normal member of each isomeric pair of enones reacted faster than its abnormal

Table 6 | Rate effects of changing the location or the presence of an electron withdrawing group (ketone carbonyl) within the triyne linker.

***normal* series**	***abnormal* series**	***non-ketonic* series**
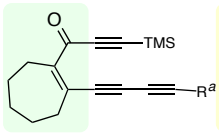	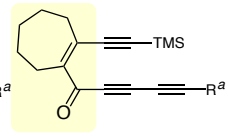	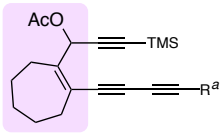
5019[c]	***5025***	***5026***
k_{rel} 80	1	
$t_{1/2}$ 3 h @ 3 ˚C	5 h @ 38 ˚C	3 h @ 115 ˚C
k_{rel} 200,000		1
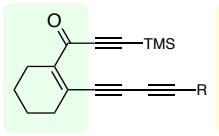	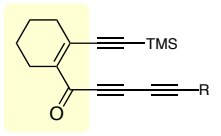	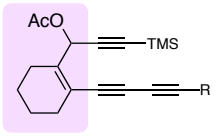
3014[c]	***5027***	***3053***
k_{rel} 60	1	
$t_{1/2}$ 7 h @ 23 ˚C	6 h @ 60 ˚C	6 h @ 125 ˚C
k_{rel} 90,000		1
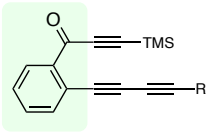	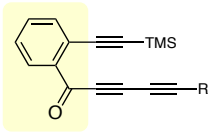	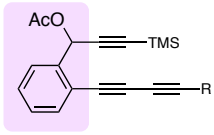
3089c[c]	***5028***	***5029***
k_{rel} 30	1	
$t_{1/2}$ 5 h @ 80 ˚C	3 h @ 115 ˚C	12 h @ 150 ˚C
k_{rel} 9000		1

[a] R = CH_2CH_2OTBS. [b] The k_{rel} values for **24a**:**1a**:**26a** are 9000:400:1 (data from Table 4).

analog, by a factor ranging from 30–80. Finally, each normal enone reacted faster than its acetate analog by a considerably larger rate factor (ca. 10^3 to $2x10^5$), which again emphasizes the significant acceleration afforded by an electron withdrawing carbonyl group.

The normal/abnormal effect illustrated in Table 6 is consistent in trend, but not in magnitude to our earlier result for the unsymmetrical tetrayne **5015** (Scheme 49). That result displayed a 2:1 preference for the normal cyclization product compared to the abnormal, while Table 6 shows a more pronounced partiality to the normal process of between 30:1 and 80:1. The substrates of Table 6 all have cycloalkene (or benzene) ring-containing tethers that limit the rotational freedom of the reacting diyne and alkyne moieties. The unsymmetrical tetrayne **5015** is less constrained, with two consecutive sp^3-hybridized atoms adjacent to the carbonyl activating group. We have synthesized two additional triyne substrates with the abnormal keto-diyne moiety to further probe this inconsistent carbonyl activating effect. We first synthesized triyne **5030** (Table 7), the abnormal variant of the sulfonamide-tethered **5004**. It cyclized much faster than we would have anticipated based on the results of Table 6, with a half-life of only three hours at 95 °C. The normal triyne **5004** undergoes HDDA reaction with an approximately equivalent rate of five hours at 90 °C. We attempted to compare this result with another

Table 7 | Rates of Additional Normal vs. Abnormal HDDA Substrates.

	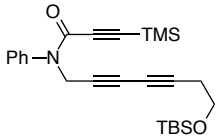	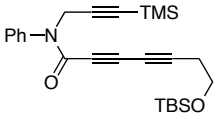
	5004	***5030***
$t_{1/2}$	5 h @ 90 °C	3 h @ 95 °C
k_{rel}	1	1
	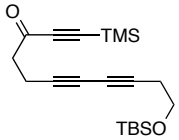	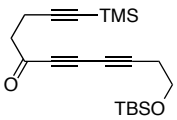
	5006	***5031***
$t_{1/2}$	6 h @ 180 °C	>50% decomp. @ 160 °C for 1 h

triyne system, the all-carbon tethered **5006**. However, in another unexpected result, the abnormally activated **5031** did not undergo clean or productive cyclization at a rate similar to its normal counterpart. Instead, we observe decomposition with no evidence for any HDDA product at 160 °C, a temperature which would produce HDDA cyclization (albeit slowly) for the normal triyne **5004**. It appears that the magnitude of the activating effect on the diyne vs. the diynophile is particularly substrate-specific.

The reduced reactivity of the acetate analogues of Table 6 is especially drastic, compared to the changes in the normal vs. abnormal substrates. Relative rates range from 9,000 to 200,000 times faster for the carbonyl vs. the corresponding acetate. This trend was examined further with non-ketonic groups other than the acetate analogues. Shown in Scheme 50, the benzyl alcohol **5032** was protected as a silyl ether of varying bulkiness and stability. The trimethylsilyl ether **5033a**, triisopropylsilyl ether **5033b**, and *tert*-butyldimethylsilyl ether **5033c**, were all prepared without complication. With these substrates in hand, one expectation was to see a rate enhancement compared to the acetate that continually increases with the size of the protecting group. We hypothesized that a larger silyl group would have greater tendency to avoid the steric interaction with the adjacent diyne substituent, thus increasing the population of the reactive conformer where the alkyne is positioned above the diyne. Yet when heated to 160 °C, a temperature which successfully cyclized the acetate analog **5029**, there was no evidence for any benzenoid product. All three of the silyl ethers were stable with no reaction indefinitely at 140 °C, with decomposition observed upon higher heating. The origin of this reduced reactivity is still in question, and might best be analyzed computationally. Perhaps the considerably larger silyl ethers (in relation to the acetate analogue) restricts free rotation enough to disallow any productive overlap of diyne and alkyne altogether.

Scheme 50 | Additional non-ketonic substrates and their failed HDDA cyclization.

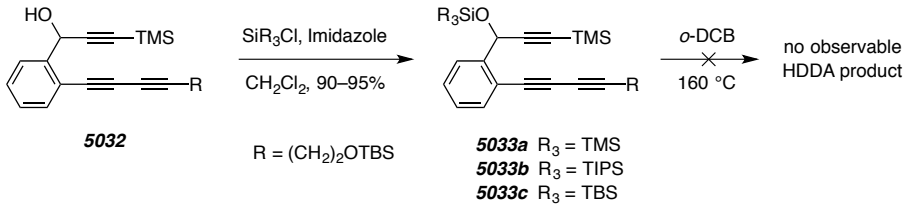

5.3. Rate Effects of Altering the Alkyne End-Groups

To expand our understanding of factors influencing rates, we set out to probe the effects of modifying the substituents at the termini of the reacting alkyne and diyne. Triynes with ester tethers were chosen for this study because their short, three-step synthetic route is easily amenable to variation at the alkyne termini. Each ester was heated in 1,2-dichlorobenzene (*o*-DCB) in the presence of 20-40 equivalents of acetic acid, which we have shown to be a particularly efficient trap of HDDA-generated benzynes. Analogous to the intramolecular cases previously discussed, half-lives were measured by following the conversion to product at various time-points via ^{1}H-NMR spectroscopy. In order to more accurately determine relative rates for these substrates, we avoided using the earlier Arrhenius factor determined for the benzene-tethered **3090c**, instead generating another Arrhenius plot with **3059** (Table 8). The Arrhenius factor for the ester-tethered **3059** was found to be more than an order of magnitude less than the benzene-tethered **3090c** (8.78×10^{8} s^{-1} vs. 1.42×10^{10} s^{-1} respectively). These ester-tethered substrates have more degrees of rotational freedom about their tethering atoms compared to the benzene-tethered substrate, which the different Arrhenius factors illustrate.

Table 8 | Determination of an Arrhenius factor (A) for ester-tethered substrates.

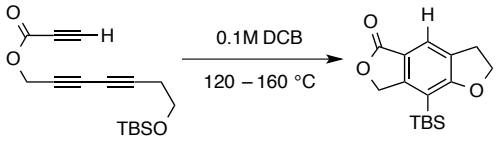

3059 ***3060***

T (°C)	$t_{1/2}$
120	7.5 h
130	3.0 h
140	1.7 h
150	0.8 h
160	0.4 h

A = 8.78 x 10^{8} s^{-1}

With an appropriate Arrhenius factor in hand, the first set of substrates studied includes the esters **3016**, **4038**, **5034**, and **5035**, shown at the top of Table 9. These differ systematically in having either a trimethylsilyl alkyne/diyne or a terminal C-H

alkyne/diyne. We found that the slowest (**5034**) and the fastest (**5035**) esters' rates of cyclization only differ by a factor less than ten. Particularly surprising was the very slight (k_{rel} = 1.2) change in rates of cyclization for the bis-trimethylsilyl capped **5034** compared to the bis-terminal C-H ester **3016**. Intuitively, the substantial increase in volume of a trimethylsilyl alkyne compared to a terminal alkyne alone would seem to slow the rate of HDDA cyclization considerably. However, it could be argued that any potential retardation of rate due to a steric increase is being offset by the increased carbon-silicon bond distance compared to an *sp*-carbon-hydrogen bond.

Table 9 | Rates of ester cyclizations with varying alkyne substituents.

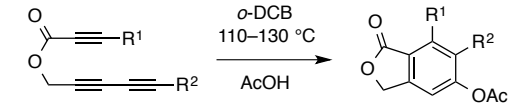

3016, 4038, 5034–5037 ***5038–5043***

	R^1	R^2	$t_{1/2}$	k_{rel}
5034	TMS	TMS	5.0 h, 130 °C	1.0
3016	H	H	4.5 h, 130 °C	1.2
4038	H	TMS	2.8 h, 130 °C	2.2
5035	TMS	H	5.0 h, 110 °C	7.9
5036	H	TBS	2.8 h, 130 °C	2.2
5037	H	$SiPh_3$	2.8 h, 130 °C	2.2

We examined the effect of steric bulk on rates of cyclization with the additional *tert*-butyldimethylsilyl and triphenylsilyl triynes **5036** and **5037** (Table 9). The three analogous triynes **4038**, **5036**, and **5037** have increasingly large silyl groups on their diyne termini. However, their rates of cyclization are identical. The consistent reactivity of these triynes speaks to the underlying mechanism of the [4+2] HDDA cycloaddition. Like the analogous Diels–Alder reaction, to which extensive mechanistic interrogation has been devoted, the HDDA could potentially proceed through one of two pathways (Figure 16). In the concerted pathway (top of figure) the a-b and c-d bonds form simultaneously. Alternatively, in a stepwise pathway (bottom) the a-b bond is formed first to create a diradical intermediate, which would then finish the cyclization with formation of the c-d bond. A concerted process, where both bonds are forming

concurrently, should show a dependence on the size differences of the substrates in Table 9. At the same time, all of our group's experimental observations to date have been consistent with the absence of radical character in both the cycloaddition and trapping processes. We decided to probe the HDDA reaction mechanism more specifically through computation of these types of substrates.

Figure 18 | Concerted vs. stepwise pathways of HDDA cyclizations.

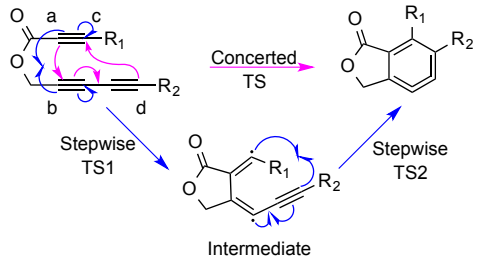

For the purposes of this study we have collaborated with the group of Professor Chris Cramer here at the University of Minnesota. Joshua Marell, a senior graduate student in the group, and Xiangyun Lei, an undergraduate researcher, performed a series of calculations on the same ester analogues from Table 9. All calculations were done at the M06-2X/6-311+G(d,p) level of theory in the gas phase. Solvent corrections were applied through single point calculations with the universal solvation model, SMD, in o-dichlorobenzene. Further correction was applied by spin purifying all open-shell singlet species. The results (Table 10) offer startling insight into the energetics of the two possible mechanistic pathways. First, the concerted transition states are considerably

Table 10 | Computed energies of concerted vs. stepwise pathways.

R1	*R2*	*Concerted TS*	*Stepwise TS1*	*Intermediate*	*Stepwise TS2*
H	H	33.78	28.10	21.62	22.19
H	TMS	33.92	27.73	20.85	20.61
TMS	H	32.12	26.82	21.09	–
TMS	TMS	–	26.26	20.05	27.04
H	ET	33.73	–	21.48	22.03
H	TBU	33.67	28.01	21.44	20.90
H	TBS	33.35	27.54	20.65	20.61

higher (>5 kcal·mol^{-1}) in energy than the transition state for step one of the radical pathway. In fact, for the most sterically encumbered triyne, with trimethylsilyl groups on both the alkyne and diyne termini, we were unable to locate the transition state for a concerted pathway. Additionally, when analyzing the stepwise radical pathway, the transition state for step two is only very slightly uphill (<2 kcal·mol^{-1}), with the exception of the bis-trimethylsilyl triyne. In fact, in two instances the step two transition state is actually lower in energy than the diradical intermediate; it is essentially a barrier-less second step.

This analysis of the HDDA reaction also allows us to compare computational results with our experimental results for the first time. We used the Arrhenius plot from Table 8 to determine the A factor for ester triyne cyclizations in order to generate accurate relative rates of different ester analogues. Yet the graph of ln(k) vs. 1/T also provides a second parameter: the experimental energy of activation (E_a). The same experimental results plotted in Table 8 correspond to an activation energy of 24.3 kcal·mol^{-1} for cyclization of ester triynes. In light of this experimental value, the computed concerted transition state has too high of a barrier to be a feasible pathway. In fact, this 24.3 kcal·mol^{-1} experimental E_a corresponds much better to the computed transition state barrier for step one of the radical pathway. We are currently in the process of optimizing the computational method. With the vast collection of experimental rate data already collected for a diverse set of triynes and tetraynes, we have substantial opportunity to examine the effects of different functionals and basis sets on predicting HDDA activation energies. The ability to find a method and protocol for computing activation energies for HDDA cyclizations that is backed by experimental data would be a powerful tool for those wishing to employ new, previously unimagined HDDA cyclizations.

Chapter 6. Differential Scanning Calorimetry Analysis of Polyynes

6.1. Different Scanning Calorimetry Introduction

Differential scanning calorimetry (DSC) is a thermoanalytical technique used primarily in polymer science to determine the thermal properties of polymers. The technique, first developed in 1962, relies on measuring the amount of heat required to increase the temperature of a sample of interest relative to a reference standard as a function of temperature. As the sample undergoes various phase transitions it will necessarily require more or less heat to keep it at the same temperature as the reference sample. These phase transitions (melting, crystallizing, boiling, etc.) can be either exothermic or endothermic. For example, as a sample reaches its melting point or boiling point, some of the heat applied to the sample will go towards affecting the phase transition from solid to liquid or liquid to gas and not to increasing the sample's temperature. Thus, the sample takes more energy relative to the reference, resulting in the same increase in temperature. These endothermic transitions appear as a sharp positive peak in the DSC trace. The example DSC trace for 2-acetonaphthone in Figure 19 shows its endothermic melting transition at 55 °C.

Figure 19 | DSC trace of 2-acetonaphthone.

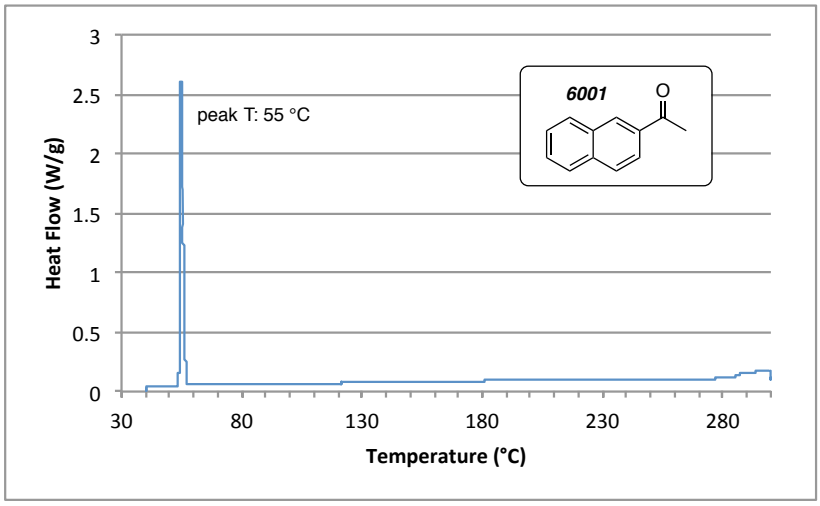

In addition to identifying physical state phase transitions, DSC allows for more subtle physical changes to be observed. DSC is most often used in this way to determine the thermal transitions of polymers. For example, glass transition temperatures (T_g) of polymers coincide with a change in heat capacity, and are seen as a "*step*" in the DSC trace. Upon further heating, crystallization temperatures can also be observed by their accompanied exothermic "*dip*" in the DSC plot. Polymers that are not completely amorphous will show this crystallization temperature dip, and also the subsequent melting temperature of the crystals. The area of endo- or exothermic peaks on the DSC trace corresponds to the energy of those polymer transitions. The percent crystallinity of the polymer can be determined from the integrals of the crystallization (exothermic) and melting (endothermic) peaks, along with the known mass of sample used for that DSC run. This extremely valuable property of a polymer indicates the amount of crystallinity in the polymer with respect to amorphous content and can have great influence on the hardness, tensile strength, and stiffness of polymers.

Initially we turned to DSC for a different, and far less thorough, purpose. While DSC is primarily utilized to determine thermal properties of polymers, small organic molecules are also capable of exhibiting interesting, and informative, behavior. Specifically, DSC can help provide decomposition details of thermally unstable, or even explosive, small molecules. For this reason DSC is a useful tool for analyzing the properties of difficult-to-handle compounds. Exothermic onset temperatures, heats of reaction, and other safety parameters are easily obtained from a DSC trace.[127] In addition to providing details of molecules that are thought to be explosive, DSC can also serve as a quick, easy, initial screen for newly isolated compounds suspected of having unstable properties.

Our HDDA projects require the synthesis and handling of a variety of polyynes. While there are occasional reports in the literature of polyynes showing explosive

[127] Cheng, S. Y.; Tseng, J. M.; Lin, S. Y.; Gupta, J. P.; Shu, C. M. Runaway reaction on tert-butyl peroxybenzoate by DSC tests. *Journal of Thermal Analysis and Calorimetry* **2008**, *93*, 121–126.

behavior,[128] to date we have not experienced any in our work. Reports of decomposition (at varying rates and temperatures) of polyynes are much more commonly found in the literature, often as a subtle comment in regards to an undetermined melting point.[129,130] We do notice similar decomposition of various polyynes under our handling and manipulation. Many times, we have found that polyynes need to be stored in solution and/or in the freezer. When left out on the bench top, neat, they decompose within a few days. With the large volume of polyynes being synthesized in our lab coupled with the reported instances of decomposition and/or explosions with polyynes, we turned to DSC as a safety and precautionary screening method.

6.2. DSC of Polyynes: Insight into Carbyne

The first polyyne we submitted to DSC was the terminal diyne **6002**, a substrate we use frequently in the synthesis of HDDA-precursor triynes. We found that the terminal diyne was susceptible to decomposition when stored neat at room temperature for an extended period. Its DSC trace, shown below, shows an exothermic downward curve with an onset temperature of 92 °C.[131] We had observed the trimethylsilyl-protected diyne **6003** to be considerably more stable and less prone to decomposition during handling. Its DSC trace, also shown in Figure 20, illustrates that, as the onset temperature has increased to 231 °C. For both of these substrates, we are unsure of the true pathway of decomposition. Whether after heating in a DSC experiment or after room temperature decomposition, all attempts to elucidate structure or physical properties of decomposition products have failed. Visually, we observe the formation of a dark, soot-like material, similar to our observations with unsuccessful HDDA cyclizations with inefficient traps. The dark, oligomeric substances are unwilling to dissolve into solutions of any solvent combination, similar to a cross-linked polymer. In the interest of

[128] Cambie, R. C.; Hirschberg, A.; Jones, E. R. H.; Lowe, G. Chemistry of the higher fungi. Part XVI. Polyacetylenic metabolites from Aleurodiscus roseus. *Journal of the Chemical Society (Resumed)* **1963**, 4120.
[129] Eisler, S.; Slepkov, A. D.; Elliott, E.; Luu, T.; McDonald, R.; Hegmann, F. A.; Tykwinski, R. R. Polyynes as a Model for Carbyne: Synthesis, Physical Properties, and Nonlinear Optical Response. *J. Am. Chem. Soc.* **2005**, *127*, 2666–2676.
[130] Chalifoux, W. A.; Tykwinski, R. R. Synthesis of polyynes to model the sp-carbon allotrope carbyne. *Nature Chemistry* **2010**, *2*, 967–971.
[131] The onset temperatures discussed in this Chapter are determined by the program software.

examining the factors effecting stability of other polyynes, we continued with this DSC analysis.

Figure 20 | DSC trace of diynes **6002** and **6003**.

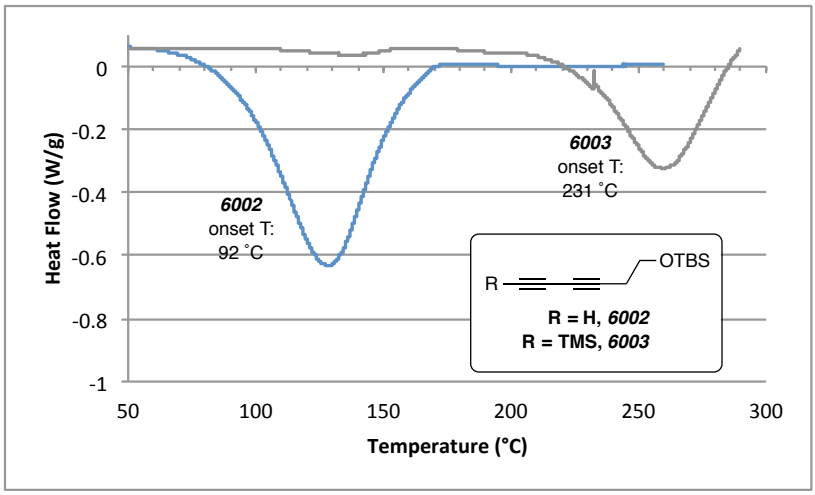

The change in onset temperature for the two diynes **6002** and **6003** is quite dramatic and suggests that substituents act to shield the reactive diynes from decomposition. A simple Glaser coupling of terminal alkynes trimethylsilyl acetylene and 2-methylbut-3-yn-2-ol produced a preliminary set of diynes to examine these steric

Figure 21 | DSC trace of diynes **6004** and **6005**.

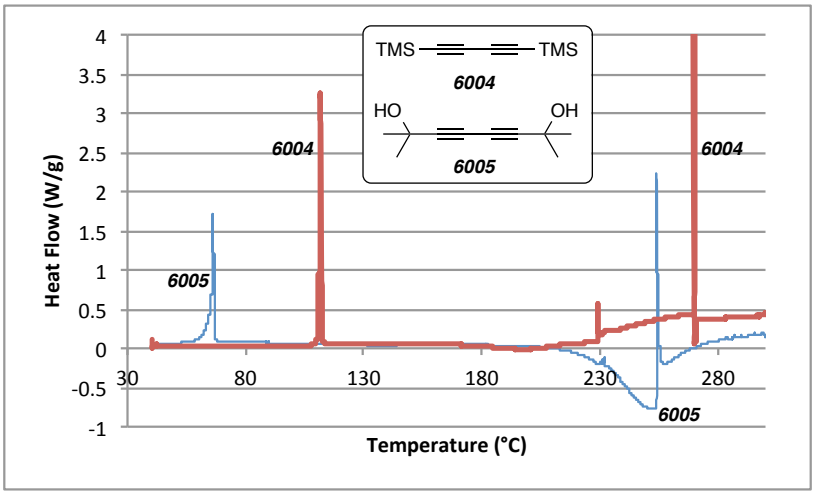

factors. The diynes **6004** and **6005** have either gem-dimethyl groups or trimethylsilyl groups to protect the diyne termini. Both of these compounds are solids at room temperature, and their melting points are clearly visible as endothermic peaks at 65 °C and 110 °C in Figure 21, which correlate with literature values. Upon further heating in the DSC instrument, however, the diol **6005** produces the characteristic decomposition exotherm near 230 °C, while the bistrimethylsilyl-1,3-butadiyne **6004** remains stable until what appears to be a boiling point endotherm arises at 270 °C. As expected, an intermediately shielded diyne such as **6006** shows an exothermic decomposition peak around 150 °C (Figure 22). A summary table on the right of Figure 22 illustrates the increasing decomposition temperature in relation to the bulk of the diyne termini. The parent compound, 1,3-butadiyne has been reported to detonate, and must be isolated in solution.[132] As you progress from a terminal diyne (onset temperature of 92 °C) to the bis-trimethylsilyl butadiyne (no decomposition exotherm observed), the onset temperature increases accordingly.

Figure 22 | DSC trace of diyne **6006** and summary table of diyne shielding effects.

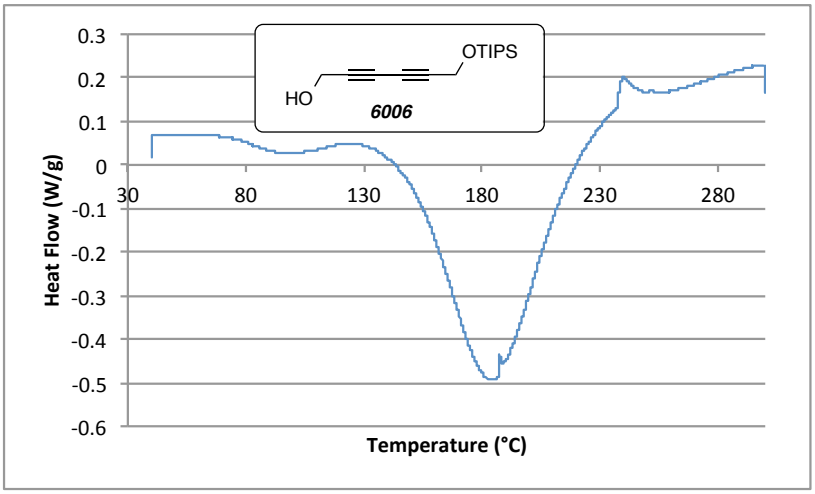

R^1	R^2	onset T
H	H	N/A
H	CH_2R	92 °C
CH_2R	CH_2R	150 °C
TMS	CH_2R	231 °C
$C(CH_3)_2OH$	$C(CH_3)_2OH$	237 °C
TMS	TMS	N/A

[132] J. B. Armitage, E. R. H. Jones, M. C. Whiting. Researches on acetylenic compounds. Part XXVIII. A new route to diacetylene and its symmetrical derivates. *J. Chem. Soc.* **1951**, 44–47.

Tykwinski has studied this trend in the context of using extended polyynes as models for the material carbyne $[(C{\equiv}C)_n]$.[133] Carbyne, sometimes referred to as linear acetylenic carbon (LAC), is the elusive *sp*-carbon allotrope (diamond and graphite representing the sp^3- and sp^2-carbon allotropes, respectively) that has intrigued scientists for years. Tykwinski has been successful at synthesizing the longest chain of conjugated polyynes to date, reaching an impressive 22 acetylene units.[134] In the course of defining the boundaries for stability of progressively longer linear conjugated polyynes, researchers in the Tykwinski laboratory have established that multi-ynes are greatly stabilized by the presence of extremely bulky α,ω-terminal substituents. At this length, the polyynes are only stable when capped with the exceedingly large tris(3,5-di-*t*-butylphenyl)methyl groups. Tykwinski and co-workers also observe similar DSC traces and trends in instability as the chain extends. To that effect, when we synthesized the

Figure 23 | DSC trace of triyne **6007** and tetrayne **6008**.

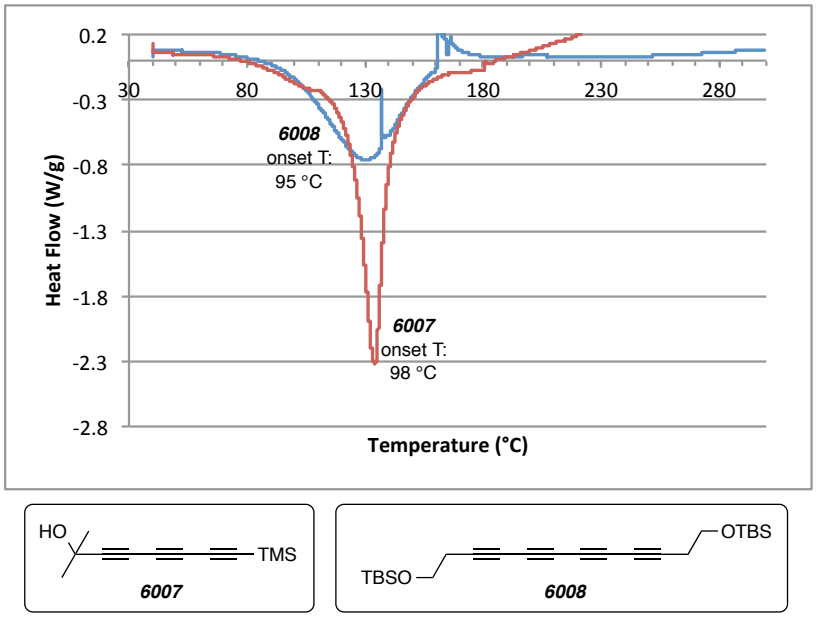

[133] (1) Eisler, S.; Slepkov, A. D.; Elliott, E.; Luu, T.; McDonald, R.; Hegmann, F. A.; Tykwinski, R. R. Polyynes as a model for carbyne: Synthesis, physical properties, and nonlinear optical response. *J. Am. Chem. Soc.* **2005**, *127*, 2666–2676.

[134] Chalifoux, W. A.; Tykwinski, R. R. Synthesis of polyynes to model the sp-carbon allotrope carbyne. *Nature Chemistry* **2010**, *2*, 967–971.

triyne **6007** and the tetrayne **6008**, they proved considerably less stable than their analogously-shielded diynes, with DSC onset temperatures of 98 and 95 °C, respectively (Figure 23).

The correlation of increasing instability with length of polyyne is similar to the trend we observed in increasing rates of HDDA reaction of tetraynes vs. triynes (cf. Sec. 5.2.1). In comparing relative rates of HDDA cyclization of a triyne vs. its otherwise analogous tetrayne, we found the presence of the additional alkyne was responsible for a relative rate enhancement of nearly five orders of magnitude. This type of activation of one π-component by a second of its own kind is well known, of course, in alkene chemistry. For example, 1,3-butadiene enters into a [4+2] cycloaddition much faster with itself than with ethylene as the dienophile, which is consistent with the lower HOMO-LUMO gap for the former pair of reactants. We suggest that this same type of behavior is operative in conjugated di-, tri-, and polyynes. Along with the fact that 1,3-butadiyne is unstable[132], a reported isolation of 1,3,5-hexatriyne (produced by a fungus) gave rise to "colorless crystals … which decomposed slowly at -20° and explosively at room temperature."[135] The Tykwinski laboratory obtained some x-ray structures of their linear polyynes and established that the extremely bulky terminal substituents on multi-ynes prevent the internal polyyne chains from associating with one another in parallel fashion.[130] Taken together with the fact that the HDDA cycloaddition of three alkynes to their corresponding benzyne is computed to be exothermic by ca. 50 kcal mol^{-1} (!),[136] we submit that the instability of unhindered, conjugated multi-alkynes is due to the fact that they enter into HDDA dimerization and, then, oligomerization with sufficiently rapid heating to result in uncontrolled (and typically unwanted) reactions. Moreover, we suggest that carbyne, the elusive missing allotrope of carbon, will most likely never be tamed as a tractable substance because its inherently low HOMO-LUMO gap will

[135] A. T. Glen, S. A. Hutchinson, N. J. McCorkindale, Hexa-1,3,5-triyne: A metabolite of Fomes Annosus. *Tetrahedron Lett*. **1996**, *35*, 4223–1225.
[136] A. Ajaz, A. Z. Bradley, R. C. Burrell, W. H. H. Li, K. J. Daoust, L. B. Bovee, K. J. DiRico, R. P. Johnson. Concerted vs stepwise mechanisms in dehydro-Diels–Alder reactions. *J. Org. Chem.* **2011**, *76,* 9320–9328.

necessarily result in facile cross-linking reactions having the nature of an HDDA process.[137]

6.3. DSC of HDDA Substrates

In the course of examining various polyynes via DSC, we recognized an opportunity to gain further understanding of energy barriers for HDDA cyclization of appropriate substrates. We quickly found that triynes and tetraynes for which we had observed successful HDDA cyclization experimentally also displayed a diagnostic exothermic peak in their DSC trace. The first HDDA substrate we submitted to DSC is the benzo-tethered **3089c**, which displays an onset temperature of 97 °C in Figure 24. This substrate has a half-life of 5 h at 80 °C, which led us to investigate the correlation between the HDDA reactivity and temperature of the DSC exotherm.

Figure 24 | DSC trace of triyne **3089c**.

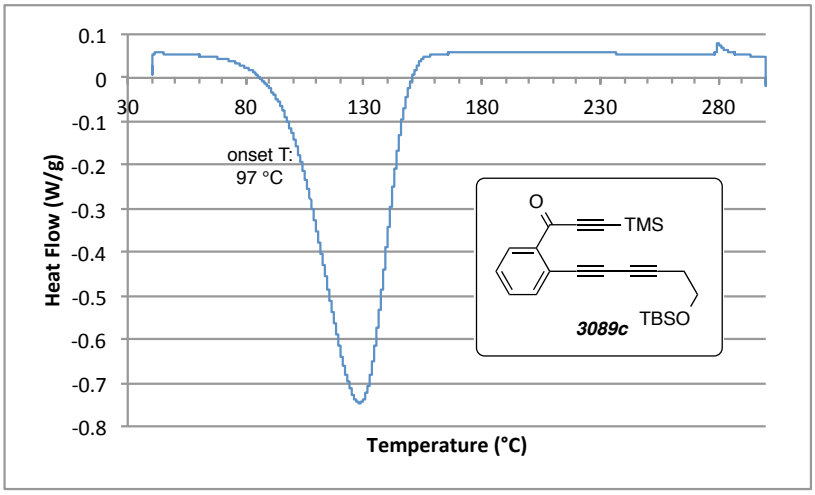

Figure 25 gives a glimpse to the relationship between HDDA reactivity and DSC trace. The rates of cyclization of triynes **5021**, **5027**, and **5028** were examined in Chapter 5 to determine effects of tether ring size and the location of carbonyl activation. The half-lives of each substrate are shown again under their structure, which vary from 6 h at 60 °C for the abnormal cyclohexene-containing **5027** to 4 h at 150 °C for the

[137] Conjugated multi-ynes preorganized in the solid state can undergo facile, controlled oligomerization: cf. J. W. Lauher, F. W. Fowler, N. S. Goroff. Single-crystal-to-single-crystal topochemical polymerizations by design. *Acc. Chem. Res*. **2008**, *41*, 1215–1229.

cyclopentene-containing **5021**. As seen in their DSC traces, the less reactive the substrate the further to the right their exotherm peak shifts. In fact, the experimentally determined half-lives of each substrate seem to fall in line particularly well with the onset temperature of the trace's exotherm. It is interesting that the shape of each of these downward exothermic peaks is similar to those in the DSC traces of decomposing diynes (cf. Fig 20), yet each of these triynes undergoes productive HDDA cyclization to the product benzenoid. One explanation is that the triynes are decomposing in a similar intermolecular fashion as the diynes when heated neat, and the DSC traces are not

Figure 25 | DSC trace of triynes **5021**, **5027**, and **5028**.

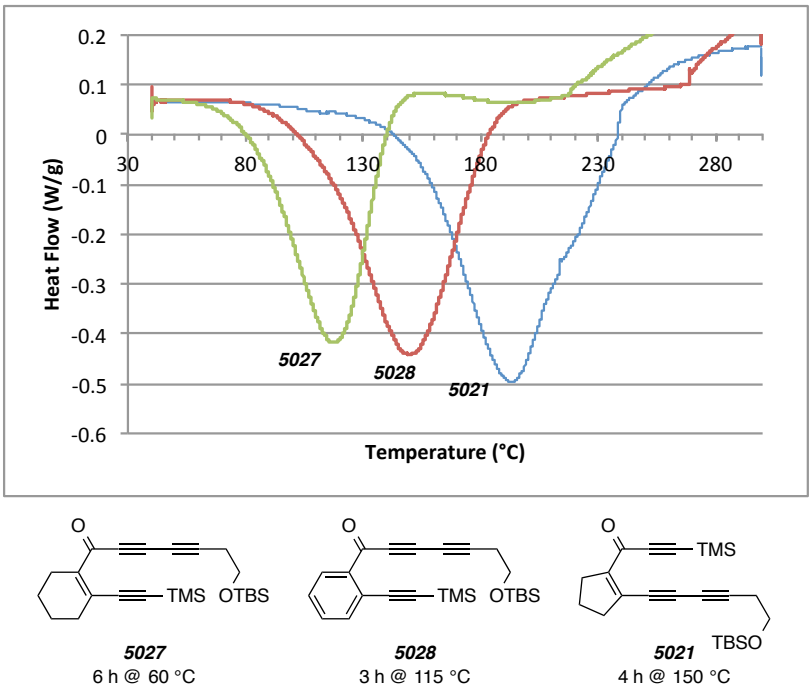

representative of any HDDA reaction. Judging from the diyne steric shielding table from Figure 20, the diyne subunit embedded in the triynes of Figures 22 and 23 should be stable in a DSC run until approximately 150 °C (cf. DSC trace of **6006**). However, the more reactive HDDA substrates **3089c**, **5021**, and **5027** each have an exotherm occurring well below that temperature, indicative of an HDDA process being responsible for the exotherm. To remove any remaining ambiguity, when the sample of **3089c** was recovered

after the DSC run and dissolved in $CDCl_3$, the ^1H NMR spectra showed clear (and clean!) evidence of the cyclized benzenoid product (estimated >50% mass recovery based on ^1H NMR). By contrast, no sample recovered after a DSC run of any of the polyynes from Sec 6.2 were at all soluble; a dark solid, soot-like mass is all that remained. This is a rather remarkable observation of a neat HDDA cyclization occurring in a DSC experiment, one that justifies the interpretation of DSC traces of polyynes as indicative of ease of HDDA cyclization.

We extended the use of DSC to include substrates for which we were not able to observe HDDA cyclization in solution. It should be noted that for our experiments, the maximum temperature comfortably reached with our silicone oil baths is in the neighborhood of 200 °C. The all-carbon tethered **5006** and **6009** show very low reactivity, making them good candidates for examination by DSC. The two-methylene variant **5006** is one of the least reactive HDDA substrates we have successfully cyclized, with a half-life of 6 h at 180 °C. With such sluggish reactivity, it came as no surprise when we could

Figure 26 | DSC trace of reactive triyne **5006** and unreactive triyne **6009**.

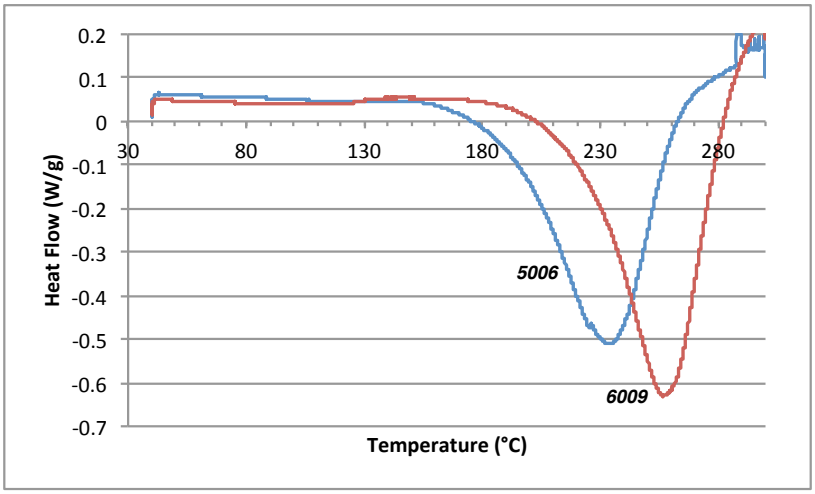

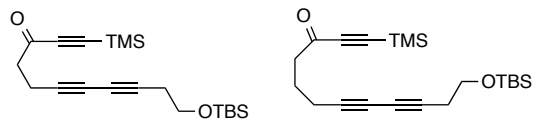

5006
$t_{1/2}$ = 6 h @ 180 °C

6009
$t_{1/2}$ = n.d.

not observe cyclization for the three-methylene tethered **6009**. The five-atom tether of **5006** produces a dihydroindenone skeleton, while the six-atom tether of **6009** would produce a dihydronaphthalenone core. To date, we have yet to initiate HDDA cyclization of any substrate with a six-atom tether. The DSC trace of **6009** (Figure 26) verifies these experimentally observed difficulties, as no exothermic onset temperature until 220 °C. By comparison, the five-atom tethered **5006** has a cyclization exotherm with an onset temperature of 191 °C-as expected based on its recorded half-life.

Figure 27 shows an additional set of substrates whose reactivity is better understood through their DSC traces. The malonate tetrayne **6010** contains a tether whose reactivity we have measured to correspond to a half-life of 4 h at 115 °C. Its DSC trace mirrors that reactivity, with an exotherm onset temperature of 119 °C. The all-methylene tethered **5018**, displays an exotherm at higher temperature, which is explained by the lack of steric buttressing present in the dimethylmalonate of **6010**. When heating **5018** in solution we do not observe HDDA product, suggesting that the DSC exotherm observed is one for decomposition. The onset temperature at 163 °C corresponds to our observations of >50% decomposition after two hours when heated in solution at 155 °C.

Figure 27 | DSC trace of polyynes **6009**, **5018**, and **5014c**.

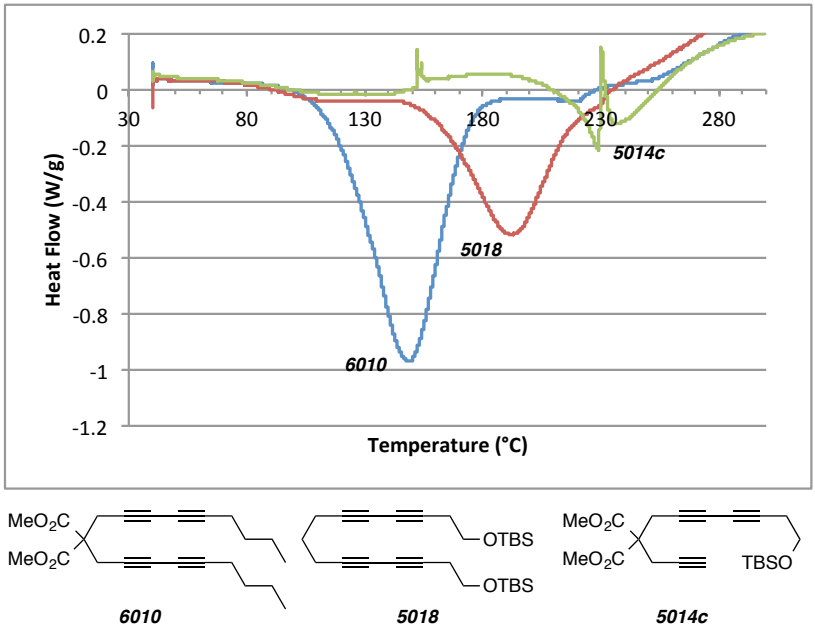

Malonate triyne **5014c** has similar correlation between its DSC trace and experimentally observed decomposition. The DSC trace shows an exothermic onset temperature of 219 °C, while we found that heating for one hour at 200 °C resulted in >50% decomposition with no sign of HDDA cyclization. We found that this same analysis can be applied to other intramolecular reactions, as shown in Figure 28. The diyne ether was synthesized originally in hopes that the diyne would trap a benzyne in a [4+2] fashion. This sort of trap would generate another benzyne, where the ether-linked prenyl group would trap via an ene reaction. However, submitting a sample of **6011** to a DSC run showed that the compound would not serve its purpose because it reacts intramolecularly with an onset temperature of 156 °C. When heated in solution, we found that an intramolecular ene reaction was taking place, with a half life of ca. 1 h at 155 °C. The ene reaction produced the exo-methylene cyclic ether **6012**, with 80% yield in solution.

Figure 28 | DSC trace of diyne ether **6011**.

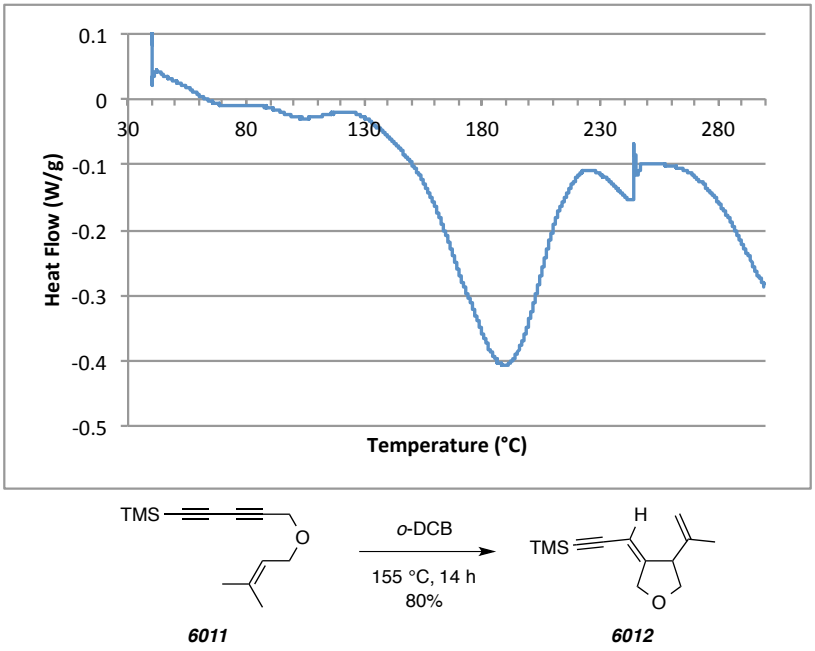

The studies described in this Chapter demonstrate the potential that DSC has in helping uncover subtle reactivity and decomposition pathways for HDDA substrates. DSC is a useful safety precaution for suspected dangerously reactive compounds, but also

as a helpful identifier of compounds susceptible to unwanted decomposition by improper storage or handling. For new compounds yet to be tested for HDDA reactivity, the DSC can serve as a valuable initial screening for insight into the activation temperature required to induce cyclization.

Supplementary Information For Chapters 2–6

General Experimental for Chapters 2–6

^{1}H and ^{13}C NMR spectra were recorded on Varian Inova 500 (500 MHz), Varian Inova 300 (300 MHz), Varian VXR 300 (300 MHz), and Bruker Avance 500 (500 MHz) spectrometers. ^{1}H NMR chemical shifts in $CDCl_3$ are referenced to TMS (δ 0.00 ppm). Non-first order multiplets are identified as "nfom". Intractable multiplets resulting from overlap of one or more peaks are labeled as “m” and denoted with a range of δ. ^{13}C NMR chemical shifts in $CDCl_3$ are referenced to chloroform (δ 77.16 ppm). The following format is used to report resonances: chemical shift in ppm [multiplicity, coupling constant(s) in Hz, integral, and assignment (when possible)]. ^{1}H NMR assignments are indicated by structure environment, e.g., CH_aH$_b$. Some complex structures are numbered in order to simplify proton assignment numbering and naming. Coupling constant analysis was guided by methods we have described elsewhere.[138,139]

Infrared spectra were recorded on a Midac Corporation Prospect 4000 FT-IR spectrometer. The most intense and/or diagnostic peaks are reported, and all spectra were collected in attenuated total reflectance (ATR) mode as thin films on a germanium window. High-resolution mass spectrometry (HRMS) measurements were performed on a Bruker BioTOF II (ESI-TOF) instrument using PEG or PPG as an internal standard/calibrant. Samples were introduced as solutions in methanol or acetonitrile. LC-MS refers to liquid chromatography mass spectrometry, which was performed on an Eclipse XDB-C18 column (4.6 mm internal diameter, 50 mm length) with 3.5 μm particle size with Solvent A containing 95% H_2O, 5% MeOH, with 15 mmol ammonium acetate and Solvent B containing 98% MeOH, 2% H_2O with 15 mmol ammonium acetate. Differential scanning calorimetry (DSC) was conducted on a TA Instruments Discovery DSC (New Castle, DE). The instrument was calibrated using an indium standard. All samples were prepared using T-Zero hermetic pans (ca. 5 mg). Samples were heated at 2 °C/min from 40–300 °C and then maintained at 300 °C for 10 min.

---

[138] Hoye, T. R.; Hanson, P. R.; Vyvyan, J. R. A practical guide to first-order multiplet analysis in ^{1}H NMR spectroscopy. *J. Org. Chem.* **1994**, *59*, 4096–4103.

[139] Hoye, T. R.; Zhao, H. A method for easily determining coupling constant values: An addendum to “A practical guide to first-order multiplet analysis in ^{1}H NMR spectroscopy.” *J. Org. Chem.* **2002**, *67*, 4014–4016.

MPLC refers to medium pressure liquid chromatography (25-200 psi) using hand-packed columns of Silasorb silica gel (18-32 μm, 60 Å pore size), a Waters HPLC pump, a Waters R401 differential refractive index detector, and a Gilson 116 UV detector. Flash chromatography was performed using E. Merck silica gel (230-400 mesh). Thin layer chromatography was performed on glass or plastic backed plates of silica gel and visualized by UV detection and/or a solution of ceric ammonium molybdate, anisaldehyde, potassium permanganate, or phosphomolybdic acid.

Reactions requiring anhydrous conditions were performed under an atmosphere of nitrogen or argon in flame or oven dried glassware. Piperidine, diisopropylamine and triethylamine for cross-coupling reactions were deaerated by a freeze-pump-thaw cycle and then stored in a Schlenk flask or by direct purging with N_2 gas immediately prior to use. Anhydrous THF, Et_2O, toluene, and CH_2Cl_2 were taken immediately prior to use after being passed through a column of activated alumina. Reported (external) reaction temperatures are the temperature of the heating bath. HDDA reactions, including those that were carried out at temperatures above the boiling point of the solvent, were typically performed in a screw-capped vial or culture tube fitted with an inert, teflon-lined cap. Those carried out in deuterated solvents were often performed directly in a capped 5 mm NMR sample tube.

General Procedure A: Alkyne Bromination

Powdered $AgNO_3$ (0.1 equiv) was added to a stirred solution of alkyne (1.0 equiv) and *N*-bromosuccinimide (NBS, 1.1 equiv) in acetone (0.1 M) at rt. After 1 h the slurry was either i) filtered through Celite® (acetone eluent) and concentrated or ii) partitioned between Et_2O and water, further extracted with Et_2O, washed with brine, dried ($MgSO_4$), and concentrated. The crude material was typically purified by flash chromatography.

General Procedure B: Cadiot–Chodkiewicz Alkyne Cross-Coupling

CuCl (0.05 equiv) was added to a stirred solution of alkyne (partner A, 1.0 equiv) and 1-bromoalkyne (partner B, 1.5 equiv) in freshly deaerated piperidine (0.3 M) at 0 ºC and under an inert atmosphere. After 1 h the reaction mixture was diluted with satd. aq. NH_4Cl and extracted with EtOAc or Et_2O. The combined organic extracts were washed with brine, dried ($MgSO_4$), and concentrated. The crude material was typically purified by flash chromatography.

General Procedure C: Tandem HDDA/Alkane Double Hydrogen Atom Transfer

A solution of HDDA triyne or tetrayne precursor in cyclooctane (ca. 0.01 M) was heated at the indicated temperature in a culture tube fitted with an inert, Teflon®-lined cap. After 12-48 h (as specified) the reaction mixture was loaded onto a bed of silica gel and washed sequentially with hexanes, to remove the excess cyclooctane, and ethyl acetate. The ethyl acetate fraction was concentrated to provide the crude product mixture. This material was typically purified by flash chromatography on silica gel.

General Procedure D. HDDA Reaction with *in situ* Dichlorination

Anhydrous lithium chloride and copper(II) chloride were combined in THF to arrive at a homogenous, red-orange stock solution of Li_2CuCl_4 (1.0 M). This was stored at room temperature in a tightly capped culture tube. Ten equivalents of this stock solution of Li_2CuCl_4 was added to the triyne substrate in a culture tube fitted with a teflon-lined cap. Additional THF was added to bring the final concentration of triyne to 0.03 M. The resulting solution was heated at the indicated temperature for the indicated time. Saturated aqueous NH_4Cl was added and the resulting mixture was extracted with EtOAc or Et_2O. The combined extracts were washed (brine), dried (Na_2SO_4), and concentrated. The crude material was purified using flash chromatography.

Experimental Section for Chapter 2

Hepta-1,6-diyn-4-ol (2001)

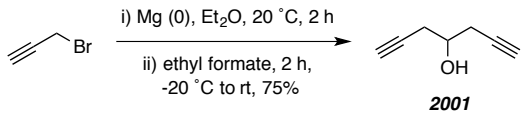

2001

[*BPW I-092*] Magnesium (2.43 g, 100 mmol, 3.30 equiv) was stirred with 10 mL of dry Et_2O in a 3-neck round-bottom flask fitted with an addition funnel and reflux condenser under an N_2 atmosphere. Mercuric chloride (*ca.* 30 mg) and propargyl bromide (0.5 mL) were added and the mixture was heated until reaction commenced. The mixture was then placed in a cool-water bath (20 °C) and a solution of propargyl bromide (7.57 mL,100 mmol, 3.3 equiv) in 50 mL of dry Et_2O was added dropwise over 2 h with stirring, keeping the temperature at 20-27 °C with cold-water cooling. At this point, practically all of the magnesium had disappeared and the reaction was stirred for a further 15 minutes at room temperature and then cooled to -20 °C (dry ice-acetone). A solution of ethyl formate (2.45 mL, 30mmol, 1 equiv) in 15 mL of Et_2O was added dropwise during 1 h with continued cooling at -20 °C. The mixture was stirred for a further 1 h without cooling and quenched with ice and ammonium chloride solution. The aqueous phase was extracted with Et_2O and the combined organic extracts were washed with brine, dried ($MgSO_4$), filtered, and concentrated under reduced pressure. Purification by flash chromatography (4:1 hexanes:EtOAc) afforded **2001** as a colorless oil (2.43 g, 23 mmol, 75%).

^{1}H NMR (500 MHz, $CDCl_3$): δ 3.96 [dtt, J = 5.5, 5.5, 5.5 Hz, 1H, $CH_2CH(OH)CH_2$], 2.48–2.58 [m, 4H, $CH_2CH(OH)CH_2$], 2.23 (d, J = 5.5 Hz, 1H, CHO*H*), and 2.08 (t, J = 2.5 Hz, 2H, $HC{\equiv}CCH_2$).

^{13}C NMR (125 MHz, $CDCl_3$): δ 80.6, 71.9, 68.9, and 26.7.

IR: 3294, 2917, 2119, 1428 and 1056 cm^{-1}.

TLC: R_f 0.3 (2:1 Hex:EtOAc).

Tetradeca-1,6,8,13-tetrayne-4,11-diol (2004) and henicosa-1,6,8,13,15,20-hexayne-4,11,18-triol (2005)

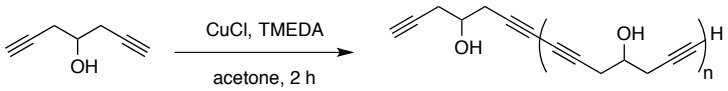

[*BPW I-086*] Hay's catalyst was prepared by adding tetramethylethylenediamine (250 µL, 1.7 mmol, 0.17 M) to a solution of copper (I) chloride (500 mg, 5.0 mmol, 0.5M) in acetone and stirred for 15 minutes. This Hay's catalyst (0.4 mL) was transferred to a 500 mL flask with 250-mL acetone and a solution of hepta-1,6-diyn-4-ol **2001** (432 mg, 4 mmol) in 30 mL acetone was added dropwise over 3 h. The mixture was stirred for 24 h and then the majority of solvent removed via rotary evaporation. The remaining solution was dissolved in EtOAc and poured over cold, dilute (0.6 M) HCl. The mixture was extracted with EtOAc (3 x 25 mL), washed with water, brine, dried ($MgSO_4$), filtered, and concentrated under reduced pressure. Purification by flash chromatography (1:1 hexanes:EtOAc) afforded **2004** as a clear, yellow oil (120 mg, 0.56 mmol, 28%) followed by **2005** (20 mg, 0.06 mmol, 5%).

Data for 2004:

^{1}H NMR (500 MHz, $CDCl_3$): δ 3.96 [dtt, *J* = 6.0, 6.0, 6.0, 2H, $CH_2CH(OH)CH_2$], 2.58–2.62 (m, 4H, $CH_2C{\equiv}CC{\equiv}CCH_2$), 2.50–2.54 [m, 4H, $CHC{\equiv}CCH_2CH(OH)$], 2.16 (d, *J* = 5.5 Hz, 2H, CHO*H*), and 2.09 (t, *J* = 2.5 Hz, 2H, $CHCCH_2$).

^{13}C NMR (125 MHz, $CDCl_3$): δ 80.4, 74.3, 72.2, 68.9, 68.3, 27.5, and 26.9.

IR: 3306, 2917, 2251, 1071 and 1054 cm^{-1}.

HR ESI-MS: calcd for $C_{14}H_{14}O_2$ $[M + Na]^+$ 237.0886, found 237.0886

TLC: R_f 0.4 (1:1 Hex:EtOAc).

Data for 2005:

^{1}H NMR (500 MHz, $CDCl_3$): δ 3.96 [dtt, *J* = 6.0, 6.0, 5.9, 3H, $CH_2CH(OH)CH_2$], 2.58–2.62 (m, 8H, $CH_2C{\equiv}CC{\equiv}CCH_2$), 2.52 [ddd, *J* = 6.6, 5.7, 2.7 Hz, 4H, $CHC{\equiv}CCH_2CH(OH)$], 2.16 (d, *J* = 5.5 Hz, 2H, CHO*H*), and 2.10 (t, *J* = 2.7 Hz, 2H, $CHCCH_2$).

^{13}C NMR (125 MHz, $CDCl_3$): δ 79.7, 73.8, 73.4, 71.5, 68.4, 68.3, 67.8, 67.6, 27.1, 26.8, and 26.3.

IR: 3393, 3295, 2916, 1420, and 1053 cm^{-1}.

HR ESI-MS: calcd for $C_{21}H_{20}O_3$ $[M + Na]^+$ 343.1305., found 343.1271

TLC: R_f 0.2 (1:1 Hex:EtOAc).

1,7-Dibromohepta-1,6-diyn-4-ol (2010)

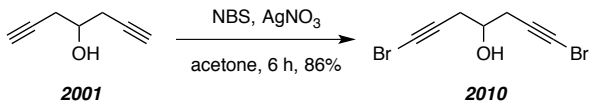

2001 ***2010***

[*BPW I-140*] To a stirring solution of the di-yne **2001** (324 mg, 3 mmol, 1.0 equiv) in dry acetone (8 mL) was added *N*-bromosuccinimide (1.12 g, 6.3 mmol, 2.1 equiv) and silver nitrate (51 mg, 0.3 mmol, 0.1 equiv). The flask was put under a N_2 atmosphere, wrapped in aluminum foil, and stirred overnight. After addition of a solution of $Na_2S_2O_3$ (10 mL) the aqueous phase was extracted with EtOAc (3x), the combined organic extracts were washed with H_2O (3x) and brine, dried ($MgSO_4$) and concentrated under reduced pressure. Purification of the crude residue by flash chromatography (4:1 Hexanes:EtOAc) provided **2010** as a yellow oil (685 mg, 2.6 mmol, 86%).

^{1}H NMR (500 MHz, $CDCl_3$): δ 3.94 (dtt, *J* = 5.9, 5.9, and 5.8 Hz, 1H, C*H*OH), 2.49–2.58 (m, 4H, HC≡CC*H*$_2$CHOH), and 2.15 (d, *J* = 5.5 Hz, 1H, CHO*H*).

LR ESI-MS: [M^+] requires 263.9; found 263.0.

TLC: R_f 0.3 (3:1 Hex:EtOAc).

1,7-Dibromohepta-1,6-diyn-4-yl acetate (2011)

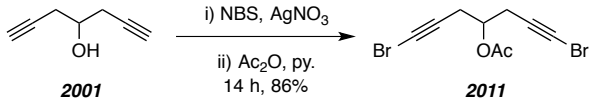

2001 ***2011***

[*BPW I-154*] To a stirring solution of di-yne **2001** (324 mg, 3 mmol, 1.0 equiv) in dry acetone (8 mL) was added *N*-bromosuccinimide (1.12 g, 6.3 mmol, 2.1 equiv) and silver nitrate (51 mg, 0.3 mmol, 0.1 equiv). The flask was put under a N_2 atmosphere, wrapped in aluminum foil, and stirred overnight. After addition of a solution of $Na_2S_2O_3$ (10 mL) the aqueous phase was extracted with EtOAc (3x), the combined organic extracts were washed with H_2O (3x) and brine, dried ($MgSO_4$) and concentrated under reduced pressure. This crude product was dissolved in pyridine (10 mL) and acetic anhydride (3 mL) was added. After being stirred overnight, the reaction was quenched by addition of dilute HCl (0.6 M) and the aqueous phase was extracted with EtOAc (3x). The combined organic extracts were washed with H_2O and brine, dried

($MgSO_4$), and concentrated under reduced pressure. Purification of the crude residue by flash chromatography (9:1 Hexanes:EtOAc) provided **2011** as a yellow oil (765 mg, 2.5 mmol, 83%).

^{1}H NMR (500 MHz, $CDCl_3$): δ 4.97 (tt, *J* = 6.0, 6.0 Hz, 1H, C*H*OAc), 2.63 (dd, *J* = 6, 3.5 Hz, 4H, CH_2CHOAc), and 2.10 (s, 3H, COCH_3).

^{13}C NMR (125 MHz, $CDCl_3$): δ 170.9, 75.5, 70.0, 41.8, 24.8, and 21.7.

IR: 2940, 2917, 2222, 1742, 1428, 1374, 1231 and 1035 cm^{-1}.

HR ESI-MS: calcd for $C_9H_8NaBr_2O_2^+$ [M + Na^+] requires 328.8783, found 328.8795

TLC: R_f 0.6 (5:1 Hex:EtOAc).

Hepta-1,6-diyn-4-yl phenylcarbamate (2012)

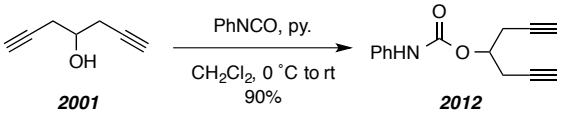

2001 ***2012***

[*BPW I-193*] Phenyl isocyanate (120 µL, 1.1 mmol) was added to a solution of alcohol **2001** (100 mg, 0.93 mmol) and pyridine (80 µL, 13 mmol) in CH_2Cl_2 at 0 °C. After warming to room temperature and stirring overnight, water was added and the organics extracted with CH_2Cl_2 (3 × 10 mL). The combined organics were washed with brine, dried over $MgSO_4$ and the crude product isolated after solvent removal purified by flash chromatography (5:1 Hex:EtOAc) to give the diyne **2012b** (190 mg, 0.84 mmol, 90%) as a yellow oil.

^{1}H NMR (500 MHz, $CDCl_3$): δ 7.39 (d, *J* = 7.8 Hz, 2H, ArH_o), 7.33 (t, *J* = 7.4 Hz, 2H, ArH_m), 7.08 (t, *J* = 7.4 Hz, 1H, ArH_p), 6.67 (br s, 1H, N*H*Ph), 5.05 (tt, *J* = 5.8, 5.8 Hz, 1H, C*H*OC=O), 2.72 (ddd *J* = 6.0, 2.7, 1.4 Hz, 4H, CH_2CHOC=O), and 2.06 (t, *J* = 2.7 Hz, 2H, $CH_2C{\equiv}CH$).

LR ESI-MS: [M^+] requires 227.1; found 227.1.

TLC: R_f 0.2 (5:1 Hex:EtOAc).

Cyclotetradeca-3,5,10,12-tetrayne-1,8-diol (2002)

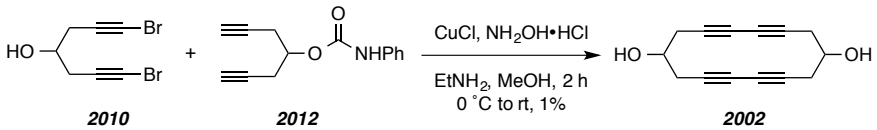

2010 ***2012*** ***2002***

[*BPW I-260*] CuCl (300 mg, 3.0 mmol) was added to a solution of MeOH/$EtNH_2$ (45:15 mL) and cooled to 0 °C. A spatula-tip of $NH_2OH \cdot HCl$ was added and the blue solution turned colorless. The diynes **2010** and **2012** were dissolved in 20 mL MeOH and added dropvise via an additional funnel over 0.5 h while the flask remained in an ice-bath. After all the alkynes were added the flask warmed to room temperature and stirred an additional 1 h. Water (20 mL) was added to quench the reaction and then most of the MeOH was removed via rotary evaporation. The green solution was extracted with Et_2O (3 × 25 mL), washed with aq. NH_4Cl (3 × 25 mL), brine, and dried ($MgSO_4$). The crude product isolated after solvent removal was purified via HPLC (1:1 Hex:EtOAc) to give the macrocycle **2002** (0.5 mg, 0.002 mmol, 1%).

^{1}H NMR (500 MHz, $CDCl_3$, **3029** diastereomer 1): δ .

HR ESI-MS calcd for $C_{14}H_{12}NaO_2^+$ [M + Na^+] requires 235.0730, found 235.0726.

TLC R_f 0.1 (1:1 hexanes:EtOAc).

Di-tert-butyl 2,2-di(prop-2-yn-1-yl)malonate (2014)

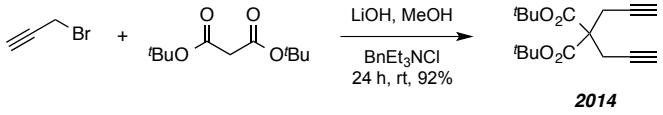

[*BPW II-064*] Lithium hydroxide (4.50 g, 188 mmol) and the phase-transfer catalyst benzyltriethylammonium chloride (1.37 g, 6.0 mmol) were stirred in 15 mL MeOH for 5 minutes. The di-*tert*-butyl 2,2-di(prop-2-yn-1-yl)malonate (1.34 mL, 6.0 mmol) and propagyl bromide (2.0 mL of 80% w sol. in toluene, 18.0 mmol) were added and the solution stirred overnight. Water was added and the organics extracted with Et_2O (3 × 15 mL). The combined organic extracts were washed 4× with water, then brine, dried ($MgSO_4$), and concentrated via rotary evaporation to give the diyne **2014** (1.62 g, 5.5 mmol, 92%) as a white solid which matched all reported spectroscopic data.[140]

---

[140] Fox, H. H.; Wolf, M. O.; Odell, R.; Lin, B. L.; Schrock, R. R.; Wrighton, M. S. Living Cyclopolymerization of 1,6-Heptadiyne Derivatives Using Well-Defined Alkylidene Complexes - Polymerization Mechanism, Polymer Structure, and Polymer Properties. *J. Am. Chem. Soc.* **1994**, *116*, 2827–2843.

Di-tert-butyl 2,2-bis(3-bromoprop-2-yn-1-yl)malonate (2013)

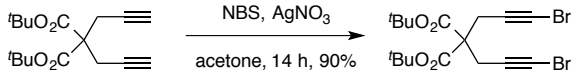

2014 ***2013***

[*BPW II-063*] To a stirring solution of di-yne **2014** (412 mg, 1.4 mmol, 1.0 equiv) in dry acetone (16 mL) was added *N*-bromosuccinimide (552 mg, 3.1 mmol, 2.2 equiv) and silver nitrate (24 mg, 0.14 mmol, 0.1 equiv). The flask was put under a N_2 atmosphere, wrapped in aluminum foil, and stirred overnight. After addition of a solution of $Na_2S_2O_3$ (10 mL) the aqueous phase was extracted with EtOAc (3x), the combined organic extracts were washed with H_2O (3x) and brine, dried ($MgSO_4$) and concentrated under reduced pressure to give the dibromo diyne **2013** (570 mg, 1.3 mmol, 90%) as an amber oil.

^{1}H NMR (500 MHz, $CDCl_3$): δ 2.87 (s, 4H, C*H*$_2$C≡CBr), and 1.46 [s, 18H, $CO_2C(CH_3)_3$].

LR ESI-MS: $[M–(^tBu)_2]^+$ requires 335.8; found 335.9.

TLC R_f 0.3 (10:1 hexanes:EtOAc).

Tetra-*tert*-butyl cyclotetradeca-3,5,10,12-tetrayne-1,1,8,8-tetracarboxylate (2015)

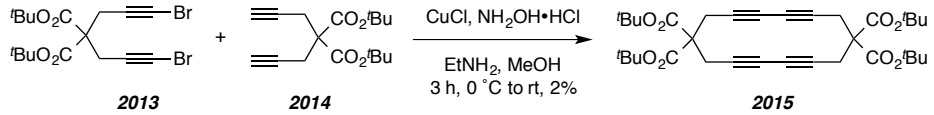

2013 ***2014*** ***2015***

[*BPW II-067*] CuCl (400 mg, 4.0 mmol) was added to a solution of MeOH/$EtNH_2$ (100:10 mL) and cooled to 0 °C. A spatula-tip of $NH_2OH \cdot HCl$ was added and the blue solution turned colorless. The diynes **2013** and **2014** were dissolved in 20 mL MeOH and added dropvise via an additional funnel over 0.5 h while the flask remained in an ice-bath. After all the alkynes were added the flask warmed to room temperature and stirred an additional 1 h. Water (20 mL) was added to quench the reaction and then most of the MeOH was removed via rotary evaporation. The green solution was extracted with Et_2O (3 × 25 mL), washed with aq. NH_4Cl (3 × 25 mL), brine, and dried ($MgSO_4$). The crude product isolated after solvent removal was purified via MPLC (10:1 Hex:EtOAc) to give the macrocycle **2015** (9 mg, 0.02 mmol, 2%).

^{1}H NMR (500 MHz, $CDCl_3$): δ 2.80 (s, 8H, C*H*$_2$C≡C), and 1.47 [s, 36H, $CO_2C(CH_3)_3$].

^{13}C NMR (125 MHz, $CDCl_3$): δ 167.9, 82.9, 75.1, 69.7, 55.2, 27.9, and 26.2.

LC / LR-MS [ES+APCI, 100 % Solvent B, 10 min run]: t_R 5.5 min; *m/z* 598 [M+NH_4^+].

TLC R_f 0.2 (10:1 hexanes:EtOAc).

Cyclotetradeca-3,5,10,12-tetrayne-1,8-diyl diacetate (2003)

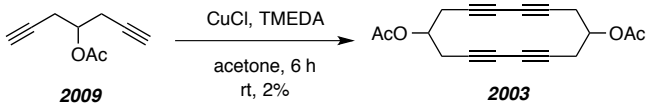

2009 ***2003***

[*BPW II-022*] Hay's catalyst was prepared by adding tetramethylethylenediamine (250 µL, 1.7 mmol) to a solution of copper (I) chloride (500 mg, 5.0 mmol) in 25 mL acetone and stirred for 15 minutes. A solution of diyne **2009** (100 mg, 0.7 mmol) in 5 mL acetone was added and the mixture was stirred for 6 h. Water was added (20 mL) the mixture was extracted with Et_2O (3 x 25 mL), washed with brine, dried ($MgSO_4$), filtered, and concentrated under reduced pressure. Purification by HPLC (1:1 hexanes:EtOAc) afforded **2003** as a clear, yellow oil (1.5 mg, 0.005 mmol, 2%).

^{1}H NMR (500 MHz, $CDCl_3$ diastereomer 1): δ 5.00 (br p, *J* = 5.9 Hz, 2H, C*H*OAc), 2.63 (d, *J* = 5.9 Hz, 8H, CH_2C≡C), and 2.08 (s, 6H, OCH_3).

^{1}H NMR (500 MHz, $CDCl_3$ diastereomer 2): δ 5.00 (br p, *J* = 5.9 Hz, 2H, C*H*OAc), 2.63 (d, *J* = 5.9 Hz, 8H, CH_2C≡C), and 2.07 (s, 6H, OCH_3).

LC / LR-MS [ES+APCI, 100 % Solv B, 10 min run]: t_R 4.3 min; *m/z* 314 [M+NH_4^+].

TLC R_f 0.3 (1:1 hexanes:EtOAc).

Hepta-1,6-diyn-4-yl methanesulfonate (S2001)

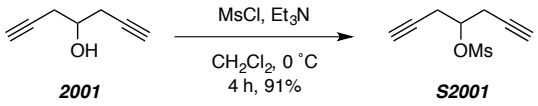

2001 ***S2001***

[*BPW II-027*] A solution of diyne **2001** (216 mg, 2.0 mmol) in CH_2Cl_2 (5 mL) was cooled to 0 °C in an ice-bath. Triethylamine (0.42 mL, 3 mmol) and methanesulfonyl chloride (185 µL, 2.4 mmol) were added and the reaction allowed to warm to room temperature. After 4 h, the solvent was removed via rotary evaporation and the remaining mixture partitioned between Et_2O and water (15:15 mL). The aqueous layer was washed with Et_2O (3 × 10 mL) and the combined organic extracts washed with brine, dried ($MgSO_4$) and concentrated. The crude product mixture

was purified via flash chromatography (3:1 Hex:EtOAc) to give the diyne **S2001** (340 mg, 1.8 mmol, 91%) as a clear oil.

^{1}H NMR (500 MHz, $CDCl_3$): δ 4.83 (tt, *J* = 6.0, 6.0 Hz, 1H, C*H*OSO_2CH_3), 3.12 (s, 3H, OSO_2CH_3), 2.77 (dt, *J* = 5.8, 2.7 Hz, 4H, $CH_2C{\equiv}CH$), and 2.11 (t, *J* = 2.7 Hz, 2H, C≡C*H*).

LR ESI-MS: $[M–C_3H_3]^+$ requires 147.0; found 147.1.

TLC R_f 0.4 (2:1 hexanes:EtOAc).

Cyclotetradeca-3,5,10,12-tetrayne-1,8-diyl dimethanesulfonate (1019)

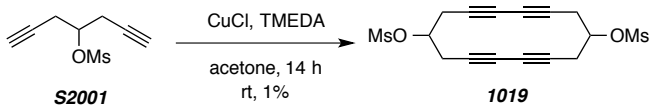

S2001 ***1019***

[*BPW II-029*] Hay's catalyst was prepared by adding tetramethylethylenediamine (375 µL, 2.6 mmol) to a solution of copper (I) chloride (750 mg, 7.5 mmol) in 125 mL acetone and stirred for 15 minutes. Diyne **S2001** (180 mg, 1.0 mmol) was added and the mixture was stirred for 6 h. The majority of solvent removed via rotary evaporation, water was added (20 mL), and the mixture was extracted with EtOAc (3 x 25 mL), washed with brine, dried ($MgSO_4$), filtered, and concentrated under reduced pressure. Purification by MPLC (2:1 hexanes:EtOAc) separated the acyclic dimer and trimer from a third, broad peak on the MPLC trace, which was concentrated and purified via HPLC (2:1 hexanes:EtOAc) to afford **1019** as a yellow oil (2 mg, 0.005 mmol, 1%).

^{1}H NMR (500 MHz, $CDCl_3$): δ 4.91 (tt, *J* = 5.5, 5.5 Hz, 2H, C*H*OSO_2CH_3), 3.09 (s, 6H, SO_2CH_3), and 2.80 (d, *J* = 5.8 Hz, 8H, $CH_2C{\equiv}C$).

LC / LR-MS [ES+APCI, 50-100 % Solv B 15 min, 22 min run]: t_R 4.8 min; *m/z* 386 $[M^+]$.

TLC R_f 0.xx (1:2 hexanes:EtOAc).

Experimental Section for Chapter 3

1-(2-(6-((*tert*-Butyldimethylsilyl)oxy)hexa-1,3-diyn-1-yl)cyclohex-1-en-1-yl)-3-(trimethylsilyl)prop-2-yn-1-yl acetate (3053)

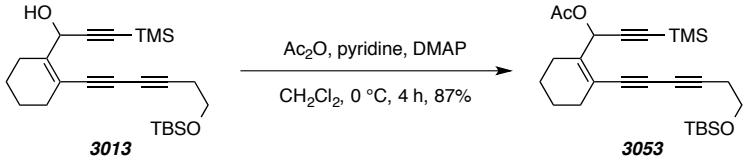

3013 ***3053***

[BPW V-087] Acetic anhydride (64 mg, 0.62 mmol) was added to a stirred solution of alcohol **3103** (52 mg, 0.13 mmol), pyridine (1.2 mL, 15.3 mmol), and DMAP (3 mg, 0.024 mmol) in CH_2Cl_2 (5 mL) at 0 ºC. After 4 h the reaction mixture was diluted with water and extracted with CH_2Cl_2. The combined organic extracts were washed with brine, dried ($MgSO_4$), and concentrated. The crude material was passed through a plug of silica gel with (hexanes:EtOAc 19:1 eluent) to give the acetate **3053** (50 mg, 0.11 mmol, 87%).

^{1}H NMR (500 MHz, $CDCl_3$): δ 6.46 (s, 1H, C*H*OAc), 3.76 (t, *J* = 7.2 Hz, 2H, SiOCH_2), 2.55 (t, *J* = 7.2 Hz, 2H, ºCCH_2), 2.39 [br d, *J*= 19 Hz, 1H,CH_aH$_b$C(CHOAc)=C], 2.20 [m, 3H, CH_aH$_b$C(CHOAc)=C and CH_2C=], 2.08 [s, 3H, C(=O)CH_3], 1.63 (nfom, 4H, CH_2(CH_2)$_2$CH_2), 0.90 [s, 9H, SiC(CH_3)$_3$], 0.17 [s, 9H, Si(CH_3)$_3$], and 0.08 [s, 6H, Si(CH_3)$_2$C].

^{13}C NMR (125 MHz, $CDCl_3$): δ 169.4, 142.6, 119.6, 100.9, 91.2, 82.7, 80.4, 78.9, 73.1, 66.2, 61.6, 30.1, 26.0, 24.4, 24.2, 22.0, 21.9, 21.2, 18.5, -0.1, and -5.2.

IR (neat): 2933, 2859, 2177, 1750, 1251, 1223, 1108, 1019, 947, 843, and 778 cm^{-1}.

HRMS (ESI-TOF): Calcd for $C_{26}H_{40}NaO_3Si_2^+$ [M+Na$^+$] requires 479.2408; found 479.2390.

TLC: R_f 0.5 (9:1 Hex/EtOAc).

10-(*tert*-Butyldimethylsilyl)-4-(trimethylsilyl)-3,5,6,7,8,9-hexahydro-2*H*-fluoreno[3,2-*b*]furan-5-yl acetate (1019)

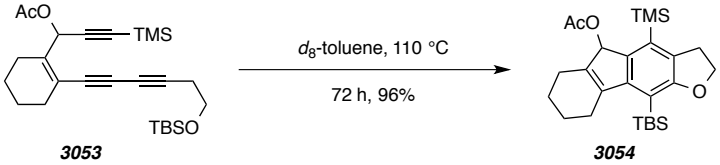

3053 ***3054***

[BPW V-160] A solution of triyne **3053** (28 mg, 0.061 mmol) in d_8-toluene (0.6 mL) was heated at 110 ºC (external bath temperature) in a sealed tube. After 72 h the solvent was evaporated and the crude residue was purified by flash chromatography (hexanes:EtOAc 49:1) to give the benzenoid **3054** (27 mg, 0.059 mmol, 96%).

^{1}H NMR (500 MHz, $CDCl_3$): δ 6.08 (d, *J* = 1.4 Hz, 1H, C*H*OAc), 4.47 (ddd, *J* =5.6 ,8.4, 10.0 Hz, 1H,OCH_aH_b), 4.30 (ddd, *J* = 9.0, 9.0, 9.0 Hz, 1H, OCH_aH_b), 3.27 (ddd, *J* = 9.7, 9.7, 15.1 Hz, 1H, ArCH_aH_b), 3.05 (ddd, *J* = 5.6, 9.4, 15.1 Hz, 1H, ArCH_aH_b), 2.49 [br d, *J* = 16.5 Hz, 1H, CH_aH_bC(CHOAc)=C], 2.36–2.47 [m, 3H, CH_aH_bC(CHOAc)=C and CH_2C=], 2.15 [s, 3H, C(=O)CH_3], 1.5–1.8 [m, 4H, $CH_2(CH_2)_2CH_2$], 0.99 [s, 9H, SiC(CH_3)$_3$], 0.344 [s, 6H, Si(CH_3)], 0.340 [s, 6H, Si(CH_3)$_2$C], and 0.33 [s, 9H, Si(CH_3)$_3$].

^{13}C NMR (125 MHz, $CDCl_3$): δ 171.7, 166.6, 151.3, 141.6, 141.5, 139.5, 132.8, 127.5, 113.4, 78.6, 69.7, 31.7, 28.4, 26.9, 25.5, 23.2, 22.5, 22.0, 19.1, 1.8, 1.4, and 1.2.

HR ESI-MS: Calcd for $C_{26}H_{40}NaO_3Si_2^+$ [M+Na^+] requires 479.2408; found 479.2414.

IR: 2929, 2856, 1737, 1370, 1301, 1255, 1225, 1015, 838, and 810 cm^{-1}.

TLC: R_f 0.52 (9:1 Hex/EtOAc).

7-((*tert*-Butyldimethylsilyl)oxy)hepta-2,4-diyn-1-ol (S3001)

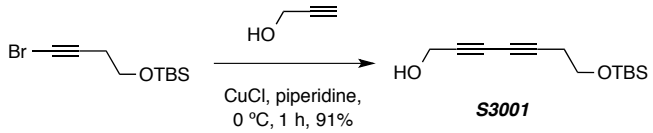

[BPW V-181] Diyne **S3001** was prepared following general procedure B from ((4-bromobut-3-yn-1-yl)oxy)(*tert*-butyl)dimethylsilane[141] (1.00 g, 3.82 mmol), propargyl alcohol (260 mg, 4.6 mmol), CuCl (40 mg, 0.40 mmol), and piperidine (4 mL). Purification by flash chromatography (hexanes:EtOAc 5:1) gave the diyne **S3001** (828 mg, 3.48 mmol, 91%) as a pale yellow oil.

^{1}H NMR (500 MHz, $CDCl_3$): δ 4.32 (dt, *J* = 6.3, 1.1 Hz, 2H, CH_2OH), 3.74 (t, *J* = 6.9 Hz, 2H, CH_2OSi), 2.50 (dt, *J* = 6.9, 1.1 Hz, 2H, C≡CC$H_2$$CH_2$), 1.55 (t, *J* = 6.3 Hz, 1H, CH_2O*H*), 0.90 [s, 9H, SiC(CH_3)$_3$], and 0.08 [s, 6H, Si(CH_3)$_2$].

^{13}C NMR (500 MHz, $CDCl_3$): δ 78.9, 73.9, 70.9, 65.6, 61.4, 51.7, 26.0, 23.9, 18.5, and -5.2.

---

[141] Villeneuve, K.; Riddell, N.; Jordan, R. W.; Tsui, G. C.; Tam, W. Ruthenium-catalyzed [2 + 2] cycloadditions between bicyclic alkenes and alkynyl halides. *Org. Lett.* **2004***, 6*, 4543–4546.

IR (neat): 3450, 2953, 2930, 2857, 2359, 2258, 1470, 1387, 1255, 1106, 913, 838, 778, and 746 cm^{-1}.

HRMS (ESI-TOF): Calcd for $C_{13}H_{22}NaO_2Si^+$ [M+Na^+] requires 261.1281; found 261.1301.

***tert*-Butyl((7-iodohepta-3,5-diyn-1-yl)oxy)dimethylsilane (S3002)**

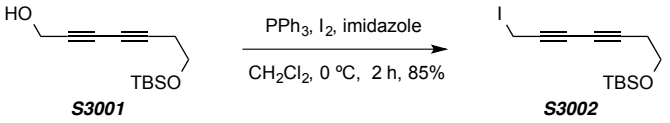

[BPW V-199] PPh_3 (288 mg, 1.1 mmol), I_2 (305 mg, 1.2 mmol), and imidazole (136 mg, 2.0 mmol) were sequentially added to a stirred solution of alcohol **S3001** (238 mg, 1.0 mmol) in CH_2Cl_2 (5 mL) at 0 °C. After 2 h the reaction mixture was diluted with CH_2Cl_2 and washed with satd. aq. $Na_2S_2O_3$. The organic extract was washed with brine, dried (Na_2SO_4), and concentrated. Purification by flash chromatography (hexanes:EtOAc 10:1) gave the iodide **S3002** (295 mg, 0.85 mmol, 85%) as a pale yellow oil.

^{1}H NMR (500 MHz, $CDCl_3$): δ 3.739 (t, *J* = 1.2 Hz, 2H, IC*H*$_2$), 3.737 (t, *J* = 7.0 Hz, 2H, SiOC*H*$_2$), 2.49 (tt, *J* = 7.0, 1.3 Hz, 2H, SiCH_2C*H*$_2$), 0.89 [s, 9H, SiC(C*H*$_3$)$_3$], and 0.07 [s, 6H, Si(*CH*$_3$)$_2$].

^{13}C NMR (125 MHz, C_6D_6): δ 80.9, 73.8, 71.4, 67.3, 61.9, 26.6, 24.5, 19.0, 4.7, and -18.5.

IR (neat): 2953, 2929, 2856, 2251, 1687, 1469, 1410, 1386, 1361, 1254, 1143, 1104, 1055, 1006, 909, and 838 cm^{-1}.

HRMS (CIMS): Calcd for $C_{13}H_{15}INOSi^+$ [M+NH_4^+] requires 366.0745; found 366.0773.

***N*-(7-((*tert*-Butyldimethylsilyl)oxy)hepta-2,4-diyn-1-yl)-*N*-phenylpropiolamide (3055)**

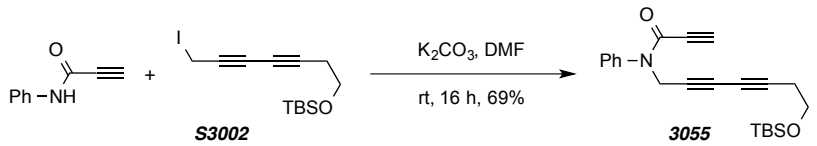

[BPW V-268] K_2CO_3 (207 mg, 1.5 mmol) was added to a stirred solution of *N*-phenylpropiolamide[142] (116 mg, 0.75 mmol) and iodide **S3002** (260 mg, 0.8 mmol) in DMF (7.0 mL) at rt. After 16 h the reaction mixture was diluted with water and washed repeatedly with EtOAc. The combined organic extracts were washed with brine, dried ($MgSO_4$) and concentrated.

---

[142] Bio, M.; Nkepang, G.; You, Y. Click and photo-unclick chemistry of aminoacrylate for visible light-triggered drug release. *Chem. Commun.* **2012**, *48*, 6517–6519.

The residue was purified by flash chromatography (hexanes:EtOAc 5:1) to give the amide **3055** (190 mg, 0.52 mmol, 69%) as a pale yellow oil.

^{1}H NMR (500 MHz, $CDCl_3$, as an 8:1 mixture of rotamers): major rotamer: δ 7.47-7.39 (m, 3H, ArH_mH_p), 7.35 (dd, J = 7.9, 1.7 Hz, 2H, ArH_o), 4.58 (t, J = 1.1 Hz, 2H, ArNCH_2), 3.72 (t, J = 6.9 Hz, 2H, SiOCH_2), 2.83 (s, 1H, C≡CH), 2.46 (tt, J = 6.9, 1.2 Hz, 2H, $SiOCH_2CH_2$), 0.89 [s, 9H, $SiC(CH_3)_3$], and 0.06 [s, 6H, $Si(CH_3)_2$]. Minor rotamer: δ 4.75 (t, J = 1.1 Hz, ArNCH_2), 3.74 (br t, J = 7.0 Hz, SiOCH_2), 2.49 (br t, J = 7.0 Hz, $SiOCH_2CH_2$), and 0.07 [s, 6H, $Si(CH_3)_2$].

^{13}C NMR (125 MHz, $CDCl_3$): δ 152.7, 140.5, 129.5, 129.0, 128.5, 80.5, 77.7, 75.8, 70.1, 69.6, 65.8, 61.4, 38.8, 26.0, 23.8, 18.4, and -5.2.

IR (neat): 3284, 2953, 2929, 2856, 2259, 2110, 1717, 1646, 1594, 1494, 1469, 1384, 1275, 1255, 1220, 1105, and 839.

HRMS (ESI-TOF): Calcd for $C_{22}H_{27}NNaO_2Si^+$ [M+Na^+] requires 388.1703; found 388.1736.

7-((*tert*-Butyldimethylsilyl)oxy)hepta-2,4-diyn-1-yl Propiolate (3059)

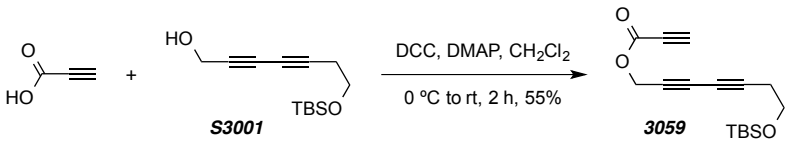

[BPW V-263] DCC (206 mg, 1.0 mmol) was added to a stirred solution of propiolic acid (70 mg, 1.0 mmol), alcohol **S3001** (119 mg, 0.50 mmol), and DMAP (12 mg, 0.1 mmol) in CH_2Cl_2 (5 mL) at 0 ºC. After 2 h the mixture was passed through a plug of Celite® (EtOAc eluent) and concentrated. Purification by flash chromatography (hexanes:EtOAc 12:1) gave the ester **3059** (80 mg, 0.28 mmol, 55%) as a pale yellow oil.

^{1}H NMR (500 MHz, $CDCl_3$): δ 4.83 (t, J = 1.1 Hz, 2H, CO_2CH_2), 3.74 (t, J = 6.9 Hz, 2H, OCH_2), 2.94 (s, 1H, C≡CH), 2.50 (tt, J = 1.1, 6.9 Hz, 2H, OCH_2CH_2), 0.90 [s, 9H, $SiC(CH_3)_3$] and 0.07 [s, 6H, $Si(CH_3)_2$].

^{13}C NMR (125 MHz, $CDCl_3$): δ 151.9, 79.9, 76.1, 74.0, 72.7, 68.1, 65.3, 61.3, 54.2, 26.0, 23.9, 18.4, and -5.2.

IR (neat): 3289, 2953, 2931, 2836, 2857, 2262, 2123, 1724, 1470, 1367, 1257, 1206, 1105, and 839cm^{-1}.

HRMS (CIMS): Calcd for $C_{16}H_{22}NaO_3Si^+$ [M+Na^+] requires 313.1230; found 313.1252.

8-(*tert*-Butyldimethylsilyl)-2,3-dihydrobenzo[1,2-b:4,5-c']difuran-5(7*H*)-one (3060)

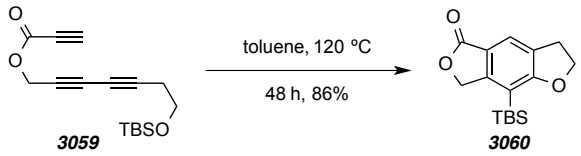

*[BPW V-267]*A solution of triyne **3059** (29 mg, 0.10 mmol) in toluene (4 mL) was heated to 120 ºC (external bath temperature) in a sealed tube. After 48 h the reaction mixture was concentrated and purified by flash chromatography (hexanes:EtOAc 4:1) gave the tricycle **3060** (25 mg, 0.086, 86%) as a white solid.

^{1}H NMR (500 MHz, $CDCl_3$): δ 7.67 (t, *J* = 1.4 Hz, 1H, Ar*H*), 5.20 (s, 2H, ArCH_2O), 4.64 (t, *J* = 8.7 Hz, 2H, $ArCH_2CH_2$), 3.25 (dt, *J* = 8.7, 1.2 Hz, 2H, $ArCH_2CH_2$), 0.89 [s, 9H, $SiC(CH_3)_3$], and 0.33 [s, 6H, $Si(CH_3)_2$].

^{13}C NMR (125 MHz, $CDCl_3$): δ 171.5, 171.4, 155.3, 128.7, 123.2, 117.9, 111.4, 71.9, 71.2, 28.7, 26.7, 18.6, and 3.8.

IR (neat): 2949, 2927, 2902, 2855, 1747, 1589, 1459, 1400, 1360, 1325, 1259, 1099, 1023, 1013, 881, and 839 cm^{-1}.

HRMS (CIMS): Calcd for $C_{16}H_{22}NaO_3Si^+$ [M+Na^+] requires 313.1230; found 313.1237.

mp: 167–169 ºC.

***tert*-Butyldimethyl((7-(prop-2-yn-1-yloxy)hepta-3,5-diyn-1-yl)oxy)silane (S3003)**

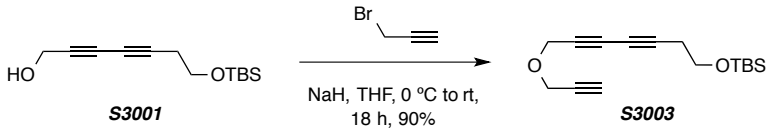

[BPW II-270] A solution of diyne **S3001** (200 mg, 0.84 mmol) in THF (2 mL) was added to a stirred suspension of NaH (67 mg, 60% suspension in mineral oil, 1.68 mmol) in THF (10 mL) at 0 ºC. The reaction mixture was allowed to warm to rt over 1 h and propargyl bromide (0.19 mL, 80 wt. % in toluene, 1.71 mmol) was added. After 18 h the mixture was cooled to 0 ºC, water was added, and the aqueous layer was extracted with diethyl ether. The combined organic extracts were washed with brine, dried ($MgSO_4$), and concentrated. Purification by flash chromatography (hexanes:EtOAc 20:1) gave the triyne **S3003** (210 mg, 0.76 mmol, 90%) as a clear yellow oil.

^{1}H NMR (500 MHz, $CDCl_3$): δ 4.32 (t, *J* = 1.1 Hz, 2H, C≡CC≡CC*H*$_2$O), 4.25 (d, *J* = 2.4 Hz, 2H, OC*H*$_2$C≡CH), 3.74 (t, *J* = 7.0 Hz, 2H, C*H*$_2$OSi), 2.50 (tt, *J* = 1.0, 7.0 Hz, C*H*$_2$CH$_2$OSi) 2.46 (t, *J* = 2.4 Hz, 1H, ≡C*H*), 0.90 [s, 9H, SiC(C*H*$_3$)$_3$], and 0.08 [s, 6H, Si(C*H*$_3$)$_2$].

^{13}C NMR (125 MHz, $CDCl_3$): δ 78.8, 78.6, 75.3, 72.0, 71.1, 65.6, 61.4, 57.1, 56.6, 26.0, 23.8, 18.4, and -5.2.

IR (neat): 3300, 2953, 2931, 2857, 2258, 1470, 1385, 1346, 1255, 1085, 839, and 779 cm^{-1}.

HRMS (ESI-TOF): Calcd for $C_{16}H_{24}NaO_2Si^+$ [M+Na$^+$] requires 299.1438; found 299.1422.

Ethyl 4-((7-((*tert*-Butyldimethylsilyl)oxy)hepta-2,4-diyn-1-yl)oxy)but-2-ynoate (3061)

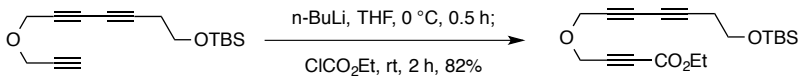

S3003 ***3061***

[BPW II-272] *n*-BuLi (0.25 mL, 2.5 M in hexanes, 0.62 mmol) was added to a stirred solution of triyne **S3003** (170 mg, 0.62 mmol) in THF (5 mL) at 0 ºC. After 0.5 h ethyl chloroformate (0.24 mL, 2.5 mmol) was added and the resulting solution was allowed to come to room temperature. After 2 h satd. aq. NH_4Cl was added and the mixture was extracted with EtOAc. The combined organic extracts were washed with brine, dried ($MgSO_4$), and concentrated. Purification by MPLC (hexanes:EtOAc 7:1) gave the triyne **3061** (178 mg, 0.51 mmol, 82%) as a clear amber oil.

^{1}H NMR (500 MHz, $CDCl_3$): δ 4.39 (s, 2H, C*H*$_2$C≡CCO$_2$Et), 4.33 (t, *J* = 1.0 Hz, 2H, C≡CC≡CC*H*$_2$O), 4.25 (q, *J* = 7.2 Hz, 2H, C*H*$_2$CH$_3$), 3.75 (t, *J* = 6.9 Hz, 2H, C*H*$_2$OSi), 2.50 (tt, *J* = 1.0, 6.9 Hz, ≡CC*H*$_2$CH$_2$) 1.32 (t, *J* = 7.2 Hz, 3H, CH$_2$C*H*$_3$), 0.90 [s, 9H, SiC(C*H*$_3$)$_3$], and 0.08 [s, 6H, Si(C*H*$_3$)$_2$].

^{13}C NMR (125 MHz, $CDCl_3$): δ 153.1, 82.2, 79.0, 78.8, 72.6, 70.4, 65.5, 62.3, 61.4, 57.7, 56.2, 26.0, 23.8, 18.4, 14.1, and -5.2.

IR (neat): 2953, 2931, 2857, 2255, 1716, 1249, 1097, 1059, 839, and 780 cm^{-1}.

HRMS (ESI-TOF): Calcd for $C_{19}H_{28}NaO_4Si^+$ [M+Na$^+$] requires 371.1649; found 371.1679.

Ethyl 8-(*tert*-Butyldimethylsilyl)-2,3,5,7-tetrahydrobenzo[1,2-*b*:4,5-*c'*]difuran-4-carboxylate (3062)

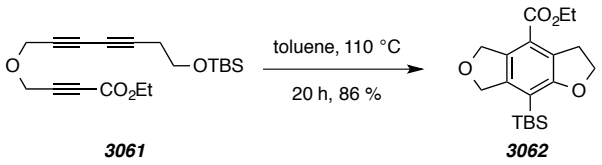

3061 ***3062***

[BPW II-267] A solution of triyne **3061** (23 mg, 0.066 mmol) in toluene (3 mL) was heated at 110 ºC (external bath temperature) in a sealed tube. After 20 h the mixture was concentrated and purified by MPLC (hexanes:EtOAc 7:1) to give the tricyclic ester **3062** (20 mg, 0.057 mmol, 86%) as a clear yellow oil.

^{1}H NMR (500 MHz, $CDCl_3$): δ 5.27 (br t, J = 2.2 Hz, 2H, OCH_2C_{Ar}=$C_{Ar}CO$), 5.06 (br s, 2H, OCH_2C_{Ar}=$C_{Ar}Si$), 4.53 (t, J = 8.8 Hz, 2H, CH_2CH_2O), 4.34 (q, J = 7.1 Hz, 2H, CH_2CH_3), 3.49 (br t, J = 8.8 Hz, 2H, CH_2CH_2O), 1.38 (t, J = 7.1 Hz, 3H, CH_2CH_3), 0.90 [s, 9H, $SiC(CH_3)_3$], and 0.31 [s, 6H, $Si(CH_3)_2$].

^{13}C NMR (125 MHz, $CDCl_3$): δ 166.9, 166.3, 146.5, 132.0, 127.9, 122.1, 116.2, 74.7, 74.5, 71.2, 61.0, 31.0, 26.8, 18.6, 14.5, and -3.4.

IR (neat): 2953, 2923, 2856, 1715, 1464, 1387, 1256, 1186, and 1038 cm^{-1}.

HRMS (ESI-TOF): Calcd for $C_{19}H_{28}NaO_4Si^+$ [M+Na^+] requires 371.1649; found 371.1674.

Dimethyl 2,2-Di(prop-2-yn-1-yl)malonate

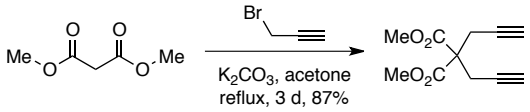

[BPW II-106] Propargyl bromide (7.8 mL, 80 wt. % in toluene, 70 mmol) was added to a stirred suspension of dimethyl malonate (2.00 mL, 17.5 mmol) and K_2CO_3 (5.32 g, 38.5 mmol) in acetone (30 mL) under a N_2 atmosphere and the mixture was brought to reflux (ca. 60 ºC). After 3 d the reaction mixture was diluted with water and extracted with CH_2Cl_2. The combined organic layers were washed with brine, dried ($MgSO_4$), and concentrated. Purification by flash chromatography (hexanes:EtOAc 3:1) gave the dimethyl 2,2-di(prop-2-yn-1-yl)malonate (3.15 g,

15.2 mmol, 87%) as a colorless oil which solidified upon standing. The spectral data were consistent with reported values.[143]

Dimethyl 2,2-Bis(3-bromoprop-2-yn-1-yl)malonate

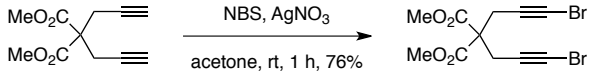

[BPW II-107] Dimethyl 2,2-bis(3-bromoprop-2-yn-1-yl)malonate was prepared following general procedure A from dimethyl 2,2-di(prop-2-yn-1-yl)malonate (1.2 g, 5.8 mmol), *N*-bromosuccinimide (2.26 g, 12.7 mmol), $AgNO_3$ (97 mg, 0.57 mmol), and acetone (40 mL). Purification by flash chromatography (hexanes:EtOAc 8:1) gave the known dibromodiyne as a clear colorless oil (2.56 g, 12.6 mmol, 76%). The spectral data were consistent with reported values.[144]

Dimethyl 2,2-Bis(8-hydroxyocta-2,4-diyn-1-yl)malonate (3065)

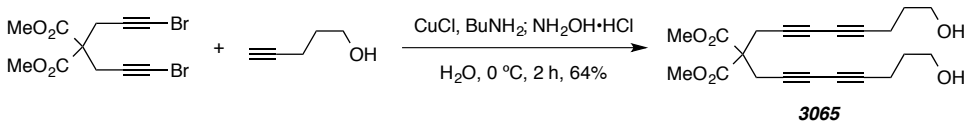

3065

[BPW II-257] CuCl (40 mg, 0.4 mmol) was added to a 30% aqueous solution of butylamine (15 mL) at 0 ºC with stirring. Hydroxylamine hydrochloride was added until the solution was colorless (~10 mg) followed by a solution of pent-4-yn-1-ol (0.2 mL, 2.2 mmol) in dichloromethane (3 mL). A solution of dimethyl 2,2-bis(3-bromoprop-2-yn-1-yl)malonate[144] (320 mg, 0.88 mmol; 5 mL CH_2Cl_2) was added dropwise to the yellow solution, and the resulting mixture allowed to come to rt. After 2 h water (10 mL) was added, the aqueous phase was extracted with CH_2Cl_2, and the combined organics were washed with satd. aq. NH_4Cl solution and brine, dried ($MgSO_4$), and concentrated. Purification by flash chromatography (hexanes:EtOAc 1:1) gave tetrayne **3065** (210 mg, 0.56 mmol, 64%) as a clear yellow oil.

^{1}H NMR (500 MHz, $CDCl_3$): δ 3.77 (s, 6H, CO_2CH_3), 3.73 (t, J = 6.1 Hz, 4H, CH_2OH), 3.06 [s, 4H, $C(CO_2Me)_2CH_2C{\equiv}C$], 2.38 (t, J = 7.0 Hz, 4H, $C{\equiv}CCH_2CH_2$), 1.77 (tt, J = 7.0, 6.1 Hz, 4H, $CH_2CH_2CH_2$), and 1.37 (br s, 2H, CH_2OH).

[143] Severa, L.; Vávra, J.; Kohoutová, A.; Čižková, M.; Šálová, T.; Hývl, J.; Saman, D.; Pohl, R.; Adriaenssens, L.; Teplý, F. Air-tolerant C–C bond formation via organometallic ruthenium catalysis: Diverse catalytic pathways involving $(C_5Me_5)Ru$ or $(C_5H_5)Ru$ are robust to molecular oxygen. *Tetrahedron Lett.***2009**, *50*, 4526–4528.

[144] Iannazzo, L.; Kotera, N.; Malacria, M.; Aubert, C.; Gandon, V. Co(I)- versus Ru(II)-catalyzed [2+2+2] cycloadditions involving alkynyl halides. *J. Organomet. Chem.* **2011**, *696*, 3906–3908.

^{13}C NMR (125 MHz, $CDCl_3$): δ 168.9, 78.1, 70.9, 68.7, 65.4, 61.4, 56.7, 53.4, 30.9, 23.9, and 15.8.

IR (neat): 3355, 2953, 2258, 1739, 1435, 1318, 1294, 1209, and 1055 cm^{-1}.

HRMS (ESI-TOF): Calcd for $C_{21}H_{24}NaO_6^+$ [M+Na^+] requires 395.1465; found 395.1461.

TLC: R_f 0.3 (1:2 Hex/EtOAc).

Dimethyl 5-(5-Hydroxypent-1-yn-1-yl)-3,4,6,8-tetrahydrocyclopenta[*g*]chromene-7,7(2*H*)-dicarboxylate (3066)

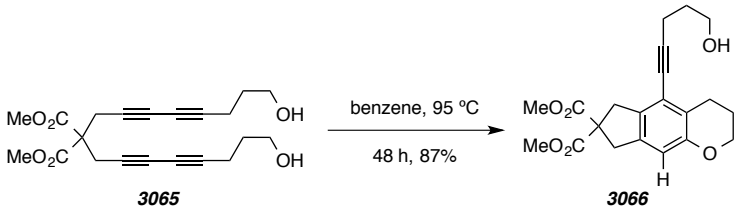

[BPW II-167] A solution of tetrayne **S23** (23 mg, 0.062 mmol) in benzene (1 mL) was heated at 95 ºC (external bath temperature) in a sealed tube. After 48 h the mixture was concentrated and the crude material was purified by MPLC (hexanes:EtOAc 1:2) to give the tricycle **3066** (20 mg, 0.054 mmol, 87%) as an amber oil.

^{1}H NMR (500 MHz, $CDCl_3$): δ 6.59 (s, 1H, Ar*H*), 4.10 (br t, *J* = 5.1 Hz, 2H, CH_2OC), 3.84 (t, *J* = 6.2 Hz, 2H, CH_2OH), 3.75 (s, 6H, CO_2CH_3), 3.56 [s, 2H, $C(CO_2Me)_2CH_2C_{Ar}{=}C_{Ar}C{\equiv}C$], 3.52 [br s, 2H, $C(CO_2Me)_2CH_2C_{Ar}{=}C_{Ar}H$], 2.79 (br t, *J* = 6.6 Hz, 2H, $CCH_2CH_2CH_2OC$), 2.61 (t, *J* = 6.9 Hz, 2H, $CH_2CH_2CH_2OH$), 1.97 (br pent, *J* = 6.5 Hz, 2H, $CCH_2CH_2CH_2OC$), and 1.88 (tt, *J* = 6.9, 6.2 Hz, 2H, $CH_2CH_2CH_2OH$).

^{13}C NMR (500 MHz, $CDCl_3$): δ 172.3, 154.4, 138.3, 134.4, 122.6, 119.9, 112.4, 97.7, 77.5, 66.2, 61.9, 60.0, 53.1, 40.9, 40.2, 31.8, 24.0, 22.3, and 16.4.

IR (neat): 3458, 2951, 2876, 2229, 1734, 1604, 1587, 1436, 1341, 1253, 1199, 1174, 1160, 1132, 1104, and 1060 cm^{-1}.

HRMS (ESI-TOF): Calcd for $C_{21}H_{24}O_6$ [M+Na^+] requires 395.1465; found 395.1495.

TLC: R_f 0.3 (1:1 Hex/EtOAc).

1,7-Dibromohepta-1,6-diyn-4-yl phenylcarbamate (S3004)

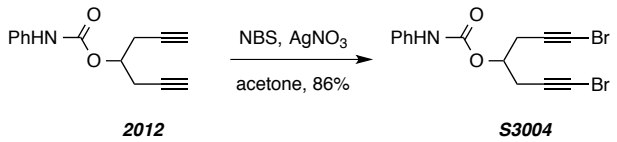

2012 ***S3004***

[*BPW II-099*] To a stirring solution of di-yne **2012** (299 mg, 1.3 mmol, 1.0 equiv) in dry acetone (15 mL) was added *N*-bromosuccinimide (515 mg, 2.9 mmol, 2.2 equiv) and silver nitrate (22 mg, 0.13 mmol, 0.1 equiv). The flask was put under a N_2 atmosphere, wrapped in aluminum foil, and stirred overnight. After addition of a solution of $Na_2S_2O_3$ (10 mL) the aqueous phase was extracted with EtOAc (3x), the combined organic extracts were washed with H_2O (3x) and brine, dried ($MgSO_4$) and concentrated under reduced pressure to give the dibromo diyne **S3004** (428 mg, 1.1 mmol, 86%) as an amber oil.

^{1}H NMR (500 MHz, $CDCl_3$): δ 7.39 (d, J = 7.7 Hz, 2H, ArH_o), 7.32 (dd, J = 7.4, 7.4 Hz, 2H, ArH_m), 7.08 (t, J = 7.3 Hz, 1H, ArH_p), 6.71 (br s, 1H, N*H*Ph), 4.98 (p, J = 5.7 Hz, 1H, C*H*OC=O), and 2.71 (d, J = 5.8 Hz, 4H, CH_2CHO).

TLC R_f 0.3 (8:1 hexanes:EtOAc).

1,17-Dihydroxyheptadeca-4,6,11,13-tetrayn-9-yl phenylcarbamate (3069)

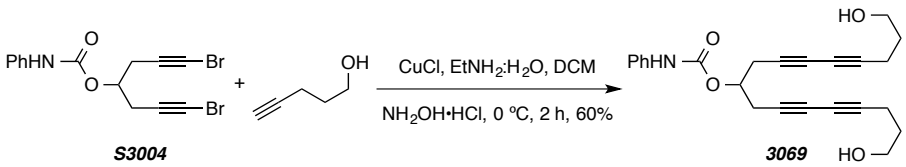

S3004 ***3069***

[*BPW II-100*] CuCl (40 mg, 0.4 mmol) was added to a 30% aqueous solution of ethylamine (10 mL) at 0 ºC with stirring. Hydroxylamine hydrochloride was added until the solution was colorless (~10 mg) followed by a solution of pent-4-yn-1-ol (160 µL mL, 1.7 mmol) in dichloromethane (3 mL). A solution of diyne **S3004** (300 mg, 0.78 mmol; 3 mL CH_2Cl_2) was added dropwise to the yellow solution, and the resulting mixture allowed to come to rt. After 2 h water (10 mL) was added, the aqueous phase was extracted with CH_2Cl_2, and the combined organics were washed with satd. aq. NH_4Cl solution and brine, dried ($MgSO_4$), and concentrated. Purification by flash chromatography (hexanes:EtOAc 1:1) gave tetrayne **3065** (183 mg, 0.47 mmol, 60%) as a clear yellow oil.

^{1}H NMR (500 MHz, $CDCl_3$): δ 7.39 (d, *J* = 7.8 Hz, 2H, ArH_o), 7.32 (dd, *J* = 7.5, 7.5 Hz, 2H, ArH_m), 7.08 (t, *J* = 7.3 Hz, 1H, ArH_p), 6.78 (br s, 1H, N*H*Ph), 4.98 (p, *J* = 5.6 Hz, 1H, C*H*OC=O), 3.75 (t, *J* = 6.1 Hz, 4H, CH_2OH), 2.77 (d, *J* = 5.7 Hz, 4H, CH_2CHOC=O), 2.40 (t, *J* = 7.0 Hz, 4H, CH_2CH$_2$CH$_2$OH), and 1.78 (p, *J* = 6.5 Hz, 4H, CH_2CH$_2$OH).

TLC R_f 0.3 (1:1 hexanes:EtOAc).

5-(5-Hydroxypent-1-yn-1-yl)-2,3,4,6,7,8-hexahydrocyclopenta[*g*]chromen-7-yl phenylcarbamate (3070)

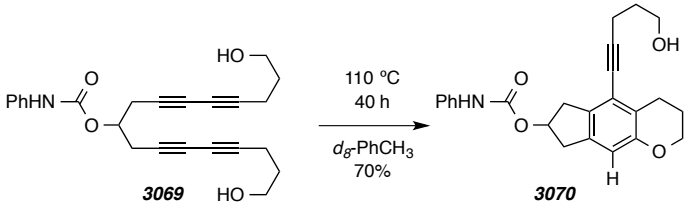

[*BPW II-103*] Tetrayne **3069** (10 mg, 0.026 mmol) in d_8-toluene (600 µL) was heated at 110 °C for 40 h. The solution was filtered through a silica plug and concentrated to give benzenoid **3070** (7 mg, 0.018 mmol, 70%) as a yellow oil.

^{1}H NMR (500 MHz, $CDCl_3$): δ 7.28-7.38 (m, 4H), 7.05 (tt, *J* = 7.4 and 1.2 Hz, 1H), 6.67 (s, CHCO), 6.56 (bs, N*H*), 5.55 (dddd, *J* = 6.1, 6.1, 2.4, 2.4 Hz, C*H*OC=O), 4.12 (bt, *J* = 5.0 Hz, CH$_2$CH$_2$CH_2OC), 3.84 (t, *J* = 6.2 Hz, CH$_2$CH$_2$CH_2OH), 3.277 (dd, *J* = 17.0, 5.8 Hz, C*H*-$_a$CHOC), 3.275 (dd, *J* = 17.0, 5.8 Hz, CH_bCHOC), 3.08 (dd, *J* = 17.3, 2.2 Hz, CH_aCC$_{ar}$H) 3.03 (dd, *J* = 17.0, 2.3, CH_bCC$_{ar}$H), 2.83 (bt, *J* = 6.5 Hz, CH_2CH$_2$CH$_2$OC), 2.60 (t, *J* = 6.9, CH_2CH$_2$CH$_2$OH), 2.00 (bp, *J* = 6.5 Hz, CH$_2$CH_2CH$_2$OC), and 1.88 (t, *J* = 6.8, 6.2 Hz, CH$_2$CH_2CH$_2$OH).

HR ESI-MS $C_{24}H_{25}NO_4$ $[M+Na]^+$ requires 414.1676; found 414.1716.

2,2,3,3,21,21,22,22-Octamethyl-4,12,20-trioxa-3,21-disilatricosa-7,9,14,16-tetrayne (3071)

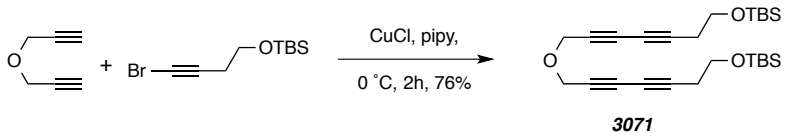

[BPW V-086] Tetrayne **3071** was prepared following the General Procedure A (Cadiot-Chodkiewicz) from ((4-bromobut-3-yn-1-yl)oxy)(tertbutyl)dimethylsilane (328 mg, 1.3 mmol), dipropargyl ether (47 mg, 0.5 mmol), CuCl (25 mg, 0.25 mmol), and piperidine (2 mL).

Purification by MPLC (hexanes:EtOAc 20:1) gave tetrayne **3071** (175 mg, 0.38 mmol, 76%) as an amber oil.

^{1}H NMR (500 MHz, $CDCl_3$): δ 4.30 (s, 4H, CH_2OCH_2), 3.74, (t, J = 7.0 Hz, 4H, CH_2OSi), 2.49 (t, J = 7.0 Hz, 4H, CH_2CH$_2$OSi), 0.90 [s, 9H, SiC(CH_3)$_3$], and 0.08 [s, 6H, Si(CH_3)$_2$].

^{13}C NMR (125 MHz, $CDCl_3$): δ 78.6, 72.1, 71.0, 65.6, 61.4, 57.2, 26.0, 23.8, 18.5, and -5.2.

IR (neat): 2955, 2930, 2857, 2259, 1255, 1107, 1082, 839, and 778 cm^{-1}.

HRMS (ESI-TOF): Calcd for $C_{26}H_{42}NaO_3Si_2^+$ [M+Na$^+$] requires 481.2565; found 481.2589.

***tert*-Butyl((4-(8-(tert-butyldimethylsilyl)-2,3,5,7-tetrahydrobenzo[1,2-b:4,5-c']difuran-4-yl)but-3-yn-1-yl)oxy)dimethylsilane (3072)**

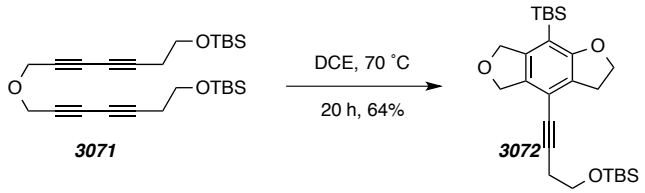

[BPW V-167] A solution of tetrayne **3071** (25 mg, 0.05 mmol) in 1,2-dichloroethane (1.1 mL) was heated in a 120 °C bath in a teflon-lined screw-capped vial. After 20 h the solvent was removed via rotary evaporation. The crude material was purified by MPLC (25:1 hexanes:EtOAc) to give the benzenoid **3072** (16 mg, 0.03 mmol, 64%) as an amber oil.

^{1}H NMR (500 MHz, $CDCl_3$): δ 5.06 (s, 2H, CH_2OC'H$_2$), 5.04 (s, 2H, CH$_2$OC'H_2), 4.51 (t, J = 8.7 Hz, 2H, CH_2OAr), 3.80 (t, J = 7.0 Hz, 2H, CH_2OSi), 3.16 (t, J = 8.7 Hz, 2H, ArCH_2CH$_2$O), 2.66 (t, J = 7.0 Hz, 2H, CH_2CH$_2$OSi), 0.91 [s, 9H, ArSiC(CH_3)$_3$], 0.87 [s, 9H, OSiC(CH_3)$_3$], 0.27 [s, 6H, ArSi(CH_3)$_2$], and 0.09 [s, 6H, OSi(CH_3)$_2$].

^{13}C NMR (125 MHz, $CDCl_3$): δ 165.8, 144.8, 132.1, 127.6, 114.9, 110.9, 94.2, 77.3, 75.9, 73.3, 70.9, 62.1, 29.3, 26.8, 26.0, 24.2, 18.6, 18.5, -3.6, and -5.1.

IR (neat): 2952, 2928, 2855, 1250, 1105, 838, and 780 cm^{-1}.

HRMS (ESI-TOF): Calcd for $C_{26}H_{42}NaO_3Si_2^+$ [M+Na$^+$] requires 481.2565; found 481.2540.

8-Methylnona-2,4-diyne-1,8-diol (3077)

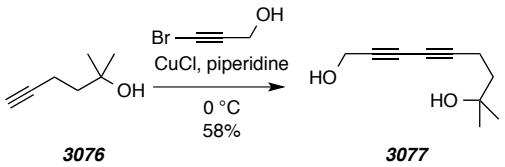

[*BPW III-051*] Diyne **3077** was prepared following the General Procedure A (Cadiot-Chodkiewicz) from 2-methylhex-5-yn-2-ol **3076** (150 mg, 1.3 mmol), bromopropargyl alcohol (268 mg, 2.0 mmol), CuCl (15 mg, 0.15 mmol), and piperidine (2 mL). Purification by flash chromatography (hexanes:EtOAc 1:1) gave diyne **3077** (125 mg, 0.75 mmol, 58%) as an amber oil.

^{1}H NMR (500 MHz, $CDCl_3$): δ 4.32 (d, *J* = 5.6 Hz, 2H, C*H*$_2$OH), 2.41 (t, *J* = 7.7 Hz, 2H, C*H*$_2$C≡C), 1.75 (t, *J* = 8.0 Hz, 2H, C*H*$_2$CH$_2$C≡C), and 1.24 [s, 6H, C(C*H*$_3$)$_2$OH].

GC-MS t_r (5025015) = 7.54 min; m/z: 166, 151, 133, 105, 91, 77, and 59.

TLC R_f 0.2 (1:1 hexanes:EtOAc).

8-Hydroxy-8-methylnona-2,4-diyn-1-yl 3-(trimethylsilyl)propiolate (3078)

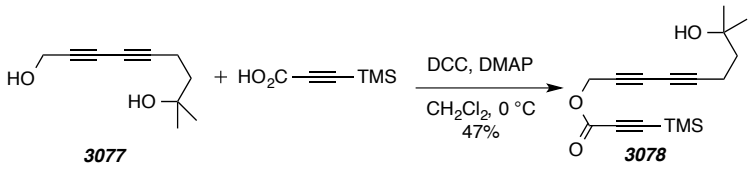

[*BPW III-054*] DCC (206 mg, 1.0 mmol) was added to a stirred solution of trimethylsilylpropiolic acid (100 mg, 0.7 mmol), alcohol **3077** (150 mg, 0.9 mmol), and DMAP (10 mg, 0.1 mmol) in CH_2Cl_2 (10 mL) at 0 ºC. After 2 h the mixture was passed through a plug of Celite® (EtOAc eluent) and concentrated. Purification by flash chromatography (hexanes:EtOAc 2:1) gave the ester **3078** (90 mg, 0.31 mmol, 47%) as a pale yellow oil.

^{1}H NMR (500 MHz, $CDCl_3$): δ 4.80 (t, *J* = 1.0 Hz, 2H, C*H*$_2$OC=O), 2.41 (tt, *J* = 7.7, 1.0 Hz, 2H, C≡CC*H*$_2$CH$_2$), 1.74 (t, *J* = 7.6 Hz, 2H, C≡CCH$_2$C*H*$_2$), 1.24 [s, 6H, C(C*H*$_3$)$_2$OH], and 0.25 [s, 9H, Si(C*H*$_3$)$_3$].

^{13}C NMR (125 MHz, $CDCl_3$): δ 152.1, 95.9, 93.7, 82.7, 72.6, 70.5, 68.4, 64.5, 53.9, 41.7, 29.3, 14.5, and -0.8.

TLC R_f 0.3 (2:1 hexanes:EtOAc).

2,2-Dimethyl-5-(trimethylsilyl)-2,3,4,8-tetrahydro-6*H*-furo[3,4-*g*]chromen-6-one (3079)

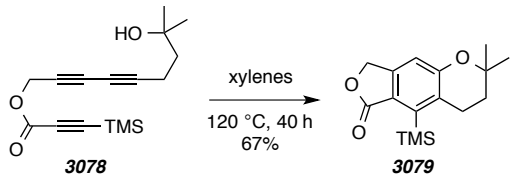

[*BPW III-088*] A solution of triyne **3078** (12 mg, 0.04 mmol) in xylenes (0.5 mL) was heated in a 120 °C bath in a teflon-lined screw-capped vial. After 40 h the solution was loaded onto a silica column and washed through with hexanes to remove xylenes. The crude material was purified by MPLC (5:1 hexanes:EtOAc) to give the benzenoid **3079** (8 mg, 0.03 mmol, 67%) as a yellow oil.

^{1}H NMR (500 MHz, $CDCl_3$): δ 6.78 (s, 1H, $C_{ar}H$), 5.14 (s, 2H, $CH_2OC{=}O$), 2.96 (t, J = 6.8 Hz, 2H, $C_{ar}CH_2$), 1.82 [t, J = 6.8 Hz, 2H, $CH_2C(CH_3)_2$], 1.36 [s, 6H, $CH_2C(CH_3)_2$], and 0.46 [s, 9H, $Si(CH_3)_3$].

^{13}C NMR (125 MHz, $CDCl_3$): δ 171.6, 158.4, 147.3, 143.0, 128.7, 122.0, 111.2, 74.8, 68.3, 33.2, 27.1, 25.1, and 2.9.

TLC R_f 0.2 (5:1 hexanes:EtOAc).

2,2-Dimethyl-5-(trimethylsilyl)-2,8-dihydro-6*H*-furo[3,4-*g*]chromen-6-one (3080)

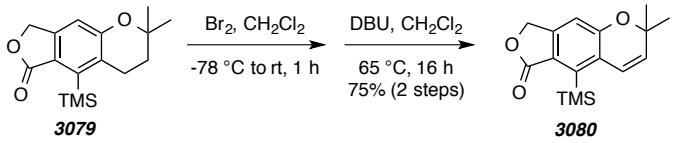

[*BPW III-125*] A solution of chromene **3079** (4 mg, 0.01 mmol) in $CDCl_3$ (200 µL) was cooled to -60 °C in a dry-ice/acetone bath. A solution of bromine (10 µL, 0.2 mmol) in $CDCl_3$ (500 µL) was added and the reaction was kept at -60 °C for 30 m and then allowed to warm to rt. After 1 h, the crude ^{1}H NMR showed full conversion of starting chromene and bromine and $CDCl_3$ were removed via rotary evaporation. This crude mixture was dissolved in 1 mL CH_2Cl_2 and DBU (5 µL, 0.03 mmol) added and heated in a sealed tube at 65 °C overnight. After solvent removal, the crude product was purified via MPLC (5:1 Hex:EtOAc) to give chromene **3080** (3 mg, 0.01 mmol, 75%) as a yellow oil.

^{1}H NMR (500 MHz, $CDCl_3$): δ 6.80 (s, 1H, $C_{ar}H$), 6.80 (d, J = 10.3 Hz, 1H, $C_{ar}CH$=CH), 5.72 (d, J = 10.3 Hz, 1H, $C_{ar}CH$=C*H*), 5.15 (s, 2H, CH_2OC=O), 1.46 [s, 6H, $CH_2C(CH_3)_2$], and 0.46 [s, 9H, $Si(CH_3)_3$].

GC-MS t_r (5025015) = 10.34 min; m/z: 288, 273, 258, 229, 199, and 129.

TLC R_f 0.2 (5:1 hexanes:EtOAc).

6-(2-(1-Hydroxy-3-(trimethylsilyl)prop-2-yn-1-yl)phenyl)hexa-3,5-diyn-1-ol (S3005-a)

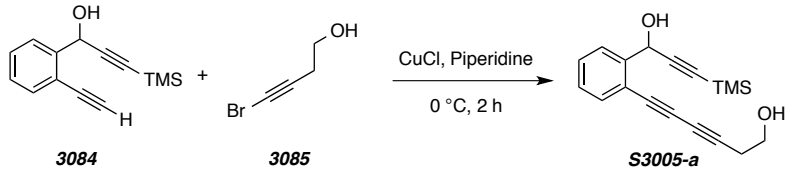

3084 ***3085*** ***S3005-a***

[*BPW II-221*] Triyne **S3005-a** was prepared following the general procedure for Cadiot-Chodkiewicz hetero-coupling from bromoalkyne **3085** (192 mg, 1.30 mmol), diyne **3084**[145] (230 mg, 1.01 mmol), CuCl (10 mg, 0.10 mmol) and piperidine (2.5 mL). The crude reaction mixture was used in the subsequent procedure without further purification, although a small amount was purified by flash chromatography (1:1 hexanes:EtOAc) for analytical purposes.

^{1}H NMR (500 MHz, $CDCl_3$): δ 7.71 (dd, J = 7.8, 1.1 Hz, 1H, $C_{aryl}H$), 7.51 (dd, J = 7.7, 1.2 Hz, 1H, $C_{aryl}H$), 7.40 (ddd, J = 7.6, 7.6, 1.3 Hz, 1H, $C_{aryl}H$), 7.29 (ddd, J = 7.6, 7.6, 1.3 Hz, 1H, $C_{aryl}H$), 5.82 (s, 1H, C*H*OH), 3.81 (t, J = 6.2 Hz, 2H, CH_2OH), 2.66 (t, J = 6.2 Hz, 2H, CH_2CH_2OH), 2.50 (br s, 1H, CHO*H*), 1.83 (br s, 1H, CH_2OH), and 0.20 [s, 9H, $Si(CH_3)_3$].

^{13}C NMR (125 MHz, $CDCl_3$): δ 143.5, 133.8, 129.7, 128.5, 127.1, 120.5, 104.2, 92.0, 82.7, 79.3, 72.6, 66.8, 63.5, 60.9, 24.2, and -0.1.

HR ESI-MS $C_{18}H_{20}O_2Si$ $[M+Na]^+$ requires 319.1125; found 319.1140.

IR: 3380, 2958, 2897, 2239, 2173, 1250, 1039 and 846 cm^{-1}.

TLC R_f 0.4 (1:1 hexanes:EtOAc).

---

[145] Suffert, J.; Abraham, E.; Raeppel, S.; Brückner, R. Synthesis of 5-/10-membered ring analogues of the dienediyne core of neocarzinostatine chromophore by palladium(0)-mediated ring-closure reaction. *Liebigs Ann.* **1996**, 447–456.

1-(2-(6-Hydroxyhexa-1,3-diyn-1-yl)phenyl)-3-(trimethylsilyl)prop-2-yn-1-one (3089-a)

[*BPW-II-284*] Triynone **3089-a** was prepared following the general procedure for MnO_2 oxidation from crude triyne **S3005-a** (87 mg, 0.3 mmol), MnO_2 (350 mg, 4 mmol), and dichloromethane (3.0 mL). Purification by MPLC (2:1 hexanes:EtOAc) gave triynone **3089-a** (80 mg, 0.27 mmol, 90%) as an amber oil.

^{1}H NMR (500 MHz, $CDCl_3$): δ = 8.11 (dd, *J* = 8.1, 1.5 Hz, 1H, $C_{aryl}H$), 7.61 (dd, *J* = 7.5, 1.5 Hz, 1H, $C_{aryl}H$), 7.51 (ddd, *J* = 7.5, 7.5, 1.5 Hz, 1H, $C_{aryl}H$), 7.46 (ddd, *J* = 7.6, 7.6, 1.4 Hz, 1H, $C_{aryl}H$), 3.80 (br dt, 2H, CH_2OH), 2.67 (t, *J* = 6.2 Hz, 2H, CH_2CH_2OH), 1.78 (br s, 1H, CH_2OH), and 0.31 [s, 9H, $Si(CH_3)_3$].

^{13}C NMR (500 MHz, $CDCl_3$): δ = 176.6, 139.1, 135.8, 132.7, 132.1, 128.7, 121.8, 101.5, 101.5, 83.4, 80.1, 73.5, 67.5, 60.9, 24.3, and -0.5.

IR (neat): 3405, 2959, 2242, 2153, 1646, 1237, 1016, and 850.

HR ESI-MS: $C_{18}H_{18}O_2Si$ $[M+Na]^+$ requires 317.0968 ; found 317.0990.

4-(Trimethylsilyl)-2,3-dihydro-5*H*-fluoreno[3,2-*b*]furan-5-one (3090-a)

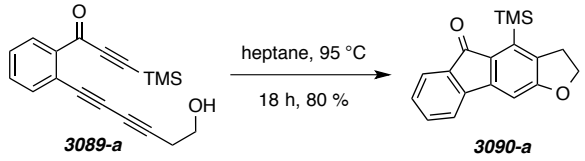

[*BPW-II-223*] A solution of triyne **3089-a** (10 mg, 0.03 mmol) in heptane (1.5 mL) was heated at 95 °C. After 18 h the mixture was concentrated and the crude material was purified by flash chromatography (15:1 hexanes:EtOAc) to give tetracycle **3090-a** (8 mg, 0.03 mmol, 80%) as a yellow solid.

^{1}H NMR (500 MHz, $CDCl_3$): δ = 7.53 (ddd, *J* = 7.3, 1.0, 1.0 Hz, 1H, Ar*H*CC=O), 7.38-7.44 (m, 2H), 7.25 (ddd, *J* = 7.2, 7.2, 1.3 Hz, 1H, Ar*H*), 6.92 (s, 1H, Ar*H*$COCH_2$), 4.63 (t, *J* = 8.8 Hz, 2H, CH_2O), and 3.27 (t, *J* = 8.8 Hz, 2H, CH_2CH_2O), and 0.40 [s, 9H, $CSi(CH_3)_3$].

^{13}C NMR (500 MHz, $CDCl_3$): δ = 193.7, 164.6, 148.2, 143.3, 138.8, 135.2, 134.0, 133.2, 132.3, 129.0, 123.4, 119.5, 103.2, 72.2, 31.4, and 1.2.

IR (neat): 2951, 2900, 1702, 1575, 1235, 1199, 866, and 844.

HR ESI-MS: $C_{18}H_{18}O_2Si$ $[M+Na]^+$ requires 317.0968 ; found 317.0980.

3-(Trimethylsilyl)-1-(2-(6-((trimethylsilyl)oxy)hexa-1,3-diyn-1-yl)phenyl)prop-2-yn-1-ol (S3005-b)

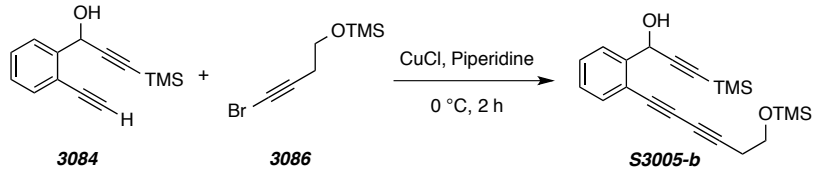

[*BPW-III-023*] Triyne **S3005-b** was prepared following the general procedure for Cadiot-Chodkiewicz hetero-coupling from bromoalkyne **3086**[146] (240 mg, 1.10 mmol), diyne **3084** (230 mg, 1.01 mmol), CuCl (10 mg, 0.10 mmol) and piperidine (2.5 mL). The crude reaction mixture was used in the subsequent procedure without further purification, although a small amount was purified by flash chromatography (10:1 hexanes:EtOAc) for analytical purposes.

^{1}H NMR (500 MHz, $CDCl_3$): δ = 7.70 (dd, *J* = 7.8, 1.4 Hz, 1H, $C_{aryl}H$), 7.50 (dd, *J* = 7.7, 1.6 Hz, 1H, $C_{aryl}H$), 7.39 (ddd, *J* = 7.6, 7.6, 1.4 Hz, 1H, $C_{aryl}H$), 7.28 (ddd, *J* = 7.6, 7.6, 1.2 Hz, 1H, $C_{aryl}H$), 5.82 (d, *J* = 5.4 Hz, 1H, C*H*OTMS), 3.76 (t, *J* = 7.1 Hz, 2H, CH_2OH), 2.60 (t, *J* = 7.1 Hz, 2H, CH_2CH$_2$OTMS), 2.50 (br s, 1H, CHO*H*) , 0.20 [s, 9H, $CSi(CH_3)_3$], and 0.15 [s, 9H, $OSi(CH_3)_3$].

^{13}C NMR (500 MHz, $CDCl_3$): δ = 143.5, 133.8, 129.6, 128.4, 127.1, 120.7, 104.2, 91.9, 83.2, 79.6, 72.3, 66.2, 63.5, 60.9, 24.1, 0.0, and -0.3.

IR (neat): 3394, 2958, 2899, 2239, 2173, 1251, 1099, 845, and 760.

HR ESI-MS: $C_{21}H_{28}O_2Si_2$ $[M+Na]^+$ requires 391.1520; found 391.1511.

---

[146] Rentsch, A.; Kalesse, M. The total synthesis of Corallopyronin A and Myxopyronin B. *Angew. Chem. Int. Ed.* **2012**, *51*, 11381–11384.

3-(Trimethylsilyl)-1-(2-(6-((trimethylsilyl)oxy)hexa-1,3-diyn-1-yl)phenyl)prop-2-yn-1-one (3089-b)

[*BPW-II-247*] Triynone **3089-b** was prepared following the general procedure for MnO_2 oxidation from crude triyne **S3005-b** (240 mg, 0.65 mmol), MnO_2 (500 mg, 5.7 mmol), and dichloromethane (6.0 mL). Purification by MPLC (10:1 hexanes:EtOAc) gave triynone **3089-b** (202 mg, 0.55 mmol, 85%) as an amber oil.

^{1}H NMR (500 MHz, $CDCl_3$): δ = 8.08 (dd, *J* = 7.8, 1.5 Hz, 1H, $C_{aryl}H$), 7.60 (dd, *J* = 7.6, 1.5 Hz, 1H, $C_{aryl}H$), 7.50 (ddd, *J* = 7.5, 7.5, 1.5 Hz, 1H, $C_{aryl}H$), 7.44 (ddd, *J* = 7.6, 7.6, 1.4 Hz, 1H, $C_{aryl}H$), 3.76 (t, *J* = 7.2 Hz, 2H, CH_2OTMS), 2.61 (t, *J* = 7.2 Hz, 2H, CH_2CH_2OTMS), 0.31 [s, 9H, CSi(CH_3)$_3$], and 0.15 [s, 9H, OSi(CH_3)$_3$].

^{13}C NMR (500 MHz, $CDCl_3$): δ = 176.6, 139.2, 135.8, 132.6, 131.9, 128.6, 122.1, 101.5, 101.5, 83.8, 80.5, 73.2, 66.8, 60.9, 24.2, -0.4, and -0.5.

IR (neat): 2957, 2874, 2360, 2340, 1649, 1251, 1234, 1102, 1015, 846, and 757.

HR ESI-MS: $C_{21}H_{26}O_2Si_2$ $[M+Na]^+$ requires 389.1364 ; found 389.1343.

4,10-Bis(trimethylsilyl)-2,3-dihydro-5*H*-fluoreno[3,2-*b*]furan-5-one (3090-b)

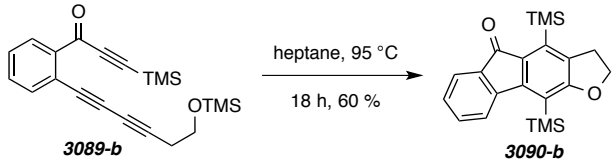

[*BPW-II-275*] A solution of triyne **3089-b** (15 mg, 0.04 mmol) in heptane (1.5 mL) was heated at 95 °C. After 18 h the mixture was concentrated and the crude material was purified by flash chromatography (15:1 hexanes:EtOAc) to give tetracycle **3090-b** (9 mg, 0.02 mmol, 60%) as a bright yellow solid.

^{1}H NMR (500 MHz, $CDCl_3$): δ = 7.57 (d, *J* = 7.6 Hz, 1H, Ar*H*CC=O), 7.55 (d, *J* = 7.2 Hz, 1H, Ar*H*CC≡C), 7.38 (ddd, *J* = 7.6, 1.3 Hz, 1H, ArH), 7.22 (ddd, *J* = 7.4, 0.8 Hz, 1H, ArH), 4.52

(t, *J* = 8.9 Hz, 2H, C*H*$_2$OC), 3.22 (t, *J* = 8.8 Hz, 2H, C*H*$_2$CH$_2$OC), 0.47 [s, 9H, Si(CH$_3$)$_3$CC-O], and 0.39, [s, 9H, Si(C*H*$_3$)$_3$CC=O].

^{13}C NMR (500 MHz, $CDCl_3$): δ = 193.8, 169.9, 154.1, 144.7, 138.9, 135.7, 133.2, 133.1, 132.1, 128.4, 124.4, 123.1, 116.9, 70.8, 31.2, 2.1, and 1.5.

IR (neat): 2952, 2898, 1702, 1606, 1506, 1381, 1291, 1247, and 846.

HR ESI-MS: $C_{21}H_{26}O_2Si_2$ $[M+Na]^+$ requires 389.1364 ; found 389.1343.

1-(2-(6-((*tert*-Butyldimethylsilyl)oxy)hexa-1,3-diyn-1-yl)phenyl)-3-(trimethylsilyl)prop-2-yn-1-ol (S3005-c)

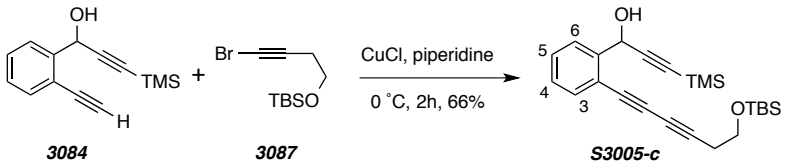

3084 ***3087*** ***S3005-c***

[BPW IV-024] Triyne **S15** was prepared following the General Procedure A (Cadiot-Chodkiewicz) from diyne **3084** (327 mg, 1.5 mmol), bromoalkyne **3087**[146] (190 mg, 0.83 mmol), CuCl (30 mg, 0.30 mmol), and piperidine (2 mL). Purification by flash chromatography (hexanes:EtOAc 6:1) gave triyne **S3005-c** (221 mg, 0.54 mmol, 66%) as a brown oil.

^{1}H NMR (500 MHz, $CDCl_3$): δ 7.69 (d, *J* = 7.8 Hz, 1H, *H3/H6*), 7.50 (d, *J* = 7.7 Hz, 1H, *H6/H3*), 7.39 (dd, *J* = 7.6, 7.6 Hz, 1H, *H4/H5*), 7.28 (dd, *J* = 7.6, 7.6 Hz, 1H, *H4/H5*), 5.82 (s, 1H, C*H*OH), 3.79 (t, *J* = 7.0 Hz, 2H, C*H*$_2$OSi), 2.59 (t, *J* = 7.0 Hz, 2H, C*H*$_2$CH$_2$OSi), 2.46 (br s, 1H, CHO*H*), 0.91[s, 9H, SiC(C*H*$_3$)$_3$], 0.20 [s, 9H, Si(C*H*$_3$)$_3$], and 0.10 [s, 6H, Si(C*H*$_3$)$_2$].

^{13}C NMR (125 MHz, $CDCl_3$): δ 143.5, 133.7, 129.5, 128.5, 127.1, 120.7, 104.2, 91.9, 83.4, 79.6, 72.2, 66.2, 63.5, 61.5, 26.0, 24.2, 18.5, 0.0, and -5.1.

IR (neat): 3424 (br), 2956, 2930, 2857, 2236, 2174, 1251, 1106, 842, and 761 cm^{-1}.

HRMS (ESI-TOF): Calcd for $C_{24}H_{34}NaO_2Si_2^+$ $[M+Na^+]$ requires 433.1990; found 433.2009.

1-(2-(6-((*tert*-Butyldimethylsilyl)oxy)hexa-1,3-diyn-1-yl)phenyl)-3-(trimethylsilyl)prop-2-yn-1-one (3089-c)

S3005-c ***3089-c***

[BPW IV-026] MnO_2 (212 mg, 2.4 mmol) was added to a stirred solution of alcohol **S3005-c** (50 mg, 0.12 mmol) in CH_2Cl_2 (1.5 mL) at room temperature. After 16 h the reaction mixture was filtered through Celite® (EtOAc eluent) and concentrated. Purification by MPLC (hexanes:EtOAc 10:1) gave the ketone **3089-c** (43 mg, 0.11 mmol, 88%) as a yellow oil.

^{1}H NMR (500 MHz, $CDCl_3$): δ 8.08 (d, *J* = 7.8 Hz, 1H, *H6*), 7.60 (d, *J* = 7.6 Hz, 1H, *H3*), 7.49 (ddd, *J* = 7.6, 7.5, 1.2 Hz, 1H, *H4*), 7.44 (t, *J* = 7.7, 7.6, 1.2 Hz, 1H, *H5*), 3.79 (t, *J* = 7.2 Hz, 2H, C*H*$_2$O), 2.59 (t, *J* = 7.2 Hz, 2H, C≡CC*H*$_2$), 0.91 [s, 9H, SiC(C*H*$_3$)$_3$], 0.30 [s, 9H, Si(C*H*$_3$)$_3$], and 0.09 [s, 6H, Si(C*H*$_3$)$_2$].

^{13}C NMR (125 MHz, $CDCl_3$): δ 176.6, 139.2, 135.8, 132.6, 131.9, 128.6, 122.1, 101.6, 101.5, 83.9, 80.6, 73.1, 66.8, 61.5, 26.0, 24.3, 18.5, -0.5, and -5.1.

IR (neat): 2956, 2930, 2858, 2244, 2153, 1649, 1252, 1234, 1108, 1014, and 844 cm^{-1}.

HRMS (ESI-TOF): Calcd for $C_{24}H_{32}NaO_2Si_2^+$ [M+Na$^+$] requires 431.1833; found 431.1839.

10-(*tert*-Butyldimethylsilyl)-4-(trimethylsilyl)-2,3-dihydro-5*H*-fluoreno[3,2-*b*]furan-5-one (3090-c)

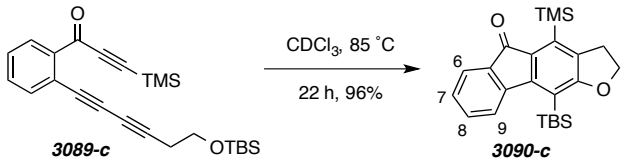

[BPW V-078] A solution of triyne **3089-c** (24 mg, 0.06 mmol) in $CDCl_3$ (2 mL) was heated at 85 °C. After 22 h the mixture was concentrated and the crude material was filtered through a plug of silica to give polycycle **3090-c** (23 mg, 0.06 mmol, 96%) as a yellow oil, which solidified upon standing.

^{1}H NMR (500 MHz, $CDCl_3$): δ 7.67 (ddd, *J* = 7.7, 0.8, 0.8 Hz, 1H, *H9*), 7.53 (ddd, *J* = 7.2, 1.3, 0.6 Hz, 1H, *H6*), 7.35 (ddd, *J* = 7.6, 7.6, 1.3 Hz, 1H, *H8*), 7.21 (ddd, *J* = 7.4, 7.4, 0.9 Hz, 1H, *H7*), 4.51 (t, *J* = 8.8 Hz, 2H, C*H*$_2$O), 3.23 (t, *J* = 8.8 Hz, 2H, C*H*$_2$CH$_2$O), 1.09 [s, 9H, SiC(C*H*$_3$)$_3$], 0.40 [s, 6H, Si(C*H*$_3$)$_2$], and 0.39 [s, 9H, Si(C*H*$_3$)$_3$].

^{13}C NMR (125 MHz, $CDCl_3$): δ 193.9, 170.6, 154.8, 144.8, 138.9, 135.5, 133.7, 132.8, 131.8, 128.4, 124.2, 123.0, 115.9, 70.7, 31.2, 28.1, 19.5, 1.6, and 0.0.

IR (neat): 2951, 2928, 2895, 2856, 1702, 1289, 1247, 843, 824 and 747 cm^{-1}.

HRMS (ESI-TOF): Calcd for $C_{24}H_{32}NaO_2Si_2^+$ [M+Na$^+$] requires 431.1833; found 431.1832.

MP: 55–58 °C.

Tri-*t*-butyl (6-(2-(3-(trimethylsilyl)propioloyl)phenyl)hexa-3,5-diyn-1-yl) silicate (3089-d)

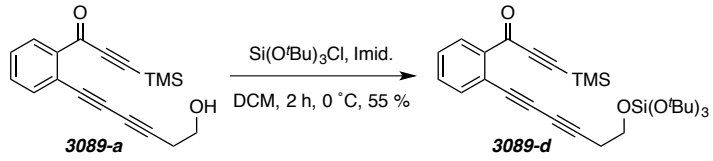

[*BPW IV-101*] To a solution of alcohol **3089-a** (100 mg, 0.34 mmol) in dichloromethane (2 mL) at 0 °C was added imidazole (50 mg, 0.74 mmol), followed by tri-*tert*-butoxylchlorosilane (143 mg, 0.48 mmol). The mixture was stirred for 2 h, filtered through silica gel and concentrated. The crude product was purified by MPLC (20:1 Hex:EtOAc) to give triyne **3089-d** (101 mg, 0.19 mmol, 55%) as a clear oil.

^{1}H NMR (500 MHz, $CDCl_3$): δ 8.06 (d, *J* = 7.7 Hz, 1H, *H6*), 7.59 (d, *J* = 7.7 Hz, 1H, *H3*), 7.49 (ddd, *J* = 7.6, 7.5, 1.3 Hz, 1H, *H4*), 7.43 (t, *J* = 7.5, 7.4, 1.2 Hz, 1H, *H5*), 3.86 (t, *J* = 7.4 Hz, 2H, C*H*$_2$O), 2.66 (t, *J* = 7.4 Hz, 2H, C≡CC*H*$_2$), 1.31 [s, 27H, Si(OC(C*H*$_3$)$_3$)$_3$], and 0.30 [s, 9H, Si(C*H*$_3$)$_3$].

^{13}C NMR (125 MHz, $CDCl_3$): δ 176.7, 139.2, 135.8, 132.6, 131.8, 128.5, 122.2, 101.6, 101.5, 84.3, 80.8, 72.95, 72.89, 66.6, 61.1, 31.5, 23.6, and -0.5.

GC-MS t_r (5027016) = 13.91 min; m/z: 540, 525, 469, 355, 339, 199, and 170.

TLC R_f 0.3 (20:1 hexanes:EtOAc).

10-(Tri-*tert*-butoxysilyl)-4-(trimethylsilyl)-2,3-dihydro-5*H*-fluoreno[3,2-*b*]furan-5-one (3090-d)

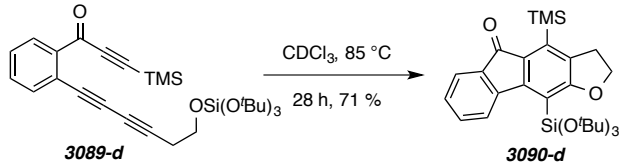

[*BPW IV-103*] A solution of triyne **3089-d** (14 mg, 0.03 mmol) in $CDCl_3$ (1.2 mL) was heated at 85 °C. After 28 h the mixture was concentrated to give tetracycle **3090-d** (10 mg, 0.02 mmol, 71%) as a bright yellow solid.

^{1}H NMR (500 MHz, $CDCl_3$): δ 8.60 (d, *J* = 7.7 Hz, 1H, *H9*), 7.49 (d, *J* = 7.2 Hz, 1H, *H6*), 7.35 (ddd, *J* = 7.6, 7.5, 1.2 Hz, 1H, *H8*), 7.18 (ddd, *J* = 7.4, 7.2, 0.6 Hz, 1H, *H7*), 4.54 (t, *J* = 8.9 Hz, 2H, C*H*$_2$O), 3.22 (t, *J* = 8.9 Hz, 2H, C*H*$_2$CH$_2$O), 1.35 [s, 27H, Si(OC(C*H*$_3$)$_3$)$_3$], and 0.39 [s, 9H, Si(C*H*$_3$)$_3$].

^{13}C NMR (125 MHz, $CDCl_3$): δ 194.3, 169.4, 154.0, 144.6, 138.7, 135.2, 133.1, 132.9, 132.4, 128.3, 127.6, 122.1, 115.8, 74.5, 70.1, 32.0, 31.1, and 1.7.

HR ESI-MS calcd for $C_{30}H_{44}NaO_5N_2$ $[M + Na]^+$ 563.2619, found 563.2636.

IR: 2976, 2933, 2902, 1703, 1507, 1382, 1364, 1296, 1244, 1186, 1048, and 845 cm^{-1}.

8-((Triisopropylsilyl)oxy)octa-2,4-diyn-1-ol (S3007)

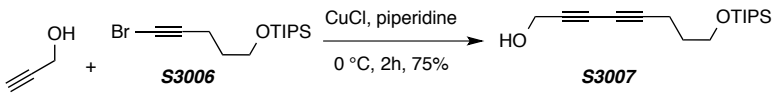

[BPW III-026] Diyne **S3007** was prepared following the General Procedure A (Cadiot-Chodkiewicz) from propargyl alcohol (0.43 mL, 7.5 mmol), bromoalkyne **S3006**[147] (1.59g, 5.0 mmol), CuCl (100 mg, 1.0 mmol), and piperidine (13 mL). Purification by flash chromatography (hexanes:EtOAc 3:1) gave diyne **S3007** (1.10 g, 3.75 mmol, 75%) as a yellow oil.

^{1}H NMR (500 MHz, $CDCl_3$): δ 4.32 (s, 2H, C*H*$_2$OH), 3.76 (t, *J* = 5.9 Hz, 2H, C*H*$_2$OSi), 2.41 (t, *J* = 7.1 Hz, 2H, C≡CC*H*$_2$), 1.76 (6.0, 7.1 Hz, 2H, C*H*$_2$CHOH), 1.04-1.08 [m, 3H, SiC*H*(CH$_3$)$_2$], and 1.06 [d, *J* = 3.3 Hz, 18H, SiCH(C*H*$_3$)$_2$].

^{13}C NMR (125 MHz, $CDCl_3$): δ 81.7, 77.4, 77.2, 76.9, 73.5, 71.1, 64.5, 61.7, 51.7, 31.6, 18.1, 15.9, 12.1

IR (neat): 2943, 2866, 2256, 1463, 1388, 1108, 1068, 1015, 882, and 684 cm^{-1}.

HRMS (ESI-TOF): Calcd for $C_{17}H_{30}NaO_2Si^+$ $[M+Na^+]$ requires 317.1907; found 317.1898.

8-((Triisopropylsilyl)oxy)octa-2,4-diyn-1-yl 3-(trimethylsilyl)propiolate (3091)

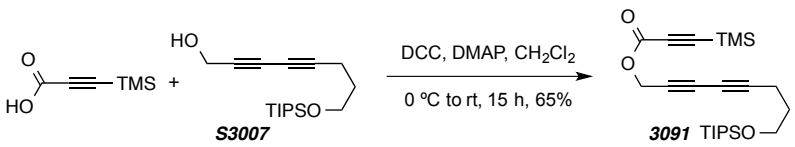

[147] Boden, C. D. J.; Pattenden, G.; Ye, T. Palladium-catalysed hydrostannylations of 1-bromoalkynes. A practical synthesis of (E)-1-stannylalk-1-enes. *J.Chem. Soc. Perk. Trans.* **1996**, 2417.

[BPW III-028] A solution of alcohol **S3007** (1.00g, 3.4 mmol) and 3-(trimethylsilyl)propiolic acid (326 mg, 2.3 mmol) in dichloromethane (12 mL) was cooled to 0 °C under a N_2 atmosphere. A separate solution of N,N'-dicyclohexylcarbodiimide (520 mg, 2.5 mmol, 1.2 equiv) and DMAP (20 mg, 0.2 mmol) in dichloromethane (5 mL) was cooled to 0 °C, added dropwise to the alcohol and acid solution and allowed to come to room temperature overnight. Dichloromethane was removed via rotary evaporation and the crude was taken up in Et_2O (50 mL) and filtered through plug of Celite, washed with H_2O (3x 50 mL), brine, dried ($MgSO_4$), and concentrated. The crude material was purified by flash chromatography (15:1 Hex:EtOAc) to give triyne **3091** (626 mg, 1.5 mmol, 65%) as an amber oil.

^{1}H NMR (500 MHz, $CDCl_3$): δ 4.80 (s, 2H, C*H*$_2$OC=O), 3.75 (t, *J* = 5.9 Hz, 2H, C*H*$_2$OSi), 2.42 (t, *J* = 7.1 Hz, 2H, C≡CC*H*$_2$), 1.75 (tt, *J* = 7.0, 5.9 Hz, 2H, C*H*$_2$CH$_2$OSi), 1.08-1.03 [m, 3H, SiC*H*(CH$_3$)$_2$], 1.05 [d, *J* = 5.1 Hz, 18H, SiCH(C*H*$_3$)$_2$], and 0.25 [s, 9H, Si(C*H*$_3$)$_3$].

^{13}C NMR (125 MHz, $CDCl_3$): δ 152.1, 95.9, 93.7, 82.6, 72.7, 68.0, 64.4, 61.7, 53.9, 31.5, 18.1, 15.9, 12.1, and -0.8.

IR (neat): 2949, 2867, 2261, 2179, 1722, 1257, 1208, 1111, and 856 cm^{-1}.

HRMS (ESI-TOF): Calcd for $C_{23}H_{38}NaO_3Si_2^+$ [M+Na$^+$] requires 441.2252; found 441.2238.

TLC R_f 0.3 (15:1 hexanes:EtOAc).

6-(3-((Diisopropyl(prop-1-en-2-yl)silyl)oxy)propyl)-7-(trimethylsilyl)isobenzofuran-1(3*H*)-one (3093)

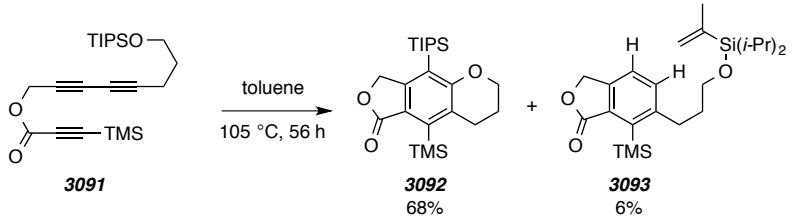

[*BPW III-034*] A solution of triyne **3091** (120 mg, 0.29 mmol) in toluene (4 mL) was heated at 105 °C. After 56 h the mixture was concentrated and the crude material was purified by MPLC (5:1 hexanes:EtOAc) to give tricycle **3092** (82 mg, 0.20 mmol, 68%) as a clear solid and tricycle **3093** (7 mg, 0.06 mmol, 6%) as a clear oil.

Characterization of 3092:

^{1}H NMR (500 MHz, $CDCl_3$): δ 5.23 (s, 2H, CH_2OC=O), 4.17 (t, J = 5.2 Hz, 2H, CH_2Oar), 2.98 (t, J = 6.5 Hz, ArCH_2), 2.00-1.95 (m, 2H, CH_2CH$_2$OAr), 1.36 [septet, J = 7.4 Hz, 3H, SiCH(CH$_3$)$_2$], 1.07 [d, J = 7.4 Hz, 18H, SiCH(CH_3)$_2$], and 0.46 [s, 9H, Si(CH_3)$_3$].

^{13}C NMR (125 MHz, $CDCl_3$): δ 171.8, 163.9, 153.7, 144.2, 128.9, 122.3, 118.7, 70.6, 65.8, 28.5, 22.5, 19.2, 12.7, and 3.1.

IR (neat): 2946, 2865, 1758, 1524, 1463, 1347, 1247, 1120, 1046, and 844 cm^{-1}.

HRMS (ESI-TOF): Calcd for $C_{23}H_{38}NaO_3Si_2^+$ [M+Na$^+$] requires 441.2252; found 441.2256.

Characterization of 3093:

^{1}H NMR (500 MHz, $CDCl_3$): δ 7.44 (d, J = 7.9 Hz, 1H, CHArCH$_2$CH$_2$), 7.34 (d, J = 7.9 Hz, 1H, CHArCCH$_2$O), 5.73 (dt, J = 3.3, 1.6 Hz, 1H, CH_2=CCH$_3$), 5.38 (dt, J = 3.3, 1.3 Hz, 1H, CH_2=CCH$_3$), 5.23 (s, 2H, CH_2OC=O), 3.73 (t, J = 6.2 Hz, 2H, CH_2OArC), 2.96 (br t, J = 8.0 Hz, 2H, ArCCH_2), 1.85 (s, 3H, CH_3C=CH$_2$), 1.78 (nfom, 2H, CH_2CH$_2$OArC), 1.01–1.07 [m, 14H, OSi(CH(CH_3)$_2$)], and 0.47 [s, 9H, Si(CH_3)$_3$].

^{13}C NMR (125 MHz, $CDCl_3$): δ 171.7, 150.4, 145.2, 142.9, 140.3, 135.7, 131.2, 128.1, 122.3, 68.8, 62.8, 37.2, 33.0, 23.7, 17.7, 17.6, 12.0, and 2.7.

IR (neat): 2944, 2867, 1759, 1459, 1353, 1249, 1091, 1030, and 850 cm^{-1}.

HRMS (ESI-TOF): Calcd for $C_{23}H_{38}NaO_3Si_2^+$ [M+Na$^+$] requires 441.2252; found` 441.2239.

6-((Triisopropylsilyl)oxy)hexa-2,4-diyn-1-ol (S3009)

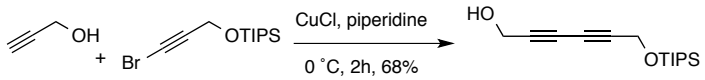

S3008 ***S3009***

[BPW IV-178] Diyne **S3009** was prepared following the General Procedure A (Cadiot-Chodkiewicz) from propargyl alcohol (0.86 mL, 15 mmol), bromoalkyne **S3008** (2.18 g, 7.5 mmol), CuCl (100 mg, 1.0 mmol), and piperidine (15 mL). Purification by flash chromatography (hexanes:EtOAc 5:1) gave diyne **S3009** (1.36 g, 5.1 mmol, 68%) as an amber oil, whose spectra matched that reported in the literature.[148]

---

[148] Xu, R.; Gramlich, V.; Frauenrath, H. Alternating Diacetylene Copolymer Utilizing Perfluorophenyl−Phenyl Interactions. *J. Am. Chem. Soc* **2006**, *128*, 5541–5547.

6-((Triisopropylsilyl)oxy)hexa-2,4-diyn-1-yl propiolate (3095)

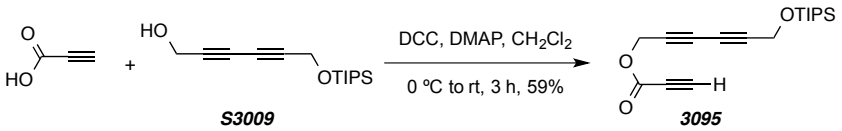

S3009 *3095*

[BPW IV-179] A solution of alcohol **S3009** (665 mg, 2.5 mmol) and propiolic acid (195 mg, 2.75 mmol) in dichloromethane (15 mL) was cooled to 0 °C under a N_2 atmosphere. N,N'-dicyclohexylcarbodiimide (550 mg, 2.75 mmol) and DMAP (30 mg, 0.25 mmol) was added and allowed to come to room temperature. After 3 h, the solution was filtered through plug of Celite, rinsing with EtOAc. After solvent removal, the crude material was purified by flash chromatography (8:1 Hex:EtOAc) to give triyne **3095** (470 mg, 1.5 mmol, 59%) as an amber oil.

^{1}H NMR (500 MHz, $CDCl_3$): δ 4.86 (s, 2H, C*H*$_2$OC=O), 4.46 (s, 2H, C*H*$_2$C≡C), 2.96 (s, 1H, C≡C*H*), 1.11 [m, 3H, SiC*H*$(CH_3)_2$], and 1.07 [d, *J* = 5.8 Hz, 18H, SiCH(C*H*$_3$)$_2$].

GC-MS t_r (5025015) = 11.34 min; m/z: 318, 275, 245, 205, 147, 119, 101, and 75.

TLC R_f 0.2 (8:1 hexanes:EtOAc).

6-(((Diisopropyl(prop-1-en-2-yl)silyl)oxy)methyl)isobenzofuran-1(3*H*)-one (3096)

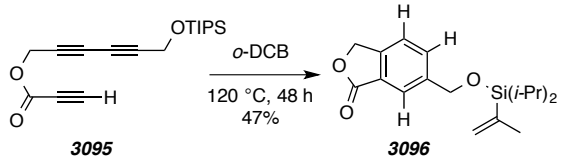

3095 *3096*

[BPW IV-181] A solution of triyne **3095** (17 mg, 0.05 mmol) in dichlorobenzene (4 mL) was heated at 120 °C. After 48 h the mixture was loaded onto a silica column and the solvent removed by washing with hexanes. The crude material was collected after washing with 1:1 Hex:EtOAC and after concentration, purified by MPLC (5:1 hexanes:EtOAc) to give benzenoid **3096** (8 mg, 0.03 mmol, 47%) as a clear oil.

^{1}H NMR (500 MHz, $CDCl_3$): δ 7.90 (s, C_{ar}*H*C_{ar}C=O), 7.70 (d, *J* = 7.8, 1.4 Hz, 1H, C_{ar}*H*$C_{ar}CH_2$OSi), 7.46 (d, *J* = 7.8 Hz, 1H, C_{ar}*H*$C_{ar}CH_2$OC=O), 5.77 (dt, *J* = 3.4, 1.7 Hz, 1H, C*H*$_2$=CCH_3), 5.40 (nfom, 1H, C*H*$_2$=CCH_3), 5.31 (s, 2H, C*H*$_2$OC=O), 4.91 (s, 2H, C*H*$_2$OSi), 1.85 (t, *J* = 1.5 Hz, 3H, C*H*$_3$C=CH_2), and 1.01–1.07 [m, 14H, OSi(C*H*$(CH_3)_2$)],.

GC-MS t_r (5025015) = 11.34 min; m/z: 318, 275, 245, 205, 147, 119, 101, and 75.

TLC R_f 0.2 (5:1 hexanes:EtOAc).

1-(2-(5-((Triisopropylsilyl)oxy)penta-1,3-diyn-1-yl)phenyl)-3-(trimethylsilyl)prop-2-yn-1-ol (S3010)

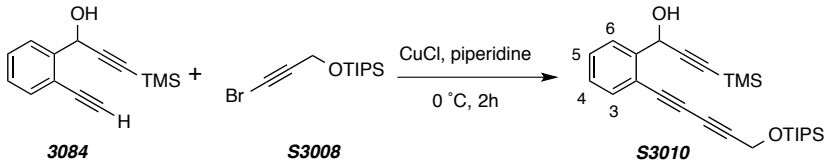

3084 ***S3008*** ***S3010***

[BPW IV-191] Triyne **S3010** was prepared following the general procedure for Cadiot-Chodkiewicz hetero-coupling from bromoalkyne **S3008** (783 mg, 2.7 mmol), diyne **3084** (410 mg, 1.8 mmol), CuCl (40 mg, 0.40 mmol) and piperidine (6 mL). The crude reaction mixture was used in the subsequent procedure without further purification, although a small amount was purified by flash chromatography (10:1 hexanes:EtOAc) for analytical purposes.

^{1}H NMR (500 MHz, $CDCl_3$): δ 7.70 (d, *J* = 7.8 Hz, 1H, *H3/H6*), 7.51 (d, *J* = 7.7 Hz, 1H, *H6/H3*), 7.40 (ddd, *J* = 7.6, 7.6 Hz, 1H, *H4/H5*), 7.29 (ddd, *J* = 7.6, 7.6, 1.2 Hz, 1H, *H4/H5*), 5.82 (s, 1H, C*H*OH), 4.54 (s, 2H, CH_2OSi), 1.11 [m, 3H, SiC*H*$(CH_3)_2$], 1.07 [d, *J* = 5.8 Hz, 18H, SiCH(CH_3)$_2$], and 0.20 [s, 9H, Si(CH_3)$_3$].

^{13}C NMR (125 MHz, $CDCl_3$): δ 143.6, 133.8, 129.8, 128.5, 127.1, 120.4, 104.1, 92.0, 83.0, 78.9, 75.1, 69.2, 63.5, 52.7, 18.1, 12.1, and -0.1.

LR ESI-MS: [M+Na^+] requires 390.2; found 390.1.

HR ESI-MS calcd for $C_{26}H_{38}NaO_2Si_2$ $[M + Na]^+$ 461.2303, found 461.2360.

IR: 2958, 2944, 2867, 2174, 1464, 1370, 1251, 1096, 1064, 845, and 761 cm^{-1}.

TLC R_f 0.2 (10:1 hexanes:EtOAc).

1-(2-(5-((Triisopropylsilyl)oxy)penta-1,3-diyn-1-yl)phenyl)-3-(trimethylsilyl)prop-2-yn-1-one (3097)

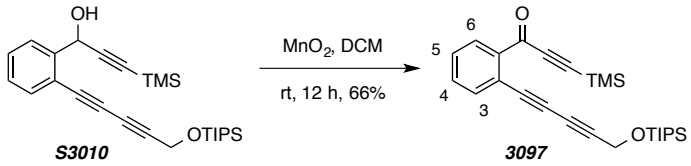

S3010 ***3097***

[*BPW III-157*] MnO_2 (1.23 g, 14.2 mmol) was added to a stirred solution of alcohol **S3010** (313 mg, 0.71 mmol) in CH_2Cl_2 (5 mL) at room temperature. After 12 h the reaction mixture was filtered through Celite® (EtOAc eluent) and concentrated. Purification by MPLC (hexanes:EtOAc 8:1) gave the ketone **3097** (203 mg, 0.47 mmol, 66%) as a yellow oil.

^{1}H NMR (500 MHz, $CDCl_3$): δ 8.09 (d, *J* = 7.7 Hz, 1H, *H6*), 7.63 (d, *J* = 7.7 Hz, 1H, *H3*), 7.51 (ddd, *J* = 7.5, 7.5, 1.4 Hz, 1H, *H4*), 7.46 (ddd, *J* = 7.6, 7.5, 1.4 Hz, 1H, *H5*), 4.55 (s, 2H, C*H*$_2$OSi), 1.13 [m, 3H, SiC*H*$(CH_3)_2$], 1.09 [d, *J* = 5.8 Hz, 18H, SiCH(C*H*$_3)_2$], and 0.31 [s, 9H, Si(C*H*$_3)_3$].

^{13}C NMR (125 MHz, $CDCl_3$): δ 176.5, 139.1, 135.9, 132.6, 131.0, 128.8, 121.7, 101.6, 101.5, 83.6, 79.8, 76.0, 69.7, 52.8, 18.1, 12.1, and -0.5.

HR ESI-MS calcd for $C_{26}H_{36}NaO_2Si_2$ $[M + Na]^+$ 459.2146, found 459.2134.

IR: 2944, 2866, 2153, 1650, 1275, 1253, 1235, 1104, 1014, 848 and 756 cm^{-1}.

TLC R_f 0.4 (8:1 hexanes:EtOAc).

2-(((Diisopropyl(prop-1-en-2-yl)silyl)oxy)methyl)-1-(trimethylsilyl)-9*H*-fluoren-9-one (3098)

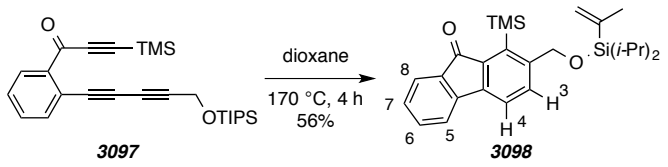

3097 ***3098***

[*BPW IV-199*] A solution of triyne **3097** (32 mg, 0.07 mmol) in dichlorobenzene (7 mL) was heated at 170 °C. After 4 h the mixture was loaded onto a silica column and the solvent removed by washing with hexanes. The crude material was collected after washing with 1:1 Hex:EtOAC and after concentration, purified by MPLC (20:1 hexanes:EtOAc) to give benzenoid **3098** (18 mg, 0.04 mmol, 56%) as a clear oil.

^{1}H NMR (500 MHz, $CDCl_3$): δ 7.74 (d, *J* = 7.7 Hz, 1H, *H4*), 7.58 (d, *J* = 7.3 Hz, 1H, *H5*), 7.53 (d, *J* = 7.7 Hz, 1H, *H4*), 7.47 (d, *J* = 7.7 Hz, 1H, *H8*), 7.45 (ddd, *J* = 7.4, 7.4, 1.2 Hz, 1H, *H6* or *H7*), 7.25 (ddd, *J* = 7.1, 7.1, 1.7 Hz, 1H, *H6* or *H7*), 5.76 (dt, *J* = 3.4, 1.7 Hz, 1H, C*H*$_2$=CCH$_3$), 5.39 (nfom, 1H, C*H*$_2$=CCH$_3$), 4.91 (s, 2H, C*H*$_2$OSi), 1.85 (t, *J* = 1.6 Hz, 3H, C*H*$_3$C=CH$_2$), 1.13–1.20 [m, 2H, OSi(C*H*$(CH_3)_2$)], 1.08 [d, *J* = 7.3 Hz, 6H, OSi(CH(C*H*$_3)_2$)], 1.08 [d, *J* = 7.2 Hz, 6H, OSi(CH(C*H*$_3)_2$)] and 0.42 [s, 9H, Si(C*H*$_3)_3$].

^{13}C NMR (125 MHz, $CDCl_3$): δ 195.7, 144.2, 143.9, 142.4, 140.0, 139.5, 134.6, 134.1, 131.4, 128.8, 128.5, 124.0, 120.9, 119.7, 66.4, 23.7, 17.7, 17.6, 12.1. and 2.5.

HR ESI-MS calcd for $C_{26}H_{36}NaO_2Si_2$ $[M + Na]^+$ 459.2146, found 459.2166.

IR: 2944, 2865, 1715, 1247, 1101, 842, 745, and 679 cm^{-1}.

TLC R_f 0.3 (20:1 hexanes:EtOAc).

1-(2-(5-((Triethylsilyl)oxy)penta-1,3-diyn-1-yl)phenyl)-3-(trimethylsilyl)prop-2-yn-1-ol (S3012)

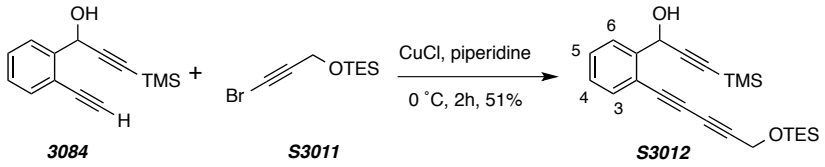

3084 ***S3011*** ***S3012***

[*BPW IV-189*] Triyne **S3012** was prepared following the general procedure for Cadiot-Chodkiewicz hetero-coupling from bromoalkyne **S3011** (453 mg, 1.8 mmol), diyne **3084** (273 mg, 1.2 mmol), CuCl (25 mg, 0.25 mmol) and piperidine (4 mL). The crude reaction mixture was purified by MPLC (10:1 hexanes:EtOAc) to give alcohol **S3012** (242 mg, 0.61 mmol, 51%) as an amber oil.

^{1}H NMR (500 MHz, $CDCl_3$): δ 7.70 (d, *J* = 7.8 Hz, 1H, *H3/H6*), 7.51 (d, *J* = 7.7 Hz, 1H, *H6/H3*), 7.41 (ddd, *J* = 7.6, 7.6, 1.3 Hz, 1H, *H4/H5*), 7.29 (dd, *J* = 7.6, 7.6 Hz, 1H, *H4/H5*), 5.81 (s, 1H, C*H*OH), 4.47 (s, 2H, CH_2OSi), 1.00 [t, *J* = 7.9 Hz, 9H, $Si(CH_2CH_3)_3$], 0.68 [q, *J* = 7.9 Hz, 6H, $Si(CH_2CH_3)_3$], and 0.20 [s, 9H, $Si(CH_3)_3$].

^{13}C NMR (125 MHz, $CDCl_3$): δ 143.6, 133.8, 129.9, 128.5, 127.1, 120.3, 104.1, 92.0, 82.8, 78.8, 75.2, 69.4, 63.5, 52.0, 6.8, 4.6, and -0.1.

HR ESI-MS calcd for $C_{23}H_{32}NaO_2Si_2$ $[M + Na]^+$ 419.1833, found 419.1887.

IR: 3376, 2957, 2877, 2238, 2174, 1370, 1250, 1092, 845, and 760 cm^{-1}.

TLC R_f 0.2 (10:1 hexanes:EtOAc).

1-(2-(5-((Triisopropylsilyl)oxy)penta-1,3-diyn-1-yl)phenyl)-3-(trimethylsilyl)prop-2-yn-1-one (3099)

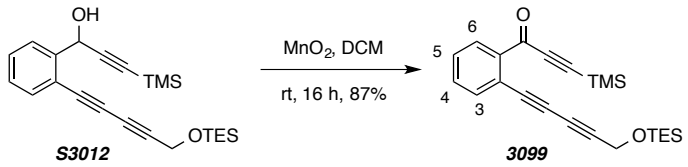

[*BPW IV-190*] MnO_2 (740 mg, 8.5 mmol) was added to a stirred solution of alcohol **S3012** (170 mg, 0.43 mmol) in CH_2Cl_2 (5 mL) at room temperature. After 16 h the reaction mixture was filtered through Celite® (EtOAc eluent) and concentrated to give ketone **3099** (147 mg, 0.37 mmol, 87%) as a yellow oil.

^{1}H NMR (500 MHz, $CDCl_3$): δ 8.10 (dd, *J* = 7.7, 1.2 Hz, 1H, *H6*), 7.62 (dd, *J* = 7.7, 1.2 Hz, 1H, *H3*), 7.51 (ddd, *J* = 7.5, 7.5, 1.4 Hz, 1H, *H4*), 7.46 (ddd, *J* = 7.6, 7.5, 1.4 Hz, 1H, *H5*), 4.47 (s, 2H, C*H*$_2$OSi), 0.99 [t, *J* = 8.0 Hz, 9H, Si(CH$_2$C*H*$_3$)$_3$], 0.67 [q, *J* = 8.0 Hz, 6H, Si(C*H*$_2$CH$_3$)$_3$], and 0.31 [s, 9H, Si(C*H*$_3$)$_3$].

^{13}C NMR (125 MHz, $CDCl_3$): δ 176.5, 139.1, 135.9, 132.7, 132.0, 128.8, 121.7, 101.6, 101.4, 83.4, 79.7, 76.1, 69.9, 52.1, 6.8, 4.6, and -0.6.

HR ESI-MS calcd for $C_{23}H_{30}NaO_2Si_2$ $[M + Na]^+$ 417.1677, found 417.1719.

IR: 2957, 2911, 2877, 2153, 1650, 1235, 1101, 1074, 1014, 849, and 755 cm^{-1}.

TLC R_f 0.3 (8:1 hexanes:EtOAc).

(1*S*,4*R*)-2,3-Dichloro-5-(((triethylsilyl)oxy)methyl)-6-(trimethylsilyl)-1,4-dihydro-7*H*-1,4-ethenobenzo[*c*]fluoren-7-one (3100)

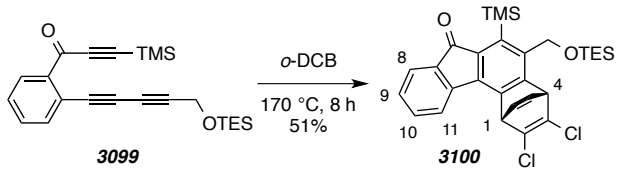

[*BPW 1-086*] A solution of triyne **3099** (17 mg, 0.04 mmol) in *o*-DCB (4.3 mL) in a sealed vial was placed in an oil bath and heated at 170 °C. After 8 h, the solution was trasfered to a silica column and the solvent removed by washing with hexanes. The curde product was collected after

flushing with 1:1 Hex:EtOAc and purified by MPLC (15:1 Hex:EtOAc) to give benzenoid **3100** (12 mg, 0.02 mmol, 51%) as a yellow oil.

^{1}H NMR (500 MHz, $CDCl_3$): δ 7.86 (d, *J* = 7.7 Hz, 1H, *H8*), 7.64 (d, *J* = 7.3 Hz, 1H, *H11*), 7.53 (ddd, *J* = 7.6, 7.6, 1.2 Hz, 1H, *H9/H10*), 7.30 (ddd, *J* = 7.5, 7.5, 0.7 Hz, 1H, *H9/H10*), 6.98 (m, 2H, *H*C=C*H*), 5.53 (dd, *J* = 5.7, 1.8 Hz, 1H, *H1*), 5.35 (dd, *J* = 5.8, 1.8 Hz, 1H, *H4*), 4.88 (d, *J* = 11.9 Hz, 1H, C$H_a$$H_b$OSi), 4.85 (d, *J* = 11.9 Hz, 1H, CH$_a$$H_b$OSi), 0.98 [t, *J* = 8.0 Hz, 9H, Si(CH$_2$CH_3)$_3$], 0.69 [q, *J* = 8.0 Hz, 6H, Si(CH_2CH$_3$)$_3$], and 0.42 [s, 9H, Si(CH_3)$_3$].

^{13}C NMR (125 MHz, $CDCl_3$): δ 194.1, 150.9, 143.6, 140.8, 140.5, 140.3, 138.8, 138.1, 137.6, 136.2, 135.5, 135.15, 135.08, 134.5, 128.8, 124.4, 122.2, 62.0, 53.5, 52.1, 7.1, 4.8, 2.7, and -0.7.

TLC R_f 0.2 (15:1 hexanes:EtOAc).

GC-MS t_r (5029021) = 16.24 min; m/z: 540, 525, 497, 409, 339, 263, 239, 87, 73, and 59.

4-(Allyloxy)but-1-yne (3103)

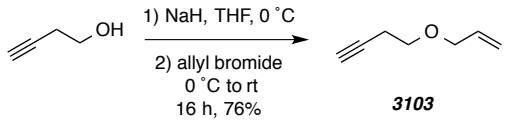

[BPW VI-222] NaH (714 mg, 17.9 mmol of a 60% w/w solid) in THF (8 mL) was cooled to 0 °C in an ice bath and 4-butyn-1-ol (767 μL, 10.2 mmol) in THF (1 mL) was added dropwise. After 45 minutes of stirring at 0 °C, allyl bromide (1.06 mL, 12.2 mmol) was added and the stirring solution allowed to warm to rt. After 16 h, the solution was cooled back to 0 °C and water added (5 mL). The mixture was extracted with diethyl ether (3 × 10 mL), washed with brine, and dried ($MgSO_4$). The crude product was purified via MPLC (5:1 Hex:EtOAc) to give the ether **3103** (852 mg, 7.8 mmol, 76%) as a clear oil, whose spectra matched that reported in the literature.[149]

4-(Allyloxy)-1-bromobut-1-yne (3104)

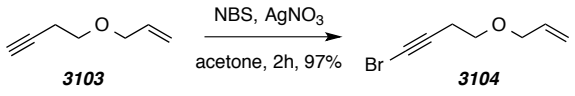

[149] Daniel, D.; Middleton, R.; Henry, H.; Okamura, W. Inhibitors of 25-hydroxyvitamin D-3-1 alpha-hydroxylase: A-ring oxa analogs of 25-hydroxyvitamin D-3. *J. Org. Chem* **1996**, *61*, 5617–5625.

[*BPW VI-223*] To a stirring solution of diyne **3103** (418 mg, 3.8 mmol, 1.0 equiv) in dry acetone (20 mL) was added *N*-bromosuccinimide (744 mg, 4.2 mmol, 2.2 equiv) and silver nitrate (65 mg, 0.38 mmol, 0.1 equiv). The flask was put under a N_2 atmosphere, wrapped in aluminum foil, and stirred 2 h. The solution was filtered through Celite® and concentrated under reduced pressure to give the crude diyne **3104** (697 mg, 3.7 mmol, 97%) which was used in the subsequent coupling step.

1-(2-(6-(Allyloxy)hexa-1,3-diyn-1-yl)phenyl)-3-(trimethylsilyl)prop-2-yn-1-ol (3105)

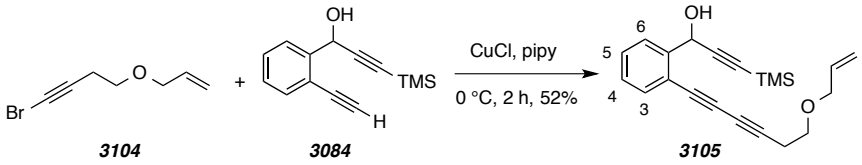

[*BPW VI-224*] Triyne **3105** was prepared following the general procedure for Cadiot-Chodkiewicz hetero-coupling from bromoalkyne **3104** (376 mg, 2.0 mmol), diyne **3084**[145] (225 mg, 1.0 mmol), CuCl (25 mg, 0.25 mmol) and piperidine (4 mL). The crude reaction mixture was purified by MPLC (5:1 hexanes:EtOAc) to give alcohol **3105** (175 mg, 0.52 mmol, 52%) as an amber oil.

^{1}H NMR (500 MHz, $CDCl_3$): δ 7.69 (dd, *J* = 7.8, 1.2 Hz, 1H, *H3/H6*), 7.50 (dd, *J* = 7.7, 1.0 Hz, 1H, *H4/H5*), 7.39 (ddd, *J* = 7.6, 7.6, 1.3 Hz, 1H, *H4/H5*), 7.28 (ddd, *J* = 7.6, 7.6, 1.3 Hz, 1H, *H4/H5*), 5.92 (ddt, *J* = 17.2, 10.4, 5.7 Hz, 1H, $OCH_2CH{=}CH_2$), 5.82 (s, 1H, C*H*OH), 5.29 (ddt, *J* = 17.2, 1.6, 1.6 Hz, 1H, $OCH_2CH{=}CH_aH_b$), 5.20 (ddt, *J* = 10.4, 1.6, 1.3 Hz, 1H, $OCH_2CH{=}CH_aH_b$), 4.04 (dt, *J* = 5.7, 1.4, Hz, 2H, $OCH_2CH{=}CH_aH_b$), 3.62 (t, *J* = 7.0 Hz, 2H, CH_2CH_2O), 2.67 (t, *J* = 6.9 Hz, 2H, CH_2CH_2O), and 0.20 [s, 9H, $Si(CH_3)_3$].

^{13}C NMR (125 MHz, $CDCl_3$): δ 143.5, 134.5, 133.8, 129.6, 128.5, 127.1, 120.7, 117.6, 104.2, 92.0, 82.9, 79.6, 72.3, 72.2, 67.8, 66.1, 63.5, 21.2, and 0.0.

HR ESI-MS calcd for $C_{21}H_{24}NaO_2Si$ $[M + Na]^+$ 359.1438, found 359.1436.

IR: 3350, 2958, 2867, 2172, 1250, 1090, 1039, 986, 844, and 759 cm^{-1}.

TLC R_f 0.3 (5:1 hexanes:EtOAc).

1-(2-(6-(Allyloxy)hexa-1,3-diyn-1-yl)phenyl)-3-(trimethylsilyl)prop-2-yn-1-one (3106)

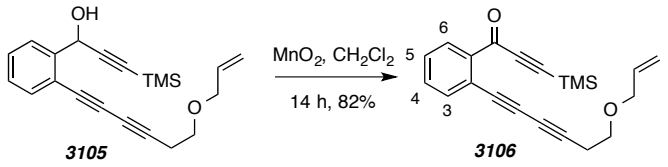

[*BPW VI-225*] MnO_2 (310 mg, 3.6 mmol) was added to a stirred solution of alcohol **3105** (80 mg, 0.24 mmol) in CH_2Cl_2 (5 mL) at room temperature. After 14 h the reaction mixture was filtered through Celite® (EtOAc eluent) and concentrated. Purification by MPLC (10:1 Hex:EtOAc) gave ketone **3106** (65 mg, 0.19 mmol, 82%) as a yellow oil.

^{1}H NMR (500 MHz, $CDCl_3$): δ 8.08 (dd, *J* = 7.7, 1.2 Hz, 1H, *H6*), 7.60 (dd, *J* = 7.7, 1.2 Hz, 1H, *H3*), 7.50 (ddd, *J* = 7.5, 7.5, 1.4 Hz, 1H, *H4*), 7.44 (ddd, *J* = 7.6, 7.6, 1.4 Hz, 1H, *H5*), 5.92 (ddt, *J* = 17.2, 10.4, 5.7 Hz, 1H, OCH_2CH=CH_2), 5.30 (ddt, *J* = 17.2, 1.6, 1.6 Hz, 1H, OCH_2CH=CH_aH_b), 5.21 (ddt, *J* = 10.4, 1.6, 1.3 Hz, 1H, OCH_2CH=CH_aH_b), 4.03 (dt, *J* = 5.7, 1.4, Hz, 2H, OCH_2CH=CH_aH_b), 3.61 (t, *J* = 6.9 Hz, 2H, CH_2CH_2O), 2.67 (t, *J* = 6.9 Hz, 2H, CH_2CH_2O), and 0.30 [s, 9H, $Si(CH_3)_3$].

^{13}C NMR (125 MHz, $CDCl_3$): δ 176.6, 139.1, 135.8, 134.5, 132.6, 131.9, 128.6, 122.0, 117.5, 101.53, 101.52, 83.6, 80.5, 73.3, 72.2, 67.8, 66.7, 21.3, and -0.5.

HR ESI-MS calcd for $C_{21}H_{22}NaO_2Si$ $[M + Na]^+$ 357.1281, found 357.1298.

IR: 2962, 2867, 2242, 2152, 1648, 1235, 1015, 847, and 755 cm^{-1}.

TLC R_f 0.2 (15:1 hexanes:EtOAc).

10-Acetyl-4-(trimethylsilyl)-2,3-dihydro-5*H*-fluoreno[3,2-*b*]furan-5-one (3111)

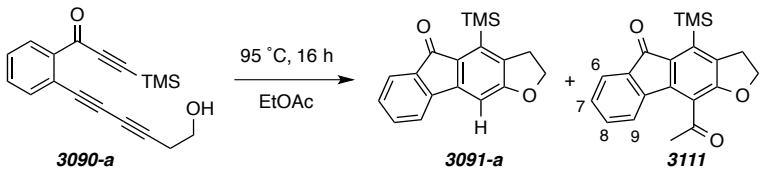

[*BPW VI-216]* A solution of triyne **3090-a** (18 mg, 0.06 mmol) in EtOAc (600 µL) in a sealed vial was heated at 95 °C for 16 h. After solvent removal, the crude product was purified by MPLC (10:1 Hex:EtOAc) to give benzenoid **3091-a** (10 mg, 0.03 mmol, 56%), which matched all

previously recorded spectra, followed by benzenoid **3111** (6 mg, 0.02 mmol, 29%) as an orange oil.

Data for **3111**:

^{1}H NMR (500 MHz, $CDCl_3$): δ 7.55 (ddd, *J* = 7.3, 0.9, 0.9 Hz, 1H, *H6*), 7.38–7.34 (m, 2H, *H7/H8/H9*), 7.25 (ddd, *J* = 6.8 6.8, 1.8 Hz, 1H, *H7/H8*), 4.69 (t, *J* = 8.9 Hz, 2H, C*H*$_2$O), 3.30 (t, *J* = 8.9 Hz, 2H, C*H*$_2$CH$_2$O), 2.67 (s, 3H, C*H*$_3$CO), and 0.40 [s, 9H, Si(CH$_3$)$_3$].

^{13}C NMR (125 MHz, $CDCl_3$): δ 202.2, 193.1, 160.9, 143.6, 141.9, 140.3, 135.1, 134.3, 134.0, 133.0, 129.3, 123.5, 122.7, 120.8, 72.8, 32.1, 31.1, and 1.3.

IR: 2979, 2950, 2903, 1703, 1536, 1390, 1287, 1248, 1128, 1008, and 844 cm^{-1}.

TLC R_f 0.2 (10:1 hexanes:EtOAc).

10-Propionyl-4-(trimethylsilyl)-2,3-dihydro-5*H*-fluoreno[3,2-*b*]furan-5-one (3112)

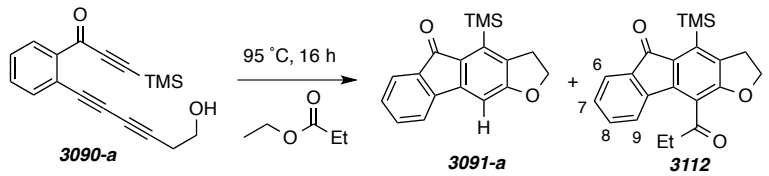

[*BPW VI-216]* A solution of triyne **3090-a** (18 mg, 0.06 mmol) in ethyl propionate (600 μL) in a sealed vial was heated at 95 °C for 16 h. After solvent removal, the crude product was purified by MPLC (10:1 Hex:EtOAc) to give benzenoid **3091-a** (8 mg, 0.03 mmol, 44%), which matched all previously recorded spectra, followed by benzenoid **3112** (7 mg, 0.02 mmol, 33%) as an orange oil.

Data for **3112**: **^{1}H NMR** (500 MHz, $CDCl_3$): δ 7.55 (d, *J* = 7.3, Hz, 1H, *H6*), 7.35 (ddd, *J* = 7.6, 7.6, 1.3 Hz, 1H, *H7/H8*), 7.25–7.21 (m, *H7/H8/H9*), 4.66 (t, *J* = 8.9 Hz, 2H, C*H*$_2$O), 3.29 (t, *J* = 8.9 Hz, 2H, C*H*$_2$CH$_2$O), 2.98 (q, *J* = 7.3 HZ, 2H, CH$_3$C*H*$_2$CO), 1.26 (t, *J* = 7.3 Hz, 3H, C*H*$_3$CH$_2$CO), and 0.40 [s, 9H, Si(CH$_3$)$_3$].

^{13}C NMR (125 MHz, $CDCl_3$): δ 205.6, 193.1, 160.5, 143.6, 141.9, 140.0, 135.1, 134.2, 133.9, 132.9, 129.3, 123.5, 122.3, 120.7, 72.7, 37.7, 31.1, 8.0, and 1.3.

HR ESI-MS calcd for $C_{21}H_{22}NaO_3Si$ $[M + Na]^+$ 373.1230, found 373.1203.

IR: 2979, 2938, 2902, 1702, 1536, 1392, 1246, 1131, and 844 cm^{-1}.

TLC R_f 0.3 (10:1 hexanes:EtOAc).

Experimental Section for Chapter 4

Dimethyl 2,2-bis(6-((tert-butyldimethylsilyl)oxy)hexa-2,4-diyn-1-yl)malonate (S4001)

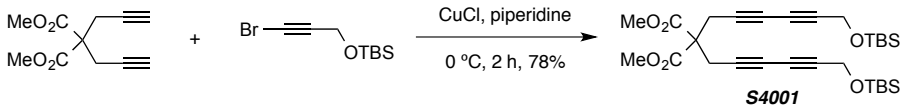

[*BPW III-293*] Tetrayne **S4001** was prepared following general procedure B from dimethyl 2,2-di(prop-2-yn-1-yl)malonate[143] (166 mg, 0.8 mmol), ((3-bromoprop-2-yn-1-yl)oxy)(*tert*-butyl)dimethylsilane (620 mg, 2.5 mmol), CuCl (30 mg, 0.30 mmol), and piperidine (3.0 mL). Purification by flash chromatography (hexanes:EtOAc 3:1) gave the tetrayne **S4001** (340 mg, 0.63 mmol, 78%) as a clear amber oil.

^{1}H NMR (500 MHz, $CDCl_3$): δ 4.35 (s, 4H, CH_2OSi), 3.77 (s, 6H, CO_2CH_3), 3.08 (s, 4H, CH_2CC), 0.90 [s, 18H, $SiC(CH_3)_3$], and 0.11 [s, 12H, $Si(CH_3)_2$].

^{13}C NMR (125 MHz, $CDCl_3$): δ 168.7, 75.8, 74.2, 69.4, 68.1, 56.8, 53.5, 52.2, 25.9, 24.0, 18.4, and -5.1.

IR (neat): 2955, 2930, 2857, 1746, 1254, 1212, 1089, 837, and 780 cm^{-1}.

HRMS (ESI-TOF): Calcd for $C_{29}H_{44}NaO_6Si_2^+$ [$M+Na^+$] requires 567.2569; found 567.2543.

TLC: R_f 0.4 (3:1 hex:EtOAc).

Dimethyl 5-(((tert-butyldimethylsilyl)oxy)methyl)-4-(3-((tert-butyldimethylsilyl)oxy)prop-1-yn-1-yl)-1*H*-indene-2,2(3*H*)-dicarboxylate (4016)

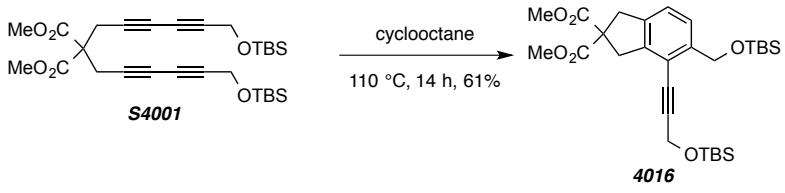

[*BPW III-295*] Indane **16b** was prepared following general procedure C (110 ºC, 14 h) from tetrayne **S5** (28 mg, 0.05 mmol) and cyclooctane (5 mL). The crude material was purified by

MPLC (hexanes:EtOAc 3:1) to give the indane **16b** (17 mg, 0.03 mmol, 61%) as a clear amber oil.

^{1}H NMR (500 MHz, $CDCl_3$): δ 7.36 (d, *J* = 7.8 Hz, 1H, *H7*), 7.15 (d, *J* = 7.8 Hz, 1H, *H6*), 4.83 (s, 2H, ArCH_2O), 4.59 (s, 2H, C≡CCH_2O), 3.75 (s, 6H, CO_2CH_3), 3.66 (s, 2H, *H3$_2$*), 3.59 (s, 2H, *H1$_2$*), 0.95 [s, 9H, SiC(CH_3)$_3$], 0.94 [s, 9H, SiC(CH_3)$_3$], 0.17 [s, 6H, Si(CH_3)$_2$], and 0.10 [s, 6H, Si(CH_3)$_2$].

^{13}C NMR (125 MHz, $CDCl_3$): δ 172.2, 142.7, 142.2, 138.2, 125.0, 124.2, 116.0, 96.4, 80.2, 63.4, 59.9, 53.1, 52.5, 40.8, 40.6, 26.1, 26.0, 18.6, 18.5, -4.9, and -5.1.

IR (neat): 2952, 2923, 2857, 1739, 1249, 1105, 1084, 838, and 780 cm^{-1}.

HRMS (ESI-TOF): Calcd for $C_{29}H_{46}NaO_6Si_2^+$ [M+Na$^+$] requires 569.2725; found 569.2704.

TLC: R_f 0.3 (6:1 hex:EtOAc).

1-(2-(7-Chlorohepta-1,3-diyn-1-yl)phenyl)-3-(trimethylsilyl)prop-2-yn-1-ol (S4002)

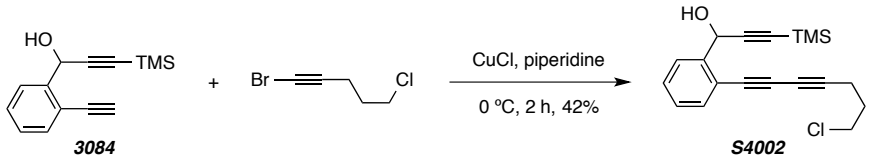

[*BPW II-214]* Triyne **S4002** was prepared following general procedure B from diyne **3084**[145] (228 mg, 1.00 mmol), 1-bromo-5-chloropent-1-yne (from 5-chloro-1-pentyne using general procedure A) (216 mg, 1.20 mmol), CuCl (30 mg, 0.30 mmol), and piperidine (2.7 mL). Purification by flash chromatography (hexanes:EtOAc 6:1) gave the triyne **S4002** (139 mg, 0.42 mmol, 42%) as a clear amber oil.

^{1}H NMR (500 MHz, $CDCl_3$): δ 7.67 (dd, *J* = 7.8, 1.6 Hz, 1H, *H6*), 7.50 (dd, *J* = 7.7, 1.5 Hz, 1H, *H3*), 7.40 (ddd, *J* = 7.7, 7.6, 1.5 Hz, 1H, *H4*), 7.29 (ddd, *J* = 7.6, 7.6, 1.4 Hz, 1H, *H5*), 5.82 (bs, 1H, ArC*H*OH), 3.68 (t, *J* = 6.3 Hz, 2H, CH_2Cl), 2.59 (t, *J* = 6.8 Hz, 2H, C≡CC*H$_2$*), 2.49, (bs, 1H, CH_2O*H*), 2.04 (p, *J* = 6.5 Hz, 2H, CH_2CH_2Cl), and 0.20 [s, 9H, Si(CH_3)$_3$].

^{13}C NMR (125 MHz, $CDCl_3$): δ 143.5, 133.8, 129.6, 128.5, 127.1, 120.6, 104.2, 91.9, 84.2, 79.4, 72.4, 66.1, 63.5, 43.5, 31.1, 17.2, and 0.1.

IR (neat): 3427, 2960, 2901, 2239, 2173, 1446, 1250, 1037, 846, and 761 cm^{-1}.

HRMS (ESI-TOF): Calcd for $C_{19}H_{21}NaClOSi^+$ [M+Na$^+$] requires 351.0942; found 351.0935.

TLC: R_f 0.2 (6:1 hex:EtOAc)

1-(2-(7-Chlorohepta-1,3-diyn-1-yl)phenyl)-3-(trimethylsilyl)prop-2-yn-1-one (4030)

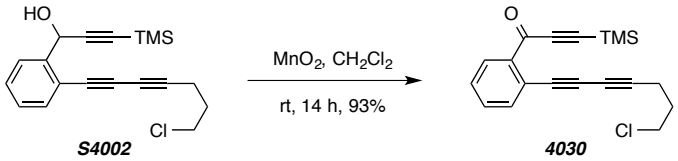

[*BPW II-244*] MnO_2 (750 mg, 8.65 mmol) was added to a stirred solution of alcohol **S4002** (268 mg, 0.82 mmol) in CH_2Cl_2 (10 mL) at room temperature. After 14 h the reaction mixture was filtered through a small column of SiO_2 (EtOAc eluent) and purified by MPLC (hexanes:EtOAc 6:1) to give the triyne **4030** (247 mg, 0.76 mmol, 93%) as an amber oil.

^{1}H NMR (500 MHz, $CDCl_3$): δ 8.10 (dd, *J* = 7.7, 1.6 Hz, 1H, *H6*), 7.60 (dd, *J* = 7.6, 1.5 Hz, 1H, *H3*), 7.51 (ddd, *J* = 7.6, 7.5, 1.5, 1H, *H4*), 7.45 (ddd, *J* = 7.6, 7.6, 1.5 Hz, 1H, *H5*), 3.68 (t, *J* = 6.3 Hz, 2H, C*H*$_2$Cl), 2.59 (t, *J* = 6.8 Hz, 2H, ArC*H*$_2$), 2.03 (p, *J* = 6.5 Hz, 2H, $CH_2CH_2CH_2Cl$), and 0.31[s, 9H, Si(C*H*$_3$)$_3$].

^{13}C NMR (125 MHz, $CDCl_3$): δ 176.6, 139.1, 135.8, 132.6, 132.0, 128.6, 121.9, 101.50, 101.49, 84.9, 80.3, 73.3, 66.6, 43.6, 31.1, 17.3, and -0.6.

IR (neat): 2964, 2243, 2152, 1641, 1560, 1481, 1296, 1250, 1232, 1012, 846, and 758 cm^{-1}.

HRMS (ESI-TOF): Calcd for $C_{19}H_{19}NaClOSi^+$ [M+Na^+] requires 349.0786; found 349.0780.

TLC: R_f 0.3 (6:1 hex:EtOAc).

2-(3-Chloropropyl)-1-(trimethylsilyl)-9*H*-fluoren-9-one (4020)

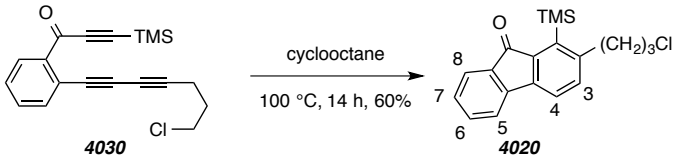

[*BPW II-267*] Fluorenone **4020** was prepared following general procedure C (100 ºC, 14 h) from triynone **4030** (10 mg, 0.03 mmol) and cyclooctane (3 mL). The crude material was purified by MPLC (hexanes:EtOAc 6:1) to give fluorenone **4020** (6 mg, 0.02 mmol, 60%) as a yellow solid.

^{1}H NMR (500 MHz, $CDCl_3$): δ 7.58 (ddd, *J* = 7.3, 0.9, 0.9 Hz, 1H, *H8*), 7.43-7.46 (m, 2H, *H6/H5*), 7.45 (d, *J* = 7.6 Hz, 1H, *H4*), 7.24-7.27 (nfom, 1H, *H7*), 7.25 (d, *J* = 7.6 Hz, 1H, *H3*),

3.55 (t, J = 6.5 Hz, 2H, CH_2Cl), 2.95 (br t, J = 7.6 Hz, 2H, ArCH_2), 1.97-2.03 (br p, J = 7.1 Hz, 2H, ArCH$_2$CH_2), and 0.44 [s, 9H, Si(CH_3)$_3$].

^{13}C NMR (125 MHz, $CDCl_3$): δ 195.4, 148.5, 144.0, 143.6, 141.2, 140.7, 135.4, 134.7, 133.9, 128.8, 124.1, 121.0, 119.6, 44.1, 36.0, 33.7, and 2.6.

IR (neat): 2950, 2898, 1711, 1606, 1438, 1247, 1182, 861, 846, and 745 cm^{-1}.

HRMS (ESI-TOF): Calcd for $C_{19}H_{21}NaClOSi^+$ [M+Na$^+$] requires 351.0942; found 351.0918.

TLC: R_f 0.2 (6:1 hex:EtOAc) .

2-Propyl-1-(trimethylsilyl)-9*H*-fluoren-9-one (4021)

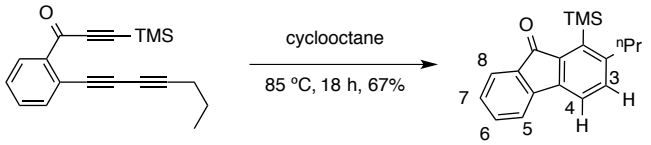

S4003 ***4021***

A solution of triynone **S4003** (1.21 g, 4.14 mol) in cyclooctane (410 mL) was heated at 85 °C in a 1000 mL round bottom flask with stirring and under inert atmosphere. After 18 h the reaction mixture was loaded onto a bed of silica gel and washed sequentially with hexanes, to remove the excess cyclooctane, and ethyl acetate. The ethyl acetate fraction was concentrated to provide the crude product mixture. The crude material was purified by flash chromatography (hexanes:EtOAc 19:1) to give fluorenone **4021** (820 mg, 2.79 mmol, 67%) as an orange oil.

^{1}H NMR (500 MHz, $CDCl_3$): δ 7.56 (ddd, J = 7.3, 1.0, 1.0 Hz, 1H, *H8*), 7.43 (m, 2H, *H5* and *H6*), 7.42 (d, J = 7.6 Hz, 1H, *H4*), 7.23 (nfom, 1H, *H7*), 7.21 (d, J = 7.6 Hz, 1H, *H3*), 2.73 (br t, J = 8.0 Hz, 2H, CH_2CH$_2$CH$_3$), 1.54 (br sext, J = 7 Hz, 2H, CH_2CH$_3$), 0.97 (t, J = 7.3 Hz, CH$_2$CH_3), and 0.43 (s, 9H, SiCH_3).

^{13}C NMR (125 MHz, $CDCl_3$): δ 195.6, 150.7, 144.2, 143.2, 141.0, 140.4, 135.4, 134.5, 134.0, 128.6, 124.0, 120.8, 119.5, 39.0, 27.1, 14.0, and 2.5.

IR (neat): 2955, 2935, 2875, 1713, 1606, 1248, 968, 861, and 846 cm^{-1}.

HRMS (ESI-TOF): Calcd for $C_{19}H_{22}NaOSi^+$ [M+Na$^+$] requires 317.1332; found 317.1358.

TLC: R_f 0.5 (9:1 Hex/EtOAc).

4,5-Dichloro-2-tosyl-6-{[(triisopropylsilyl)oxy]methyl}-7-{3-[(triisopropylsilyl)oxy]prop-1-yn-1-yl}isoindoline (4025c)

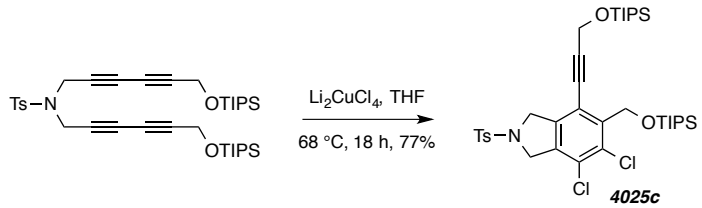

Dichloride **4025c** was prepared following General Procedure C from known tetrayne[150] (20 mg, 0.03 mmol), Li_2CuCl_4 (0.3 mL, 1M in THF, 0.3 mmol), and THF (0.7 mL). Purification by flash chromatography (hexanes:EtOAc 12:1 to 5:1) gave the dichloride **4025c** (17 mg, 0.023 mmol, 77%) as a colorless solid.

^{1}H NMR (500 MHz, $CDCl_3$): δ 7.77 (d, J = 8.0 Hz, 2H, $SO_2Ar\mathit{H}_o$), 7.33 (d, J = 8.0 Hz, 2H, $SO_2Ar\mathit{H}_M$), 4.97 (s, 2H, $C\mathit{H}_2$), 4.68 (s, 2H, $C\mathit{H}_2$), 4.65 (s, 2H, $C\mathit{H}_2$), 4.61 (s, 2H, $C\mathit{H}_2$), 2.42 (s, 3H, $ArC\mathit{H}_3$), 1.20-1.08 (m, 2H, $SiC\mathit{H}(CH_3)_2$], 1.12 [d, J = 5.9 Hz, 6H, $SiCH(C\mathit{H}_3)_2$], and 1.07 [d, J = 6.5 Hz, 6H, $SiCH(C\mathit{H}_3)_2$].

^{13}C NMR (125 MHz, $CDCl_3$): δ 144.2, 141.3, 138.9, 136.0, 133.7, 133.5, 130.2, 128.2, 127.8, 118.2, 97.6, 78.8, 62.5, 55.1, 54.7, 52.7, 21.8, 18.2, 12.3, and 12.2.

IR (neat): 2944, 2891, 2863, 2362, 2343, 1463, 1356, 1167, 1100, 1068, 883, and 813 cm^{-1}.

HRMS (ESI-TOF): Calcd for $C_{37}H_{57}Cl_2NNaO_4SSi_2^+$ [M+Na^+] requires 760.2816; found 760.2839.

mp: 122–126 °C.

Dimethyl 2,2-di(nona-2,4-diyn-1-yl)malonate (S4004)

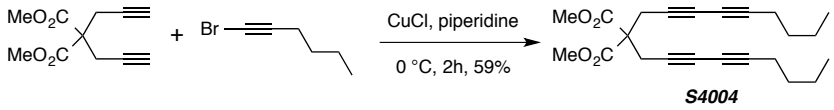

[*BPW V-038*] Tetrayne **S4004** was prepared following the General Procedure B from bromohexyne (480 mg, 3.0 mmol), dimethyl 2,2-di(prop-2-yn-1-yl)malonate[143] (208 mg, 1.0

[150] R Hoye, T.; Chen, J.; Baire, B. Cycloaddition Reactions of Azide, Furan, and Pyrrole Units with Benzynes Generated by the Hexadehydro-Diels–Alder (HDDA) Reaction. *HETEROCYCLES* **2014**, *88*, 1191.

mmol), CuCl (20 mg, 0.20 mmol), and piperidine (5 mL). Purification by flash chromatography (hexanes:EtOAc 3:1) gave tetrayne **S4005** (216 mg, 0.59 mmol, 59%) as a yellow oil.

^{1}H NMR (500 MHz, $CDCl_3$): δ 3.77 (s, 6H, CO_2CH_3), 3.06 [s, 4H, $CH_2C(CO_2Me)_2$], 2.24 (t, J = 6.9 Hz, 4H, $CH_2C{\equiv}C$), 1.50 (br tt, J = 7.0, 7.0 Hz, 4H, $C{\equiv}CCH_2CH_2$), 1.40 (br tq, J = 7.0, 7.0 Hz, 4H, CH_2CH_3), and 0.91 (t, J = 7.3 Hz, 6H, CH_3).

^{13}C NMR (125 MHz, $CDCl_3$): δ 169.0, 79.2, 70.7, 68.9, 65.0, 56.9, 53.5, 30.4, 24.0, 22.1, 19.1, and 13.7.

IR (neat): 2957, 2934, 2873, 2259, 1744, 1435, 1320, 1292, 1210, 1184, 1072, and 1054 cm^{-1}.

HRMS (ESI-TOF): Calcd for $C_{23}H_{28}NaO_4^+$ [$M+Na^+$] requires 391.1880; found 391.1885.

Dimethyl 5-butyl-6,7-dichloro-4-(hex-1-yn-1-yl)-1,3-dihydro-2H-indene-2,2-dicarboxylate (4026)

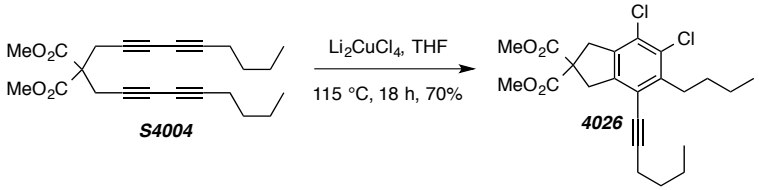

[*BPW V-072*] Dichloride **4026** was prepared following General Procedure D from tetrayne **S4004** (30 mg, 0.08 mmol), Li_2CuCl_4 (0.8 mL, 1M in THF, 0.8 mmol), and THF (1.9 mL). Purification by MPLC (hexanes:EtOAc 8:1) gave the dichloride **4026** (25 mg, 0.057 mmol, 70%) as a colorless solid.

^{1}H NMR (500 MHz, $CDCl_3$): δ 3.77 (s, 6H, CO_2CH_3), 3.67 [s, 2H, $CH_2C(CO_2Me)_2$], 3.65 [s, 2H, $C'H_2C(CO_2Me)_2$], 2.92 (nfom, 2H, $ArCH_2$), 2.47 (t, J = 7.0 Hz, 2H, $C{\equiv}CCH_2$), 1.61 (m, 2H, CH_2CH_2Ar), 1.52 (m, 4H, $\equiv CCH_2CH_2$, $CH_2CH_2CH_3$), 1.41 (tq, J = 7, 7 Hz, 2H, CH_2CH_3), 0.96 (t, J = 7.3 Hz, 3H, CH_3), and 0.95 (t, J = 7.3 Hz, 3H, CH_3).

^{13}C NMR (125 MHz, $CDCl_3$): δ 171.8, 143.3, 141.9, 137.0, 130.7, 128.2, 119.7, 99.1, 76.5, 58.8, 53.3, 41.7, 41.3, 33.2, 31.2, 30.9, 23.0, 22.1, 19.5, 14.0, and 13.7.

IR (neat): 2957, 2933, 2872, 2245, 1740, 1434, 1276, 1249, 1199, and 1074 cm^{-1}.

HRMS (ESI-TOF): Calcd for $C_{23}H_{28}NaO_4^+$ [$M+Na^+$] requires 461.1257; found 461.1331.

1-(Nona-2,4-diyn-1-yloxy)nona-2,4-diyne (S4005)

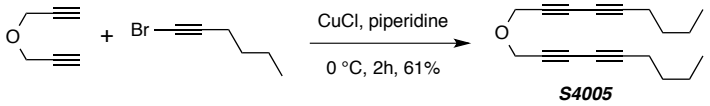

[*BPW V-080*] Tetrayne **S4005** was prepared following the General Procedure B from 1-bromohexyne (400 mg, 2.5 mmol), dipropargyl ether (94 mg, 1.0 mmol), CuCl (20 mg, 0.20 mmol), and piperidine (5 mL). Purification by flash chromatography (hexanes:EtOAc 20:1) gave tetrayne **S4005** (156 mg, 0.61 mmol, 61%) as a yellow oil.

^{1}H NMR (500 MHz, $CDCl_3$): δ 4.31 (s, 4H, OCH_2), 2.29 (t, J = 6.9 Hz, 4H, C≡CCH_2), 1.52 (tt, J = 7,7 Hz, 4H, C≡CCH$_2$CH_2), 1.42 (tq, J = 7, 7 Hz, 4H, CH_2CH$_3$), and 0.91 (t, J = 7.3 Hz, 6H, CH$_2$CH_3).

^{13}C NMR (125 MHz, $CDCl_3$): δ 81.8, 72.3, 70.8, 64.6, 57.3, 30.3, 22.1, 19.2, and 13.7.

IR (neat): 2959, 2934, 2873, 2363, 2342, 2255, 1345, and 1077 cm^{-1}.

HRMS (ESI-TOF): Calcd for $C_{18}H_{22}NaO^+$ [M+Na$^+$] requires 277.1563; found 277.1532.

5-Butyl-6,7-dichloro-4-(hex-1-yn-1-yl)-1,3-dihydroisobenzofuran (4027)

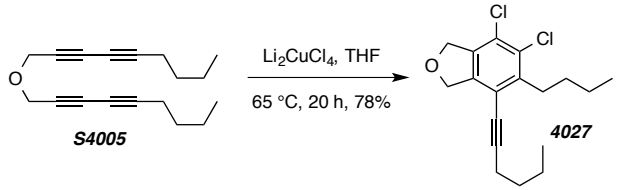

[*BPW V-094*] Dichloride **4027** was prepared following General Procedure D from tetrayne **S4006** (20 mg, 0.079 mmol), Li_2CuCl_4 (0.8 mL, 1M in THF, 0.8 mmol), and THF (1.9 mL). Purification by MPLC (hexanes:EtOAc 20:1) gave the dichloride **4027** (20 mg, 0.062 mmol, 78%) as a colorless solid.

^{1}H NMR (500 MHz, $CDCl_3$): δ 5.17 (s, 2H, OCH_2), 5.14 (s, 2H, OCH_2), 2.97 (nfom, 2H, ArCH_2), 2.48 (t, J = 6.8 Hz, 2H, C≡CCH_2), 1.60 (m, 2H, CH_2CH$_2$Ar), 1.51 (m, 4H, ≡CCH$_2$CH_2, CH$_2$CH_2CH$_3$), 1.45 (tq, J = 7, 7 Hz, 2H, CH_2CH$_3$), 0.98 (t, J = 7.3 Hz, 3H, CH_3), and 0.98 (t, J = 7.3 Hz, 3H, CH_3).

^{13}C NMR (125 MHz, $CDCl_3$): δ 143.9, 141.5, 136.5, 131.1, 125.7, 117.1, 99.2, 76.0, 75.3, 74.6, 33.0, 31.3, 30.9, 23.1, 22.2, 19.5, 14.1, and 13.8.

IR (neat): 2958, 2932, 2861, 2227, 1781, 1465, 1457, 1420, 1360, 1082, 1061, 904, 764, and 757 cm^{-1}.

HRMS (ESI-TOF): Calcd for $C_{18}H_{22}Cl_2NaO^+$ [M+Na^+] requires 347.0940; found 347.0925.

6-Oxo-5-(trimethylsilyl)-2,3,4,6-tetrahydroindeno[2,1-*g*]chromene-11-carbaldehyde (4031)

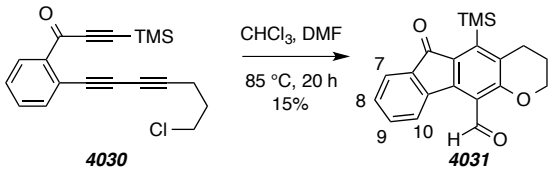

4030 ***4031***

[*BPW II-204*] A solution of triyne **4030** (45 mg, 0.14 mmol) in chloroform (1 mL) with DMF (380 µL, 5 mmol) was heated in a sealed vial at 85 °C. After 20 h the solvent was removed via rotary evaporation and the crude product purified via MPLC (3:1 Hex:EtOAc) to give the aldehyde **4031** (7 mg, 0.02 mmol, 15%) as a yellow oil.

^{1}H NMR (500 MHz, $CDCl_3$): δ 10.61 (s, C*H*O), 8.23 (d, *J* = 7.7 Hz, *H7*), 7.58 (d, *J* = 6.8 Hz, *H10*), 7.45 (ddd, *J* = 7.6, 7.6, 1.3 Hz, *H8*/*H9*), 7.31 (ddd, *J* = 7.4, 7.4, 0.8 Hz, 1H, *H8*/*H9*), 4.32 (t, *J* = 5.0 Hz, CH_2O), 2.93 (t, *J* = 6.4 Hz, C$H_2$$CH_2$$CH_2$O), and 2.06 (tt, *J* = 6.4, 5.0 Hz, CH_2C$H_2$$CH_2$Cl), and 0.44 [s, Si(C$H_3$)$_3$].

GC-MS t_r (5025015) = 13.60 min; m/z: 336, 321, 293, 265, 207, 178, 163, and 73.

5-(Trimethylsilyl)penta-2,4-diyn-1-yl propiolate (4038)

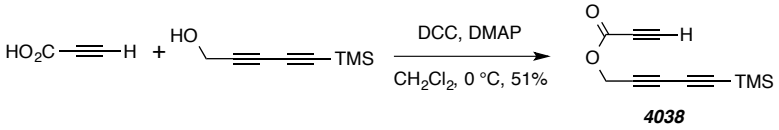

4038

[*BPW V-258*] A solution of 5-(trimethylsilyl)penta-2,4-diyn-1-ol[151] (230 mg, 1.5 mmol) and propiolic acid (110 µL, 1.8 mmol) in dichloromethane (10 mL) was cooled to 0 °C. N,N'-dicyclohexylcarbodiimide (370 mg, 1.8 mmol) and DMAP (15 mg, 0.12 mmol) was added and allowed to come to room temperature. After 4 h, the solution was filtered through plug of Celite, rinsing with EtOAc. After solvent removal, the crude material was purified by MPLC (15:1 Hex:EtOAc) to give triyne **4038** (155 mg, 0.76 mmol, 51%) as an amber oil.

---

[151] Bowling, N. P.; Burrmann, N. J.; Halter, R. J.; Hodges, J. A.; McMahon, R. J. Synthesis of simple diynals, diynones, their hydrazones, and diazo compounds: Precursors to a family of dialkynyl carbenes (R 1—C≡C—C̈—C≡C—R_2). *J. Org. Chem.* **2010**, *75*, 6382–6390.

^{1}H NMR (500 MHz, $CDCl_3$): δ 4.84 (s, 2H, CH_2O), 2.96 (s, 1H, C≡CH), and 0.20 [s, 9H, Si(CH_3)$_3$].

^{13}C NMR (125 MHz, $CDCl_3$): δ 151.7, 89.1, 86.7, 76.3, 73.8, 72.5, 69.9, 53.9, and -0.5.

IR: 3291, 2963, 2123, 1724, 1252, 1207, 966, 848, and 753 cm^{-1}.

HR ESI-MS calcd for $C_{11}H_{12}NaO_2Si$ $[M + Na]^+$ 227.0499, found 227.0451.

Ethyl 3-oxo-5-(trimethylsilyl)-1,3,6,7-tetrahydrocyclobuta[*e*]isobenzofuran-7-carboxylate (4039)

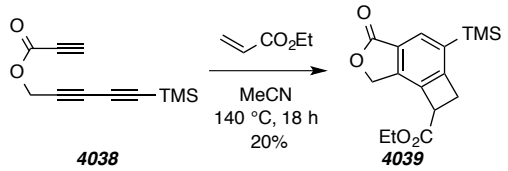

4038 ***4039***

[*BPW VI-239*] A solution of **4038** (25 mg, 0.12 mmol) in *o*-DCB (1.1 mL) with ethyl acrylate (200 µL, 1.8 mmol) was heated in a sealed vial to 140 °C. After 18 h the solution was loaded on a silica column and the solvent removed by flushing with hexanes followed by 1:1 Hex:EtOAc to obtain the crude product. This was purified via MPLC (2:1 Hex:EtOAC) to obain **4039** (8 mg, 0.3 mmol, 20%) as a yellow oil.

^{1}H NMR (500 MHz, $CDCl_3$): δ 7.98 (s, 1H, $C_{ar}H$), 5.28 (d, J = 15.6 Hz, 1H, CHCH_aCH$_b$), 5.22 (d, J = 15.6 Hz, 1H, CHCH$_a$CH_b), 4.41 (dd, J = 5.7, 2.6 Hz, 1H, CHCH$_2$), 4.22 (q, J = 7.1 Hz, 2H, CH_2CH$_3$), 3.55 (ddd, J = 14.2, 5.7, 0.8 Hz, 1H, OCH_aCH$_b$), 3.44 (ddd, J = 14.2, 3.5, 0.9 Hz, 1H, OCH$_a$CH_b), 1.30 (t, J = 7.1 Hz, 3H, CH$_2$CH_3), and 0.30 [s, 9H, Si(CH_3)$_3$].

^{13}C NMR (125 MHz, $CDCl_3$): δ 172.0, 171.5, 154.4, 141.4, 137.5, 137.2, 131.3, 125.4, 68.1, 61.4, 48.3, 33.7, 14.3, and -1.0.

IR: 2956, 2901, 1764, 1731, 1621, 1249, 1162, 1078, 1047, 1006, and 843 cm^{-1}.

HR ESI-MS calcd for $C_{11}H_{12}NaO_2Si$ $[M + Na]^+$ xxx.0499, found xxx.0451.

6,6-Dimethylhepta-2,4-diyn-1-yl propiolate (4053)

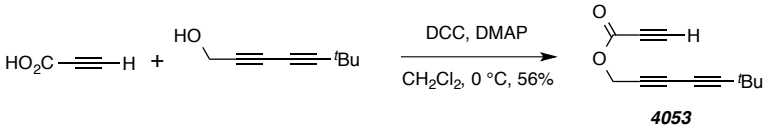

4053

[*BPW VI-121*] A solution of 6,6-dimethylhepta-2,4-diyn-1-ol[151] (65 mg, 0.48 mmol) and proiolic acid (62 µL, 1.0 mmol) in dichloromethane (4 mL) was cooled to 0 °C. N,N'-dicyclohexylcarbodiimide (206 mg, 1.0 mmol) and DMAP (5 mg, 0.04 mmol) was added and allowed to come to room temperature. After 4 h, the solution was filtered through plug of Celite, rinsing with EtOAc. After solvent removal, the crude material was purified by MPLC (10:1 Hex:EtOAc) to give triyne **4053** (50 mg, 0.27 mmol, 56%) as a yellow oil.

^{1}H NMR (500 MHz, $CDCl_3$): δ 4.83 (s, 2H, C*H*$_2$O), 2.95 (s, 1H, C≡C*H*), and 1.25 [s, 9H, C(C*H*$_3$)$_3$].

^{13}C NMR (125 MHz, $CDCl_3$): δ 151.8, 90.3, 76.1, 73.9, 72.7, 69.0, 62.9, 54.2, 30.3, and 28.2.

IR: 3285, 2972, 2868, 2255, 2124, 1722, 1366, 1206, 1178, 968, and 752 cm^{-1}.

GC-MS t_r (5025015) = 6.36 min; m/z: 188, 173, 145, 117, 91, 77, and 53.

5-(*tert*-Butyl)-6-(3,3-dimethylbut-1-yn-1-yl)naphtho[1,2-*c*:7,8-*c′*]difuran-3,8(1*H*,10*H*)-dione (4055)

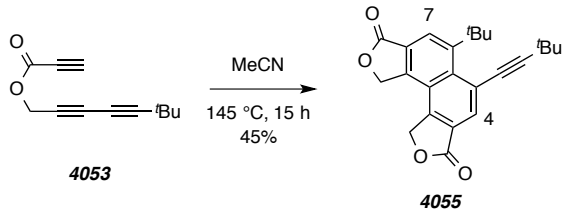

4053 *4055*

[*BPW VI-177*] A solution of **4053** (100 mg, 0.53 mmol) in acetonitrile (0.5 mL) was heated in a sealed vial to 145 °C. After 15 h the solvent was removed via rotary evaporation and the crude product was purified via MPLC (2:1 Hex:EtOAC) to obain **4055** (45 mg, 0.12 mmol, 20%) as a white solid.

^{1}H NMR (500 MHz, $CDCl_3$): δ 8.37 (s, 1H, *H4),* 8.30 (s, 1H, *H7*), 5.63 (s, 2H, C*H*$_2$O), 5.60 (s, 2H, CH_2O), 1.82 [s, 9H, $CH_7C(CH_3)_3$], and 1.39 [s, 9H, C≡CC(C*H*$_3$)$_3$].

^{13}C NMR (125 MHz, $CDCl_3$): δ 170.6, 169.7, 152.3, 145.2, 144.1, 137.9, 134.3, 125.2, 124.7, 124.1, 123.3, 123.2, 107.9, 83.7, 69.8, 69.5, 38.0, 34.5, 30.5, and 28.8.

IR: 2967, 2868, 2361, 2339, 1765, 1457, 1411, 1365, 1238, 1019, 912, 842, and 762 cm^{-1}.

HR ESI-MS calcd for $C_{24}H_{24}NaO_4$ $[M + Na]^+$ 399.1567, found 399.1525.

Experimental Section for Chapter 5

_N_-(7-((_tert_-Butyldimethylsilyl)oxy)hepta-2,4-diyn-1-yl)-N-phenyl-3-(trimethylsilyl)-propiolamide (5004)

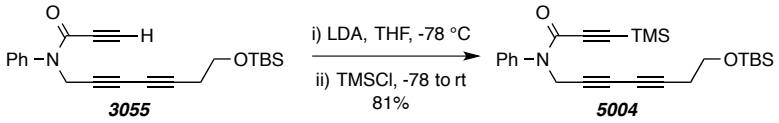

[*BPW V-246*] A stirred solution of amide **3055** (60 mg, 0.16 mmol) in THF (1 mL) was cooled in a dry ice/acetone bath. Freshly prepared lithium diisopropylamide (0.5 mL of a 0.4 M solution in THF/hexanes, 0.2 mmol, 1.3 equiv) was added dropwise, and the resulting solution was stirred for 40 minutes. Trimethylsilyl chloride (25 μL, 0.19 mmol, 1.2 equiv) was added and the mixture was allowed to warm to room temperature. After 20 min satd aq. NH_4Cl was added and the mixture was extracted with EtOAc. The combined organic extracts were washed with brine, dried ($MgSO_4$), and concentrated. The crude material was purified via MPLC (7:1 hexanes:EtOAc) to give the amide **5004** (56 mg, 0.13 mmol, 81%) as a clear amber oil.

^{1}H NMR (500 MHz, $CDCl_3$): major rotamer: δ 7.47–7.39 (m, 3H, PhH_mH_p), 7.35 (dd, J = 8.1, 2.1 Hz, 2H, PhH_o), 4.57 (s, 2H, CH_2N), 3.72 (t, J = 7.0 Hz, 2H, CH_2OSi), 2.46 (t, J = 7.0 Hz, 2H, CH_2CH$_2$O), 0.90 [s, 9H, SiC(CH_3)$_3$], 0.07 [s, 9H, SiCH_3)$_3$], and -0.04 [s, 6H, Si(CH_3)$_2$]. Minor rotamer (the resonances from the aliphatic protons of the minor constituent in the ca. 7:1 ratio of rotamers): 4.74 (br s, 2H, CH_2N), 3.74 (t, J = 6.9 Hz, 2H, CH$_2$OSi), 2.49 (t, J = 6.9 Hz, 2H, CH_2CH$_2$O), 0.90 [s, 9H, SiC(CH_3)$_3$], 0.07 [s, 6H, Si(CH_3)$_2$], and -0.04 [s, 9H, Si(CH_3)$_3$].

^{13}C NMR (125 MHz, $CDCl_3$): δ 153.2, 140.9, 129.2, 128.7, 128.6, 99.6, 96.1, 77.5, 70.4, 69.3, 65.8, 61.4, 38.4, 26.0, 23.8, 18.4, -1.0, and -5.2.

IR (neat): 2957, 2930, 2857, 2260, 1648, 1596, 1494, 1378, 1275, 1253, 1106, 843, 776, and 761 cm^{-1}.

HRMS (ESI-TOF): Calcd for $C_{25}H_{35}NNaO_2Si_2^+$ [M+Na$^+$] requires 460.2099; found 460.2123.

8-(*tert*-Butyldimethylsilyl)-6-phenyl-4-(trimethylsilyl)-2,3,6,7-tetrahydro-5H-furo[2,3-f]isoindol-5-one (5007)

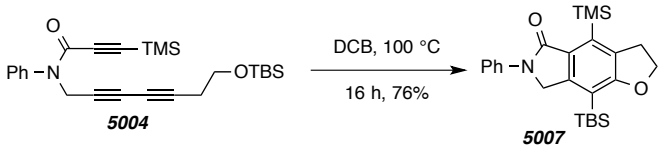

[*BPW V-253*] A solution of triyne **5004** (17 mg, 0.04 mmol) in DCB (0.39 mL) was heated at 100 °C. After 16 h the solution was loaded onto a column of silica and DCB was removed by initial elution with hexanes. Subsequent elution with hexanes:EtOAc (5:1) gave the crude material. Purification of the residue from these more polar fractions via flash chromatography (8:1 hexanes:EtOAc) gave the isoindolone **5007** (13 mg, 0.03 mmol, 76%) as a yellow solid.

^{1}H NMR (500 MHz, $CDCl_3$): δ 7.81 (dd, *J* = 8.7, 1.0 Hz, 2H, PhH_o), 7.40 (dd, *J* = 8.7, 7.4 Hz, 2H, PhH_m), 7.13 (tt, *J* = 7.4, 1.1, 1H, PhH_p), 4.72 (s, 2H, CH_2N), 4.52 (t, *J* = 8.7 Hz, 2H, CH_2O), 3.31 (t, *J* = 8.7 Hz, 2H, CH_2CH_2O), 0.93 [s, 9H, SiC(CH_3)$_3$], 0.46 [s, 9H, Si(CH_3)$_3$], and 0.40 [s, 6H, Si(CH_3)$_2$].

^{13}C NMR (125 MHz, $CDCl_3$): δ 168.3, 168.3, 148.4, 140.0, 137.0, 133.3, 129.9, 129.2, 123.9, 119.3, 112.1, 70.7, 52.3, 31.4, 26.9, 18.7, 2.2, and -3.1.

IR (neat): 2951, 2928, 2896, 2855, 1694, 1600, 1501, 1376, 1322, 1239, 1179, 1106, 842, and 809 cm^{-1}.

HRMS (ESI-TOF): Calcd for $C_{25}H_{36}NO_2Si_2^+$ [M+H$^+$] requires 438.2279; found 438.2294.

MP: 185–189 °C.

7-((*tert*-Butyldimethylsilyl)oxy)hepta-2,4-diyn-1-yl 3-(trimethylsilyl)propiolate (5005)

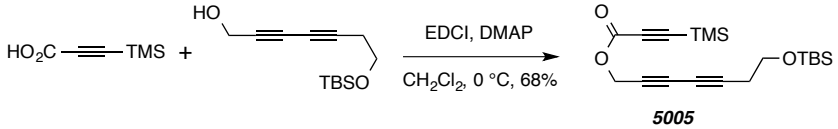

[*BPW V-109*] The following reagents were added in sequence to CH_2Cl_2 (5 mL) at 0 °C: 7-((*tert*-butyldimethylsilyl)oxy)hepta-2,4-diyn-1-ol[51a] (120 mg, 0.5 mmol), 3-trimethylsilylpropynoic acid (64 mg, 0.45 mmol), EDCI (78 mg, 0.45 mmol), and DMAP (6 mg, 0.05 mmol). The resulting homogenous solution quickly became cloudy. After 1 h the suspension was diluted with H_2O and extracted with CH_2Cl_2. The combined organic extracts were washed with brine, dried ($MgSO_4$),

and concentrated. Purification by MPLC (12:1 hexanes:EtOAc) gave the ester **5005** (110 mg, 0.30 mmol, 68%) as a clear oil.

^{1}H NMR (500 MHz, $CDCl_3$): δ 4.80 (s, 2H, C*H*$_2$OC=O), 3.74 (t, *J* = 6.9 Hz, 2H, C*H*$_2$OSi), 2.50 (t, *J* = 6.9 Hz, 2H, C≡CC*H*$_2$CH$_2$), 0.89 [s, 9H, SiC(C*H*$_3$)$_3$], 0.25 [s, 9H, Si(C*H*$_3$)$_3$], and 0.07 [s, 6H, Si(C*H*$_3$)$_2$].

^{13}C NMR (125 MHz, $CDCl_3$): δ 152.1, 96.0, 93.7, 79.9, 72.5, 68.6, 65.4, 61.3, 53.9, 26.0, 23.9, 18.4, -0.8, and -5.2.

IR (neat): 2955, 2930, 2857, 2262, 2176, 1718, 1254, 1203, 1108, 853 cm^{-1}.

HRMS (ESI-TOF): Calcd for $C_{19}H_{30}NaO_3Si_2^+$ [M+Na$^+$] requires 385.1626; found 385.1664.

8-(*tert*-Butyldimethylsilyl)-4-(trimethylsilyl)-3,7-dihydrobenzo[1,2-b:4,5-c']difuran-5(2H)-one (5008)

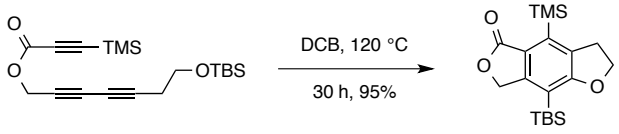

5005 ***5008***

[*BPW V-202*] A solution of ester **5005** (21 mg, 0.06 mmol) in DCB (1.2 mL) was heated at 120 °C. After 30 h the solution was loaded onto a column of silica gel and DCB was removed by initial elution with hexanes. Subsequent elution with a more polar mixture of hexanes:EtOAc gave benzenoid **5008** (20 mg, 0.06 mmol, 95%) as an off-white solid.

^{1}H NMR (500 MHz, $CDCl_3$): δ 5.16 (s, 2H, C*H*$_2$OC=O), 4.56 (t, *J* = 8.7 Hz, 2H, C*H*$_2$OAr), 3.30 (t, *J* = 8.7 Hz, 2H, C*H*$_2$CH$_2$O, 0.90 [s, 9H, SiC(C*H*$_3$)$_3$], 0.42 [s, 9H, Si(C*H*$_3$)$_3$], and 0.32 [s, 6H, Si(C*H*$_3$)$_2$].

^{13}C NMR (125 MHz, $CDCl_3$): δ 171.7, 169.6, 155.8, 138.5, 134.3, 121.8, 111.5, 71.2, 70.6, 31.0, 26.8, 18.6, 1.4, and -3.6.

IR (neat): 2950, 2928, 2896, 2856, 1754, 1241, 1094, 842, and 826 cm^{-1}.

HRMS (ESI-TOF): Calcd for $C_{19}H_{30}NaO_3Si_2^+$ [M+Na$^+$] requires 385.1626; found 385.1638.

MP: 164–167 °C.

9-((*tert*-Butyldimethylsilyl)oxy)nona-4,6-diyn-1-ol (S5001)

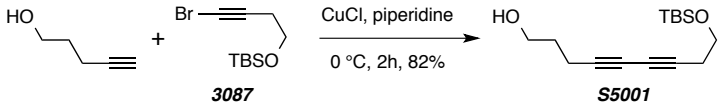

[*BPW IV-215*] Diyne **S5001** was prepared following the General Procedure A (Cadiot-Chodkiewicz) from **3087**[146] (524 mg, 2.0 mmol), pent-4-yn-1-ol (0.37 mL, 4.0 mmol), CuCl (40 mg, 0.40 mmol), and piperidine (6 mL). Purification by flash chromatography (hexanes:EtOAc 2.5:1) gave diyne **S5001** (437 mg, 1.64 mmol, 82%) as a yellow oil.

^{1}H NMR (500 MHz, $CDCl_3$): δ 3.74 (br t, J = 5.7 Hz, 2H, CH_2OH), 3.73 (t, J = 7.1 Hz, 2H, CH_2OSi), 2.46 (t, J = 7.1 Hz, 2H, CH_2CH$_2$CH$_2$OH), 2.39 (t, J = 6.9 Hz, 2H, CH_2CH$_2$CH$_2$OSi), 1.78 (pentet, J = 6.6 Hz, 2H, CH_2CH$_2$OH), 1.37 (br s, 1H, OH), 0.89 [s, 9H, SiC(CH_3)$_3$], and 0.07 [s, 6H, Si(CH_3)$_2$].

^{13}C NMR (125 MHz, $CDCl_3$): δ 74.7, 66.4, 65.8, 61.7, 61.6, 31.1, 26.0, 23.8, 18.5, 15.9, and -5.2.

IR (neat): 3350, 2952, 2929, 2857, 1471, 1255, 1105, 1055, 910, and 838 cm^{-1}.

HRMS (ESI-TOF): Calcd for $C_{15}H_{26}NaO_2Si^+$ [M+Na$^+$] requires 289.1594; found 289.1600.

9-((*tert*-Butyldimethylsilyl)oxy)nona-4,6-diynal (S5002)

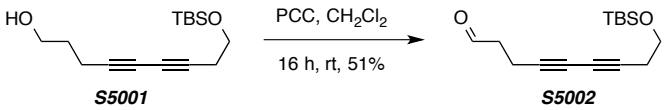

[*BPW IV-216*] PCC (645 mg, 3 mmol) was added to a stirred solution of alcohol **S5001** (400 mg, 1.5 mmol) in CH_2Cl_2 (12 mL) at room temperature. After 16 h the reaction mixture was filtered through Celite® (CH2Cl2 eluent) and concentrated. Purification by flash chromatography (7:1 hexanes:EtOAc) gave aldehyde **S5002** (201 mg, 0.76 mmol, 51%) as a yellow oil.

^{1}H NMR (500 MHz, $CDCl_3$): δ 9.79 (t, J = 1.0 Hz, 1H, CHO), 3.72 (t, J = 7.1 Hz, 2H, CH_2OSi), 2.70 (br tt, J = 7.5, 1.0 Hz, 2H, CH_2CH$_2$COH), 2.57 (br td, J = 6.9, 1.0 Hz, 2H, CH_2CHO), 2.46 (tt, J = 7.1, 1.1 Hz, 2H, CH_2CH$_2$OSi), 0.89 [s, 9H, SiC(CH_3)$_3$], and 0.07 [s, 6H, Si(CH_3)$_2$].

^{13}C NMR (125 MHz, $CDCl_3$): δ 199.8, 75.4, 75.2, 66.3, 66.2, 61.6, 42.3, 26.0, 23.8, 18.5, 12.6, and -5.2.

IR (neat): 2954, 2929, 2856, 2734, 1727, 1252, 1105, 913, 838, and 779 cm^{-1}.

HRMS (ESI-TOF): Calcd for $C_{15}H_{24}NaO_2Si^+$ [M+Na^+] requires 287.1438; found 287.1434.

11-((*tert*-Butyldimethylsilyl)oxy)-1-(trimethylsilyl)undeca-1,6,8-triyn-3-ol (S5003)

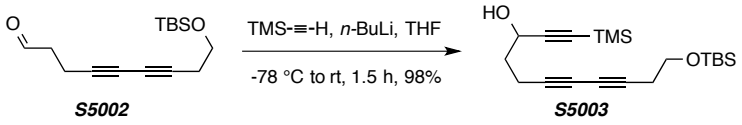

S5002 ***S5003***

[*BPW IV-219*] *n*-BuLi (0.36 mL, 2.5 M in hexanes, 0.9 mmol) was added to a stirred solution of trimethylsilylacetylene (145 µL, 1 mmol) in THF (6 mL) at -78 °C. After 1 h a solution of aldehyde **S5002** (180 mg, 0.68 mmol) in THF (1 mL) was added, and the resulting mixture was allowed to warm to room temperature. After 20 min satd aq. NH_4Cl was added and the mixture was extracted with EtOAc. The combined organic extracts were washed with brine, dried ($MgSO_4$), and concentrated to give the alcohol **S5003** (241 mg, 0.67 mmol, 98%) as a clear amber oil.

^{1}H NMR (500 MHz, $CDCl_3$): δ 4.50 (t, *J* = 6.4 Hz, 1H, C*H*OH), 3.73 (t, *J* = 7.1 Hz, 2H, CH_2OSi), 2.46 (t, *J* = 7.0 Hz, 2H, $CH_2C{\equiv}CC{\equiv}CCH_2CH_2OSi$), 2.51–2.38 (m, 2H, $CH_aH_bC{\equiv}CC{\equiv}CCH_2CH_2OSi$), 1.90 (br q, *J* = 6.6 Hz, 2H, $CHCH_2CH_2C{\equiv}$), 1.86 (br s, 0.89 [s, 9H, $SiC(CH_3)_3$], 0.17 [s, 9H, $Si(CH_3)_3$], and 0.07 [s, 6H, $Si(CH_3)_2$].

^{13}C NMR (125 MHz, $CDCl_3$): δ 105.7, 90.5, 77.4, 76.4, 74.5, 66.4, 66.0, 61.7, 36.1, 26.0, 23.8, 18.5, 15.4, 0.0, and 5.2.

IR (neat): 3497, 2956, 2930, 2857, 2173, 1251, 1106, and 843 cm^{-1}.

HRMS (ESI-TOF): Calcd for $C_{20}H_{34}NaO_2Si_2^+$ [M+Na^+] requires 385.1990; found 385.2004.

11-((*tert*-Butyldimethylsilyl)oxy)-1-(trimethylsilyl)undeca-1,6,8-triyn-3-one (5006)

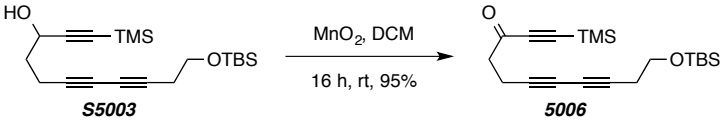

S5003 ***5006***

[*BPW IV-220*] MnO_2 (785 mg, 9.2 mmol) was added to a stirred solution of alcohol **S5003** (220 mg, 0.61 mmol) in CH_2Cl_2 (7 mL) at room temperature. After 16 h the reaction mixture was filtered through Celite® (CH_2Cl_2 eluent) and concentrated to give ketone **5006** (207 mg, 0.58 mmol, 95%) as an amber oil.

^{1}H NMR (500 MHz, $CDCl_3$): δ 3.72 (t, *J* = 7.1 Hz, 2H, C*H*$_2$OSi), 2.81 [br t, *J* = 7.3 Hz, 2H, $CH_2CH_2C(=O)$], 2.58 [br t, *J* = 7.5 Hz, 2H, $CH_2CH_2C(=O)$], 2.46 (tt, *J* = 7.1, 1.1 Hz, 2H, $C{\equiv}CCH_2CH_2OSi$), 0.89 [s, 9H, $SiC(CH_3)_3$], 0.25 [s, 9H, $Si(CH_3)_3$], and 0.07 [s, 6H, $Si(CH_3)_2$].

^{13}C NMR (125 MHz, $CDCl_3$): δ 184.8, 101.4, 99.4, 75.2, 75.1, 66.3, 66.2, 61.6, 43.7, 26.0, 23.8, 18.5, 14.0, -0.7, and -5.2.

IR (neat): 2956, 2930, 2857, 2229, 2153, 1681, 1253, 1109, and 845 cm^{-1}.

HRMS (ESI-TOF): Calcd for $C_{20}H_{32}NaO_2Si_2^+$ [M+Na$^+$] requires 383.1833; found 383.1844.

8-(*tert*-Butyldimethylsilyl)-4-(trimethylsilyl)-2,3,6,7-tetrahydro-5H-indeno[5,6-b]furan-5-one (5009)

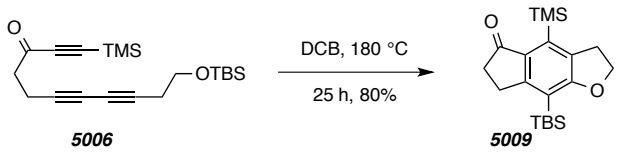

5006 ***5009***

[*BPW IV-236*] A solution of triyne **5006** (75 mg, 0.21 mmol) in DCB (2.1 mL) was heated at 180 °C. After 25 h the solution was cooled and loaded onto a column of silica gel and the DCB was removed by initial elution with hexanes. The crude product was eluted with a more polar solvent (hexanes:EtOAc 5:1). The residue from those fractions was purified via MPLC (20:1 hexanes:EtOAc) to give the indanone **5009** (60 mg, 0.17 mmol, 80%) as an off-white solid.

^{1}H NMR (500 MHz, $CDCl_3$): δ 4.51 (t, *J* = 8.6 Hz, 2H, C*H*$_2$O), 3.25 (t, *J* = 8.6 Hz, 2H, $ArCH_2CH_2O$), 3.07 [br t, *J* = 5.9 Hz, 2H, $CH_2CH_2C(=O)$], 2.58 [br t, *J* = 5.9 Hz, 2H, $CH_2CH_2C(=O)$], 0.92 [s, 9H, $SiC(CH_3)_3$], 0.36 [s, 6H, $Si(CH_3)_2$], and 0.35 [s, 9H, $Si(CH_3)_3$].

^{13}C NMR (125 MHz, $CDCl_3$): δ 205.8, 170.4, 165.2, 137.5, 134.9, 133.2, 114.9, 70.9, 36.4, 31.0, 28.7, 27.0, 18.8, 1.7, and -2.4.

IR (neat): 2951, 2928, 2896, 2855, 1697, 1296, 1246, 1220, 842, and 826 cm^{-1}.

HRMS (ESI-TOF): Calcd for $C_{20}H_{32}NaO_2Si_2^+$ [M+Na$^+$] requires 383.1833; found 383.1845.

MP: 128–129 °C.

Dimethyl 2,2-bis(7-((tert-Butyldimethylsilyl)oxy)hepta-2,4-diyn-1-yl)malonate (5011)

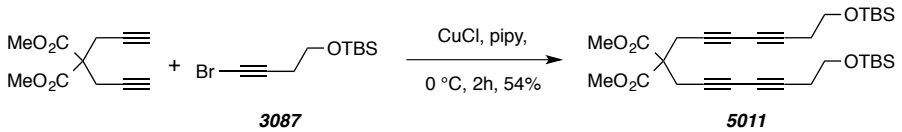

3087 ***5011***

[*BPW V-164*] Tetrayne **5011** was prepared following the General Procedure A (Cadiot-Chodkiewicz) from **3087**[146] (328 mg, 1.3 mmol), dimethyl 2,2-di(prop-2-yn-1-yl)malonate[143] (104 mg, 0.5 mmol), CuCl (25 mg, 0.25 mmol), and piperidine (2 mL). Purification by MPLC (hexanes:EtOAc 10:1) gave tetrayne **5011** (155 mg, 0.27 mmol, 54%) as an amber oil.

^{1}H NMR (500 MHz, $CDCl_3$): δ 3.76 (s, 6H, CO_2CH_3), 3.72 (t, J = 7.1 Hz, 4H, CH_2OSi), 3.05 [s, 4H, $CH_2C(CO_2Me)_2$], 2.45 (t, J = 7.1 Hz, 4H, CH_2CH_2OSi), 0.89 [s, 9H, $SiC(CH_3)_3$], and 0.07 [s, 6H, $Si(CH_3)_2$].

^{13}C NMR (125 MHz, $CDCl_3$): δ 168.8, 75.9, 71.0, 68.6, 66.1, 61.5, 56.8, 53.4, 26.0, 23.8, 23.7, 18.5, and -5.2.

IR (neat): 2954, 2930, 2857, 2262, 1745, 1293, 1249, 1212, 1107, 839, and 780 cm^{-1}.

HRMS (ESI-TOF): Calcd for $C_{31}H_{48}NaO_6Si_2^+$ [M+Na$^+$] requires 595.2882; found 595.2904.

Dimethyl 8-(tert-butyldimethylsilyl)-4-(4-((tert-butyldimethylsilyl)oxy)but-1-yn-1-yl)-2,3,5,7-tetrahydro-6H-indeno[5,6-b]furan-6,6-dicarboxylate (5013)

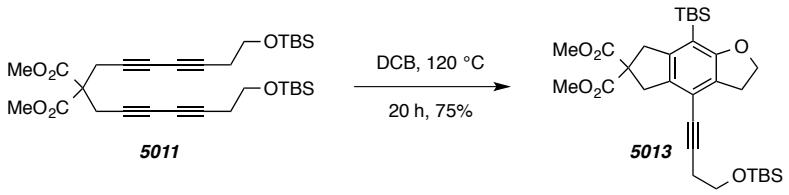

[*BPW V-172*] A solution of tetrayne **5011** (20 mg, 0.03 mmol) in DCB (3.5 mL) was heated at 120 °C. After 20 h the solution was cooled and loaded onto a column of silica gel and the DCB was removed by initial elution with hexanes. The crude product was eluted with a more polar mixture of hexanes:EtOAc. The residue from those fractions was purified via MPLC (6:1 hexanes:EtOAc) to give the benzenoid **5013** (15 mg, 0.03 mmol, 75%) as a yellow oil.

^{1}H NMR (500 MHz, $CDCl_3$): δ 4.44 (t, J = 8.7 Hz, 2H, CH_2OAr), 3.80 (t, J = 7.1 Hz, 2H, CH_2OSi), 3.73 (s, 6H, CO_2CH_3), 3.54 [s, 2H, $CH_2C(CO_2Me)_2$], 3.50 s, 2H, $C'H_2C(CO_2Me)_2$], 3.11 (t, J = 8.7 Hz, 2H, CH_2CH_2O), 2.66 (t, J = 7.1 Hz, 2H, CH_2CH_2OSi), 0.91 [s, 9H, $ArSiC(CH_3)_3$], 0.88 [s, 9H, $OSiC(CH_3)_3$], 0.32 [s, 6H, $ArSi(CH_3)_2$], and 0.09 [s, 6H, $OSi(CH_3)_2$].

^{13}C NMR (125 MHz, $CDCl_3$): δ 172.3, 165.4, 145.1, 133.1, 127.1, 117.6, 113.7, 94.0, 77.9, 70.6, 62.1, 60.2, 53.0, 43.2, 39.2, 29.5, 26.7, 26.0, 24.2, 18.5, 18.5, -2.7, and -5.1.

IR (neat): 2952, 2928, 2855, 1739, 1249, 1235, 838, and 781 cm^{-1}.

HRMS (ESI-TOF): Calcd for $C_{31}H_{48}NaO_6Si_2^+$ [M+Na$^+$] requires 595.2882; found 595.2879.

_N_-(7-((*tert*-Butyldimethylsilyl)oxy)hepta-2,4-diyn-1-yl)-4-methyl-_N_-(prop-2-yn-1-yl)benzenesulfonamide (5014b)

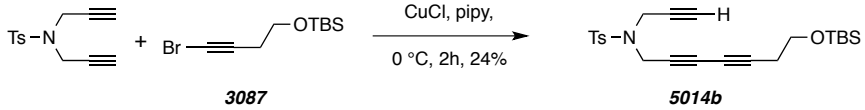

3087 ***5014b***

[*BPW VI-060*] Triyne **5014b** was prepared following the General Procedure A (Cadiot-Chodkiewicz) from **3087**[146] (140 mg, 0.5 mmol), 4-methyl-*N*,*N*-di(prop-2-yn-1-yl)benzenesulfonamide[152] (124 mg, 0.5 mmol), CuCl (25 mg, 0.25 mmol), and piperidine (2 mL). Purification by MPLC (hexanes:EtOAc 4:1) gave triyne **5014b** (51 mg, 0.12 mmol, 24%) as an amber oil.

^{1}H NMR (500 MHz, $CDCl_3$): δ 7.70 (d, *J* = 8.3 Hz, 2H, $SO_2Ph\mathit{H}_o$), 7.31 (d, *J* = 8.3 Hz, 2H, $SO_2Ph\mathit{H}_m$), 4.22 (s, 2H, $C\mathit{H}_2C{\equiv}CC{\equiv}C$), 4.12 (d, *J* = 2.4 Hz, 2H, $C\mathit{H}_2C{\equiv}C$), 3.71 (t, *J* = 6.9 Hz, 2H, $C\mathit{H}_2OSi$), 2.45 (t, *J* = 6.9 Hz, 2H, $C\mathit{H}_2CH_2OSi$), 2.43 (s, 3H, $ArC\mathit{H}_3$), 2.16 (t, *J* = 2.4 Hz, 1H, $C{\equiv}C\mathit{H}$), 0.89 [s, 9H, $OSiC(C\mathit{H}_3)_3$], and 0.07 [s, 6H, $Si(C\mathit{H}_3)_2$].

^{13}C NMR (125 MHz, $CDCl_3$): δ 144.2, 135.0, 129.7, 128.0, 77.9, 76.2, 74.3, 70.8, 68.4, 65.5, 61.4, 37.1, 36.6, 26.0, 23.7, 21.7, 18.5, and -5.2.

IR (neat): 3288, 2955, 2929, 2857, 2259, 1355, 1164, 1096, and 838 cm^{-1}.

HRMS (ESI-TOF): Calcd for $C_{23}H_{31}NNaO_3SSi^+$ [M+Na$^+$] requires 452.1686; found 452.1694.

Dimethyl 2-(7-((*tert*-Butyldimethylsilyl)oxy)hepta-2,4-diyn-1-yl)-2-(prop-2-yn-1-yl)malonate (5014c)

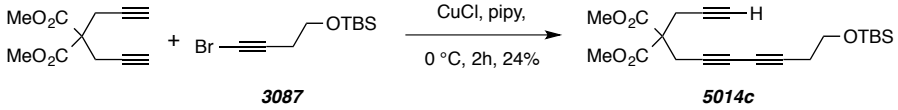

3087 ***5014c***

[*BPW VI-059*] Triyne **5014c** was prepared following the General Procedure A (Cadiot-Chodkiewicz) from **3087**[146] (200 mg, 0.75 mmol), dimethyl 2,2-di(prop-2-yn-1-yl)malonate[143] (150 mg, 0.75 mmol), CuCl (25 mg, 0.25 mmol), and piperidine (2 mL). Purification by MPLC (hexanes:EtOAc 10:1) gave triyne **5014c** (70 mg, 0.18 mmol, 24%) as an amber oil.

---

[152] Trost, B. M.; Rudd, M. T. Ruthenium-Catalyzed Cycloisomerizations of Diynols. *J. Am. Chem. Soc* **2005**, *127*, 2763–4776.

^{1}H NMR (500 MHz, $CDCl_3$): δ 3.77 (s, 6H, CO_2CH_3), 3.72 (t, *J* = 7.1 Hz, 2H, CH_2OSi), 3.07 (s, 2H, $CH_2C{\equiv}CC{\equiv}C$), 2.98 (d, *J* = 2.6 Hz, 2H, $CH_2C{\equiv}CH$), 2.45 (t, *J* = 7.1 Hz, 2H, CH_2CH_2OSi), 2.03 (t, *J* = 2.6 Hz, 1H, $C{\equiv}CH$), 0.89 [s, 9H, $OSiC(CH_3)_3$], and 0.07 [s, 6H, $Si(CH_3)_2$].

^{13}C NMR (125 MHz, $CDCl_3$): δ 169.0, 78.3, 75.8, 72.0, 71.0, 68.5, 66.1, 61.5, 56.7, 53.4, 26.0, 23.7, 23.6, 23.0, 18.5, and -5.2.

IR (neat): 3290, 2954, 2930, 2857, 1744, 1436, 1293, 1212, 1106, 839, and 778 cm^{-1}.

HRMS (ESI-TOF): Calcd for $C_{21}H_{30}NaO_5Si^+$ [$M+Na^+$] requires 413.1755; found 413.1760.

2,2,3,3,21,21,22,22-Octamethyl-4,20-dioxa-3,21-disilatricosa-7,9,14,16-tetrayne (5018)

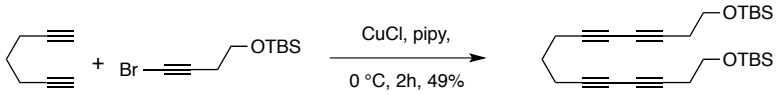

3087 ***5018***

[*BPW VI-052*] Tetrayne **16** was prepared following the General Procedure A (Cadiot-Chodkiewicz) from **3087**[146] (786 mg, 3.0 mmol), 1,6-heptadiyne (70 mg, 0.75 mmol), CuCl (40 mg, 0.4 mmol), and piperidine (5 mL). Purification by MPLC (hexanes:EtOAc 50:1) gave the tetrayne **5018** (169 mg, 0.37 mmol, 49%) as a colorless oil.

^{1}H NMR (500 MHz, $CDCl_3$): δ 3.73 (t, *J* = 7.1 Hz, 4H, CH_2OSi), 2.46 (tt, *J* = 7.1, 1.1 Hz, 4H, CH_2CH_2OSi), 2.38 (tt, *J* = 6.9, 1.1 Hz, 4H, $CH_2C{\equiv}CC{\equiv}C$), 1.73 (pentet, *J* = 6.9 Hz, 2H, $CH_2CH_2C{\equiv}C$), 0.89 [s, 18H, $OSiC(CH_3)_3$], and 0.07 [s, 12H, $Si(CH_3)_2$].

^{13}C NMR (125 MHz, $CDCl_3$): δ 76.3, 74.8, 66.4, 66.1, 61.6, 27.2, 26.0, 23.8, 18.47, 18.45, and -5.2.

IR (neat): 2953, 2929, 2857, 1255, 1106, 838, and 776 cm^{-1}.

HRMS (ESI-TOF): Calcd for $C_{27}H_{44}NaO_2Si_2^+$ [$M+Na^+$] requires 479.2772; found 479.2790.

8-((*tert*-Butyldimethylsilyl)oxy)octa-3,5-diyn-2-ol (S5004)

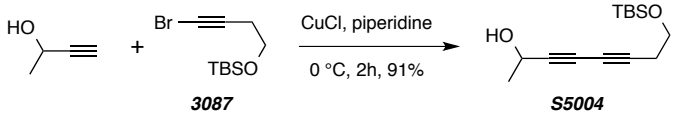

3087 ***S5004***

[*BPW VI-160*] Diyne **S5004** was prepared following the General Procedure A (Cadiot-Chodkiewicz) from **3087**[146] (130 mg, 0.5 mmol), but-3-yn-2-ol (140 mg, 2.0 mmol), CuCl (20 mg, 0.2 mmol), and piperidine (4 mL). Purification by MPLC (hexanes:EtOAc 6:1) gave diyne **S5004** (115 mg, 0.46 mmol, 91%) as a yellow oil.

^{1}H NMR (500 MHz, $CDCl_3$): δ 4.56 (q, *J* = 6.5 Hz, 1H, C*H*OH), 3.74 (t, *J* = 7.0 Hz, 2H, CH_2OSi), 2.49 (dt, *J* = 7.0, 0.8 Hz, 2H, CH_2CH$_2$OSi), 1.46 (d, *J* = 6.6 Hz, 3H, CHCH_3), 0.90 [s, 9H, SiC(CH_3)$_3$], and 0.07 [s, 6H, Si(CH_3)$_2$].

^{13}C NMR (125 MHz, $CDCl_3$): δ 78.9, 77.5, 69.2, 65.5, 61.5, 58.9, 26.0, 24.2, 23.9, 18.5, and -5.2.

IR: cm^{-1}.

8-((*tert*-Butyldimethylsilyl)oxy)octa-3,5-diyn-2-yl propiolate (3059-Me)

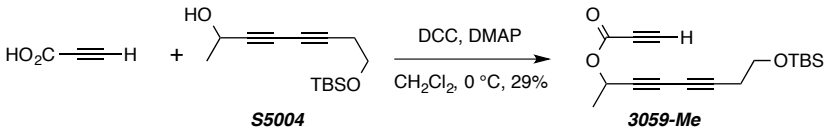

S5004 ***3059-Me***

[*BPW VI-182*] The following reagents were added in sequence to CH_2Cl_2 (1 mL) at 0 °C: **S5004** (100 mg, 0.4 mmol), propiolic acid (37 mg, 0.6 mmol), DCC (123 mg, 0.6 mmol), and DMAP (10 mg, 0.06 mmol). The resulting homogenous solution quickly became cloudy. After 16 h the suspension was diluted with H_2O and extracted with CH_2Cl_2. The combined organic extracts were washed with brine, dried ($MgSO_4$), and concentrated. Purification by MPLC (20:1 hexanes:EtOAc) gave the ester **3059-Me** (35 mg, 0.12 mmol, 29%) as a clear oil.

^{1}H NMR (500 MHz, $CDCl_3$): δ 5.52 (q, *J* = 6.7 Hz, 1H, C*H*OC=O), 3.74 (t, *J* = 7.0 Hz, 2H, CH_2OSi), 2.92 (s, 1H, C≡C*H*), 2.49 (dt, *J* = 7.0, 0.8 Hz, 2H, CH_2CH$_2$OSi), 1.55 (d, *J* = 6.7 Hz, 3H, CHCH_3), 0.90 [s, 9H, SiC(CH_3)$_3$], and 0.07 [s, 6H, Si(CH_3)$_2$].

^{13}C NMR (125 MHz, $CDCl_3$): δ 151.5, 79.9, 75.6, 74.3, 72.4, 70.9, 65.3, 62.8, 61.3, 26.0, 23.8, 21.1, 18.4, and -5.2.

IR (neat): 3290, 2953, 2930, 2857, 2260, 2119, 1720, 1216, 1105, 1079, 837, and 777 cm^{-1}.

HRMS (ESI-TOF): Calcd for $C_{17}H_{24}NaO_3Si^+$ [M+Na$^+$] requires 327.1387; found 327.1382.

8-(*tert*-Butyldimethylsilyl)-7-methyl-3,7-dihydrobenzo[1,2-*b*:4,5-*c'*]difuran-5(2*H*)-one (3060-Me)

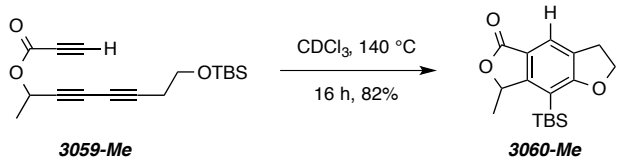

3059-Me ***3060-Me***

[*BPW VI-202*] A solution of triyne **3059-Me** (12 mg, 0.04 mmol) in $CDCl_3$ (0.4 mL) was heated at 140 °C. After 16 h the solution was cooled and solvent removed to give the benzenoid **3060-Me** (10 mg, 0.03 mmol, 82%) as a yellow oil.

^{1}H NMR (500 MHz, $CDCl_3$): δ 7.66 (t, *J* = 1.1 Hz, 1H, $C_{ar}H$), 5.51 (q, *J* = 6.4 Hz, 1H, $CHCH_3$), 4.63 (t, *J* = 8.2 Hz, 1H, CH_aH_bO), 4.62 (t, *J* = 8.5 Hz, 1H, CH_aH_bO), 3.24 (nfom, 2H, CH_2CH_2O), 1.59 (d, *J* = 6.4 Hz, 3H, $CHCH_3$), 0.95 [s, 9H, $SiC(CH_3)_3$], 0.37 (s, 3H, $Si(CH_3)_2$), and 0.31 [s, 3H, $Si(CH_3)_2$].

^{13}C NMR (125 MHz, $CDCl_3$): δ 171.6, 170.8, 160.2, 128.5, 123.5, 118.0, 111.8, 78.4, 71.7, 28.7, 27.9, 23.7, 18.4, and -2.7.

IR (neat): 2953, 2931, 2857, 1756, 1396, 1312, 1248, 1113, and 1040 cm^{-1}.

HRMS (ESI-TOF): Calcd for $C_{17}H_{24}NaO_3Si^+$ [$M+Na^+$] requires 327.1387; found 327.1391.

2-(6-((*tert*-Butyldimethylsilyl)oxy)hexa-1,3-diyn-1-yl)cyclohept-1-ene-1-carbaldehyde (S5005)

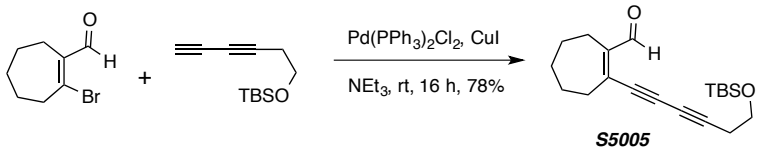

S5005

[*BPW VI-060*] $Pd(PPh_3)_2Cl_2$ (14 mg, 0.02 mmol) was added to a solution of aldehyde 2-bromocyclohept-1-ene-1-carbaldehyde[153] (182 mg, 0.9 mmol) and *tert*-butyl(hexa-3,5-diyn-1-yloxy)dimethylsilane[154] (291 mg, 1.4 mmol) in triethylamine (3.5 mL) under an atmosphere of N_2 and stirred for 15 minutes. CuI (5 mg) was added and the reaction mixture was allowed to stir at

[153] Auer, D.; Maywald, M.; Schmittel, M.; Steffen, J.-P. Ring strain effects in enyne-allene thermolysis: switch from the Myers-Saito reaction to the C2-C6 biradical cyclization. *Tetrahedron Lett.* **1997**, *38*, 6177–6180.

[154] Wang, K.-P.; Cho, E. J.; Yun, S. Y.; Rhee, J. Y.; Lee, D. Regio- and steroselectivity in the concatenated enyne cross metathesis-metallotropic [1,3]-shift of terminal 1,3-diyne. *Tetrahedron*. **2013**, *69*, 9105–9110.

room temperature. After 16 h the mixture was washed with satd. aq. NH_4Cl. The aqueous phase was extracted with EtOAc and the combined organic extracts were washed with brine, dried ($MgSO_4$), and concentrated. Purification by MPLC (hexanes:EtOAc 15:1) gave the diyne **S5005** (231 mg, 0.7 mmol, 78%) as a clear brown oil.

^{1}H NMR (500 MHz, $CDCl_3$): δ 10.08 (s, 1H, C*H*O), 3.78 (t, *J* = 6.9 Hz, 2H, CH_2OSi), 2.59 (t, *J* = 6.9 Hz, 2H, CH_2CH$_2$OSi), 2.59 (nfom, 2H, CH_2CCHO), 2.50 (nfom, 2H, CH_2CC≡C), 1.79 (nfom, 2H, CH_2CH$_2$CCHO), 1.62 (nfom, 2H, CH_2 CH$_2$CC≡C), 1.44 (nfom, 2H, CH_2CH$_2$CH$_2$), 0.90 [s, 9H, SiC(CH_3)$_3$], and 0.08 [s, 6H, Si(CH_3)$_2$].

^{13}C NMR (125 MHz, $CDCl_3$): δ 191.8, 152.1, 144.6, 86.7, 85.2, 73.0, 66.0, 61.4, 37.2, 32.3, 26.0, 25.8, 25.7, 24.5, 24.4, 18.5, and -5.2.

IR (neat): 2953, 2928, 2855, 2229, 1673, 1254, 1237, 1108, 838, and 778 cm^{-1}.

HRMS (ESI-TOF): Calcd for $C_{20}H_{30}NaO_2Si^+$ [M+Na$^+$] requires 353.1907; found 353.1914.

1-(2-(6-((*tert*-Butyldimethylsilyl)oxy)hexa-1,3-diyn-1-yl)cyclohept-1-en-1-yl)-3-(trimethylsilyl)prop-2-yn-1-ol (S5006)

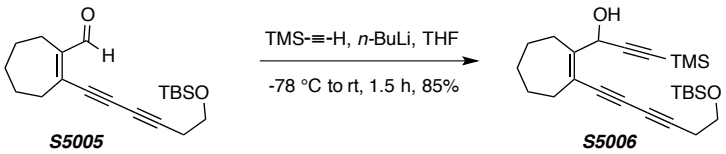

[*BPW VI-064*] *n*-BuLi (0.3 mL, 2.5 M in hexanes, 0.75 mmol) was added to a stirred solution of trimethylsilylacetylene (120 µL, 0.84 mmol) in THF (6 mL) at -78 °C. After 1 h a solution of aldehyde **S5005** (180 mg, 0.55 mmol) in THF (2 mL) was added, and the mixture was allowed to warm to room temperature. After 30 min satd aq. NH_4Cl was added and the mixture was extracted with EtOAc. The combined organic extracts were washed with brine, dried ($MgSO_4$), and concentrated. Purification by MPLC (hexanes:EtOAc 15:1) gave the alcohol **S5006** (203 mg, 0.47 mmol, 85%) as a clear amber oil.

^{1}H NMR (500 MHz, $CDCl_3$): δ 5.54 (d, *J* = 4.0, 1H, C*H*OH), 3.76 (t, *J* = 7.1 Hz, 2H, CH_2OSi), 2.56 (t, *J* = 7.1 Hz, 2H, CH_2CH$_2$OSi), 2.47 [ddd, *J* = 14.8, 8.3, 2.2 Hz, 1H, =C(CHOH)CH_aH$_b$], 2.40 [ddd, *J* = 14.7, 8.6, 2.9 Hz, 1H, =C(C≡C)CH_aH$_b$], 2.39 [ddd, *J* = 14.7, 8.9, 2.7 Hz, 1H, =C(CHOH)CH$_a$$H_b$], 2.35 [ddd, *J* = 14.7, 7.7, 2.8 Hz, 1H, =C(C≡C)CH$_a$$H_b$], 1.87 (d, *J* = 4.1 Hz, 1H, CHO*H*), 1.82–1.68 (overlapping nfom, 2H,

=CCH$_2$C*H$_2$*), 1.60–1.46 [overlapping nfom, 4H, =CCH$_2$(C*H$_2$*)$_2$], 0.90 [s, 9H, SiC(C*H$_3$*)$_3$], 0.17 [s, 9H, Si(C*H$_3$*)$_3$], and 0.08 [s, 6H, Si(C*H$_3$*)$_2$].

^{13}C NMR (125 MHz, $CDCl_3$): δ 152.3, 123.3, 104.1, 90.8, 83.1, 78.8, 75.0, 66.4, 65.6, 61.6, 34.5, 32.6, 29.1, 27.1, 26.1, 26.0, 24.2, 18.5, 0.0, and -5.1.

IR (neat): 3426, 2954, 2927, 2855, 2171, 1250, 1106, 1029, 843, and 778 cm^{-1}.

HRMS (ESI-TOF): Calcd for $C_{25}H_{40}NaO_2Si_2^+$ [M+Na$^+$] requires 451.2459; found 451.2460.

11-(*tert*-Butyldimethylsilyl)-4-(trimethylsilyl)-3,6,7,8,9,10-hexahydrocyclohepta[2,3]-indeno[5,6-b]furan-5(2H)-one (5022) via ketone (5019)

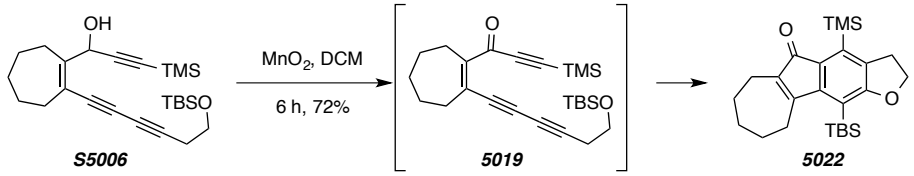

[*BPW VI-068*] MnO_2 (113 mg, 1.3 mmol) was added to a stirred solution of alcohol **S5006** (28 mg, 0.065 mmol) in CH_2Cl_2 (1 mL) at room temperature. After 6 h the reaction mixture was filtered through Celite® (EtOAc eluent) and concentrated. Purification by MPLC (hexanes:EtOAc 30:1) gave benzenoid **5022** (20 mg, 0.047 mmol, 72%) as an orange solid.

^{1}H NMR (500 MHz, $CDCl_3$): δ 4.43 (t, *J* = 8.9 Hz, 2H, C*H$_2$*OAr), 3.15 (t, *J* = 8.9 Hz, 2H, ArC*H$_2$*), 2.64 (br t, *J* = 5 Hz, 2H, =CC*H$_2$*), 2.35 (br t, *J* = 5 Hz, 2H, =C-C*H$_2$*), 1.82 (m, 2H, =C-CH$_2$C*H$_2$*), 1.59 (m, 2H, =C-CH$_2$C*H$_2$*), 1.51 [m, 2H, =C(CH$_2$)$_2$C*H$_2$*], 1.03 [s, 9H, SiC(C*H$_3$*)$_3$], 0.33 [s, 9H, Si(C*H$_3$*)$_3$], and 0.30 [s, 6H, Si(C*H$_3$*)$_2$].

^{13}C NMR (125 MHz, $CDCl_3$): δ 197.4, 169.2, 161.6, 156.0, 137.8, 136.4, 130.1, 128.1, 116.1, 70.4, 32.3, 31.1, 30.7, 28.5, 27.2, 26.4, 23.4, 18.8, 1.5, and 0.9.

IR (neat): 2927, 2855, 1696, 1493, 1376, 1311, 1299, 1261, 1248, 1111, 844, 765, and 753 cm^{-1}.

HRMS (ESI-TOF): Calcd for $C_{25}H_{38}NaO_2Si_2^+$ [M+Na$^+$] requires 449.2303; found 449.2296.

MP: 127–129 °C.

(*Z*)-2-(6-((*tert*-Butyldimethylsilyl)oxy)hexa-1,3-diyn-1-yl)cyclooct-1-ene-1-carbaldehyde (S5007)

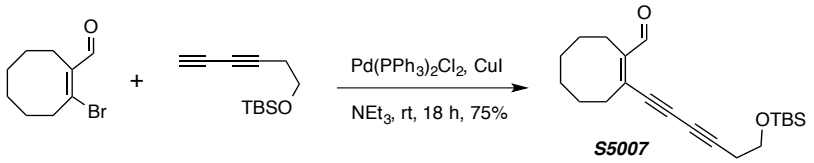

[*BPW V-248*] $Pd(PPh_3)_2Cl_2$ (5 mg, 0.01 mmol) was added to a solution of (Z)-2-bromocyclooct-1-ene-1-carbaldehyde[155] (50 mg, 0.23 mmol), tert-butyl(hexa-3,5-diyn-1-yloxy)dimethylsilane[154] (100 mg, 0.48 mmol), and triethylamine (1 mL) under an atmosphere of N_2, and the resulting mixture was stirred for 15 minutes. CuI (2 mg, 0.01 mmol) was added and the mixture was stirred at room temperature for 18 h. The mixture was partitioned between satd. aq. NH_4Cl and EtOAc, the aqueous layer was extracted with additional EtOAc, and the combined organic extracts were washed with brine, dried ($MgSO_4$), and concentrated. Purification of the residue by MPLC (hexanes:EtOAc 12:1) gave the aldehyde **S5007** (59 mg, 0.17 mmol, 75%) as a clear brown oil.

^{1}H NMR (500 MHz, $CDCl_3$): δ 10.12 (s, 1H, C*H*O), 3.78 (t, *J* = 6.9 Hz, 2H, CH_2OSi), 2.59 (t, *J* = 6.9 Hz, 2H, CH_2CH$_2$O), 2.60 (br t, *J* = 6.3 Hz, 2H, CH_2CC=O), 2.45 (br t, *J* = 6.1 Hz, 2H, CH_2C=CC=O), 1.76 (br pentet, 2H, CH_2CH$_2$C=CC=O), 1.54 [br pentet, 4H, (CH_2)$_2$(CH$_2$)$_2$C=C], 0.91 [s, 9H, SiC(CH_3)$_3$], and 0.09 [s, 6H, Si(CH_3)$_2$].

^{13}C NMR (125 MHz, $CDCl_3$): δ 192.1, 149.7, 141.9, 85.8, 83.9, 72.3, 66.0, 61.3, 34.0, 29.9, 29.0, 26.5, 25.99, 25.98, 24.3, 23.9, 18.5, and -5.1.

IR (neat): 2929, 2856, 2230, 1675, 1106, 813, and 775 cm^{-1}.

HRMS (ESI-TOF): Calcd for $C_{21}H_{32}NaO_2Si^+$ [M+Na$^+$] requires 367.2064; found 367.2097.

(*Z*)-1-(2-(6-((*tert*-Butyldimethylsilyl)oxy)hexa-1,3-diyn-1-yl)cyclooct-1-en-1-yl)-3-(trimethylsilyl)prop-2-yn-1-ol (S5008)

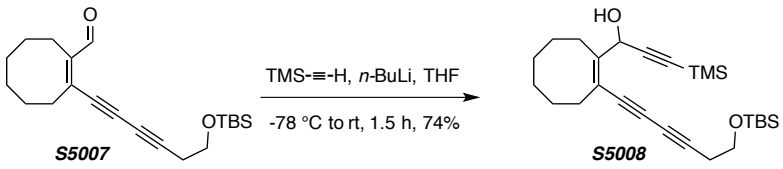

[155] Peng, Y.; Yu, M.; Zhang, L. Au-Catalyzed synthesis of 5,6-dihydro-8*H*-indolizin-7-ones from *N*-(pent-2-en-4-ynyl)-β-lactams *Org. Lett.* **2008**, *10*, 5187–5190.

[*BPW IV-242*] *n*-BuLi (0.45 mL, 2.5 M in hexanes, 1.1 mmol) was added to a stirred solution of trimethylsilylacetylene (175 µL, 1.2 mmol) in THF (8 mL) at -78 °C. After 1 h a solution of aldehyde **S5007** (285 mg, 0.83 mmol) in THF (2 mL) was added, and the mixture was allowed to warm to room temperature. After 15 min satd aq. NH_4Cl was added and the mixture was extracted with EtOAc. The combined organic extracts were washed with brine, dried ($MgSO_4$), and concentrated. Purification by MPLC (hexanes:EtOAc 15:1) gave the alcohol **S5008** (270 mg, 0.61 mmol, 74%) as a clear amber oil.

^{1}H NMR (500 MHz, $CDCl_3$): δ 5.62 (d, *J* = 4.4, 1H, C*H*OH), 3.76 (t, *J* = 7.1 Hz, 2H, CH_2OSi), 2.56 (t, *J* = 7.1 Hz, 2H, CH_2CH$_2$OSi), 2.51 (ddd, *J* = 13.9, 7.7, 3.8Hz, 1H, =CCH_a), 2.42–2.35 (m, 2H, =CCH$_a$$H_b$ and =C'C'H_aH$_b$), 2.30 (ddd, *J* = 13.4, 5.2, 5.2, Hz, 1H, =C'C'H$_a$$H_b$), 1.92 (d, *J* = 4.4 Hz, 1H, CHO*H*), 1.80 (m, 1H, =C-CH$_2$CH_a), 1.71 (m, 1H, =C-CH$_2$CH_b), 1.64 (br pentet, 2H, CH$_2$), 1.47 [m, 4H, CH$_2$(CH_2)$_2$], 0.90 [s, 9H, SiC(CH_3)$_3$], 0.17 [s, 9H, Si(CH_3)$_3$], and 0.08 [s, 6H, Si(CH_3)$_2$].

^{13}C NMR (125 MHz, $CDCl_3$): δ 149.3, 121.0, 104.5, 90.9, 82.5, 78.3, 77.4, 66.5, 65.2, 61.6, 31.6, 31.5, 28.7, 27.3, 26.7, 26.0 (2x), 24.2, 18.5, 0.1, and -5.1.

IR (neat): 3431 (br), 2955, 2929, 2856, 1471, 1251, 1106, 861, and 778 cm^{-1}.

HRMS (ESI-TOF): Calcd for $C_{26}H_{42}NaO_2Si_2^+$ [M+Na$^+$] requires 465.2616; found 465.2636.

12-(*tert*-Butyldimethylsilyl)-4-(trimethylsilyl)-2,3,6,7,8,9,10,11-octahydro-5H-cycloocta-[2,3]indeno[5,6-b]furan-5-one (5023) via ketone **5020**

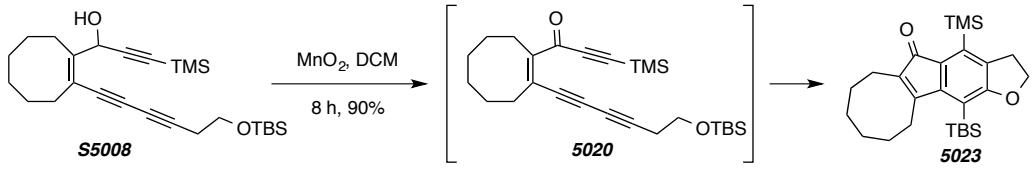

[*BPW IV-243*] MnO_2 (60 mg, 0.7 mmol) was added to a stirred solution of alcohol **S5008** (20 mg, 0.05 mmol) in CH_2Cl_2 (1 mL) at room temperature. After 6 h the reaction mixture was filtered through Celite® (EtOAc eluent) and concentrated to give the benzenoid **5023** (18 mg, 0.04 mmol, 90%) as an orange solid.

^{1}H NMR (500 MHz, $CDCl_3$): δ 4.44 (t, *J* = 8.9 Hz, 2H, CH_2O), 3.15 (t, *J* = 8.9 Hz, 2H, CH_2CH$_2$O), 2.75 (br t, *J* = 6.2 Hz, 2H, CH_2CC=O), 2.36 (br t, *J* = 6.2 Hz, 2H, CH_2C=CC=O), 1.69–1.63 (m, 2H, CH_2CH$_2$CC=O), 1.60 (br pentet, 2H, CH_2CH$_2$C=CC=O), 1.51–1.44 [m,

4H, ($C\mathit{H}_2$)$_2$(CH_2)$_2$C=C], 1.03 [s, 9H, SiC($C\mathit{H}_3$)$_3$], 0.34 [s, 9H, Si($C\mathit{H}_3$)$_3$], and 0.3 [s, 6H, Si($C\mathit{H}_3$)$_2$].

^{13}C NMR (125 MHz, $CDCl_3$): δ 197.6, 169.2, 159.5, 156.5, 136.7, 136.4, 131.3, 128.1, 116.2, 70.5, 31.3, 30.0, 29.3, 28.2, 27.0, 26.5, 26.0, 22.0, 18.9, 1.4, and 0.6.

IR (neat): 2928, 2855, 1696, 1299, 1246, 1079, 1010, and 859 cm^{-1}.

HRMS (ESI-TOF): Calcd for $C_{26}H_{40}NaO_2Si_2^+$ [M+Na$^+$] requires 463.2459; found 463.2474.

MP: 149–150 °C.

2-(6-((*tert*-Butyldimethylsilyl)oxy)hexa-1,3-diyn-1-yl)cyclopent-1-ene-1-carbaldehyde (S5009)

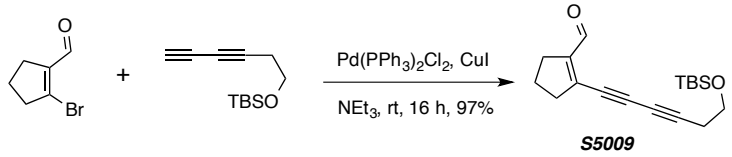

[*BPW V-062*] $Pd(PPh_3)_2Cl_2$ (25 mg, 0.05 mmol) was added to a solution of 2-bromocyclopent-1-ene-1-carbaldehyde[156] (210 mg, 1.2 mmol), *tert*-butyl(hexa-3,5-diyn-1-yloxy)dimethylsilane[154] (290 mg, 1.4 mmol), and triethylamine (5 mL) under an atmosphere of N_2, and the solution was stirred for 15 minutes. CuI (5 mg, 0.02 mmol) was added and the reaction mixture was stirred at room temperature. After 18 h, EtOAc was added and the mixture was washed with satd. aq. NH_4Cl. The aqueous phase was extracted with additional EtOAc, and the combined organic extracts were washed with wish brine, dried ($MgSO_4$), and concentrated to give the aldehyde **S5009** (353 mg, 1.17 mmol, 97%) as a clear brown oil.

^{1}H NMR (500 MHz, $CDCl_3$): δ 10.01 (s, 1H, C*H*O), 3.78 (t, *J* = 6.8 Hz, 2H, $C\mathit{H}_2$OSi), 2.71 (tt, *J* = 7.5, 2.3 Hz, 2H, $C\mathit{H}_2$CCHO), 2.63 (tt, *J* = 7.5, 2.3 Hz, 2H, $C\mathit{H}_2$C=CCHO), 2.60 (t, *J* = 6.8 Hz, 2H, $C\mathit{H}_2CH_2$OSi), 1.97 (pentet, *J* = 7.9 Hz, 2H, $CH_2C\mathit{H}_2CH_2$), 0.91 [s, 9H, SiC($C\mathit{H}_3$)$_3$], and 0.09 [s, 6H, Si($C\mathit{H}_3$)$_2$].

^{13}C NMR (125 MHz, $CDCl_3$): δ188.5, 151.7, 141.9, 86.8, 85.4, 68.6, 65.8, 61.2, 38.9, 29.8, 26.0, 24.3, 22.3, 18.4, and –5.2.

IR (neat): 2954, 2930, 2856, 2232, 1671, 1251, 1107, 838, and 778 cm^{-1}.

---

[156] Delort, E.; Klotz, P.; Salem, B.; Suffert, J. Cyclocarbopalladation: 5-Exo-dig Cyclization versus direct Stille cross-coupling reaction. The influence of the α,β-propargylic substitution. *Org. Lett.* **2003**, *5*, 2307–2310.

HRMS (ESI-TOF): Calcd for $C_{18}H_{26}NaO_2Si^+$ [M+Na^+] requires 325.1594; found 325.1596.

1-(2-(6-((*tert*-Butyldimethylsilyl)oxy)hexa-1,3-diyn-1-yl)cyclopent-1-en-1-yl)-3-(trimethylsilyl)prop-2-yn-1-ol (S5010)

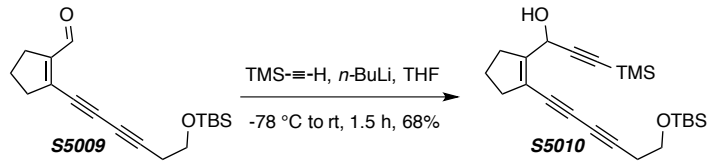

[*BPW IV-047*] *n*-BuLi (0.54 mL, 2.5 M in hexanes, 1.4 mmol) was added to a stirred solution of trimethylsilylacetylene (215 µL, 1.5 mmol) in THF (8 mL) at -78 °C. After 1 h a solution of aldehyde **S5009** (300 mg, 1.0 mmol) in THF (1 mL) was added, and the mixture was allowed to warm to room temperature. After 20 min satd aq. NH_4Cl was added and the mixture was extracted with EtOAc. The combined organic extracts were washed with brine, dried ($MgSO_4$), and concentrated. The crude material was purified via MPLC (10:1 hexanes:EtOAc) to give the alcohol **S5010** (273 mg, 0.68 mmol, 68%) as a clear amber oil.

^{1}H NMR (500 MHz, $CDCl_3$): δ 5.39 (br s, 1H, C*H*OH), 3.76 (t, *J* = 7.1 Hz, 2H, CH_2OSi), 2.67–2.57 (m, 2H, CH_2C=), 2.56 (t, *J* = 7.1 Hz, 2H, CH_2CH_2OSi), 2.56–2.47 (m, 2H, C'H_2C'=), 2.03 (br s, 1H, CHO*H*), 1.98–1.86 (m, 2H, $CH_2CH_2CH_2$), 0.90 [s, 9H, SiC(CH_3)$_3$], 0.18 [s, 9H, Si(CH_3)$_3$], and 0.08 [s, 6H, Si(CH_3)$_2$].

^{13}C NMR (125 MHz, $CDCl_3$): δ 152.0, 120.9, 103.5, 90.8, 83.1, 80.0, 70.3, 66.3, 61.5, 60.5, 36.9, 31.4, 26.0, 24.2, 22.3, 18.5, 0.0, and -5.2.

IR (neat): 3450, 2956, 2930, 2857, 2172, 1251, 1109, 842, and 778 cm^{-1}.

HRMS (ESI-TOF): Calcd for $C_{23}H_{36}NaO_2Si_2^+$ [M+Na^+] requires 423.2146; found 423.2138.

1-(2-(6-((*tert*-Butyldimethylsilyl)oxy)hexa-1,3-diyn-1-yl)cyclopent-1-en-1-yl)-3-(trimethylsilyl)prop-2-yn-1-one (5021)

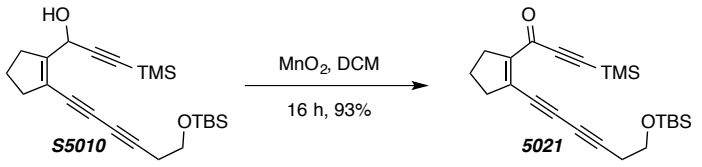

[*BPW IV-063*] MnO_2 (880 mg, 10.2 mmol) was added to a stirred solution of alcohol **S5010** (273 mg, 0.68 mmol) in CH_2Cl_2 (10 mL) at room temperature. After 16 h the reaction mixture was

filtered through Celite® (CH_2Cl_2 eluent) and concentrated to give ketone **5021** (252 mg, 0.63 mmol, 93%) as an amber oil.

^{1}H NMR (500 MHz, $CDCl_3$): δ 3.77 (t, *J* = 7.1 Hz, 2H, C*H*$_2$OSi), 2.77–2.71 (m, 4H, C*H*$_2$CH$_2$C*H*$_2$), 2.59 (t, *J* = 7.1 Hz, 2H, C*H*$_2$CH$_2$O), 1.90 (pentet, *J* = 7.7 Hz, 2H, C*H*$_2$CH$_2$C=C), 0.90 [s, 9H, SiC(C*H*$_3$)$_3$], 0.29 [s, 9H, Si(C*H*$_3$)$_3$], and 0.07 [s, 6H, Si(C*H*$_3$)$_2$].

^{13}C NMR (125 MHz, $CDCl_3$): δ 173.3, 149.1, 136.9, 101.9, 100.4, 87.8, 87.3, 70.6, 66.9, 61.3, 41.0, 32.8, 26.0, 24.3, 21.8, 18.4, -0.5, and -5.1.

IR (neat): 2955, 2930, 2857, 2228, 1609, 1252, 1107, and 846 cm^{-1}.

HRMS (ESI-TOF): Calcd for $C_{23}H_{34}NaO_2Si_2^+$ [M+Na$^+$] requires 421.1990; found 421.2000.

9-(*tert*-Butyldimethylsilyl)-4-(trimethylsilyl)-3,6,7,8-tetrahydrocyclopenta[2,3]indeno[5,6-b]furan-5(2H)-one (5024)

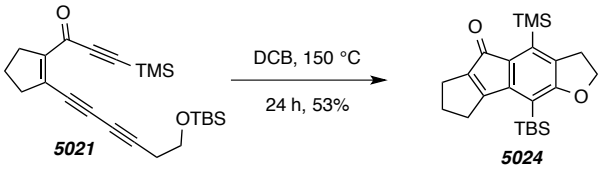

[*BPW V-245*] A solution of triyne **5021** (30 mg, 0.08 mmol) in DCB (0.75 mL) was heated at 180 °C. After 24 h the solution was loaded onto a column of silica and DCB was removed by elution with hexanes. Subsequent elution with hexanes:EtOAc (5:1) gave the crude material. Purification of the residue from these more polar fractions via flash chromatography (25:1 hexanes:EtOAc) gave the benzenoid **5024** (16 mg, 0.04 mmol, 53%) as an orange solid.

^{1}H NMR (500 MHz, $CDCl_3$): δ 4.42 (t, *J* = 8.9 Hz, 2H, C*H*$_2$O), 3.14 (t, *J* = 8.9 Hz, 2H, C*H*$_2$CH$_2$O), 2.75 (tt, *J* = 6.9, 2.8 Hz, 2H, C*H*$_2$CC=O), 2.41 (tt, *J* = 7.3, 3.0 Hz, 2H, C*H*$_2$CAr), 2.26 (br pentet, *J* = 7.3 Hz, 2H, CH$_2$C*H*$_2$CH$_2$), 0.94 [s, 9H, SiC(C*H*$_3$)$_3$], 0.34 [s, 6H, Si(C*H*$_3$)$_2$], and 0.33 [s, 9H, Si(C*H*$_3$)$_3$].

^{13}C NMR (125 MHz, $CDCl_3$): δ 193.9, 169.6, 168.3, 150.0, 145.2, 137.1, 134.7, 128.0, 116.1, 70.3, 33.1, 31.5, 27.7, 27.5, 24.5, 18.5, 1.6, and -0.2.

IR (neat):, 2952, 2928, 2895, 2855, 1698, 1497, 1375, 1301, 1247, 1111, 844, and 809 cm^{-1}.

HRMS (ESI-TOF): Calcd for $C_{23}H_{34}NaO_2Si_2^+$ [M+Na$^+$] requires 421.1990; found 421.2022.

MP: 148–153 °C.

2-((Trimethylsilyl)ethynyl)cyclohept-1-ene-1-carbaldehyde (S5011)

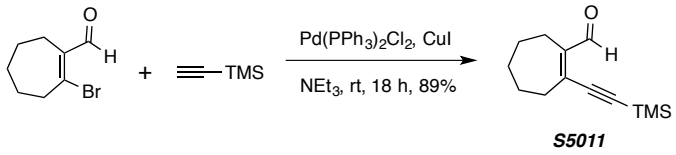

S5011

[*BPW IV-059*] $Pd(PPh_3)_2Cl_2$ (25 mg, 0.04 mmol) was added to a solution of 2-bromocyclohept-1-ene-1-carbaldehyde[153] (200 mg, 1.0 mmol), trimethylsilylacetylene (0.35 mL, 2.5 mmol), and triethylamine (4 mL) under an atmosphere of N_2. This solution was stirred for 15 minutes at ambient temperature. CuI (5 mg, 0.03 mmol) was added and the mixture was allowed to stir at room temperature. After 18 h the reaction mixture was washed with satd. aq. NH_4Cl. The aqueous phase was extracted with EtOAc and the combined organic extracts were washed with brine, dried ($MgSO_4$), and concentrated. Purification by MPLC (hexanes:EtOAc 15:1) gave the aldehyde **S5011** (196 mg, 0.89 mmol, 89%) as a clear brown oil.

^{1}H NMR (500 MHz, $CDCl_3$): δ 10.18 (s, 1H, C*H*O), 2.59 (nfom, 2H, =CCH_2), 2.49 (nfom, 2H, =C'C'H_2), 1.79 (br pentet, 2H, CH_2CH$_2$CCHO), 1.64 (br pentet, 2H, CH_2CH$_2$CC≡C), 1.44 (pentet, 2H, J = 6.0 Hz, CH_2CH$_2$CH$_2$), and 0.22 [s, 9H, Si(CH_3)$_3$].

^{13}C NMR (125 MHz, $CDCl_3$): δ 192.7, 149.5, 145.6, 106.5, 102.8, 37.4, 32.3, 25.8, 25.7, 24.3, and 0.1.

IR (neat): 2957, 2925, 2852, 2133, 1675, 1251, 1159, 857, 846, and 761 cm^{-1}.

HRMS (ESI-TOF): Calcd for $C_{13}H_{20}NaOSi^+$ [M+Na$^+$] requires 243.1176; found 243.1191.

7-((*tert*-Butyldimethylsilyl)oxy)-1-(2-((trimethylsilyl)ethynyl)cyclohept-1-en-1-yl)hepta-2,4-diyn-1-ol (S5012)

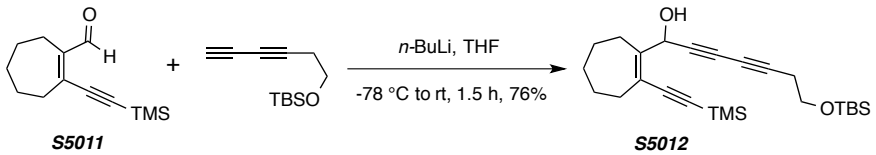

S5011 ***S5012***

[*BPW IV-062*] *n*-BuLi (0.3 mL, 2.5 M in hexanes, 0.75 mmol) was added to a stirred solution of *tert*-butyl(hexa-3,5-diyn-1-yloxy)dimethylsilane[154] (166 mg, 0.8 mmol) in THF (6 mL) at -78 °C. After 1 h a solution of aldehyde **S5011** (120 mg, 0.55 mmol) in THF (2 mL) was added and the mixture was allowed to warm to room temperature. After 30 min satd aq. NH_4Cl was added and the mixture was extracted with EtOAc. The combined organic extracts were washed with brine,

dried ($MgSO_4$), and concentrated. Purification by MPLC (hexanes:EtOAc 15:1) gave the alcohol **S5012** (180 mg, 0.42 mmol, 76%) as a clear amber oil.

^{1}H NMR (500 MHz, $CDCl_3$): δ 5.66 (d, *J* = 4.5 Hz, 1H, C*H*OH), 3.74 (t, *J* = 7.0 Hz, 2H, CH_2OSi), 2.49 (td, *J* = 7.0, 0.9 Hz, 2H, CH_2CH$_2$OSi), 2.45–2.32 (m, 4H, =C-CH_2), 1.96 (d, *J* = 4.6 Hz, 1H, CHO*H*), 1.80–1.69 (m, 2H, =C-CH$_2$CH_2), 1.60–1.49 [m, 4H, =C-CH$_2$(CH_2)$_2$], 0.90 [s, 9H, SiC(CH_3)$_3$], 0.19 [s, 9H, Si(CH_3)$_3$], and 0.07 [s, 6H, Si(CH_3)$_2$].

^{13}C NMR (125 MHz, $CDCl_3$): δ 148.9, 124.7, 104.9, 99.4, 78.8, 74.7, 70.2, 65.8, 65.6, 61.5, 34.8, 32.5, 29.0, 27.0, 26.1, 26.0, 23.9, 18.5, 0.2, and -5.2.

IR (neat): 3450, 2954, 2927, 2855, 2255, 2134, 1250, 1108, 857, 842, 779, and 760 cm^{-1}.

HRMS (ESI-TOF): Calcd for $C_{25}H_{40}NaO_2Si_2^+$ [M+Na$^+$] requires 451.2459; found 451.2452.

7-((*tert*-Butyldimethylsilyl)oxy)-1-(2-((trimethylsilyl)ethynyl)cyclohept-1-en-1-yl)hepta-2,4-diyn-1-one (5025)

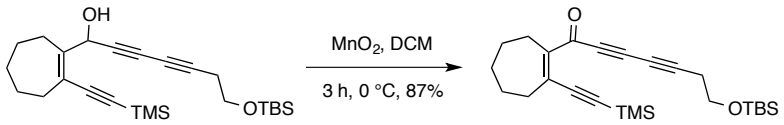

S5012 ***5025***

[*BPW V-117*] MnO_2 (120 mg, 1.4 mmol) was added to a stirred solution of alcohol **S5012** (30 mg, 0.07 mmol) in CH_2Cl_2 (1 mL) at 0 °C. After 3 h the reaction mixture was filtered through Celite® (EtOAc eluent) and concentrated at 0 °C to give ketone **5025** (28 mg, 0.07 mmol, 93%) as an orange oil.

^{1}H NMR (500 MHz, $CDCl_3$): δ 3.76 (t, *J* = 7.0 Hz, 2H, CH_2OSi), 2.61–2.58 (m, 4H, =C-CH_2), 2.58 (t, *J* = 7.0 Hz, 2H, C≡CCH_2CH$_2$), 1.77 (br pentet, *J* = 5.7 Hz, 2H, =C-CH$_2$CH_2), 1.62 (br pentet, *J* = 5.9 Hz, 2H, =C-CH$_2$CH_2), 1.49 (pentet, *J* = 6.0 Hz, 2H, =C-CH$_2$CH$_2$CH_2), 0.89 [s, 9H, SiC(CH_3)$_3$], 0.24 [s, 9H, Si(CH_3)$_3$], and 0.07 [s, 6H, Si(CH_3)$_2$].

^{13}C NMR (125 MHz, $CDCl_3$): δ 177.5, 148.4, 138.3, 108.9, 105.2, 87.8, 79.4, 73.4, 66.2, 61.1, 38.8, 32.2, 28.6, 26.0, 26.0, 25.5, 24.3, 18.4, 0.0, and -5.2.

IR (neat): 2955, 2928, 2855, 2232, 2140, 1604, 1251, 1108, 855, 844, 778, and 763 cm^{-1}.

HRMS (ESI-TOF): Calcd for $C_{25}H_{38}NaO_2Si_2^+$ [M+Na$^+$] requires 449.2303; found 449.2312.

4-(*tert*-Butyldimethylsilyl)-11-(trimethylsilyl)-3,6,7,8,9,10-hexahydrocyclohepta[2,3]indeno-[5,6-b]furan-5(2H)-one (S5013)

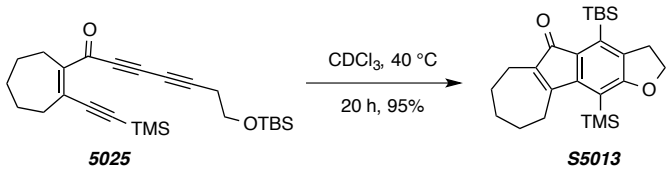

[*BPW IV-065*] A solution of triyne **5025** (20 mg, 0.05 mmol) in $CDCl_3$ (1 mL) was heated at 40 °C. After 20 h the mixture was concentrated and the crude material filtered through a plug of silica (hexanes:EtOAc 5:1) to give polycycle **S5013** (19 mg, 0.05 mmol, 95%) as a red solid.

^{1}H NMR (500 MHz, $CDCl_3$): δ 4.36 (t, *J* = 8.7 Hz, 2H, C*H*$_2$OAr), 3.14 (t, *J* = 8.7 Hz, 2H, ArC*H*$_2$CH$_2$), 2.73 (nfom, 2H, =C-C*H*$_2$), 2.34 (nfom, 2H, =C-C*H*$_2$), 1.82 (br pentet, *J* = 5.9 Hz, 2H, =C-CH$_2$C*H*$_2$), 1.65 (br pentet, *J* = 5.6 Hz, 2H, =C-CH$_2$C*H*$_2$), 1.50 (br pentet, *J* = 5.9 Hz, 2H, =C-CH$_2$CH$_2$C*H*$_2$), 0.94 [s, 9H, SiC(C*H*$_3$)$_3$], 0.40 [s, 9H, Si(C*H*$_3$)$_3$], and 0.34 [s, 6H, Si(C*H*$_3$)$_2$].

^{13}C NMR (125 MHz, $CDCl_3$): δ 197.1, 164.8, 163.9, 145.7, 139.5, 136.2, 134.0, 131.2, 119.9, 69.9, 33.0, 32.4, 31.4, 27.6, 27.1, 26.4, 23.2, 19.2, 3.8, and -1.3.

IR (neat): 2924, 2852, 1704, 1422, 1310, 1270, 1253, 844, 826, 736, and 690 cm^{-1}.

HRMS (ESI-TOF): Calcd for $C_{25}H_{38}NaO_2Si_2^+$ [M+Na$^+$] requires 449.2303; found 449.2320.

MP: 148–152 °C.

1-(2-(6-((*tert*-Butyldimethylsilyl)oxy)hexa-1,3-diyn-1-yl)cyclohept-1-en-1-yl)-3-(trimethylsilyl)prop-2-yn-1-yl acetate (5026)

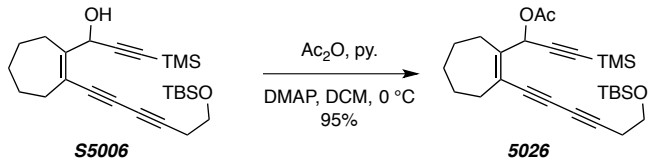

[*BPW IV-091*] Acetic anhydride (31 mg, 0.28 mmol) was added to a stirred solution of alcohol **S5006** (25 mg, 0.06 mmol), pyridine (0.4 mL, 5 mmol), and DMAP (1 mg, 0.008 mmol) in CH_2Cl_2 (2 mL) at 0 °C. After 2 h the reaction mixture was diluted with water and extracted with CH_2Cl_2. The combined organic extracts were washed with brine, dried ($MgSO_4$), and concentrated. The crude material was purified by MPLC (19:1 hexanes:EtOAc) to give acetate **5026** (26 mg, 0.06 mmol, 95%).

^{1}H NMR (500 MHz, $CDCl_3$): δ 6.39 (s, 1H, C*H*OAc), 3.76 (t, *J* = 7.3 Hz, 2H, CH_2OSi), 2.55 (t, *J* = 7.3 Hz, 2H, CH_2CH$_2$OSi), 2.41 (nfom, 4H, =C-CH_2), 2.07 (s, 3H, COCH_3), 1.75 (nfom, 2H, =C-CH$_2$CH_2), 1.52 [nfom, 4H, =C-CH$_2$(CH_2)$_2$], 0.90 [s, 9H, SiC(CH_3)$_3$], 0.17 [s, 9H, Si(CH_3)$_3$], and 0.08 [s, 6H, Si(CH_3)$_2$].

^{13}C NMR (125 MHz, $CDCl_3$): δ 169.3, 148.2, 125.2, 100.9, 91.3, 83.4, 79.6, 74.5, 67.2, 66.4, 61.6, 34.6, 32.5, 29.6, 26.8, 26.0, 25.9, 24.2, 21.2, 18.5, 0.1, and -5.2.

IR (neat): 2955, 2928, 2855, 2177, 1750, 1251, 1222, 1108, 845, and 778 cm^{-1}.

HRMS (ESI-TOF): Calcd for $C_{27}H_{42}NaO_3Si_2^+$ [M+Na$^+$] requires 493.2565; found 493.2558.

11-(*tert*-Butyldimethylsilyl)-4-(trimethylsilyl)-2,3,5,6,7,8,9,10-octahydrocyclohepta[2,3]-indeno[5,6-b]furan-5-yl acetate (S5014)

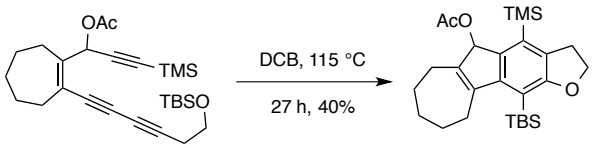

5026 ***S5014***

[*BPW V-153*] A solution of triyne **5026** (20 mg, 0.04 mmol) in DCB (425 μL) was heated at 115 °C. After 27 h the solution was added to a column of silica gel and the DCB removed by elution with hexanes. Subsequent elution with a more polar solvent mixture (hexanes:EtOAc 5:1) and concentration provided the crude mixture of products. This material was purified by MPLC (hexanes:EtOAc 30:1) to give polycycle **S5014** (8 mg, 0.02 mmol, 40%) as an amber oil.

^{1}H NMR (500 MHz, $CDCl_3$): δ 6.22 (s, 1H, C*H*OAc), 4.47 (ddd, *J* = 10.1, 8.4, 5.7 Hz, 1H, CH_aH$_b$OSi), 4.31 (ddd, *J* = 9.3, 9.3, 8.4 Hz, 1H, CH$_a$$H_b$OSi), 3.26 (ddd, *J* = 15.1, 10.0, 9.3 Hz, 1H, CH_aH$_b$CH$_2$OSi), 3.05 (ddd, *J* = 15.1, 9.4, 5.7 Hz, 1H, CH$_a$$H_bCH_2$OSi), 2.63 (ddd, *J* = 15.3, 8.3, 2.5 Hz, 1H, =CCH_aH$_b$), 2.55 (br dddd, *J* = 15.4, 9.0, 2.3, 1.3 Hz, 1H, =CCH$_a$$H_b$), 2.50 (ddd, *J* = 15.8, 9.0, 2.4 Hz, 1H, =C'C'H_aH$_b$), 2.42 [ddd, *J* = 15.8, 9.1, 2.4 Hz, 1H, =C'C'H_aH$_b$), 2.13 (s, 3H, COCH_3), 1.83–1.74 (m, 2H, =C-CH$_2$CH_2), 1.63–1.56 [m, 1H, =C-CH$_2$CH_2), 1.55–1.44 (m, 3H, =C'C'H$_a$$H_b$ and =C(CH$_2$)CH_2], 1.03 [s, 9H, SiC(CH_3)$_3$], 0.33 [s, 9H, Si(CH_3)$_3$], 0.30 [s, 3H, Si(CH_3)$_a$(CH$_3$)$_b$], and 0.29 [s, 3H, Si(CH$_3$)$_a$(CH_3)$_b$].

^{13}C NMR (125 MHz, $CDCl_3$): δ 172.1, 166.8, 152.3, 146.7, 146.4, 139.2, 132.9, 130.7, 113.5, 79.6, 69.8, 32.3, 31.7, 29.0, 28.6, 28.1, 27.5, 26.3, 22.2, 19.0, 1.2, and -0.9.

IR (neat): 2950, 2925, 2853, 1735, 1370, 1248, 1226, 840, and 809 cm^{-1}.

HRMS (ESI-TOF): Calcd for $C_{27}H_{42}NaO_3Si_2^+$ [M+Na^+] requires 493.2565; found 493.2584.

7-((*tert*-Butyldimethylsilyl)oxy)-1-(2-((trimethylsilyl)ethynyl)cyclohex-1-en-1-yl)hepta-2,4-diyn-1-ol (S5015)

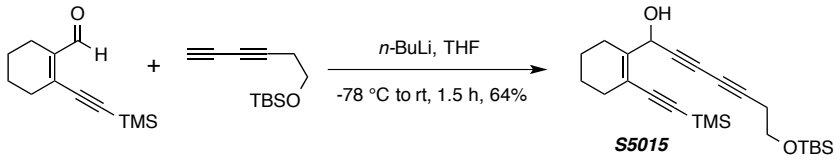

[*BPW IV-127*] *n*-BuLi (0.5 mL, 2.5 M in hexanes, 1.3 mmol) was added to a stirred solution of *tert*-butyl(hexa-3,5-diyn-1-yloxy)dimethylsilane[154] (290 mg, 1.4 mmol) in THF (10 mL) at -78 °C. After 1 h a solution of 2-((trimethylsilyl)ethynyl)cyclohex-1-ene-1-carbaldehyde[156] (230 mg, 1.1 mmol) in THF (3 mL) was added, and the mixture was allowed to warm to room temperature. After 30 min satd aq. NH_4Cl was added and the mixture was extracted with EtOAc. The combined organic extracts were washed with brine, dried ($MgSO_4$), and concentrated. Purification by MPLC (hexanes:EtOAc 20:1) gave the alcohol **S5015** (292 mg, 0.71 mmol, 64%) as a clear amber oil.

^{1}H NMR (500 MHz, $CDCl_3$): δ 5.63 (d, *J* = 5.0 Hz, 1H, C*H*OH), 3.74 (t, *J* = 7.0 Hz, 2H, CH_2O), 2.50 (t, *J* = 7.0 Hz, 2H, C≡CCH_2), 2.29 (br tt, *J* = 6.1, 2.4 Hz, 2H, =C-CH_2), 2.19 (br tt, *J* = 5.9, 2.4 Hz, 2H, =C-CH_2), 2.10 (d, *J* = 5.2 Hz, CHO*H*), 1.62 [m, 4H, $CH_2(CH_2)_2CH_2$], 0.89 [s, 9H, $SiC(CH_3)_3$], 0.19 [s, 9H, $Si(CH_3)_3$], and 0.07 [s, 6H, $Si(CH_3)_2$].

^{13}C NMR (125 MHz, $CDCl_3$): δ 143.7, 119.0, 103.6, 99.1, 78.8, 74.8, 70.2, 65.8, 64.6, 61.5, 30.2, 26.0, 24.0, 23.9, 22.1, 22.0, 18.5, 0.1, and -5.2.

IR (neat): 3420 (br), 2954, 2931, 2858, 2140, 1471, 1250, 1107, 878, 842, and 778 cm^{-1}.

HRMS (ESI-TOF): Calcd for $C_{24}H_{38}NaO_2Si_2^+$ [M+Na^+] requires 437.2303; found 437.2320.

7-((*tert*-Butyldimethylsilyl)oxy)-1-(2-((trimethylsilyl)ethynyl)cyclohex-1-en-1-yl)hepta-2,4-diyn-1-one (5027)

[*BPW IV-130*] MnO_2 (210 mg, 2.4 mmol) was added to a stirred solution of alcohol **S5015** (50 mg, 0.12 mmol) in CH_2Cl_2 (1 mL) at room temperature. After 17 h the reaction mixture was

filtered through Celite® (EtOAc eluent) and concentrated. Purification by MPLC (hexanes:EtOAc 20:1) gave the ketone **5027** (46 mg, 0.11 mmol, 93%) as a red oil.

^{1}H NMR (500 MHz, $CDCl_3$): δ 3.76 (t, *J* = 7.0 Hz, 2H, C*H*$_2$O), 2.58 (t, *J* = 7.0 Hz, 2H, ≡CC*H*$_2$), 2.41 (br t, *J* = 5.4 Hz, 2H, =C-C*H*$_2$), 2.38 (br t, *J* = 5.7 Hz, 2H, =C-C*H*$_2$), 1.65–1.59 [m, 4H, CH_2(C*H*$_2$)$_2$$CH_2$], 0.89 [s, 9H, SiC(C*H*$_3$)$_3$], 0.23 [s, 9H, Si(C*H*$_3$)$_3$], and 0.07 [s, 6H, Si(C*H*$_3$)$_2$].

^{13}C NMR (125 MHz, $CDCl_3$): δ 177.4, 142.4, 133.1, 107.3, 103.8, 87.7, 79.2, 73.3, 66.2, 61.1, 33.9, 26.0, 25.3, 24.3, 21.9, 21.6, 18.4, 0.0, and -5.2.

IR (neat): 2951, 2930, 2858, 2359, 2340, 2232, 2141, 1605, 1250, 1107, 842, and 779 cm^{-1}.

HRMS (ESI-TOF): Calcd for $C_{24}H_{36}NaO_2Si_2^+$ [M+Na$^+$] requires 435.2146; found 435.2151.

10-(*tert*-Butyldimethylsilyl)-4-(trimethylsilyl)-2,3,5,6,7,8-hexahydro-9H-fluoreno[2,3-b]furan-9-one (S5016)

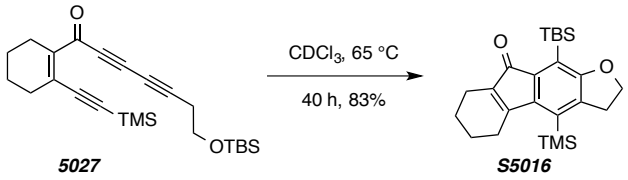

5027 ***S5016***

[*BPW IV-146*] A solution of triyne **5027** (23 mg, 0.06 mmol) in $CDCl_3$ (2 mL) was heated at 65 °C. After 40 h the mixture was concentrated and the crude material purified by flash chromatography (hexanes:EtOAc 20:1) to give polycycle **S5016** (19 mg, 0.05 mmol, 83%) as a red oil.

^{1}H NMR (500 MHz, $CDCl_3$): δ 4.36 (t, *J* = 8.7 Hz, 2H, C*H*$_2$O), 3.15 (t, *J* = 8.7 Hz, 2H, ArC*H*$_2$), 2.58 (tt, *J* = 5.7, 2.6 Hz, 2H, =C-C*H*$_2$), 2.21 (tt, *J* = 6.1, 2.7 Hz, 2H, =C-C*H*$_2$), 1.77–1.71 (m, 2H, =C-CH_2C*H*$_2$), 1.70–1.65 (m, 2H, =C-CH_2C*H*$_2$), 0.94 [s, 9H, SiC(C*H*$_3$)$_3$], 0.41 [s, 9H, Si(C*H*$_3$)$_3$], and 0.33 [s, 6H, Si(C*H*$_3$)$_2$].

^{13}C NMR (125 MHz, $CDCl_3$): δ 197.9, 164.8, 159.5, 145.4, 139.8, 133.8, 132.3, 131.1, 119.7, 69.9, 33.0, 28.0, 27.7, 23.3, 21.6, 20.1, 19.2, 4.2, and -1.3.

IR (neat): 2936, 2928, 2892, 2854, 1706, 1423, 1310, 1253, 844, and 826 cm^{-1}.

HRMS (ESI-TOF): Calcd for $C_{24}H_{36}NaO_2Si_2^+$ [M+Na$^+$] requires 435.2146; found 435.2152.

7-((*tert*-Butyldimethylsilyl)oxy)-1-(2-((trimethylsilyl)ethynyl)phenyl)hepta-2,4-diyn-1-ol (S5017)

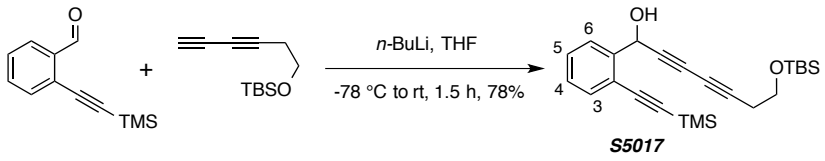

[*BPW III-298*] *n*-BuLi (0.5 mL, 2.5 M in hexanes, 1.3 mmol) was added to a stirred solution of *tert*-butyl(hexa-3,5-diyn-1-yloxy)dimethylsilane[154] (290 mg, 1.4 mmol) in THF (4 mL) at -78 °C. After 1 h a solution of 2-((trimethylsilyl)ethynyl)benzaldehyde[157] (200 mg, 1.0 mmol) in THF (1 mL) was added, and the mixture was allowed to warm to room temperature. After 60 min satd aq. NH_4Cl was added and the mixture was extracted with EtOAc. The combined organic extracts were washed with brine, dried ($MgSO_4$), and concentrated. Purification by MPLC (hexanes:EtOAc 10:1) gave the alcohol **S5017** (320 mg, 0.78 mmol, 78%) as a clear amber oil.

^{1}H NMR (500 MHz, $CDCl_3$): δ 7.58 (d, *J* = 7.7 Hz, 1H, Ar*H6*/*H3*), 7.47 (d, *J* = 7.6 Hz, 1H Ar*H3/H6*), 7.35 (dd, *J* = 7.5, 7.5 Hz, 1H, Ar*H4/H5*), 7.27 (dd, *J* = 7.6, 7.6 Hz, 1H, Ar*H4/H5*), 5.82 (d, *J* = 5.7 Hz, 1H ArC*H*), 3.73 (t, *J* = 7.0 Hz, 2H, CH_2OSi), 2.82 (br m, 1H, CHO*H*), 2.50 (t, *J* = 7.0 Hz, 2H, C≡CCH_2), 0.90 [s, 9H, SiC(CH_3)$_3$], 0.27 [s, 9H, Si(CH_3)$_3$], and 0.07 [s, 6H, Si(CH_3)$_2$].

^{13}C NMR (125 MHz, $CDCl_3$): δ 142.2, 132.9, 129.3, 128.4, 126.9, 121.3, 102.2, 101.2, 79.4, 74.6, 71.5, 65.8, 63.9, 61.5, 26.0, 23.9, 18.5, 0.0, and -5.2.

IR (neat): 3396 (br), 2956, 2857, 2157, 1472, 1251, 1105, 865, 843, 778, and 761 cm^{-1}.

HRMS (ESI-TOF): Calcd for $C_{24}H_{34}NaO_2Si_2^+$ [M+Na$^+$] requires 433.1990; found 433.2002.

7-((*tert*-Butyldimethylsilyl)oxy)-1-(2-((trimethylsilyl)ethynyl)phenyl)hepta-2,4-diyn-1-one (5028)

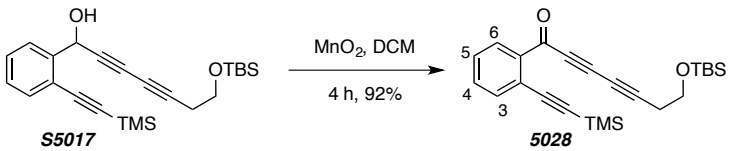

[157] Abbiati, G.; Dell;Acqua, M.; Facoetti, D.; Rossi. Selective base-promoted synthesis of dihydroisobenzofurans by domino addition/annulation reactions of *ortho*-alkynylbenzaldehydes *Synthesis* **2010**, *14*, 2367–2378.

[*BPW IV-023*] MnO_2 (430 mg, 4.9 mmol) was added to a stirred solution of alcohol **S5017** (102 mg, 0.25 mmol) in CH_2Cl_2 (2.5 mL) at room temperature. After 4 h the reaction mixture was filtered through Celite® (EtOAc eluent) and concentrated. Purification by MPLC (hexanes:EtOAc 10:1) gave the ketone **5028** (93 mg, 0.23 mmol, 92%) as a yellow oil.

^{1}H NMR (500 MHz, $CDCl_3$): δ 8.00 (d, *J* = 7.8 Hz, 1H, *H6*), 7.58 (d, *J* = 7.6 Hz, 1H, *H3*), 7.49 (ddd, *J* = 7.5, 7.5 Hz, 1H, *H4*), 7.41 (t, *J* = 7.6, 7.6 Hz, 1H, *H5*), 3.80 (t, *J* = 6.8 Hz, 2H, C*H*$_2$O), 2.61 (t, *J* = 6.8 Hz, 2H, C≡CC*H*$_2$), 0.90 [s, 9H, SiC(C*H*$_3$)$_3$], 0.28 [s, 9H, Si(C*H*$_3$)$_3$], and 0.09 [s, 6H, Si(C*H*$_3$)$_2$].

^{13}C NMR (125 MHz, $CDCl_3$): δ 176.6, 138.4, 135.2, 132.7, 131.4, 128.4, 123.0, 102.7, 102.2, 88.4, 78.9, 72.5, 65.6, 61.0, 26.0, 24.3, 18.4, 0.0, and -5.2.

IR (neat): 2956, 2929, 2857, 2234, 2145, 1648, 1297, 1251, 1108, 865, 843, and 757 cm^{-1}.

HRMS (ESI-TOF): Calcd for $C_{24}H_{32}NaO_2Si_2^+$ [M+Na$^+$] requires 431.1833; found 431.1805.

10-(*tert*-Butyldimethylsilyl)-4-(trimethylsilyl)-2,3-dihydro-9H-fluoreno[2,3-b]furan-9-one (S5018)

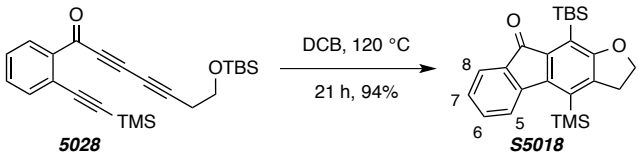

[*BPW V-248*] A solution of triyne **5028** (48 mg, 0.12 mmol) in DCB (1.2 mL) was heated at 120 °C. After 21 h the solution was added to a column of silica and the DCB was removed by washing with hexanes and subsequent elution with a more polar solvent mixture (hexanes:EtOAc 5:1) gave the benzenoid **S5018** (45 mg, 0.11 mmol, 94%) as an orange solid.

^{1}H NMR (500 MHz, $CDCl_3$): δ 7.53 (ddd, *J* = 7.2, 1.3, 0.6 Hz, 1H, *H8*), 7.50 (ddd, *J* = 7.7, 0.7, 0.7 Hz, 1H, *H5*), 7.36 (ddd, *J* = 7.6, 7.6, 1.4 Hz, 1H, *H6*), 7.14 (ddd, *J* = 7.4, 7.4, 0.8 Hz, 1H, *H7*), 4.44 (t, *J* = 8.8, 2H, C*H*$_2$O), 3.25 (t, *J* = 8.8 Hz, 2H, ArC*H*$_2$), 0.98 [s, 9H, SiC(C*H*$_3$)$_3$], 0.50 [s, 9H, Si(C*H*$_3$)$_3$], and 0.38 [s, 6H, Si(C*H*$_3$)$_2$].

^{13}C NMR (125 MHz, $CDCl_3$): δ 194.4, 166.1, 145.6, 144.9, 141.7, 137.6, 134.9, 133.5, 132.9, 127.0, 123.9, 123.5, 120.1, 69.9, 32.7, 27.7, 19.4, 2.5, and -1.2.

IR (neat): 2953, 2895, 2853, 1715, 1292, 1254, 902, 845, 825, 763, and 752 cm^{-1}.

HRMS (ESI-TOF): Calcd for $C_{24}H_{32}NaO_2Si_2^+$ [M+Na$^+$] requires 431.1833; found 431.1853.

MP: 159–162 °C

1-(2-(6-((*tert*-Butyldimethylsilyl)oxy)hexa-1,3-diyn-1-yl)phenyl)-3-(trimethylsilyl)prop-2-yn-1-yl acetate (5029)

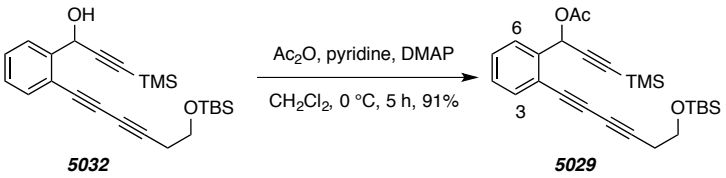

[*BPW V-130*] Acetic anhydride (78 mg, 0.76 mmol) was added to a stirred solution of alcohol **5032** (78 mg, 0.146 mmol), pyridine (0.7 mL, 8.7 mmol), and DMAP (2 mg, 0.02 mmol) in CH_2Cl_2 (6 mL) at 0 °C. After 5 h the reaction mixture was diluted with water and extracted (3 × 5 mL) with CH_2Cl_2. The combined organics were washed with brine, dried ($MgSO_4$), and concentrated. After passing the crude material through a silica plug (hexanes:EtOAc 10:1 eluent), the acetate **5029** (60 mg, 0.133 mmol, 91%) was obtained as a golden oil.

^{1}H NMR (500 MHz, $CDCl_3$): δ 7.73 (dddd, *J* = 7.7, 1.3, 0.5, 0.5 Hz, 1H, *H6*), 7.52 (ddd, *J* = 7.7, 1.4, 0.6 Hz, 1H, *H3*), 7.41 (dddd, *J* = 7.9, 7.5, 1.4, 0.4 Hz, 1H, *H4*), 7.32 (dddd, *J* = 7.8, 7.5, 1.4, 0.3 Hz, 1H, *H5*), 6.73 (ddd, *J* = 0.4, 0.4, 0.4 Hz, 1H, C*H*OAc), 3.80 (t, *J* = 7.1 Hz, 2H, CH_2O), 2.60 (t, *J* = 7.1 Hz, 2H, C≡CCH_2), 2.13 (s, 3H, COCH_3), 0.92 [s, 9H, SiC(CH_3)$_3$], 0.21 [s, 9H, Si(CH_3)$_3$], and 0.11 [s, 6H, Si(CH_3)$_2$].

^{13}C NMR (125 MHz, $CDCl_3$): δ 169.5, 139.7, 133.7, 129.3, 128.9, 128.0, 121.6, 100.8, 92.9, 83.2, 79.7, 71.7, 66.1, 64.3, 61.5, 26.0, 24.2, 21.0, 18.5, 0.1, and -5.1.

IR (neat): 2956, 2929, 2857, 2370, 2182, 1750, 1251, 1220, 1106, 1045, and 844 cm^{-1}.

HRMS (ESI-TOF): Calcd for $C_{26}H_{36}NaO_3Si_2^+$ [M+Na$^+$] requires 475.2095; found 475.2144.

10-(*tert*-Butyldimethylsilyl)-4-(trimethylsilyl)-3,5-dihydro-2*H*-fluoreno[3,2-*b*]furan-5-yl acetate (S5019)

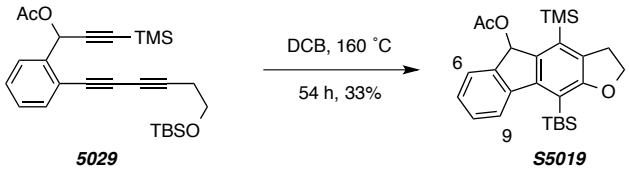

[*BPW V-203*] A solution of triyne **5029** (27 mg, 0.06 mmol) in degassed DCB (1.2 mL) was heated at 160 °C under N_2 atmosphere. After 54 h the solution was added to a column of silica

and the DCB was removed by washing with hexanes. Subsequent elution with a more polar solvent mixture (hexanes:EtOAc 5:1) and concentration provided the crude mixture of products. The crude material was purified by MPLC (hexanes:EtOAc 20:1) to give the polycycle **S5019** (9 mg, 0.02 mmol, 33%) as a yellow oil.

^{1}H NMR (500 MHz, $CDCl_3$): δ 7.84 (ddd, *J* = 7.8, 0.8, 0.8 Hz, 1H, *H9*), 7.71 (dddd, *J* = 7.5, 1.4, 0.7, 0.7 Hz, 1H, *H6*), 7.29 (dddd, *J* = 7.6, 7.6, 1.2, 0.4 Hz, 1H, *H8/H7*), 7.17 (ddd, *J* = 7.5, 7.5, 1.1 Hz, 1H, *H7/H8*), 6.66 (dd, *J* = 0.4, 0.4 Hz, 1H, C*H*OAc), 4.54 (ddd, *J* = 10.1, 8.4, 5.6 Hz, 1H, CH_aH$_b$O), 4.39 (ddd, *J* = 9.4, 9.4, 8.4 Hz, 1H, CH$_a$$H_b$O), 3.32 (ddd, *J* = 15.3, 10.1, 9.1 Hz, 1H, ArCH_aCH$_b$), 3.15 (ddd, *J* = 15.2, 9.5, 5.6 1H, ArCH$_a$CH_b), 2.12 (s, 3H, C=OCH_3), 1.10 [s, 9H, SiC(CH_3)$_3$], 0.41 [s, 6H, Si(CH_3)$_2$], and 0.38 [s, 9H, Si(CH_3)$_3$].

^{13}C NMR (125 MHz, $CDCl_3$): δ 172.1, 167.2, 147.7, 143.7, 142.1, 139.4, 134.8, 131.4, 128.1, 127.1, 126.6, 124.1, 114.5, 75.9, 70.0, 31.7, 28.3, 22.0, 19.6, 1.2, and 0.2.

IR (neat): 2954, 2928, 2895, 2855, 1736, 1471, 1249, 1230, 1013, 840, and 824 cm^{-1}.

HRMS (ESI-TOF): Calcd for $C_{26}H_{36}NaO_3Si_2^+$ [M+Na$^+$] requires 475.2095; found 475.2115.

7-((*tert*-Butyldimethylsilyl)oxy)-N-phenylhepta-2,4-diynamide (S5020)

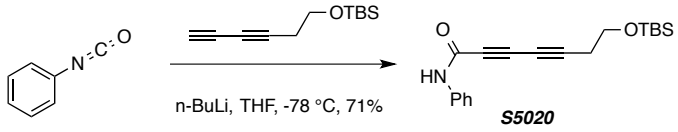

[*BPW VI-093*] *n*-BuLi (0.76 mL, 2.5 M in hexanes, 1.9 mmol) was added to a stirred solution of *tert*-butyl(hexa-3,5-diyn-1-yloxy)dimethylsilane[154] (416 mg, 2.0 mmol) in THF (10 mL) at -78 °C. After 40 min a solution of phenylisocyanate (186 µL, 1.7 mmol) in THF (2 mL) was added and the mixture was allowed to warm to room temperature. After 30 min satd aq. NH_4Cl was added and the mixture was extracted with EtOAc. The combined organic extracts were washed with brine, dried ($MgSO_4$), and concentrated. Purification by flash chromatography on silica gel (8:1 hexanes:EtOAc) gave the amide **S5020** (395 mg, 1.2 mmol, 71%) as a clear amber oil.

^{1}H NMR (500 MHz, $CDCl_3$): δ 7.70 (br s, 1H, PhN*H*), 7.51 (dd, *J* = 8.8, 1.3 Hz, 2H, PhH_o), 7.33 (dd, *J* = 8.5, 7.5 Hz, 2H, PhH_m), 7.13 (tt, *J* = 7.4, 1.2 Hz, 1H, PhH_p) 3.77 (t, *J* = 6.7 Hz, 2H, CH_2OSi), 2.56 (t, *J* = 6.7 Hz, 2H, CH_2CH$_2$O), 0.91 [s, 9H, SiC(CH_3)$_3$], and 0.09 [s, 9H, SiCH_3)$_3$].

^{13}C NMR (125 MHz, $CDCl_3$): δ 149.9, 137.2, 129.2, 125.2, 120.0, 84.8, 71.2, 68.4, 64.8, 61.0, 26.0, 24.1, 18.4, and -5.2.

IR (neat): 3265 (br), 3134, 3060, 2953, 2929, 2882, 2857, 2242, 1642, 1598, 1544, 1443, 1319, 1255, 1106, 787, and 777 cm^{-1}.

HRMS (ESI-TOF): Calcd for $C_{19}H_{25}NNaO_2Si^+$ [M+Na^+] requires 350.1547; found 350.1569.

7-((*tert*-Butyldimethylsilyl)oxy)-N-phenyl-N-(3-(trimethylsilyl)prop-2-yn-1-yl)hepta-2,4-diynamide (5030)

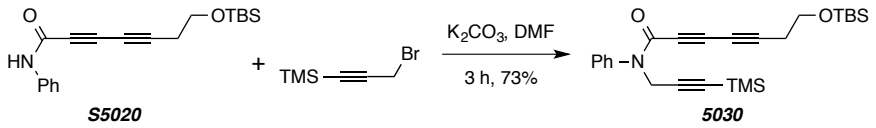

S5020 ***5030***

[*BPW VI-103*] K_2CO_3 (30 mg, 0.22 mmol) was added to a stirred solution of amide **S5020** (33 mg, 0.1 mmol) and (3-bromoprop-1-yn-1-yl)trimethylsilane (45 mg, 0.24 mmol) in DMF (0.8 mL). After 3 h the reaction mixture was diluted with EtOAc (10 mL) and washed with water (3 × 15 mL), brine, and dried ($MgSO_4$). Purification by MPLC (10:1 hexanes:EtOAc) gave the triyne **5030** (32 mg, 0.07 mmol, 73%) as a clear yellow oil.

^{1}H NMR (500 MHz, $CDCl_3$): major rotamer: δ 7.45–7.39 (m, 3H, PhH_mH_p), 7.33 (dd, J = 8.3, 1.8 Hz, 2H, PhH_o), 4.52 (s, 2H, CH_2N), 3.67 (t, J = 6.6 Hz, 2H, CH_2OSi), 2.44 (t, J = 6.6 Hz, 2H, C$H_2$$CH_2O$), 0.86 [s, 9H, SiC(C$H_3$)$_3$], 0.10 [s, 9H, SiC$H_3$)$_3$], and 0.02 [s, 6H, Si(C$H_3$)$_2$]. Minor rotamer (the resonances from the aliphatic protons of the minor constituent in the ca. 7:1 ratio of rotamers): 4.65 (br s, 2H, CH_2N), 3.80 (t, J = 6.7 Hz, 2H, CH_2OSi), 2.60 (t, J = 6.7 Hz, 2H, C$H_2$$CH_2O$), 0.91 [s, 9H, SiC(C$H_3$)$_3$], 0.15 [s, 6H, Si(C$H_3$)$_2$], and 0.02 [s, 9H, Si(C$H_3$)$_3$].

^{13}C NMR (125 MHz, $CDCl_3$): δ 152.7, 140.3, 129.3, 128.9, 128.6, 99.6, 90.1, 85.7, 77.2, 66.6, 64.8, 60.9, 38.9, 25.9, 24.1, 18.4, -0.2, and -5.2.

IR (neat): 2956, 2929, 2857, 2242, 2180, 2154, 1645, 1388, 1251, 1108, and 842 cm^{-1}.

HRMS (ESI-TOF): Calcd for $C_{25}H_{35}NNaO_2Si_2^+$ [M+H^+] requires 460.2099; found 460.2118.

8-(*tert*-Butyldimethylsilyl)-6-phenyl-4-(trimethylsilyl)-2,3,5,6-tetrahydro-7H-furo[2,3-f]isoindol-7-one (S5021)

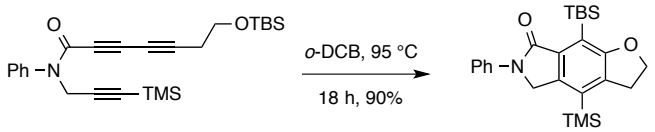

5030 ***S5021***

[*BPW VI-105*] A solution of triyne **5030** (41 mg, 0.09 mmol) in DCB (0.94 mL) was heated at 95 °C. After 18 h the solution was loaded onto a column of silica and DCB was removed by initial elution with hexanes. Subsequent elution with hexanes:EtOAc (5:1) gave the crude material. Purification of the residue from these more polar fractions via MPLC (10:1 hexanes:EtOAc) gave the isoindolone **5021** (37 mg, 0.08 mmol, 90%) as a white solid.

^{1}H NMR (500 MHz, $CDCl_3$): δ 7.79 (dd, *J* = 8.8, 1.1 Hz, 2H, PhH_o), 7.40 (dd, *J* = 8.6, 7.4 Hz, 2H, PhH_m), 7.13 (tt, *J* = 7.4, 1.1 Hz, 1H, PhH_p), 4.72 (s, 2H, CH_2N), 4.50 (t, *J* = 8.6 Hz, 2H, CH_2OAr), 3.27 (t, *J* = 8.6 Hz, 2H, CH_2CH$_2$O), 0.99 [s, 9H, SiC(CH_3)$_3$], 0.46 [s, 6H, Si(CH_3)$_2$], and 0.42 [s, 9H, SiCH_3)$_3$].

^{13}C NMR (125 MHz, $CDCl_3$): δ 167.8, 166.3, 140.0, 139.0, 137.5, 136.7, 130.8, 129.2, 124.1, 119.7, 117.0, 69.9, 51.5, 31.4, 27.7, 19.0, 0.9, and -0.7.

IR (neat): 2954, 2926, 2892, 2854, 1701, 1600, 1501, 1375, 1316, 1251, 1238, 842, and 753 cm^{-1}.

HRMS (ESI-TOF): Calcd for $C_{25}H_{35}NNaO_2Si_2^+$ [M+H$^+$] requires 460.2099; found 460.2126.

MP: 168–170 °C.

11-((*tert*-Butyldimethylsilyl)oxy)-1-(trimethylsilyl)undeca-1,6,8-triyn-5-ol (S5022)

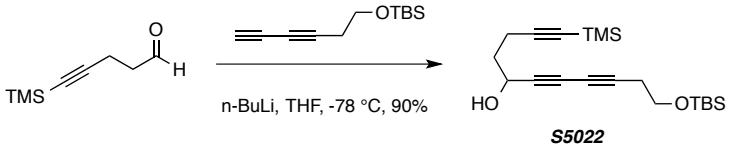

S5022

[*BPW VI-076*] *n*-BuLi (0.4 mL, 2.5 M in hexanes, 1.0 mmol) was added to a stirred solution of *tert*-butyl(hexa-3,5-diyn-1-yloxy)dimethylsilane[154] (208 mg, 1.0 mmol) in THF (10 mL) at -78 °C. After 40 min a solution of 5-(trimethylsilyl)pent-4-ynal (110 mg, 0.7 mmol) in THF (5 mL) was added and the mixture was allowed to warm to room temperature. After 30 min satd aq. NH_4Cl was added and the mixture was extracted with EtOAc. The combined organic extracts were washed with brine, dried ($MgSO_4$), and concentrated. Purification by MPLC (9:1 hexanes:EtOAc) gave the triyne **S5022** (228 mg, 0.63 mmol, 90%) as a clear yellow oil.

^{1}H NMR (500 MHz, $CDCl_3$): δ 4.57 (dt, *J* = 6.2, 6.2 Hz, 1H, C*H*OH), 3.74 (t, *J* = 7.0 Hz, 2H, CH_2OSi), 2.50 (dt, *J* = 7.0, 1.0 Hz, 2H, CH_2CH$_2$OSi), 0.90 [s, 9H, SiC(CH_3)$_3$], 0.19 [s, 9H, SiC(CH_3)$_3$], and 0.07 [s, 6H, Si(CH_3)$_2$].

^{13}C NMR (125 MHz, $CDCl_3$): δ 105.8, 85.9, 79.0, 75.9, 70.4, 65.5, 61.9, 61.4, 36.2, 26.0, 23.8, 18.4, 16.0, 0.2, and -5.2.

IR: 3464, 2956, 2930, 2857, 2257, 2175, 1251, 1106, 841, and 777 cm^{-1}.

HR ESI-MS calcd for $C_{20}H_{34}NaO_2Si_2$ $[M + Na]^+$ 385.1990, found 385.1998.

11-((*tert*-Butyldimethylsilyl)oxy)-1-(trimethylsilyl)undeca-1,6,8-triyn-5-one (5031) and (*E*)-11-((*tert*-Butyldimethylsilyl)oxy)-1-(trimethylsilyl)undeca-3-en-1,6,8-triyn-5-one (S5023)

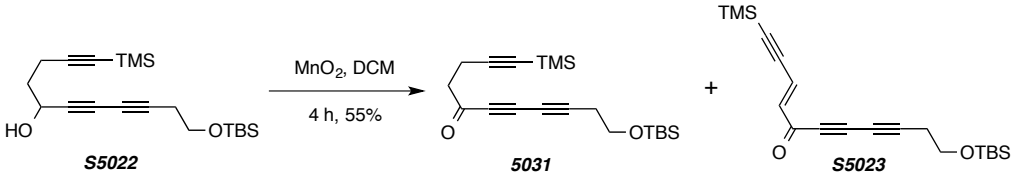

[*BPW VI-077*] MnO_2 (516 mg, 6.0 mmol) was added to a stirred solution of alcohol **S5022** (110 mg, 0.3 mmol) in CH_2Cl_2 (6 mL) at room temperature. After 4 h the reaction mixture was filtered through Celite® (EtOAc eluent) and concentrated. Purification by MPLC (hexanes:EtOAc 25:1) gave the ketone **5031** (40 mg, 0.11 mmol, 37%) as a yellow oil and **S5023** (20 mg, 0.06 mmol, 19%) as a yellow oil.

Data for 5031:

^{1}H NMR (500 MHz, $CDCl_3$): δ 3.78 (t, J = 6.7 Hz, 2H, CH_2OSi), 2.82 (t, J = 7.3 Hz, 2H, CH_2C=O), 2.59 (t, J = 6.7 Hz, 2H, C$H_2$$CH_2$OSi), 2.56 (t, J = 7.4 Hz, 2H, CH_2C≡CSi), 0.90 [s, 9H, SiC(CH_3)$_3$], 0.14 [s, 9H, Si(CH_3)$_3$], and 0.07 [s, 6H, Si(CH_3)$_2$].

^{13}C NMR (125 MHz, $CDCl_3$): δ 184.7, 104.5, 88.4, 85.9, 77.0, 71.8, 64.8, 60.9, 44.4, 26.0, 24.3, 18.4, 14.7, 0.2, and -5.2.

IR: 2956, 2930, 2857, 2236, 2178, 2146, 1675, 1251, 1108, 1080, 841, and 777 cm^{-1}.

HR ESI-MS calcd for $C_{20}H_{32}NaO_2Si_2$ $[M + Na]^+$ 383.1833, found 383.1853.

Data for S5023:

^{1}H NMR (500 MHz, $CDCl_3$): δ 6.89 (d, J = 16.1 Hz, 1H, CH=CHC=O), 6.53 (d, J = 16.1 Hz, 1H, CH=CHC=O), 3.78 (t, J = 6.7 Hz, 2H, CH_2OSi), 2.59 (t, J = 6.7 Hz, 2H, C$H_2$$CH_2$O), 0.91 [s, 9H, SiC(C$H_3$)$_3$], 0.23 [s, 9H, Si(C$H_3$)$_3$], and 0.09 [s, 6H, Si(C$H_3$)$_2$].

^{13}C NMR (125 MHz, $CDCl_3$): δ 176.5, 140.1, 129.1, 110.8, 101.2, 88.0, 77.5, 70.5, 64.9, 60.9, 25.9, 24.3, 18.4, 0.4, and -5.2.

IR: 2956, 2930, 2858, 2234, 1635, 1254, 1108, 844, and 777 cm^{-1}.

HR ESI-MS calcd for $C_{20}H_{30}NaO_2Si_2$ $[M + Na]^+$ 381.1677, found 381.1684.

***tert*-Butyldimethyl((6-(2-(3-(trimethylsilyl)-1-((trimethylsilyl)oxy)prop-2-yn-1-yl)phenyl)hexa-3,5-diyn-1-yl)oxy)silane (5033a)**

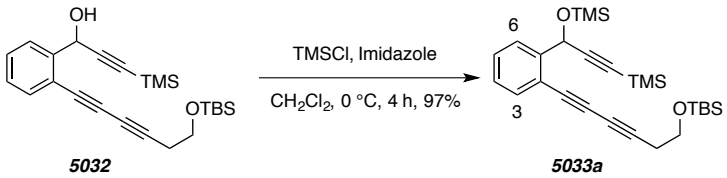

5032 ***5033a***

[*BPW V-213*] To a solution of alcohol **5032** (48 mg, 0.12 mmol) in CH_2Cl_2 (1 mL) was added trimethylsilylchloride (22 µL, 0.18 mmol) and imidazole (16 mg, 0.24 mmol) at 0 °C. The solution was allowed to warm to rt and after 4 h the solution was filtered through a plug of Celite, rinsing with EtOAc. After solvent removal, the crude material was purified by MPLC (20:1 Hex:EtOAc) to give triyne **5033a** (55 mg, 0.11 mmol, 97%) as an clear oil.

^{1}H NMR (500 MHz, $CDCl_3$): δ 7.72 (dd, *J* = 7.9, 1.3 Hz, 1H, *H6*), 7.46 (dd, *J* = 7.7, 1.4 Hz, 1H, *H3*), 7.37 (ddd, *J* = 7.6, 7.6, 1.4 Hz, 1H, *H4*), 7.24 (ddd, *J* = 7.6, 7.6, 1.3 Hz, 1H, *H5*), 5.81 (s, 1H, C*H*OSi), 3.79 (t, *J* = 7.0 Hz, 2H, CH_2OSi), 2.60 (t, *J* = 7.0 Hz, 2H, CH_2CH_2O), 0.92 [s, 9H, SiC(CH_3)$_3$], 0.22 [s, 9H, OSi(CH_3)$_3$], 0.17 [s, 9H, Si(CH_3)$_3$], and 0.10 [s, 6H, Si(CH_3)$_2$].

^{13}C NMR (125 MHz, $CDCl_3$): δ 144.2, 133.4, 129.4, 127.9, 127.1, 120.4, 105.5, 90.9, 82.8, 79.2, 72.6, 66.4, 63.3, 61.5, 26.0, 24.2, 18.5, 0.4, -0.1, and -5.1.

IR: 2957, 2930, 2858, 2330, 2174, 1251, 1106, 1068, 1011, 871, and 775 cm^{-1}.

HR ESI-MS calcd for $C_{27}H_{42}NaO_2Si_3$ $[M + Na]^+$ 505.2385, found 505.2411.

***tert*-Butyldimethyl((6-(2-(1-((triisopropylsilyl)oxy)-3-(trimethylsilyl)prop-2-yn-1-yl)phenyl)hexa-3,5-diyn-1-yl)oxy)silane (5033b)**

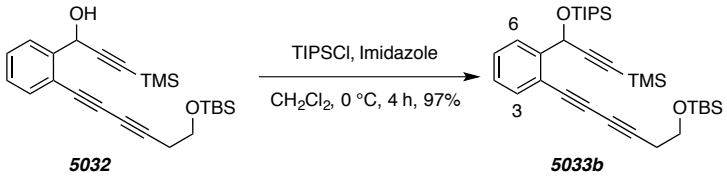

5032 ***5033b***

[*BPW V-215*] To a solution of alcohol **5032** (30 mg, 0.07 mmol) in CH_2Cl_2 (1 mL) was added triisopropylsilylchloride (25 μL, 0.11 mmol) and imidazole (16 mg, 0.24 mmol) at 0 °C. The solution was allowed to warm to rt and after 4 h the solution was filtered through a plug of Celite, rinsing with EtOAc. After solvent removal, the crude material was purified by MPLC (20:1 Hex:EtOAc) to give triyne **5033b** (40 mg, 0.07 mmol, 97%) as an clear oil.

^{1}H NMR (500 MHz, $CDCl_3$): δ 7.72 (dd, *J* = 7.9, 1.4 Hz, 1H, *H6*), 7.44 (dd, *J* = 7.7, 1.4 Hz, 1H, *H3*), 7.37 (ddd, *J* = 7.6, 7.6, 1.4 Hz, 1H, *H4*), 7.22 (ddd, *J* = 7.6, 7.6, 1.3 Hz, 1H, *H5*), 5.86 (s, 1H, C*H*OSi), 3.79 (t, *J* = 7.0 Hz, 2H, CH_2OSi), 2.60 (t, *J* = 7.0 Hz, 2H, CH_2CH$_2$O), 1.21 [sept, *J* = 7.1 Hz, 3H, Si(C*H*(CH$_3$)$_2$)$_3$], 1.11 [d, *J* = 7.3 Hz, 9H, Si(CH(CH_3)$_2$)$_3$], 1.05 [d, *J* = 7.3 Hz, 9H, Si(CH(CH_3)$_2$)$_3$] 0.92 [s, 9H, SiC(CH_3)$_3$], 0.14 [s, 9H, Si(CH_3)$_3$], and 0.10 [s, 6H, Si(CH_3)$_2$].

^{13}C NMR (125 MHz, $CDCl_3$): δ 145.4, 133.2, 129.4, 127.5, 126.5, 119.5, 106.1, 89.6, 82.6, 79.3, 72.6, 66.4, 63.4, 61.6, 26.0, 24.2, 18.2, 18.1, 12.4, -0.9, and -5.1.

IR: 2944, 2867, 2360, 2339, 1463, 1104, 1063, 1011, 913, 882, and 842 cm^{-1}.

HR ESI-MS calcd for $C_{33}H_{54}NaO_2Si_3$ $[M + Na]^+$ 589.3324, found 589.3344.

***tert*-Butyl((6-(2-(1-((*tert*-butyldimethylsilyl)oxy)-3-(trimethylsilyl)prop-2-yn-1-yl)phenyl)hexa-3,5-diyn-1-yl)oxy)dimethylsilane (5033c)**

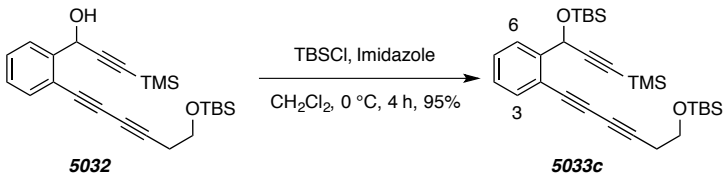

5032 ***5033c***

[*BPW V-214*] To a solution of alcohol **5032** (48 mg, 0.12 mmol) in CH_2Cl_2 (1 mL) was added *tert*-butyldimethylsilylchloride (26 mg, 0.18 mmol) and imidazole (16 mg, 0.24 mmol) at 0 °C. The solution was allowed to warm to rt and after 4 h the solution was filtered through a plug of Celite, rinsing with EtOAc. After solvent removal, the crude material was purified by MPLC (20:1 Hex:EtOAc) to give triyne **5033c** (58 mg, 0.11 mmol, 95%) as an clear oil.

^{1}H NMR (500 MHz, $CDCl_3$): δ 7.70 (dd, *J* = 7.9, 1.4 Hz, 1H, *H6*), 7.45 (dd, *J* = 7.7, 1.4 Hz, 1H, *H3*), 7.37 (ddd, *J* = 7.6, 7.6, 1.4 Hz, 1H, *H4*), 7.23 (ddd, *J* = 7.6, 7.6, 1.3 Hz, 1H, *H5*), 5.79 (s, 1H, C*H*OSi), 3.79 (t, *J* = 7.0 Hz, 2H, CH_2OSi), 2.60 (t, *J* = 7.0 Hz, 2H, CH_2CH$_2$O), 0.92 [s,

18H, SiC(C*H*$_3$)$_3$], 0.20 [s, 3H, OSi(C*H*$_3$)$_2$], 0.16 [s, 9H, Si(C*H*$_3$)$_3$], 0.15 [s, 3H, Si(C*H*$_3$)$_2$] and 0.10 [s, 6H, Si(C*H*$_3$)$_2$].

^{13}C NMR (125 MHz, $CDCl_3$): δ 144.7, 133.3, 129.3, 127.7, 126.8, 120.1, 105.8, 90.3, 82.7, 79.3, 72.7, 66.4, 63.5, 61.6, 26.0, 26.0, 24.2, 18.4, -0.1, -4.3, -4.6, and -5.1.

IR: 2956, 2930, 2857, 2330, 2174, 1471, 1252, 1106, and 774 cm^{-1}.

HR ESI-MS calcd for $C_{30}H_{48}NaO_2Si_3$ $[M + Na]^+$ 547.2854, found 547.2869.

5-(Trimethylsilyl)penta-2,4-diyn-1-yl 3-(trimethylsilyl)propiolate (5034)

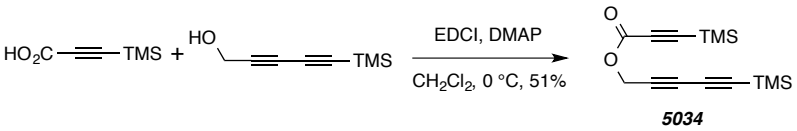

5034

[*BPW V-221*] The following reagents were added in sequence to CH_2Cl_2 (5 mL) at 0 °C: 5-(trimethylsilyl)penta-2,4-diyn-1-ol[151] (137 mg, 0.9 mmol), 3-trimethylsilylpropynoic acid (142 mg, 1.0 mmol), EDCI (170 mg, 1.1 mmol), and DMAP (12 mg, 0.1 mmol). The resulting homogenous solution quickly became cloudy. After 3 h the suspension was diluted with H_2O and extracted with CH_2Cl_2. The combined organic extracts were washed with brine, dried ($MgSO_4$), and concentrated. Purification by MPLC (10:1 hexanes:EtOAc) gave the ester **5034** (140 mg, 0.51 mmol, 51%) as a clear oil.

^{1}H NMR (500 MHz, $CDCl_3$): δ 4.81 (s, 2H, C*H*$_2$O), 0.25 [s, 9H, C=OC≡CSi(C*H*$_3$)$_3$], and 0.20 [s, 9H, Si(C*H*$_3$)$_3$].

^{13}C NMR (125 MHz, $CDCl_3$): δ 152.0, 96.2, 93.5, 88.9, 86.8, 72.3, 70.3, 53.6, -0.4, and -0.8.

IR: 2965, 2903, 2114, 1721, 1253, 1205, 851, and 760 cm^{-1}.

HR ESI-MS calcd for $C_{14}H_{20}NaO_2Si_2$ $[M + Na]^+$ 299.0894, found 299.0898.

1-Oxo-6-(trimethylsilyl)-1,3-dihydroisobenzofuran-5-yl acetate (5038)

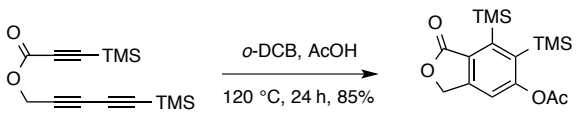

5034 ***5038***

[*BPW V-264*] A solution of triyne **5032** (27 mg, 0.10 mmol) and acetic acid (60 µL, 10 equiv) in DCB (1.0 mL) was heated at 120 °C. After 24 h the solution was loaded onto a column of silica

and DCB was removed by initial elution with hexanes. Subsequent elution with hexanes:EtOAc (5:1) gave the benzenoid **5038** (28 mg, 0.08 mmol, 85%) as a yellow oil.

^{1}H NMR (500 MHz, $CDCl_3$): δ 7.16 (s, 1H, Ar*H*), 5.24 (s, 2H, CH_2O), 2.36 (s, 3H, CH_3), 0.44 [s, 9H, Si(CH_3)$_3$], and 0.39 [s, 9H, Si(CH_3)$_3$].

^{13}C NMR (125 MHz, $CDCl_3$): δ 171.1, 169.0, 159.2, 155.3, 148.1, 143.0, 129.3, 115.0, 68.6, 21.9, and 2.7 (2).

IR (neat): 2952, 2902, 1760, 1249, 1190, 1141, 1058, 1017, 844, and 757 cm^{-1}.

HRMS (ESI-TOF): Calcd for $C_{16}H_{24}NaO_4Si_2^+$ [M+H$^+$] requires 359.1105; found 359.1113.

5-Acetoxy-phthalide (5039)

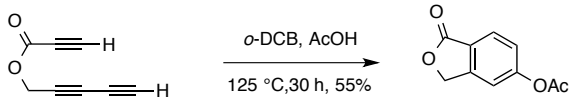

3016 ***5039***

[*BPW V-283*] A solution of triyne **5034** (5 mg, 0.04 mmol) and acetic acid (45 µL, 20 equiv) in DCB (0.4 mL) was heated at 125 °C. After 30 h the solution was loaded onto a column of silica and DCB was removed by initial elution with hexanes. Subsequent elution with hexanes:EtOAc (5:1) gave the benzenoid **5039** (4 mg, 0.02 mmol, 55%) as a yellow oil whose spectra matched that reported in the literature.

1-Oxo-6-(trimethylsilyl)-1,3-dihydroisobenzofuran-5-yl acetate (5040)

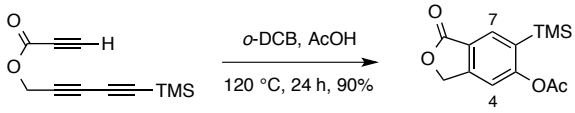

4038 ***5040***

[*BPW V-265*] A solution of triyne **4038** (24 mg, 0.12 mmol) and acetic acid (70 µL, 10 equiv) in DCB (1.0 mL) was heated at 120 °C. After 24 h the solution was loaded onto a column of silica and DCB was removed by initial elution with hexanes. Subsequent elution with hexanes:EtOAc (2:1) gave the benzenoid **5040** (28 mg, 0.11 mmol, 90%) as a yellow oil.

^{1}H NMR (500 MHz, $CDCl_3$): δ 8.05 (d, *J* = 0.6 Hz, 1H, *H7*), 7.27 (t, *J* = 0.8 Hz, 1H, *H4*), 5.30 (d, *J* = 1.2 Hz, 2H, CH_2O), 2.37 (s, 3H, CH_3), and 0.33 [s, 9H, Si(CH_3)$_3$].

^{13}C NMR (125 MHz, $CDCl_3$): δ 170.5, 168.8, 159.7, 149.2, 134.2, 133.2, 122.8, 115.8, 69.2, 21.6, and -1.0.

IR (neat): 2954, 2900, 1762, 1618, 1248, 1190, 1136, 1068, 1010, and 843 cm^{-1}.

HRMS (ESI-TOF): Calcd for $C_{13}H_{16}NaO_4Si^+$ [M+H^+] requires 287.0710; found 287.0721.

Penta-2,4-diyn-1-yl 3-(trimethylsilyl)propiolate (5035)

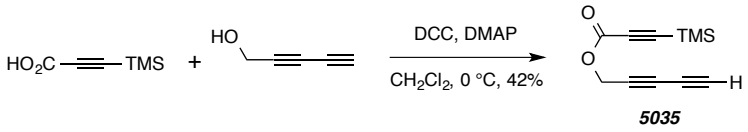

5035

[*BPW V-252*] A solution of penta-2,4-diyn-1-ol[158] (60 mg, 0.75 mmol) and 3-trimethylsilylpropynoic acid (140 mg, 1.0 mmol) in dichloromethane (7 mL) was cooled to 0 °C. N,N'-dicyclohexylcarbodiimide (206 mg, 1.0 mmol) and DMAP (10 mg, 0.08 mmol) was added and allowed to come to room temperature. After 4 h, the solution was filtered through plug of Celite, rinsing with EtOAc. After solvent removal, the crude material was purified by MPLC (20:1 Hex:EtOAc) to give triyne **5035** (65 mg, 0.32 mmol, 42%) as an amber oil.

^{1}H NMR (500 MHz, $CDCl_3$): δ 4.81 (s, 2H, CH_2O), 2.23 (s, 1H, C≡C*H*), and 0.26 [s, 9H, Si(CH_3)$_3$].

^{13}C NMR (125 MHz, $CDCl_3$): δ 151.9, 96.3, 93.4, 71.6, 69.3, 69.1, 67.1, 53.4, and -0.8.

IR: 3294, 2965, 2363, 2344, 2175, 2118 1719, 1253, 1205, 848, and 760 cm^{-1}.

HR ESI-MS calcd for $C_{11}H_{12}NaO_2Si$ [M + Na]$^+$ 227.0499, found 227.0489.

1-Oxo-7-(trimethylsilyl)-1,3-dihydroisobenzofuran-5-yl acetate (5041)

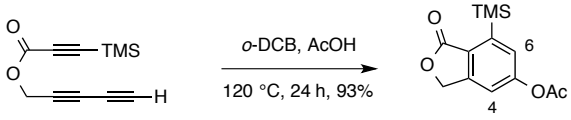

5035 ***5041***

[*BPW V-288*] A solution of triyne **5035** (20 mg, 0.10 mmol) and acetic acid (110 µL, 20 equiv) in DCB (9.0 mL) was heated at 125 °C. After 24 h the solution was loaded onto a column of silica and DCB was removed by initial elution with hexanes. Subsequent elution with hexanes:EtOAc (2:1) gave the crude product. Purification via MPLC (5:1 Hex:EtOAc) gave benzenoid **5041** (24 mg, 0.09 mmol, 93%) as a yellow oil.

---

[158] Turlington, M.; Du, Y.; Ostrum, S. G.; Santosh, V.; Wren, K.; Lin, T.; Sabat, M.; Pu, L. From highly enantioselective catalytic reaction of 1,3-diynes with aldehydes to facile asymmetric synthesis of polycyclic compounds. *J. Am. Chem. Soc.* **2011**, *133*, 11780–11794.

^{1}H NMR (500 MHz, $CDCl_3$): δ 7.31 (d, *J* = 2.0 Hz, 1H, *H6*), 7.23 (dt, *J* = 1.9, 0.9 Hz, 1H, *H4*), 5.29 (d, *J* = 0.7 Hz, 2H, CH_2O), 2.36 (s, 3H, CH_3), and 0.40 [s, 9H, $Si(CH_3)_3$].

^{13}C NMR (125 MHz, $CDCl_3$): δ 170.9, 169.1, 154.2, 148.6, 144.4, 128.8, 127.5, 115.9, 69.0, 21.3, and -1.2.

IR (neat): 2934, 2855, 1759, 1588, 1194, 1128, 1048, 1010, 843, and 757 cm^{-1}.

HRMS (ESI-TOF): Calcd for $C_{13}H_{16}NaO_4Si^+$ [M+H$^+$] requires 287.0710; found 287.0705.

5-(*tert*-Butyldimethylsilyl)penta-2,4-diyn-1-yl propiolate (5036)

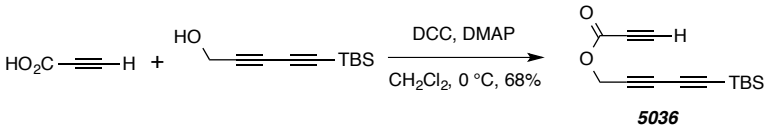

5036

[*BPW VI-112*] A solution of 5-(*tert*-butyldimethylsilyl)penta-2,4-diyn-1-ol[159] (194 mg, 1.0 mmol) and propiolic acid (75 µL, 1.2 mmol) in dichloromethane (8 mL) was cooled to 0 °C. N,N'-dicyclohexylcarbodiimide (247 mg, 1.2 mmol) and DMAP (15 mg, 0.12 mmol) was added and allowed to come to room temperature. After 2 h, the solution was filtered through plug of Celite, rinsing with EtOAc. After solvent removal, the crude material was purified by MPLC (10:1 Hex:EtOAc) to give triyne **5036** (168 mg, 0.68 mmol, 68%) as an amber oil.

^{1}H NMR (500 MHz, $CDCl_3$): δ 4.85 (s, 2H, CH_2O), 2.96 (s, 1H, C≡C*H*), 0.94 [s, 9H, $SiC(CH_3)_3$ and 0.14 [s, 6H, $Si(CH_3)_2$].

^{13}C NMR (125 MHz, $CDCl_3$): δ 151.8, 87.9, 87.4, 76.3, 73.9, 72.7, 69.4, 54.0, 26.1, 16.8, and -4.8.

IR: 3290, 2954, 2931, 2858, 2123, 1725, 1208, 830, and 778 cm^{-1}.

HR ESI-MS calcd for $C_{14}H_{18}NaO_2Si$ [M + Na]$^+$ 269.0972, found 269.0957.

6-(*tert*-Butyldimethylsilyl)-1-oxo-1,3-dihydroisobenzofuran-5-yl acetate (5042)

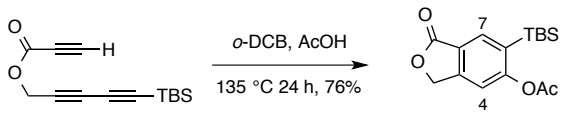

5036 ***5042***

---

[159] Marino, J. P.; Nguyen, H. N. Bulky trialkylsilyl acetylenes in the Cadiot−Chodkiewicz cross-coupling reaction. *J. Org. Chem.* **2002**, *67*, 6841–6844.

[*BPW VI-115*] A solution of triyne **5036** (35 mg, 0.14 mmol) and acetic acid (80 µL, 10 equiv) in DCB (1.4 mL) was heated at 135 °C. After 18 h the solution was loaded onto a column of silica and DCB was removed by initial elution with hexanes. Subsequent elution with hexanes:EtOAc (2:1) gave benzenoid **5042** (33 mg, 0.11 mmol, 76%) as a yellow oil.

^{1}H NMR (500 MHz, $CDCl_3$): δ 8.05 (s, 1H, *H7*), 7.28 (t, *J* = 0.8 Hz, 1H, *H4*), 5.31 (d, *J* = 0.9 Hz, 2H, C*H*$_2$O), 2.36 (s, 3H, C*H*$_3$), 0.90 [s, 9H, SiC(C*H*$_3$)$_3$ and 0.35 [s, 6H, Si(C*H*$_3$)$_2$].

^{13}C NMR (125 MHz, $CDCl_3$): δ 170.6, 168.9, 159.7, 149.0, 134.5, 131.7, 122.6, 116.1, 69.2, 60.6, 53.6, 26.7, 21.8, 17.6, and -4.7.

IR (neat): 2953, 2930, 2883, 2857, 1764, 1618, 1250, 1189, 1065, 1010, 837, and 768 cm^{-1}.

HRMS (ESI-TOF): Calcd for $C_{16}H_{22}NaO_4Si^+$ [M+H$^+$] requires 326.1180; found 326.1182.

5-(Triphenylsilyl)penta-2,4-diyn-1-yl propiolate (5037)

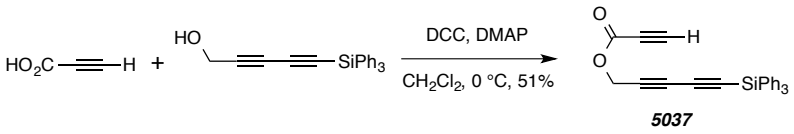

5037

[*BPW VI-116*] A solution of 5-(triphenylsilyl)penta-2,4-diyn-1-ol (110 mg, 0.32 mmol) and propiolic acid (30 µL, 0.48 mmol) in dichloromethane (3 mL) was cooled to 0 °C. N,N'-dicyclohexylcarbodiimide (100 mg, 0.48 mmol) and DMAP (5 mg, 0.04 mmol) was added and allowed to come to room temperature. After 4 h, the solution was filtered through plug of Celite, rinsing with EtOAc. After solvent removal, the crude material was purified by MPLC (12:1 Hex:EtOAc) to give triyne **5037** (65 mg, 0.17 mmol, 51%) as a clear oil.

^{1}H NMR (500 MHz, $CDCl_3$): δ 7.62 [dd, *J* = 8.0, 1.4 Hz, 6H, Si(Ph*H*$_o$)$_3$], 7.45 [ddd, *J* = 7.3, 7.3, 1.4 Hz, 3H, Si(Ph*H*$_p$)$_3$], 7.39 [ddd, *J* = 7.5, 6.8, 1.4 Hz, 6H, Si(Ph*H*$_m$)$_3$], and 4.86 (s, 2H, C*H*$_2$O), 2.95 (s, 1H, C≡C*H*).

^{13}C NMR (125 MHz, $CDCl_3$): δ 151.7, 135.7, 132.2, 130.4, 128.3, 90.7, 84.0, 76.5, 73.8, 72.6, 71.3, and 53.9.

IR: 3272, 3069, 3050, 3023, 2119, 1724, 1429, 1208, 1113, 967, 806, and 749 cm^{-1}.

HR ESI-MS calcd for $C_{26}H_{18}NaO_2Si$ [M + Na]$^+$ 413.0968, found 413.0979.

Experimental Section for Chapter 6

2-Methyl-6-(trimethylsilyl)hexa-3,5-diyn-2-ol (S6001)

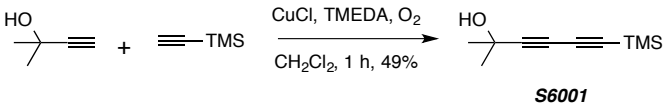

[*BPW IV-275*] To a solution of CuCl (500 mg, 5.0 mmol) in CH_2Cl_2 (50 mL) was added tetramethylethylenediamine (1.9 mL, 12.7 mmol) and oxygen was bubbled in with stirring for 10 minutes at rt. Trimethylsilylacetylene (0.71 mL, 5.0 mmol) and 2-methylbut-3-yn-2-ol (0.48 mL, 5.0 mmol) was added and the reaction stirred, uncovered, for 1 h. Aqueous NH_4Cl was added (10 mL), and the organic layer was washed with water, brine, dried ($MgSO_4$), filtered, and concentrated under reduced pressure. The crude product was purified via flash chromatography (3:1 Hex:EtOAc) to give **S6001** (440 mg, 2.4 mmol, 49%) as a clear oil.

^{1}H NMR (500 MHz, $CDCl_3$): δ 2.0 (br s, 1H, O*H*), 1.53 [s, 6H, C(C*H*$_3$)$_2$], and 0.2 [s, 9H, Si(C*H*$_3$)$_3$].

^{13}C NMR (125 MHz, $CDCl_3$): δ 87.9, 87.3, 82.1, 67.4, 65.7, 31.2, and -0.3.

IR: 3350 (br), 2984, 2963, 2231, 2103, 1251, 1092, 863, 846, and 761 cm^{-1}.

2-Methyl-8-(trimethylsilyl)octa-3,5,7-triyn-2-ol (6007)

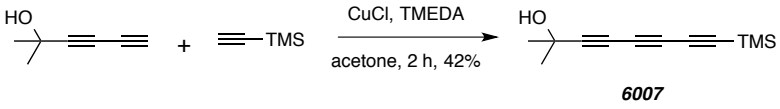

[*BPW V-215*] To a solution of CuCl (100 mg, 1.0 mmol) in acetone (15 mL) was added tetramethylethylenediamine (50 µL, 0.33 mmol) and stirred for 10 minutes at rt. Trimethylsilylacetylene (2.8 mL, 20 mmol) and 2-methylhexa-3,5-diyn-2-ol[160] (270 mg, 2.5 mmol) in acetone (2 mL) was added dropwise over 5 minutes and the reaction stirred, uncovered, for 2 h. Water was added (10 mL), and the mixture was extracted with EtOAc (3 x 20 mL), washed with brine, dried ($MgSO_4$), filtered, and concentrated under reduced pressure. Purification by MPLC (3:1 hexanes:EtOAc) gave **6007** (215 mg, 1.1 mmol, 42%) as a yellow oil.

[160] Dunetz, J. R.; Danheiser, R. L. Synthesis of highly substituted indolines and indoles via intramolecular [4 + 2] cycloaddition of ynamides and conjugated enynes. *J. Am. Chem. Soc.* **2005**, *127*, 5776–5777.

^{1}H NMR (500 MHz, $CDCl_3$): δ 1.54 [s, 6H, C(CH_3)$_2$], and 0.21 [s, 9H, Si(CH_3)$_3$].

^{13}C NMR (125 MHz, $CDCl_3$): δ 88.0, 87.8, 82.5, 67.5, 65.8, 64.1, 61.1, 31.1, and -0.4.

IR: 3300 (br), 2984, 2962, 2901, 2166, 2075, 1292, 1251, 962, 850, and 761 cm^{-1}.

GC-MS t_r (5025015) = 7.07 min; m/z: 204, 189, 171, 147, and 75.

2,2,3,3,18,18,19,19-Octamethyl-4,17-dioxa-3,18-disilaicosa-7,9,11,13-tetrayne (6008)

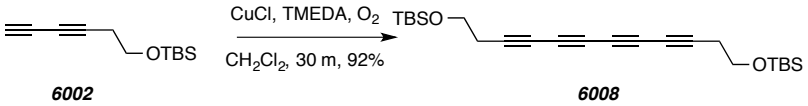

6002 ***6008***

[*BPW IV-275*] To a solution of CuCl (60 mg, 0.6 mmol) in CH_2Cl_2 (10 mL) was added tetramethylethylenediamine (230 µL, 1.5 mmol) and oxygen was bubbled in with stirring for 10 minutes at rt. Diyne **6002**[154] (75 mg, 0.36 mmol) was added and the reaction stirred, uncovered, for 30 min. Aqueous NH_4Cl was added (10 mL), and the organic layer was washed with water, brine, dried ($MgSO_4$), filtered, and concentrated under reduced pressure. The crude product was filtered through a plug of silica to give **6008** (69 mg, 0.17 mmol, 42%) as a clear oil.

^{1}H NMR (500 MHz, $CDCl_3$): δ 3.75 (t, J = 6.8 Hz, 4H, CH_2OSi), 2.52 (t, J = 6.8 Hz, 4H, CH_2CH_2O), 0.90 [s, 18H, SiC(CH_3)$_3$], and 0.07 [s, 12H, Si(CH_3)$_2$].

^{13}C NMR (125 MHz, $CDCl_3$): δ 77.8, 66.9, 61.5, 61.2, 60.9, 26.0, 24.1, 18.4, and -5.1.

IR: 3300 (br), 2954, 2929, 2857, 2228, 1255, 1108, 838, and 778 cm^{-1}.

HR ESI-MS calcd for $C_{24}H_{38}NaO_2Si_2$ $[M + Na]^+$ 437.2303, found 437.2313.

12-((*tert*-Butyldimethylsilyl)oxy)-1-(trimethylsilyl)dodeca-1,7,9-triyn-3-one (6009)

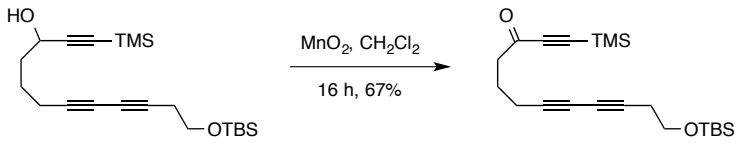

S6002 ***6009***

[*BPW IV-217*] MnO_2 (278 mg, 3.2 mmol) was added to a stirred solution of alcohol **S6002** (60 mg, 0.16 mmol) in CH_2Cl_2 (2.0 mL) at room temperature. After 16 h the reaction mixture was filtered through Celite® (EtOAc eluent) and concentrated to give the ketone **6009** (41 mg, 0.11 mmol, 67%) as a yellow oil.

^{1}H NMR (500 MHz, $CDCl_3$): δ 3.73 (t, *J* = 7.1 Hz, 2H, C*H*$_2$O), 2.70 (t, *J* = 7.3 Hz, C*H*$_2$C=O), 2.47 (tt, *J* = 7.1, 1.1 Hz, 2H, C*H*$_2$CH$_2$OSi), 2.33 (tt, *J* = 6.9, 1.1 Hz, 2H, C*H*$_2$CH$_2$CH$_2$C=O), 1.86 (tt, *J* = 7.2, 7.0 Hz, 2H, CH$_2$C*H*$_2$CH$_2$C=O), 0.90 [s, 9H, SiC(C*H*$_3$)$_3$], 0.25 [s, 9H, Si(C*H*$_3$)$_3$], and 0.07 [s, 6H, Si(C*H*$_3$)$_2$].

^{13}C NMR (125 MHz, $CDCl_3$): δ 186.8, 102.0, 98.3, 76.4, 74.9, 66.4, 66.3, 61.6, 44.0, 26.0, 23.8, 22.5, 18.6, 18.5, -0.6, and -5.1.

IR: 2955, 2930, 2857, 2149, 1679, 1253, 1110, 846, and 778 cm^{-1}.

HR ESI-MS calcd for $C_{21}H_{34}NaO_2Si_2$ $[M + Na]^+$ 397.1990, found 397.2007.

Dimethyl 2,2-di(nona-2,4-diyn-1-yl)malonate (6010)

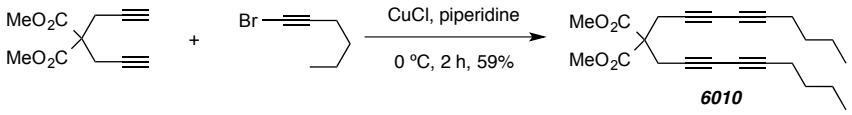

[*BPW V-038*] Diyne **6010** was prepared following the General Procedure A (Cadiot-Chodkiewicz) from dimethyl 2,2-di(prop-2-yn-1-yl)malonate[143] (208 mg, 1.0 mmol), 1-bromopentyne (480 mg, 3.0 mmol), CuCl (40 mg, 0.4 mmol), and piperidine (5 mL). Purification by MPLC (hexanes:EtOAc 3:1) gave tetrayne **6010** (216 mg, 0.6 mmol, 59%) as a reddish oil.

^{1}H NMR (500 MHz, $CDCl_3$): δ 3.77 (s, 6H, CO$_2$C*H*$_3$), 3.06 [s, 4H, C*H*$_2$C(CO$_2$CH$_3$)$_2$], 2.24 (t, *J* = 6.9 Hz, 4H, C≡CC*H*$_2$), 1.50 (br p, *J* = 7.1 Hz, 4H, C≡CCH$_2$C*H*$_2$), 1.41 (br sex, *J* = 7.1 Hz, 4H, C*H*$_2$CH$_3$), and 0.91 (t, *J* = 7.3 Hz, 6H, CH$_2$C*H*$_3$).

^{13}C NMR (125 MHz, $CDCl_3$): δ 168.9, 79.1, 70.6, 68.8, 64.9, 56.9, 53.4, 30.3, 23.9, 22.1, 19.0, and 13.7.

IR: 2957, 2934, 2872, 2259, 1744, 1435, 1292, 1210, 1072, 1054, 956, and 847 cm^{-1}.

HR ESI-MS calcd for $C_{23}H_{28}NaO_4$ $[M + Na]^+$ 391.1880, found 391.1885.

Trimethyl(5-((3-methylbut-2-en-1-yl)oxy)penta-1,3-diyn-1-yl)silane (6011)

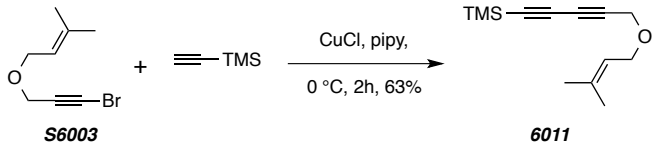

[*BPW VI-046*] Diyne **6011** was prepared following the General Procedure A (Cadiot-Chodkiewicz) from **S6003** (1.0 g, 5.0 mmol), trimethylsilylacetylene (1.4 mL, 10.0 mmol), CuCl (75 mg, 0.75 mmol), and piperidine (25 mL). Purification by MPLC (hexanes:EtOAc 20:1) gave diyne **6011** (693 mg, 3.2 mmol, 63%) as a yellow oil.

^{1}H NMR (500 MHz, $CDCl_3$): δ 5.32 (t, *J* = 6.7 Hz, 1H, C=C*H*), 4.19 (s, 2H,C≡CCH_2), 4.05 (d, *J* = 7.1 Hz, 2H, =CHCH_2O), 1.76 (s, 3H, CH_3C=C), 1.71 (s, 3H, CH_3C=C), and 0.20 [s, 9H, Si(CH_3)$_3$].

GC-MS t_r (5027016) = 6.61 min; m/z: 220, 205, 190, 175, 159, 131, 83, 73, and 59. t_{r2} 7.19 min; m/z: 219, 205, 175, 137, 121, 107, 97, 83, 73, and 53.

(*Z*)-Trimethyl(3-(4-(prop-1-en-2-yl)dihydrofuran-3(2*H*)-ylidene)prop-1-yn-1-yl)silane (6012)

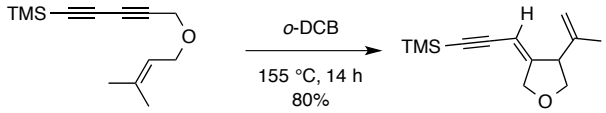

6011 ***6012***

[*BPW VI-176*] A solution of ether **6011** (20 mg, 0.09 mmol) in DCB (0.9 mL) was heated at 155 °C. After 14 h the solution was loaded onto a column of silica and DCB was removed by initial elution with hexanes. Subsequent elution with hexanes:EtOAc (2:1) gave **6012** (16 mg, 0.7 mmol, 80%) as a yellow oil.

^{1}H NMR (500 MHz, $CDCl_3$): δ 5.40 (q, *J* = 2.6 Hz, 1H, C=C*H*C≡C), 4.88 (m, 1H, C=CH_aH$_b$), 4.87 (m, 1H, C=CH$_a$$H_b$) 4.55 (ddd, *J* = 15.4, 4.1, 2.7, 1.4 Hz, 1H, OCH_aH$_b$C=C), 4.49 (dd, *J* = 15.4, 2.8, 0.5 Hz, 1H, OCH$_a$$H_b$C=C) 4.06 (dd, *J* = 8.7, 7.2 Hz, 1H, OCH_aH$_b$CH), 3.77 (dd, *J* = 8.7, 7.1 Hz, 1H, OCH$_a$$H_b$CH), 3.45 (qt, *J* = 7.3, 2.1 Hz, 1H, C*H*C=C), 1.68 (s, 3H, C=CCH_3), and 0.19 [s, 9H, Si(CH_3)$_3$].

^{13}C NMR (125 MHz, $CDCl_3$): δ 158.1, 143.0, 114.5, 101.8, 101.2, 99.8, 72.7, 71.9, 52.7, 19.0, and 0.1.

IR: 2959, 2898, 2859, 2129, 1644, 1250, 1070, 844, and 759 cm^{-1}.

GC-MS t_{r1} (5027016) = 6.61 min; m/z: 220, 205, 190, 175, 159, 131, 83, 73, and 59.

Computational Details

General Computational Details

DFT calculations were carried out in Gaussian 09[161] using the M06-2X/6-311+G(d,p)[162] functional basis set for geometry optimizations and frequency calculations (unless otherwise specified, e.g., 2H atom transfer from ethane). To identify starting geometries for the DFT calculations of the various hydrocarbon donors, Monte Carlo conformational searches were carried out in MacroModel version 10.0.[163] Each of the identified conformers was subjected to geometry optimization using the above DFT method. The optimized reactant and product geometries were found to have no imaginary frequencies and the optimized transition structure geometries were found to have only one imaginary frequency.

Computational Details for Table 5

To identify starting geometries for the DFT calculations, Monte Carlo conformational searches were carried out in MacroModel version 10.0. The alkyne-to-1,3-diyne dihedral angle in each lowest-energy conformer was then modified to and fixed at 0° in GaussView.[164] This was then used as the starting geometry for a DFT geometry optimization, which was carried out in Gaussian 09 using M06-2X/6-31+G(d,p). The DFT optimized geometries were found to have no imaginary frequencies. The coordinates for each final geometry for each of triynes **5019–5021**, **3014**, and **3089c** is given on the following pages. The energy value corresponding to the "Sum of electronic and thermal Free Energies=" is also given for each substrate, which, even though not

---

[161] Gaussian 09, Revision A.1, Frisch, M. J.; Trucks, G. W.; Schlegel, H. B.; Scuseria, G. E.; Robb, M. A.; Cheeseman, J. R.; Scalmani, G.; Barone, V.; Mennucci, B.; Petersson, G. A.; Nakatsuji, H.; Caricato, M.; Li, X.; Hratchian, H. P.; Izmaylov, A. F.; Bloino, J.; Zheng, G.; Sonnenberg, J. L.; Hada, M.; Ehara, M.; Toyota, K.; Fukuda, R.; Hasegawa, J.; Ishida, M.; Nakajima, T.; Honda, Y.; Kitao, O.; Nakai, H.; Vreven, T.; Montgomery, Jr., J. A.; Peralta, J. E.; Ogliaro, F.; Bearpark, M.; Heyd, J. J.; Brothers, E.; Kudin, K. N.; Staroverov, V. N.; Kobayashi, R.; Normand, J.; Raghavachari, K.; Rendell, A.; Burant, J. C.; Iyengar, S. S.; Tomasi, J.; Cossi, M.; Rega, N.; Millam, N. J.; Klene, M.; Knox, J. E.; Cross, J. B.; Bakken, V.; Adamo, C.; Jaramillo, J.; Gomperts, R.; Stratmann, R. E.; Yazyev, O.; Austin, A. J.; Cammi, R.; Pomelli, C.; Ochterski, J. W.; Martin, R. L.; Morokuma, K.; Zakrzewski, V. G.; Voth, G. A.; Salvador, P.; Dannenberg, J. J.; Dapprich, S.; Daniels, A. D.; Farkas, Ö.; Foresman, J. B.; Ortiz, J. V.; Cioslowski, J.; Fox, D. J. Gaussian, Inc., Wallingford CT, 2009.

[162] Zhao, Y.; Truhlar, D. G. The M06 suite of density functionals for main group thermochemistry, thermochemical kinetics, noncovalent interactions, excited states, and transition elements: Two new functionals and systematic testing of four M06 functionals and twelve other functionals. *Theor. Chem. Acc.* **2008**, *120*, 215–241. (b) Zhao, Y.; Truhlar, D. G. Density functionals with broad applicability in chemistry. *Acc. Chem. Res.* **2008**, *41*, 157–167.

[163] MacroModel, version 10.0, Schrödinger, LLC, New York, NY, 2013. (b) Chang, G.; Guida, W. C.; Still, W. C. An internal coordinate Monte Carlo method for searching conformational space. *J. Am. Chem. Soc.* **1989**, *111*, 4379–4386.

[164] GaussView, Version 5, Dennington, R.; Keith, T.; Millam, J. Semichem Inc., Shawnee Mission KS, 2009.

highly relevant given the dihedral angle constraint that was imposed, still serves as an additional check parameter for anyone repeating one of these computations.

Computed energy and geometry for 5019' (entry 1, Table 5)

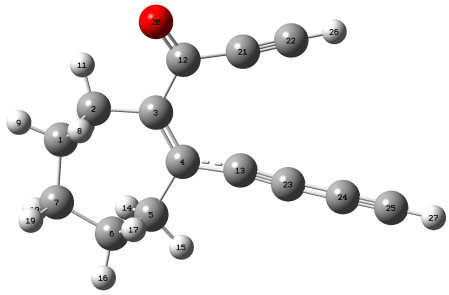

Energy: -1063.103622

Center Number	Atomic Number	Coordinates X	Y	Z
1	6	0.804418	0.680686	0.358900
2	6	0.115027	-0.504626	0.385477
3	6	0.844866	-1.809043	0.645732
4	6	1.821629	-2.197709	-0.472736
5	6	3.167704	-1.487170	-0.404240
6	6	3.113096	0.031766	-0.505415
7	6	2.286567	0.699444	0.602458
8	6	1.260810	-0.660787	0.143140
9	6	2.437072	-0.995014	0.050736
10	6	-3.759322	-1.259103	-0.062889
11	6	-4.951585	-1.490957	-0.165866
12	6	0.201160	1.986937	0.038329
13	8	0.897924	3.000208	-0.089599
14	6	-1.227997	2.140661	-0.130838
15	6	-2.388055	2.460763	-0.285509
16	1	1.394750	-1.724257	1.593866
17	1	0.105722	-2.601901	0.782456
18	1	1.991550	-3.278212	-0.409408
19	1	1.344164	-2.020855	-1.445547
20	1	3.649672	-1.753101	0.548311
21	1	3.819798	-1.880658	-1.193017
22	1	4.135832	0.422015	-0.456618
23	1	2.716963	0.336469	-1.483371
24	1	2.505830	0.200636	1.557372
25	1	2.593864	1.740756	0.710492
26	1	-5.994358	-1.697252	-0.255574
27	1	-3.424929	2.679615	-0.415834

Computed energy and geometry for 5020' (entry 2, Table 5)

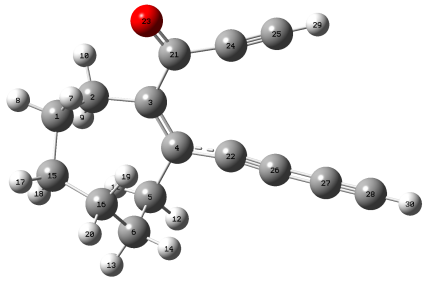

Energy: -1102.372234

Center Number	Atomic Number	Coordinates X	Y	Z
1	6	2.027200	0.861674	0.936033
2	6	2.977187	0.729424	-0.271213
3	6	2.745960	-0.509473	-1.140480
4	6	2.774204	-1.851948	-0.385596
5	6	1.407100	-2.466173	-0.058209
6	6	0.565431	-1.731968	0.999720
7	6	-0.060304	-0.438725	0.500315
8	6	0.583833	0.752127	0.526466
9	6	0.001902	2.034425	0.029113
10	8	0.723791	2.969837	-0.240467
11	6	-1.444616	2.208129	-0.065143
12	6	-2.616394	2.459983	-0.122856
13	6	-1.349156	-0.639339	-0.073991
14	6	-2.512807	-0.962520	-0.135504
15	6	-3.852730	-1.245944	-0.203203
16	6	-5.030732	-1.489841	-0.263188
17	1	2.267215	0.094313	1.672400
18	1	2.197772	1.832185	1.404538
19	1	2.883773	1.626417	-0.887323
20	1	4.001691	0.710116	0.115370
21	1	1.795956	-0.414392	-1.677463
22	1	3.522631	-0.513701	-1.909758
23	1	3.311996	-2.586010	-0.991760
24	1	3.356927	-1.746663	0.538504
25	1	0.818150	-2.554968	-0.978042
26	1	1.565518	-3.485586	0.306186
27	1	-0.249565	-2.388655	1.309735
28	1	1.172661	-1.537048	1.886059
29	1	-3.661259	2.656266	-0.179733
30	1	-6.070260	-1.709961	-0.318554

Computed energy and geometry for 3014' (entry 3, Table 5)

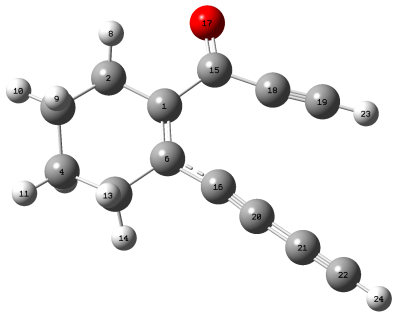

Energy: -1023.842978

Center Number	Atomic Number	Coordinates X	Y	Z
1	6	1.088329	0.497378	-0.005659
2	6	0.390929	-0.676087	0.014927
3	6	1.092076	-2.037047	0.042469
4	6	2.563730	-1.945573	-0.394297
5	6	3.232117	-0.811836	0.395303
6	6	2.612798	0.532337	-0.037469
7	6	-1.020060	-0.790590	0.001142
8	6	-2.206209	-0.945239	0.019286
9	6	-3.581438	-1.124539	0.040367
10	6	-4.773376	-1.279844	0.058690
11	6	0.437320	1.861015	-0.007845
12	8	1.151855	2.873965	0.002685
13	6	-1.047020	2.054928	-0.077811
14	6	-2.232073	2.212679	-0.068339
15	1	0.560684	-2.717941	-0.605081
16	1	1.038214	-2.408949	1.048462
17	1	3.049789	-2.889699	-0.193487
18	1	2.634938	-1.737468	-1.453388
19	1	3.081913	-0.974437	1.451751
20	1	4.295905	-0.786469	0.199029
21	1	2.954039	1.321001	0.610604
22	1	2.929114	0.763911	-1.041674
23	1	-5.840384	-1.332127	0.017491
24	1	-3.261792	2.484971	0.060228

Computed energy and geometry for 3089c' (entry 4, Table 5)

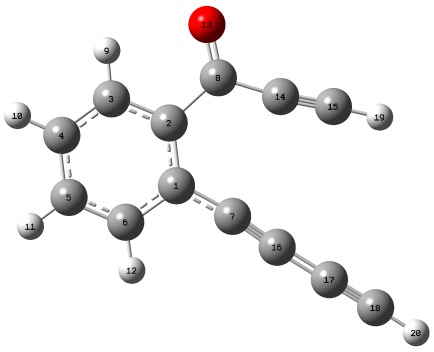

Energy: -1021.489335

Center Number	Atomic Number	Coordinates X	Y	Z
1	6	-1.239325	0.475938	-0.013633
2	6	-2.636089	0.547196	-0.029969
3	6	-3.384223	-0.629334	-0.012398
4	6	-2.739691	-1.891938	0.014630
5	6	-1.383494	-1.954667	0.031385
6	6	-0.612522	-0.782079	0.004935
7	6	0.782547	-0.862399	-0.006862
8	6	1.977415	-0.946826	-0.015311
9	6	3.321152	-1.061765	-0.018139
10	6	4.535738	-1.169725	-0.018983
11	6	-0.391333	1.766913	0.004726
12	8	-0.955017	2.905792	0.001816
13	6	1.156791	1.675056	0.025254
14	6	2.349655	1.685395	0.022803
15	1	-3.126518	1.490880	-0.052834
16	1	-4.448123	-0.569718	-0.024820
17	1	-3.322436	-2.811266	0.021903
18	1	-0.901077	-2.905453	0.069491
19	1	5.595943	-1.325528	0.014420
20	1	3.422619	1.764163	0.026678

Computed energy and geometry for 5021' (entry 5, Table 5)

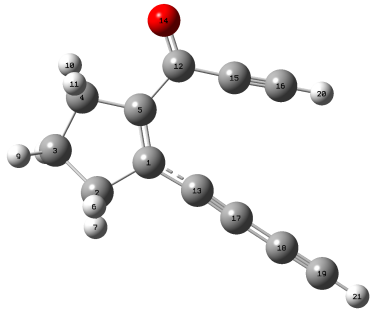

Energy: -984.571116

Center Number	Atomic Number	Coordinates X	Y	Z
1	6	1.343647	0.114366	-0.024634
2	6	0.400448	-0.852695	-0.030443
3	6	1.041453	-2.228085	-0.102927
4	6	2.505533	-1.948438	0.275721
5	6	2.732335	-0.471696	-0.091521
6	6	-1.009008	-0.730322	-0.030451
7	6	1.176445	1.581784	-0.027342
8	8	2.139680	2.308710	-0.138831
9	6	-0.161821	2.142980	0.117791
10	6	-1.250443	2.646852	0.145016
11	1	0.544388	-2.942990	0.554655
12	1	0.942230	-2.604087	-1.127514
13	1	2.625447	-2.073008	1.354242
14	1	3.204184	-2.622723	-0.219071
15	1	3.423943	0.045372	0.574857
16	1	3.126040	-0.352210	-1.107383
17	1	-2.223605	3.078855	0.168056
18	6	-2.217976	-0.726271	-0.030647
19	6	-3.587823	-0.664376	-0.025620
20	6	-4.790548	-0.604357	-0.020161
21	1	-5.853525	-0.557339	-0.015876

Computational Details for Section 4.4.2.

A total of six stable conformers of the substrate triyne **3016** were found (cf. **3016-comp-a-f**). Only a single geometry was identified for benzyne **3017**. A total of nine stable conformers of the substrate **4059** were found (cf. **4059-a-i**). Only a single geometry was identified for substrate **4060**. Only a single geometry was identified for naphthalene **4061**. Boltzmann analysis was conducted on all conformers of **3016** and **4059** to determine the equilibrium ratio of the conformers. The Boltzmann analysis was carried out at 298 K by the following equation,

$$\begin{array}{c}\text{percentage}\\ \text{(mole fraction)}\\ \text{of the } i\text{th component}\\ \text{of } n \text{ species}\\ \text{in equilibrium}\end{array} = \frac{e^{\left(-\Delta E_i^* / RT\right)}}{\sum_{i=1}^{n} e^{\left(-\Delta E_i^* / RT\right)}}$$

where ΔE_i is the difference in free energy between the i^{th} component and the lowest energy component.

Energy of 4060 (relative to 4061)

Structure	**Free Energy (rel to 4061) (kcal•mol^{-1})**
4061-comp	0.0
4060-comp	88.1

Boltzmann Analysis to Determine Energy of 4059 (relative to 4061)

Structure of each component *i*	**Free Energy (rel to 4061-comp) (kcal•mol^{-1})**	**mol fraction of each of the *i* components**
4059-comp-a	115.7	0.211
4059-comp-b	115.7	0.211
4059-comp-c	115.7	0.211
4059-comp-d	115.7	0.211
4059-comp-e	116.5	0.054
4059-comp-f	116.5	0.054
4059-comp-g	117.0	0.022

4059-comp-h	117.0	0.022
4059-comp-i	118.0	0.004

which corresponds to an energy of 115.8 kcal•mol^{-1}

Boltzmann Analysis to Determine Energy of 3016+3017 (relative to 4061)

Structure of each component *i*	Free Energy + 3017 (rel to 4061-comp) (kcal•mol^{-1})	mol fraction of each of the *i* components
3016-comp-a	176.2	0.380
3016-comp-b	176.3	0.310
3016-comp-c	176.3	0.310
3016-comp-d	180.8	1.42×10^{-4}
3016-comp-e	180.8	1.42×10^{-4}
3016-comp-f	181.8	2.73×10^{-5}

which corresponds to an energy of 176.2 kcal•mol^{-1}

Boltzmann Analysis to Determine Energy of 3016+3016 (relative to 4061)

Structure of each component *i*	Free Energy x 2 (rel to 4061-comp) (kcal•mol^{-1})	mol fraction of each of the *i* components
3016-comp-a	227.6	0.428
3016-comp-b	227.8	0.286
3016-comp-c	227.8	0.286
3016-comp-d	236.9	5.97×10^{-8}
3016-comp-e	236.9	5.97×10^{-8}
3016-comp-f	238.9	2.21×10^{-9}

which corresponds to an energy of 227.7 kcal•mol^{-1}

Computed energy and geometry for 3016-a

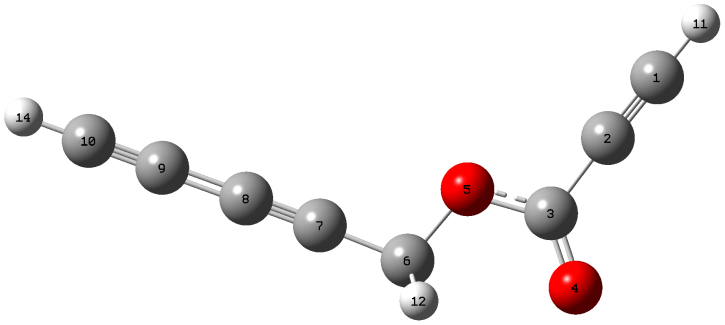

Sum of electronic and thermal Free Energies = -457.272413 A.U.[a]

Atom Type	Cartesian Coordinates (x,y,z)		
C	3.753607	1.772959	-0.00003
C	2.993677	0.838896	0.000014
C	2.11542	-0.320718	-0.000022
O	2.493395	-1.465207	-0.000189
O	0.826277	0.050005	0.000164
C	-0.098871	-1.048862	0.000118
C	-1.453151	-0.507812	0.000044
C	-2.589653	-0.093874	0.000008
C	-3.885612	0.379976	-0.000032
C	-5.02072	0.795114	-0.00007
H	4.425276	2.603589	-0.000036
H	0.076156	-1.668773	0.88515
H	0.076267	-1.668799	-0.884871
H	-6.023251	1.161514	-0.000221

[a] Atomic Units = Hartrees

Computed energy and geometry for 3016-b

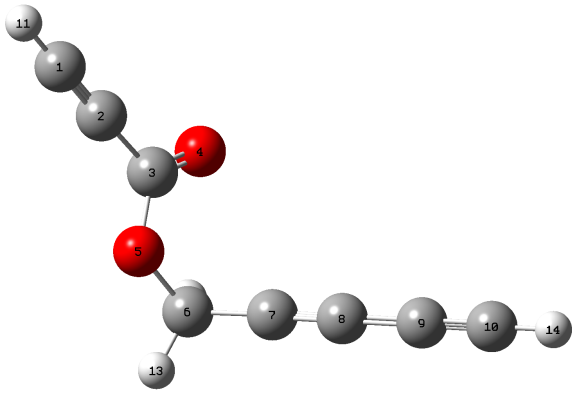

Sum of electronic and thermal Free Energies = -457.272222 A.U.[a]

Atom Type	Cartesian Coordinates (x,y,z)		
C	3.710164	1.397547	-0.545757
C	2.778788	0.736905	-0.163068
C	1.659998	-0.040216	0.348469
O	1.252223	0.013985	1.47912
O	1.148802	-0.835138	-0.609403
C	0.018776	-1.62107	-0.204096
C	-1.207944	-0.82495	-0.153323
C	-2.232228	-0.181473	-0.123227
C	-3.39993	0.55234	-0.084886
C	-4.422634	1.195892	-0.051577
H	4.535975	1.985582	-0.882544
H	0.214968	-2.070725	0.773177
H	-0.064556	-2.401478	-0.961737
H	-5.324519	1.766003	-0.021839

[a] Atomic Units = Hartrees

Computed energy and geometry for 3016-c

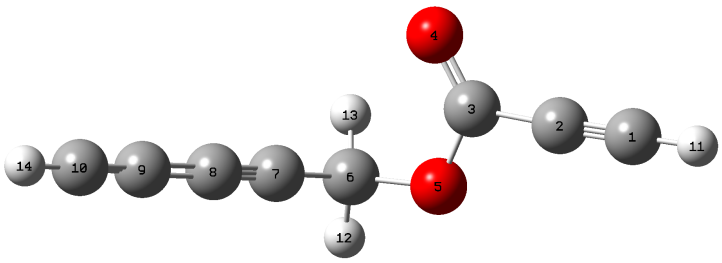

Sum of electronic and thermal Free Energies = -457.272222 A.U.[a]

Atom Type	Cartesian Coordinates (x,y,z)		
C	-3.709814	1.397738	-0.545783
C	-2.77858	0.736914	-0.163074
C	-1.659702	-0.040097	0.348393
O	-1.251553	0.014639	1.478861
O	-1.148797	-0.835478	-0.609261
C	-0.018869	-1.621468	-0.203858
C	1.207984	-0.825657	-0.153071
C	2.232293	-0.182242	-0.123041
C	3.399168	0.552825	-0.085009
C	4.421798	1.196466	-0.051769
H	-4.535565	1.985903	-0.882494
H	0.064325	-2.401992	-0.961415
H	-0.21514	-2.070976	0.773473
H	5.323508	1.766906	-0.023102

[a] Atomic Units = Hartrees

Computed energy and geometry for 3016-d

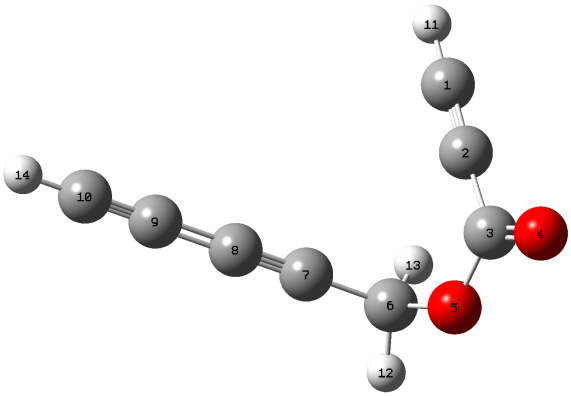

Sum of electronic and thermal Free Energies = -457.264954 A.U.[a]

Atom Type	Cartesian Coordinates (x,y,z)		
C	1.306104	2.192977	-0.760495
C	1.581859	1.150736	-0.221525
C	1.960039	-0.078605	0.474144
O	2.734444	-0.092999	1.388676
O	1.40825	-1.226474	0.025952
C	0.430733	-1.193345	-1.017056
C	-0.873139	-0.721867	-0.545966
C	-1.958259	-0.344707	-0.165116
C	-3.192429	0.09137	0.270636
C	-4.273254	0.474269	0.653122
H	1.061076	3.120874	-1.230306
H	0.356282	-2.227709	-1.357438
H	0.778182	-0.573551	-1.850115
H	-5.227016	0.811205	0.994366

[a] Atomic Units = Hartrees

Computed energy and geometry for 3016-e

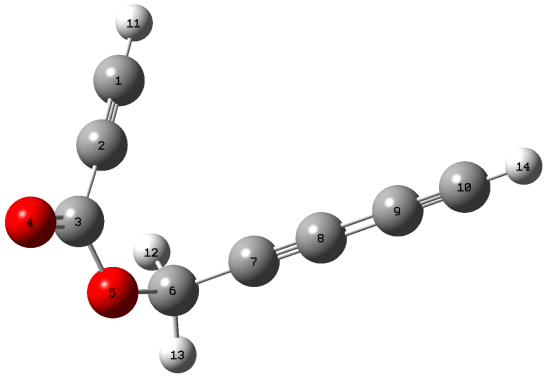

Sum of electronic and thermal Free Energies = -457.264954 A.U.[a]

Atom Type	Cartesian Coordinates (x,y,z)		
C	-1.306544	2.192984	-0.760452
C	-1.582078	1.150679	-0.221483
C	-1.959989	-0.078718	0.474213
O	-2.734226	-0.093208	1.388892
O	-1.408215	-1.22653	0.025821
C	-0.430636	-1.193277	-1.017136
C	0.873202	-0.721689	-0.546039
C	1.958309	-0.34454	-0.165178
C	3.192517	0.091459	0.270498
C	4.273335	0.474278	0.65305
H	-1.061695	3.120917	-1.230283
H	-0.778138	-0.573573	-1.85024
H	-0.356041	-2.227651	-1.357461
H	5.226712	0.811155	0.995431

[a] Atomic Units = Hartrees

Computed energy and geometry for 3016-f

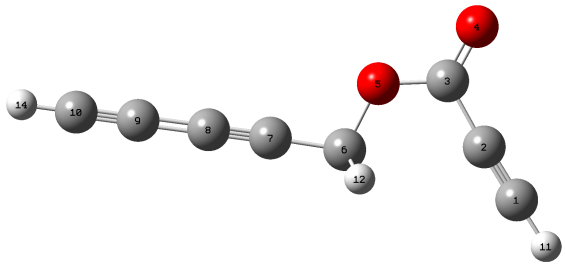

Sum of electronic and thermal Free Energies = -457.263397 A.U.[a]

Atom Type	Cartesian Coordinates (x,y,z)		
C	3.446188	-1.580018	-0.000442
C	2.816703	-0.551767	-0.000284
C	2.107873	0.729301	-0.000048
O	2.680712	1.78228	-0.000265
O	0.762148	0.674205	0.000492
C	0.111279	-0.602942	0.00066
C	-1.330294	-0.378572	0.00025
C	-2.528935	-0.218096	0.000111
C	-3.896724	-0.036456	-0.00017
C	-5.094652	0.12348	-0.000464
H	4.017065	-2.48354	-0.000586
H	0.401617	-1.172682	0.889831
H	0.40206	-1.173189	-0.888033
H	-6.152246	0.267947	-0.000703

[a] Atomic Units = Hartrees

Computed energy and geometry for 3017

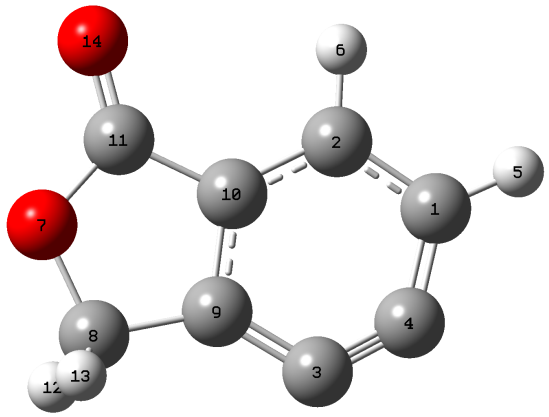

Sum of electronic and thermal Free Energies = -457.354225 A.U.[a]

Atom Type	Cartesian Coordinates (x,y,z)		
C	-2.428727	-0.846041	-0.000183
C	-1.095998	-1.299297	-0.000043
C	-1.535444	1.380421	0.000059
C	-2.455775	0.53845	0.000003
H	-3.275967	-1.519277	-0.0002
H	-0.881834	-2.363987	0.000065
O	2.065776	0.559096	-0.000164
C	1.147765	1.656682	-0.00016
C	-0.203717	1.006404	0.000097
C	-0.03695	-0.382407	0.00021
C	1.424216	-0.648733	0.000783
H	1.325946	2.263385	-0.892691
H	1.326257	2.263635	0.892135
O	2.010896	-1.693674	-0.000324
C	-2.428727	-0.846041	-0.000183
C	-1.095998	-1.299297	-0.000043

[a] Atomic Units = Hartrees

Computed energy and geometry for 4059-a

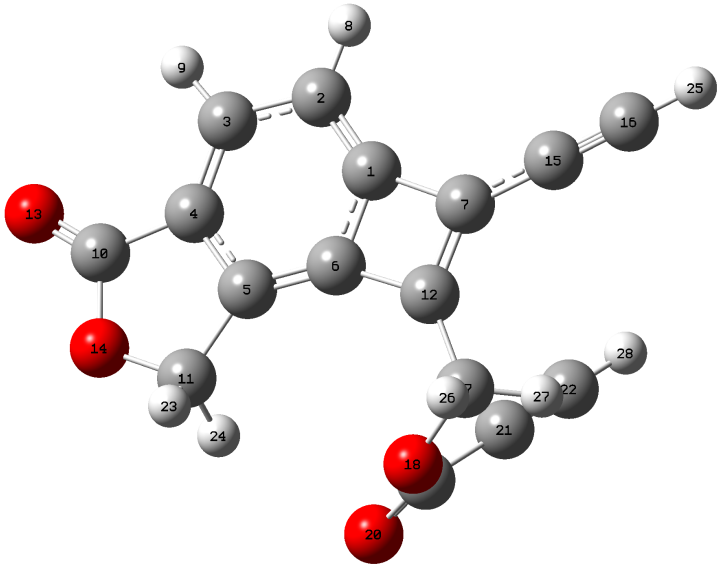

Sum of electronic and thermal Free Energies = -914.723179 A.U.[a]

Atom Type	Cartesian Coordinates (x,y,z)		
C	-0.227062	1.801721	-0.000822
C	0.717538	2.647033	0.501122
C	2.047187	2.121105	0.571586
C	2.290837	0.838217	0.147114
C	1.297268	-0.033973	-0.37507
C	0.04242	0.480346	-0.442049
C	-1.700373	1.577034	-0.352636
H	0.497931	3.655072	0.834205
H	2.864895	2.721684	0.958575
C	3.578106	0.100034	0.138362
C	1.960709	-1.340744	-0.714391
C	-1.421169	0.317972	-0.774683
O	4.667051	0.462656	0.489094
O	3.339108	-1.145927	-0.36308
C	-2.879829	2.344778	-0.247974
C	-3.884025	3.012317	-0.14918
C	-2.180116	-0.840183	-1.314934
O	-1.475139	-2.053008	-1.021722
C	-1.363919	-2.47402	0.255849

O	-0.627403	-3.380511	0.533187
C	-2.182287	-1.785101	1.249873
C	-2.838502	-1.240792	2.102007
H	1.907204	-1.578833	-1.780297
H	1.565783	-2.184294	-0.140366
H	-4.769455	3.603866	-0.070409
H	-2.221557	-0.812039	-2.407149
H	-3.202232	-0.867957	-0.923001
H	-3.412195	-0.75765	2.863564

[a] Atomic Units = Hartrees

Computed energy and geometry for 4059-b

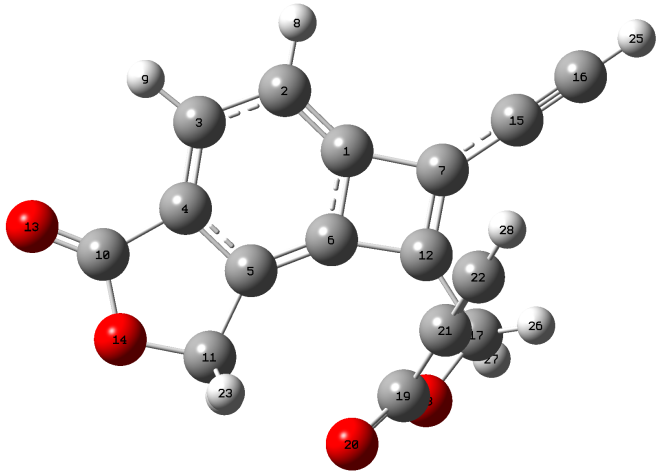

Sum of electronic and thermal Free Energies = -914.723178 A.U.[a]

Atom Type	Cartesian Coordinates (x,y,z)		
C	-0.227357	1.801581	0.000676
C	0.717105	2.646895	-0.501537
C	2.046836	2.121151	-0.571871
C	2.290705	0.838415	-0.147071
C	1.297275	-0.033785	0.375309
C	0.042337	0.480328	0.44217
C	-1.700552	1.576844	0.352825
H	0.497393	3.654819	-0.83489
H	2.864426	2.721764	-0.959052
C	3.578014	0.100315	-0.138376
C	1.960784	-1.340487	0.71464
C	-1.421187	0.31787	0.775
O	4.666921	0.463023	-0.489159
O	3.339154	-1.145662	0.363083
C	-2.88002	2.344572	0.24814
C	-3.884235	3.012081	0.149382
C	-2.179599	-0.840678	1.315221
O	-1.474083	-2.053087	1.021479
C	-1.363623	-2.47414	-0.256163

O	-0.627246	-3.380613	-0.533887
C	-2.182395	-1.785076	-1.249751
C	-2.838778	-1.240548	-2.101615
H	1.565819	-2.18411	0.140748
H	1.907497	-1.578514	1.780566
H	-4.769672	3.603615	0.070591
H	-3.201763	-0.868784	0.923469
H	-2.220815	-0.81287	2.407448
H	-3.412721	-0.757253	-2.862886

[a] Atomic Units = Hartrees

Computed energy and geometry for 4059-c

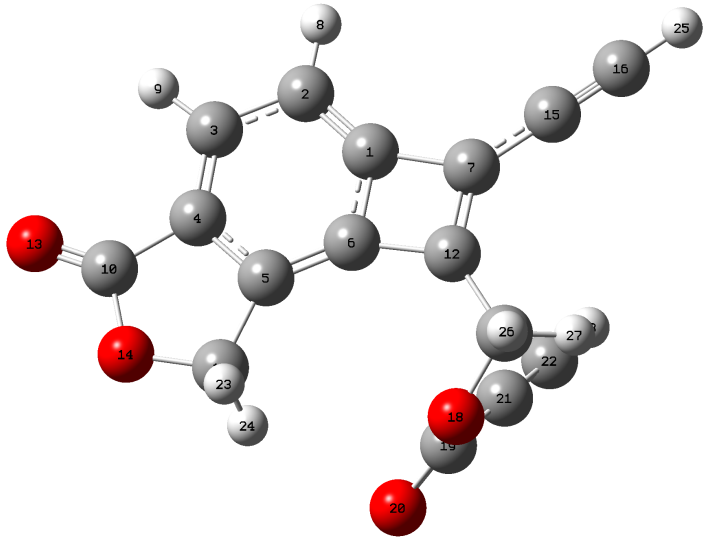

Sum of electronic and thermal Free Energies = **-914.723177** A.U.[a]

Atom Type	Cartesian Coordinates (x,y,z)		
C	0.227197	1.801604	0.000689
C	-0.717311	2.646888	-0.501481
C	-2.047011	2.121069	-0.571845
C	-2.290812	0.838308	-0.147085
C	-1.297327	-0.033849	0.375276
C	-0.042417	0.48033	0.442142
C	1.700414	1.576948	0.352817
H	-0.497653	3.654839	-0.834793
H	-2.864629	2.721655	-0.95901
C	-3.578084	0.100134	-0.138407
C	-1.960768	-1.340596	0.714588
C	1.421122	0.31795	0.77498
O	-4.667009	0.462779	-0.489186
O	-3.339152	-1.145832	0.36305
C	2.879842	2.344734	0.248127
C	3.884017	3.012303	0.149367
C	2.179632	-0.84053	1.315211
O	1.474258	-2.053024	1.021492
C	1.363917	-2.474135	-0.256143

O	0.627661	-3.3807	-0.53388
C	2.182641	-1.784982	-1.249707
C	2.83902	-1.240355	-2.101511
H	-1.907462	-1.578643	1.780509
H	-1.565767	-2.184188	0.140675
H	4.769434	3.603864	0.070553
H	2.220838	-0.812705	2.407438
H	3.201804	-0.868541	0.923466
H	3.412954	-0.757005	-2.862755

[a] Atomic Units = Hartrees

Computed energy and geometry for 4059-d

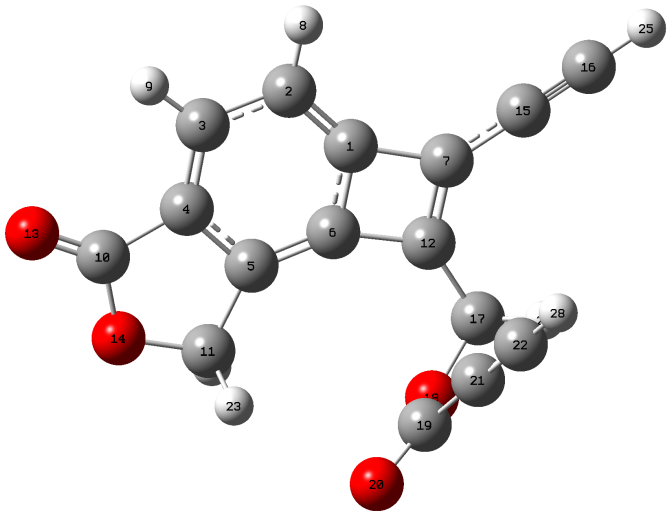

Sum of electronic and thermal Free Energies = -914.723176 A.U.[a]

Atom Type	Cartesian Coordinates (x,y,z)		
C	0.227212	1.801667	-0.000266
C	-0.71749	2.647108	0.501289
C	-2.047159	2.121213	0.571562
C	-2.290821	0.838327	0.147085
C	-1.297183	-0.033889	-0.374896
C	-0.042244	0.480274	-0.441397
C	1.700467	1.577129	-0.352393
H	-0.497996	3.65522	0.834221
H	-2.864872	2.721889	0.958391
C	-3.578071	0.100101	0.13821
C	-1.960505	-1.34069	-0.714229
C	1.421304	0.318014	-0.774317
O	-4.667079	0.462732	0.48873
O	-3.338987	-1.145903	-0.363088
C	2.879768	2.345152	-0.248037
C	3.883828	3.012942	-0.149564
C	2.18	-0.840201	-1.314819
O	1.4747	-2.052875	-1.021843
C	1.363783	-2.474316	0.25563

O	0.627347	-3.380897	0.532851
C	2.182319	-1.7856	1.249647
C	2.838553	-1.241358	2.101814
H	-1.565642	-2.184201	-0.140107
H	-1.906927	-1.578889	-1.780104
H	4.769147	3.604689	-0.071032
H	3.20209	-0.868301	-0.922849
H	2.221487	-0.81179	-2.40703
H	3.41229	-0.758317	2.863404

[a] Atomic Units = Hartrees

Computed energy and geometry for 4059-e

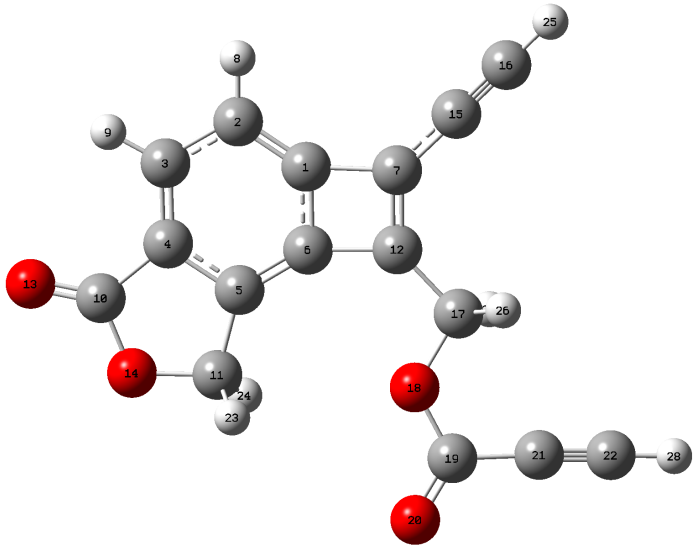

Sum of electronic and thermal Free Energies = -914.721889 A.U.[a]

Atom Type	Cartesian Coordinates (x,y,z)		
C	-0.996164	1.899604	0.002663
C	-2.315631	2.240529	0.040161
C	-3.240184	1.14778	0.015477
C	-2.764317	-0.139706	-0.038067
C	-1.385069	-0.480399	-0.07628
C	-0.521	0.565135	-0.06235
C	0.461566	2.373905	0.016356
H	-2.664928	3.265562	0.090256
H	-4.311378	1.322834	0.044408
C	-3.533686	-1.408519	-0.055089
C	-1.277286	-1.979101	-0.110043
C	0.891569	1.088316	-0.052078
O	-4.721228	-1.581528	-0.03892
O	-2.63771	-2.437547	-0.094145
C	1.097234	3.632432	0.077609
C	1.626086	4.719002	0.13372
C	2.201186	0.39416	-0.124431

O	1.933836	-0.961445	0.256697
C	2.912855	-1.886809	0.226768
O	2.677952	-3.029737	0.50399
C	4.242405	-1.415886	-0.154967
C	5.355886	-1.073134	-0.46445
H	-0.755936	-2.386779	0.760044
H	-0.796862	-2.3528	-1.018346
H	2.091236	5.678625	0.18635
H	2.933352	0.852023	0.549365
H	2.601619	0.420233	-1.145839
H	6.347401	-0.781481	-0.737215

[a] Atomic Units = Hartrees

Computed energy and geometry for 4059-f

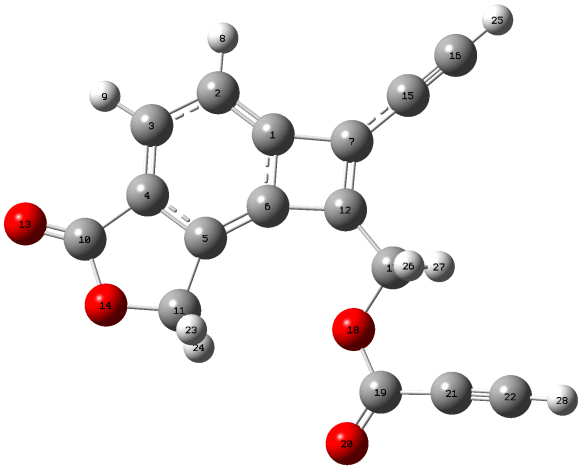

Sum of electronic and thermal Free Energies = -914.721885 A.U.[a]

Atom Type	Cartesian Coordinates (x,y,z)		
C	0.996166	1.89963	0.002564
C	2.31564	2.240505	0.040158
C	3.24016	1.147727	0.015518
C	2.764242	-0.139741	-0.038007
C	1.384986	-0.480388	-0.076325
C	0.520962	0.565175	-0.062486
C	-0.461551	2.373968	0.016299
H	2.664973	3.265525	0.090323
H	4.31136	1.322728	0.044552
C	3.533575	-1.408574	-0.054786
C	1.277161	-1.979086	-0.110127
C	-0.891587	1.088399	-0.052261
O	4.721118	-1.581607	-0.038883
O	2.637576	-2.437571	-0.094097
C	-1.097189	3.632507	0.077626
C	-1.625979	4.719099	0.133835
C	-2.201187	0.394201	-0.124577
O	-1.933711	-0.961418	0.256451
C	-2.912707	-1.88681	0.226692
O	-2.67772	-3.029724	0.50391
C	-4.242341	-1.415925	-0.154789

C	-5.355904	-1.073266	-0.464077
H	0.796824	-2.35273	-1.018502
H	0.755689	-2.386787	0.759876
H	-2.09112	5.678724	0.186511
H	-2.601702	0.420295	-1.145953
H	-2.933327	0.851958	0.549314
H	-6.347478	-0.781689	-0.736703

[a] Atomic Units = Hartrees

Computed energy and geometry for 4059-g

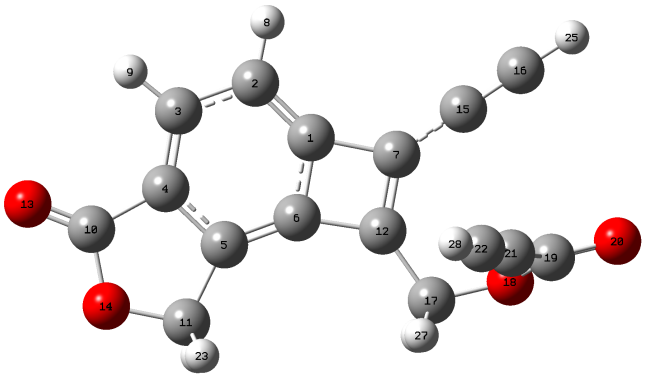

Sum of electronic and thermal Free Energies = -914.721041 A.U.[a]

Atom Type	Cartesian Coordinates (x,y,z)		
C	-0.431673	1.357059	-0.082768
C	-1.393279	2.273633	0.225171
C	-2.727417	1.767668	0.316941
C	-2.957275	0.431462	0.098964
C	-1.943519	-0.513458	-0.219392
C	-0.679557	-0.023172	-0.305798
C	1.050745	1.098966	-0.336141
H	-1.179753	3.323026	0.393055
H	-3.559853	2.422437	0.556238
C	-4.248058	-0.294909	0.146625
C	-2.60657	-1.856338	-0.375919
C	0.804106	-0.219192	-0.545655
O	-5.350645	0.114347	0.380468
O	-3.996181	-1.610103	-0.135562
C	2.215186	1.896175	-0.317933
C	3.215976	2.574013	-0.287906
C	1.645351	-1.398742	-0.869731
O	3.006215	-1.036079	-1.073396
C	3.821887	-0.802557	-0.022494
O	4.964169	-0.485988	-0.197975
C	3.246584	-0.972768	1.311523

C	2.829151	-1.098438	2.435503
H	-2.255906	-2.591686	0.354366
H	-2.499222	-2.269841	-1.383009
H	4.113432	3.152686	-0.269202
H	1.324244	-1.84747	-1.815026
H	1.553587	-2.162058	-0.085682
H	2.465182	-1.200923	3.435039

[a] Atomic Units = Hartrees

Computed energy and geometry for 4059-h

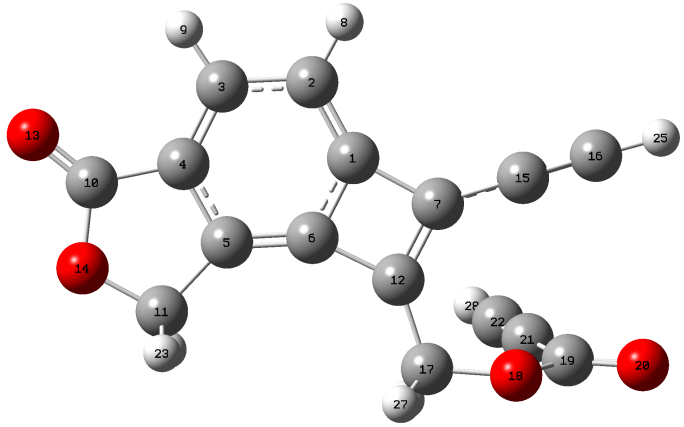

Sum of electronic and thermal Free Energies = -914.721032 A.U.[a]

Atom Type	Cartesian Coordinates (x,y,z)		
C	0.431515	1.357107	-0.082696
C	1.393109	2.273595	0.22549
C	2.727241	1.767645	0.317233
C	2.957116	0.431497	0.098996
C	1.943378	-0.513338	-0.219598
C	0.679428	-0.023054	-0.30601
C	-1.050884	1.099043	-0.336163
H	1.179554	3.322953	0.393578
H	3.559658	2.422373	0.556701
C	4.247897	-0.294877	0.146528
C	2.606414	-1.856212	-0.376289
C	-0.804213	-0.219046	-0.545988
O	5.350441	0.114287	0.380706
O	3.996006	-1.610037	-0.13579
C	-2.215314	1.89627	-0.317954
C	-3.216096	2.574127	-0.288058
C	-1.645408	-1.398536	-0.870338
O	-3.006376	-1.0359	-1.073371
C	-3.821645	-0.802616	-0.022102
O	-4.964023	-0.486146	-0.19708
C	-3.245834	-0.973093	1.311666

C	-2.827933	-1.099122	2.435419
H	2.499119	-2.269558	-1.383449
H	2.255669	-2.591658	0.353859
H	-4.11361	3.152714	-0.26946
H	-1.553268	-2.16216	-0.086635
H	-1.324527	-1.846837	-1.815912
H	-2.463602	-1.201801	3.434795

[a] Atomic Units = Hartrees

Computed energy and geometry for 4059-i

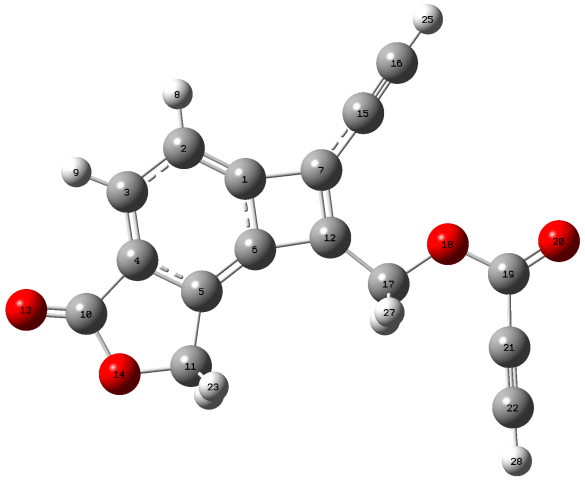

Sum of electronic and thermal Free Energies = -914.719393 A.U.[a]

Atom Type	Cartesian Coordinates (x,y,z)		
C	0.901616	1.603246	0.000246
C	2.08361	2.283164	0.000633
C	3.264933	1.477507	0.000617
C	3.146525	0.109402	0.00026
C	1.906236	-0.585796	-0.000231
C	0.790301	0.188682	-0.00021
C	-0.623438	1.692115	0.000027
H	2.143849	3.365525	0.000981
H	4.251912	1.930332	0.001001
C	4.228521	-0.902595	0.000431
C	2.211767	-2.060119	-0.000789
C	-0.717075	0.337613	-0.000495
O	5.418411	-0.754397	0.000073
O	3.641435	-2.139666	-0.000471
C	-1.526368	2.77632	0.000212
C	-2.260377	3.736486	0.000685
C	-1.819993	-0.649846	-0.001072
O	-3.046099	0.073212	-0.001518
C	-4.220032	-0.587077	-0.000458
O	-5.260258	0.007822	-0.000804
C	-4.145996	-2.048994	0.001059

C	-4.140549	-3.254528	0.002293
H	1.839646	-2.572138	-0.893314
H	1.839201	-2.572987	0.891059
H	-2.926235	4.570969	0.001257
H	-1.751814	-1.293986	0.886262
H	-1.751108	-1.293785	-0.888507
H	-4.151453	-4.323186	0.003765

[a] Atomic Units = Hartrees

Computed energy and geometry for 4060

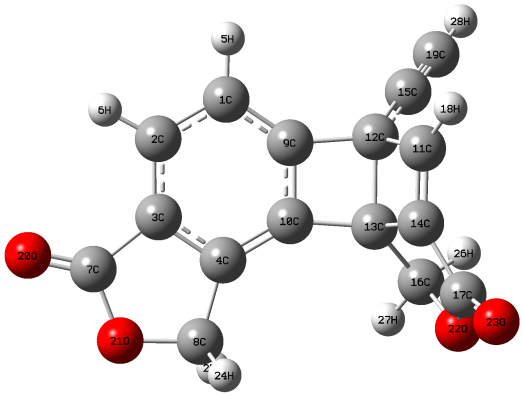

Sum of electronic and thermal Free Energies = -914.767139 A.U.[a]

Atom Type	Cartesian Coordinates (x,y,z)		
C	1.101339	2.216756	-0.782883
C	2.38212	1.660003	-0.69202
C	2.528206	0.368813	-0.184606
C	1.472976	-0.430176	0.248908
H	0.949411	3.220039	-1.166154
H	3.26446	2.211225	-1.002663
C	3.785113	-0.402332	-0.001945
C	2.037391	-1.743585	0.715208
C	0.05549	1.421	-0.332392
C	0.210198	0.1306	0.171412
C	-2.263405	0.745372	-1.332733
C	-1.466382	1.399645	-0.180362
C	-1.273553	-0.087445	0.364513
C	-2.083357	-0.485037	-0.843543
C	-2.145209	2.399437	0.611962
C	-1.995198	-0.884938	1.436005
C	-2.687124	-1.82093	-0.612574
H	-2.826736	1.177853	-2.150722
C	-2.724552	3.22733	1.272031
O	4.915627	-0.086738	-0.244846
O	3.449858	-1.617698	0.524711
O	-2.54748	-2.030781	0.73348

O	-3.208205	-2.606833	-1.347917
H	1.680546	-2.59243	0.124327
H	1.846853	-1.938452	1.774764
H	-2.818192	-0.314741	1.879196
H	-1.346557	-1.276713	2.219822
H	-3.232504	3.96256	1.856126

[a] Atomic Units = Hartrees

Computed energy and geometry for 4061

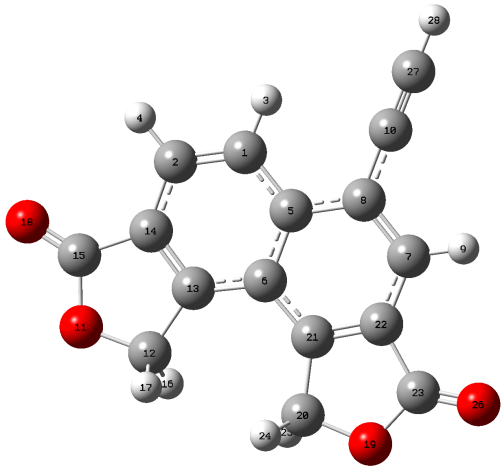

Sum of electronic and thermal Free Energies = -914.907487 A.U.[a]

Atom Type	Cartesian Coordinates (x,y,z)		
C	-1.007586	2.210482	0.000011
C	-2.301265	1.751335	0.000008
H	-0.802745	3.275624	0.000008
H	-3.151136	2.425848	0.000008
C	0.099595	1.312939	0.000019
C	-0.130054	-0.100187	0.000023
C	2.525552	0.944733	0.000012
C	1.452091	1.813111	0.000012
H	3.546205	1.312596	0.000017
C	1.691928	3.227444	0.000012
O	-3.475444	-1.72424	-0.000021
C	-2.062896	-1.927504	-0.000008
C	-1.475351	-0.54005	0.000015
C	-2.506178	0.358298	0.000014
C	-3.785949	-0.392329	0.000032
H	-1.797207	-2.504078	-0.892319
H	-1.797228	-2.504101	0.892295
O	-4.911588	0.016735	-0.000038
O	2.512037	-2.71798	-0.000023
C	1.109436	-2.45654	-0.000016

C	0.998779	-0.953748	0.00002
C	2.264184	-0.435261	0.000024
C	3.235074	-1.557615	0.000056
H	0.672551	-2.916646	0.892665
H	0.672551	-2.916593	-0.892724
O	4.43214	-1.532253	-0.000044
C	1.908002	4.415674	-0.000008
H	2.107673	5.464559	-0.000306

[a] Atomic Units = Hartrees

Bibliography and Notes

1. Lee, M.; Dunne, T.; Chang, C.; Siegel, M. Calicheamicins, a novel family of antitumor antibiotics. 4. Structure elucidation of calicheamicins β_1^{Br}, Υ_1^{Br}, α_2^I, α_3^I, β_1^I, Υ_1^I, and δ_1^I. *J. Am. Chem. Soc.* **1992**, 11*4*, 985–997.

2. Golik, J.; Dubay, G.; Groenewold, G.; Kawaguchi, H.; Konishi, M.; Krishnan, B.; Ohkuma, H.; Saitoh, K.; Doyle, T. Esperamicins, a novel class of potent antitumor antibiotics. 3. Structures of Esperamicins A1, A2, and A1b. *J. Am. Chem. Soc.* **1987,** *109* , 3462–3464

3. Wang, X.; Xie, H. C-1027. *Drugs of the Future* **1999,** *24*, 847–852.

4. Sugimoto, Y.; Otani, T.; Oie, S.; Wierzba, K.; Yamada, Y. Mechanism of action of a new macromolecular antitumor antibiotic, C-1027. *The Journal of Antibiotics* **1990**, *43*, 417–421.

5. Liu, W.; Christenson, S.; Standage, S.; Shen, B. Biosynthesis of the enediyne antitumor antibiotic C-1027. *Science* **2002**; *297*, 1170–1173.

6. Maeda, H. Enediyne Antibiotics as Antitumor Agents. New York, 1995.

7. Brukner, I. Curr. Opin. Oncol. Endocr. Met. Invest. Drugs **2000,** 2, 344.

8. Rezanka, T.; Dembitsky, V. Novel brominated lipidic compounds from lichens of Central Asia. *Phytochemistry* **1999**, *51*, 963-968.

9. Sondheimer, F.; Amiel, Y.; Wolovsky, R. Unsaturated macrocyclic compounds. V. 1 large ring poly-acetylenes. *J. Am. Chem. Soc.* **1957**, *79*, 4247–4248.

10. Sondheimer, F.; Wolovsky, R. Unsaturated macrocyclic compounds. VI. The synthesis of cyclo-octadeca-1, 3, 7, 9, 13, 15-hexane-5, 11, 17-triyne, a completely conjugated eighteen-membered ring cyclic system. *J. Am. Chem. Soc.* **1959**, *81*, 1771.

11. Sondheimer, F.; Amiel, Y.; Gaoni, Y. Unsaturated macrocyclic compounds. VII. 1 Synthesis of cyclooctadeca-1, 3, 7, 9, 13, 15-hexaene-5, 11, 17-triyne from 1, 5-hexadiyn-3-ol. *J. Am. Chem. Soc.* **1959**, *81*, 1771–1772.

12. Mayer, J.; Sondheimer, F. 1, 5, 9-Tridehydro [14] annulene and bicyclo [9.3. 0] tetradeca-1, 5, 7, 11, 13-pentaene-3, 9-diyne, an acetylenic homolog of azulene containing fused five- and eleven-membered rings. *J. Am. Chem. Soc.* **1966**, *88*, 602–603.

13. Thorson, J.; Shen, B.; Whitwam, R.; Liu, W.; Li, Y.; Ahlert, J. Enediyne biosynthesis and self-resistance: a progress report. *Bioorg. Chem.* **1999,** *27*, 172–188.

14. Smith, A.; Nicolaou, K. C. The enediyne antibiotics. *J. Med. Chem.* **1996**, *39*, 2103–2117.

15. Nicolaou, K.; Zuccarello, G.; Riemer, C.; Estevez, V.; Dai, W. Design, synthesis, and study of simple monocyclic conjugated enediynes. The 10-membered ring enediyne moiety of the enediyne anticancer antibiotics. *J. Am. Chem. Soc.* **1992,** *114*, 7360–7371.

16. Snyder, J. Monocyclic enediyne collapse to 1, 4-diyl biradicals: a pathway under strain control. *J. Am. Chem. Soc.* **1990,** *112*, 5367–5369.

17. Nicolaou, K.; Sorensen, E.; Discordia, R.; Hwang, C.; Bergman, R.; Minto, R.; Bharucha, K. Ten-membered ring enediynes with remarkable chemical and biological profiles. *Angew. Chem., Int. Ed.* **1992,** *31*, 1044–1046.

18. Nicolaou, K.; Hummel, C.; Nakada, M.; Shibayama, K.; Pitsinos, E.; Saimoto, H.; Mizuno, Y.; Baldenius, K.; Smith, A. Total synthesis of calicheamicin. gamma. 1I. 3. The final stages. *J. Am. Chem. Soc.* **1993,** *115* , 7625–7635.

19. Danishefsky, S.; Shair, M. Observations in the chemistry and biology of cyclic enediyne antibiotics: Total syntheses of calicheamicin [gamma] 1I and dynemicin A. *J. Org. Chem* **1996,** *61*, 16–44.

20. Myers, A.; Fraley, M.; Tom, N.; Cohen, S.; Madar, D. Synthesis of (+)-dynemicin A and analogs of wide structural variability: establishment of the absolute configuration of natural dynemicin A. *Chem. Biol.* **1995**, *2*, 33–43.

21. Myers, A.; Liang, J.; Hammond, M.; Harrington, P.; Wu, Y.; Kuo, E. Total synthesis of (+)-neocarzinostatin chromophore. *J. Am. Chem. Soc.* **1998,** *120*, 5319–5320.

22. Myers, A.; Hammond, M.; Wu, Y.; Xiang, J.; Harrington, P.; Kuo, E. Enantioselective synthesis of neocarzinostatin chromophore aglycon. *J. Am. Chem. Soc* **1996,** *118*, 10006–10007.

23. Myers, A.; Harrington, P.; Kuo, E. Enantioselective synthesis of the epoxy diyne core of neocarzinostatin chromophore. *J. Am. Chem.* Soc. **1991,** *113*, 694–695.

24. Danishefsky, S.; Mantlo, N.; Yamashita, D.; Schulte, G. A concise route to the calicheamicin− esperamicin series: the crystal structure of a core subunit. *J. Am. Chem. Soc.* **1988,** *110*, 6890–6891.

25. Inoue, M.; Sasaki, T.; Hatano, S.; Hirama, M. Synthesis of the C-1027 chromophore framework through atropselective macrolactonization. *Angew. Chem., Int. Ed.* **2004,** *43*, 6500–6505.

26. Ren, F.; Hogan, P.; Anderson, A.; Myers, A. Kedarcidin chromophore: Synthesis of its proposed structure and evidence for a stereochemical revision. *J. Am. Chem. Soc.* **2007,** *129*, 5381–5383.

27. Glaser, C. Contribution to the Chemistry of Phenylacetylenes. *Ber.* **1869**, *2*, 422–424.

28. Myers, A.; Goldberg, S. Concise synthesis of the bicyclic core of the chromoprotein antibiotics kedarcidin and neocarzinostatin by transannular reductive cyclization of a tetrayne precursor. *Tetrahedron Lett.* **1998**, *39*, 9633–9636.

29. Myers, A.; Goldberg, S. Synthesis of the kedarcidin core structure by a transannular cyclization pathway. *Angew. Chem., Int. Ed.* **2000,** *112*, 2844–2847.

30. Eglinton, G.; Galbraith, A. Macrocyclic acetylenic compounds. Part I. Cyclotetradeca-1: 3-diyne and related compounds. *Journal of the* Chemical *Society (Resumed)* **1959**, *27*, 3320–3321.

31. (a) Hensens, O.; Giner, J.; Goldberg, I. Biosynthesis of NCS chrom A, the chromophore of the antitumor antibiotic neocarzinostatin. *J. Am.* Chem. *Soc.* **1989**, *111*, 3295–3299; (b) Tokiwa, Y.; Miyoshi-Saitoh, M.; Kobayashi, H.; Sunaga, R.; Konishi, M.; Oki, T.; Iwasaki, S. Biosynthesis of dynemicin A, a 3-ene-1, 5-diyne antitumor antibiotic. *J. Am. Chem. Soc.* **1992,** *114*, 4107–4110; (c) Lam, K.; Veitch, J.; Golik, J.; Krishnan, B. Biosynthesis of esperamicin A1, an enediyne antitumor antibiotic. *J. Am. Chem. Soc.* **1993**, *115*, 12340–12345.

32. (a) Liu, W.; Christenson, S.; Standage, S.; Shen, B. Biosynthesis of the enediyne antitumor antibiotic C-1027. *Science (Washington, DC, U.S.)* **2002,** *297*, 1170; (b) Liu, W.; Nonaka, K.; Nie, L.; Zhang, J.; Christenson, S. The neocarzinostatin biosynthetic gene cluster from Streptomyces carzinostaticus ATCC 15944 involving two iterative type I polyketide synthases. *Chem. Biol.* **2005**, *12*, 293–302; (c) Lomovskaya, N.; Whitwam, R.; Thorson, J.; Czisny, A. The Calicheamicin Gene Cluster and Its Iterative Type I Enediyne PKS. *Science (Washington, DC, U.S.)* **2002**, *297*, 1173–1176; (d) Liu, W.; Ahlert, J.; Gao, Q.; Wendt-Pienkowski, E.; Shen, B.; Thorson, J. Rapid PCR amplification of minimal enediyne polyketide synthase cassettes leads to a predictive familial classification model. *Proc. Natl. Acad. Sci. U.S.A.* **2003,** *100*, 11959; (e) Zazopoulos, E.; Huang, K.; Staffa, A.; Liu, W.; Bachmann, B.; Nonaka, K.; Ahlert, J.; Thorson, J.; Shen, B.; Farnet, C. A genomics-guided approach for discovering and expressing cryptic metabolic pathways. *Nat. Biotechnol.* **2003,** *21*, 187–190; (f) Van Lanen,

S.; Oh, T.; Liu, W.; Wendt-Pienkowski, E., Shen, B. Characterization of the maduropeptin biosynthetic gene cluster from Actinomadura madurae ATCC 39144 supporting a unifying paradigm for enediyne biosynthesis. *J. Am. Chem. Soc.* **2007**, *129*, 13082–13094.

33. Ben, S.; Wen, L.; Koichi, N. Enediyne natural products: biosynthesis and prospect towards engineering novel antitumor agents. *Curr. Med. Chem.* **2003,** *10*, 2317–2325.

34. Zhang, J.; Van Lanen, S.; Ju, J.; Liu, W.; Dorrestein, P.; Li, W.; Kelleher, N.; Shen, B. A phosphopantetheinylating polyketide synthase producing a linear polyene to initiate enediyne antitumor antibiotic biosynthesis. *Proc. Natl. Acad. Sci. U.S.A.* **2008,** *105*, 1460–1465.

35. Kong, R.; Goh, L.; Liew, C.; Ho, Q.; Murugan, E.; Li, B.; Tang, K.; Liang, Z. Characterization of a carbonyl-conjugated polyene precursor in 10-membered enediyne biosynthesis. *J. Am. Chem. Soc.* **2008,** *130* , 8142–8143.

36. Belecki, K.; Crawford, J. M.; Townsend, C. A. Production of octaketide polyenes by the calicheamicin polyketide synthase CalE8: Implications for the biosynthesis of enediyne core structures. *J. Am. Chem. Soc.* **2009,** *131*, 12564–12566.

37. Sun, H.; Kong, R.; Zhu, D.; Lu, M.; Ji, Q.; Liew, C.; Lescar, J.; Zhong, G.; Liang, Z. Products of the iterative polyketide synthases in 9-and 10-membered enediyne biosynthesis. *Chem. Commun. (Cambridge, U.K.)* **2009,** *47*, 7399–7401.

38. Chen, X. G., P. Lai; Sze, K.; Guo, Z. Identification of a nonaketide product for the iterative polyketide synthase in biosynthesis of the nine-membered enediyne C-1027. *Angew. Chem., Int. Ed.* **2010,** *49*, 7926–7928.

39. Chen, Y.; Thorson, J.; Shen, B. Polyketide synthase chemistry does not direct biosynthetic divergence between 9-and 10-membered enediynes. *Proc. Natl. Acad. Sci. U.S.A.* **2010**, *107*, 11331–11335.

40. Belecki, K.; Townsend, C. A. Environmental Control of the Calicheamicin Polyketide Synthase Leads to Detection of a Programmed Octaketide and a Proposal for Enediyne Biosynthesis. *Angew. Chem. Int. Ed.* **2012**, *51*, 11316–11319.

41. (1) Belecki, K.; Townsend, C. A. Biochemical Determination of Enzyme-Bound Metabolites: Preferential Accumulation of a Programmed Octaketide on the Enediyne Polyketide Synthase CalE8. *J. Am. Chem. Soc* **2013**, *135*, 14339–14348.

42. Li, L.; Wang, J.; Zhang, G.; Liu, Q. A mild copper-mediated Glaser-type coupling reaction under the novel CuI/NBS/DIPEA promoting system. *Tetrahedron Lett.* **2009**, *50*, 4033–4036.

43. Hay, A. Oxidative Coupling of Acetylenes. II1. *J. Org. Chem.* **1962**, *27*, 3320–3321.

44. Denmeade, S.; Chiang, M.; Breslow, R. Efficient triple coupling reaction to produce a self-adjusting molecular cage. *J. Am. Chem. Soc.* **1985**, *107*, 5544–5545.

45. Klebanskii, A. L. G., I. V.; Kuznetsova, O. M. Reaction of formation of diacetylenic compounds, from monosubstituted derivatives of acetylene. *Zh.* Obshch. *Khim.* **1957,** *27*, 2977–2983.

46. Chodkiewicz, W. *Chemistry of Acetylenes*. Dekker: New York, 1957.

47. Stille, J. The palladium-catalyzed cross-coupling reactions of organotin reagents with organic electrophiles [new synthetic methods (58)]. Angew. Chem., Int. Ed. 1986, 25, 508–524.

48. (a) Mio, M. J.; Kopel, L. C.; Braun, J. B.; Gadzikwa, T. L.; Hull, K. L.; Brisbois, R. G.; Markworth, C. J.; Grieco, P. A. One-pot synthesis of symmetrical and unsymmetrical bisarylethynes by a modification of the sonogashira coupling reaction. *Org. Lett.* **2002,** *4*, 3199–202; (b) Kende, A.; Smith, C. A mild synthesis of 1, 3-Diynes. *J. Org. Chem.* **1988**, *53*, 2655–2657.

49. Marshall, J.; Wang, X. Synthesis of enantioenriched homopropargylic alcohols through diastereoselective SE'additions of chiral allenylstannanes to aldehydes. *J. Org. Chem.* **1992**, *57*, 1242–1252.

50. Saccavini, C.; Tedeschi, C.; Maurette, L. Functional [6] pericyclynes: Synthesis through [14+ 4] and [8+ 10] cyclization strategies. *Chem.*-Eur. *J.* **2007**, *13*, 5378–5387.

51. a) Hoye, T. R.; Baire, B.; Niu, D.; Willoughby, P. H.; Woods, B. P. The hexadehydro-Diels–Alder reaction. *Nature* **2012**, *490*, 208–212. b) Niu, D.; Willoughby, P. H.; Woods, B. P.; Baire, B.; Hoye, T. R. Alkane desaturation via concerted double hydrogen atom transfer to benzyne. *Nature* **2013**, *501*, 531–534.

52. Bailey, W. F.; Jiang, X. Stereochemistry of the cyclization of 4-(*t*-butyldimethyl)siloxy-5-hexenyllithium: *cis*-Selective ring-closure accompanied by retro-[1,4]-Brook rearrangement. *ARKIVOK* **2005**, *6*, 25–32.

53. a) Heine, H. W. Personal communication. *Bucknell* University **1969**; b) Hoye, T. R. Personal communication. *University of Minnesota* **2011**.

54. Diels, O.; Alder, K. Syntheses in the hydroaromatic series [in German]. *Justus Liebigs Ann. Chem.* **1928**, *460*, 98–122.

55. Michael, A.; Bucher, J. E. Über die Einwirkung von Eissigsäureanhydrid auf Phenylpropiolsäure. *Chem. Zentrblt*. **1898**, 731–733.

56. Bradley, A.; Johnson, R. Thermolysis of 1,3,8-nonatriyne: Evidence for intramolecular [2+4] cycloaromatization to a benzyne intermediate. *J. Am. Chem. Soc.* **1997**, *119*, 9917–9918.

57. Brown, R. F.; Coulston, K. J.; Eastwood, F. W. Formation of biphenylene by elimination of C_2 from 9, 10-didehydrophenanthrene at 1100 ºC. *Tetrahedron Lett.* **1996**, *37*, 6819–6820.

58. Miyawaki, K.; Suzuki, R.; Kawano, T.; Ueda, I. Cycloaromatization of a non-conjugated polyenyne system: Synthesis of 5H-benzo[d]fluoreno[3,2-b]pyrans via diradicals generated from 1-[2-{4-(2-alkoxymethylphenyl)butan-1,3-diynyl}]phenylpentan-2,4-diyn-1-ols and trapping evidence for the 1,2-didehydrobenzene diradical. *Tetrahedron Lett.* **1997**, *38*, 3943–3946.

59. a) Miyawaki, K.; Kawano, T.; Ueda, I. Multiple cycloaromatization of novel aromatic enediynes bearing a triggering device on the terminal acetylene carbon. *Tetrahedron Lett.* **1998**, *39*, 6923–6926. b) Ueda, I.; Sakurai, Y.; Kawano, T.; Wada, Y.; Futai, M. An unprecedented arylcarbene formation in thermal reaction of non-conjugated aromatic enetetraynes and DNA strand cleavage. *Tetrahedron Lett.* **1999**, *40*, 319–322. c) Miyawaki, K.; Kawano, T.; Ueda, I. Domino thermal radical cycloaromatization of non-conjugated aromatic hexa- and heptaynes: Synthesis of fluoranthene and benzo[*a*]rubicene skeletons. *Tetrahedron Lett.* **2000**, *41*, 1447–1451. d) Kawano, T.; Inai, H.; Miyawaki, K.; Ueda, I. Synthesis of indenothiophenone derivatives by cycloaromatization of non-conjugated thienyl tetraynes. *Tetrahedron Lett.* **2005**, *46*, 1233–1236. e) Kawano, T.; Inai, H.; Miyawaki, K.; Ueda, I. Effect of water molecules on the cycloaromatization of non-conjugated aromatic tetraynes. *Bull. Chem. Soc. Jpn.* **2006**, *79*, 944–949. f) Kawano, T.; Suehiro, M.; Ueda, I. Synthesis and inclusion properties of 6,6′-Bi(benzo[*b*]fluoren-5-ol) derivative by cycloaromatization. *Chem. Lett.* **2006**, *35*, 58–59. g) Kimura, H.; Torikai, K.; Miyawaki, K.; Ueda, I. Scope of the thermal cyclization of nonconjugated ene–yne–nitrile system: A facile synthesis of cyanofluorenol derivatives. *Chem. Lett.* **2008**, *37*, 662–663. h) Torikai, K.; Otsuka, Y.; Nishimura, M.; Sumida, M.; Kawai, T.; Sekiguchi, K.; Ueda, I. Synthesis and DNA cleaving activity of water-soluble non-conjugated thienyl tetraynes. *Bioorgan. Med. Chem.* **2008**, *16*, 5441–5451.

60. Tsui, J. A.; Sterenberg, B. T. A Metal-Templated 4 + 2 Cycloaddition Reaction of an Alkyne and a Diyne To Form a 1,2-Aryne. *Organometallics* **2009**, *28*, 4906–4908.

61. For the purposes of this Thesis, i) an aryne (or *o*-aryne) will refer to any aromatic ring containing an adjacent pair of sp-hybridized carbon atoms (this includes any of the subfamilies of, for example, benzynes, pyridynes, naphthalynes, or indolynes); ii) *o*-benzyne will refer to the parent 1,2-dehydrobenzene; iii) a benzyne derivative (collectively, "benzynes") refers to any substituted *o*-benzyne analog; this may or may not be fused to an additional, non-aromatic ring.

62. Wenk, H. H.; Winkler, M.; Sander, W. One century of aryne chemistry. *Angew. Chem. Int. Ed.* **2003**, *42*, 502–528.

63. Stoermer, R; Kahlert, B. Ueber das 1- und 2-brom-cumaron. *Ber. Dtsch. Chem. Ges.* **1902**, *35*, 1633–1640.

64. Roberts, J.D.; Simmons, H.E.; Carlsmith, L.A.; Vaughan, C.W. Rearrangement in the reaction of chlorobenzene-1-C^{14} with potassium amide. *J. Am. Chem. Soc.* **1953**, *75*, 3290–3291. b) Huisgen, R.; Rist, H. Über Umlagerungen bei nucleophilen Substitutionen in der aromatischen Reihe und ihre Deutung. *Naturwissenschaften* **1954**, *41*, 358–359. c) Wittig, G.; Pohmer, L. Intermediäre Bildung von Dehydrobenzol (Cyclohexadienin). *Angew. Chem.* **1955**, *67*, 348.

65. Hoffmann, R.W. Dehydrobenzone and Cycloalkynes. *Organic Chemistry, a Series of Monographs*, 11; Academic Press, 1967.

66. Tadross, P. M.; Stoltz, B. M. A comprehensive history of arynes in natural product total synthesis. *Chem. Rev.* **2012**, *112*, 3550–3577.

67. Stiles, M.; Miller, R. G.; Burckhardt, U. Reactions of benzyne intermediates in non-basic media. *J. Am. Chem. Soc.* **1963**, *85*, 1792–1797.

68. Wittig, G.; Hoffmann, R. W. 1,2,3-Benzothiadiazole 1,1-dioxide. *Org. Syn.* **1967**, *47*, 4–9.

69. Himeshima, Y.; Sonoda, T.; Kobayashi, H. Fluoride-induced 1, 2-elimination of *o*-trimethylsilylphenyl triflate to benzyne under mild conditions. *Chem. Lett.* **1983**, 1211–1214.

70. Kitamura, T.; Yamane, M. (Phenyl)[*o*-(trimethylsilyl)phenyl]iodonium triflate. A new and efficient precursor of benzyne. *Chem. Commun.* **1995**, 983–984.

71. Bronner, S. M.; Garg, N. K. Efficient synthesis of 2-(trimethylsilyl)phenyl trifluoromethanesulfonate: A versatile precursor to *o*-benzyne. *J. Org. Chem.* **2009**, *74*, 8842–8843.

72. a) Bhunia, A.; Yetra, S. R.; Biju, A. T. Recent advances in transition-metal-free carbon-carbon and carbon-heteroatom bond-forming reactions using arynes.

Chem. Soc. Rev. **2012**, *41*, 3140–3152. b) Yoshida, H.; Takaki, K. Aryne insertion reactions into carbon-carbon σ-bonds. *Synlett.* **2012**, *23*, 1725–1732.

73. Gampe, C. M.; Carreira, E. M. Arynes and cyclohexyne in natural product synthesis. *Angew. Chem. Int. Ed.* **2012**, *51*, 3766–3778.

74. Wang, K.-P.; Yun, S. Y.; Mamidipalli, P.; Lee, D. Silver-mediated fluorination, trifluoromethylation, and trifluoromethylthiolation of arynes. *Chem. Sci.* **2013**, *4*, 3205–3211.

75. Matsumoto, K.; Nagashima, K.; Kamigauchi, T.; Kawamura, Y.; Yasuda, Y.; Ishii, K.; Uotani, N.; Sato, T.; Nakai, H.; Terui, Y. Salfredins, new aldose reductase inhibitors produced by Crucibulum sp. RF-3817. I. Fermentation, isolation and structures of salfredins. *J. Antiobiot.* **1995**, *48*, 439–446.

76. Hoye, T. R.; Baire, B.; Wang, T. Tactics for probing aryne reactivity: mechanistic studies of silicon–oxygen bond cleavage during the trapping of (HDDA-generated) benzynes by silyl ethers. *Chem. Sci.* **2013**, *5*, 545.

77. Tamao, K.; Ishida, N.; Tanaka, T.; Kumada, M. Silafunctional compounds in organic synthesis. Part 20. Hydrogen peroxide oxidation of the silicon-carbon bond in organoalkoxysilanes. *Organometallics* **1983**, *2*, 1694–1696.

78. The product mixture of the reaction of **3095** also contained a minor (~20%) amount of the *o*-DCB-trapped product, as evidenced by GC-MS and crude ^{1}H-NMR.

79. Liu, Z.; Larock, R. C. Facile O-Arylation of Phenols and Carboxylic Acids. *Org. Lett.* **2004**, *6*, 99–102.

80. Cheong, P. H.-Y.; Paton, R. S.; Bronner, S. M.; Im, G.-Y. J.; Garg, N. K.; Houk, K. N. Indolyne and aryne distortions and nucleophilic regioselectivites. *J. Am. Chem. Soc.* **2010**, *132*, 1267–1269.

81. Zhang, H.; Hu, Q.; Li, L.; Hu, Y.; Zhou, P.; Zhang, X.; Xie, H.; Yin, F.; Hu, Y.; Wang, S. Convenient one-step construction of yne-functionalized aryl halides through domino cyclization from tetraynes. *Chem. Commun.* **2014**, *50*, 3335.

82. Hamura, T.; Ibusuki, Y.; Sato, K.; Matsumoto, T.; Osamura, Y.; Suzuki, K. Strain-Induced Regioselectivities in Reactions of Benzyne Possessing a Fused Four-Membered Ring. *Org. Lett.* **2003**, *5*, 3551–3554.

83. a) Finnegan, R. A. Organometallic Chemistry. IX. The Metalation of Benzocyclobutene with Sodium and Potassium Alkyls1, 2. *J. Org. Chem.* **1965**, *30*, 1333–1335. b) Streitwieser, A., Jr; Ziegler, G. R.; Mowery, P. C.; Lewis, A.;

Lawler, R. G. Some generalizations concerning the reactivity of aryl positions adjacent to fused strained rings. *J. Am. Chem. Soc.* **1968**, *90*, 1357–1358.

84. Garr, A. N.; Luo, D.; Brown, N.; Cramer, C. J.; Buszek, K. R.; VanderVelde, D. Experimental and Theoretical Investigations into the Unusual Regioselectivity of 4,5-, 5,6-, and 6,7-Indole Aryne Cycloadditions. *Org. Lett.* **2010**, *12*, 96–99.

85. Im, G.-Y. J.; Bronner, S. M.; Goetz, A. E.; Paton, R. S.; Cheong, P. H.-Y.; Houk, K. N.; Garg, N. K. Indolyne Experimental and Computational Studies: Synthetic Applications and Origins of Selectivities of Nucleophilic Additions. *J. Am. Chem. Soc.* **2010**, *132*, 17933–17944.

86. Hunig, S.; Muller, H.; Thier, W. Reduktionen mit diimide. *Tetrahedron Lett.* **1961**, *2*, 353–357.

87. Corey, E. J.; Pasto, D. J.; Mock, W. L. Chemistry of diimide. II. Stereochemistry of hydrogen transfer to carbon-carbon multiple bonds. *J. Am. Chem. Soc.* **1961**, *83*, 2957–2958.

88. Fernández, I.; Cossío, F. P.; Sierra, M. A. Dyotropic Reactions: Mechanisms and Synthetic Applications. *Chem. Rev. (Washington, DC, U.S.)* **2013**, *109*, 6687–6711.

89. Fernández, I.; Sierra, M. A.; Cossío, F. P. In-Plane Aromaticity in Double Group Transfer Reactions. *J. Org. Chem.* **2007**, *72*, 1488–1491.

90. de Almeida, G.; Townsend, L. C.; Bertozzi, C. R. Synthesis and reactivity of dibenzoselenacycloheptynes. *Org. Lett.* **2013**, *15*, 3038–3041.

91. a) Buist, P. H. Fatty acid desaturases: selecting the dehydrogenation channel. *Nat.Prod. Rep*. **2004**, *21*, 249–262. b) Bhattacharya, A. et al. Characterization of the fungal gibberellin desaturase as a 2-oxoglutarate-dependent dioxygenase and its utilization for enhancing plantgrowth. *Plant Physiol.* **2012**, *160*, 837–845. c) Moran, N. A.; Jarvik, T. Lateral transfer of genes from fungi underlies carotenoid production in aphids. *Science* **2010**, *328*, 624–627.

92. Davies, H. M. L.; Du Bois, J.; Yu, J.-Q. C–H functionalization in organic synthesis. *Chem. Soc. Rev*. **2011**, *40*, 1855–1856.

93. Niu, D.; Wang, T.; Woods, B. P.; Hoye, T. R. Dichlorination of (Hexadehydro-Diels–Alder Generated) Benzynes and a Protocol for Interrogating the Kinetic Order of Bimolecular Aryne Trapping Reactions. *Org. Lett.* **2014**, *16*, 254–257.

94. Noyori, S.; Nishihara, Y. Recent Advances in Cross-Coupling Reactions with Aryl Chlorides, Tosylates, and Mesylates. Applied Cross-Coupling Reactions; *Springer: Berlin Heidelberg*, **2013**; pp 177−202.

95. (a) Friedman, L.; Logullo, F. M. Substitution reactions with photochemically produced acyl radicals. *Angew. Chem., Int. Ed. Engl*. **1965**, *4*, 239−240. (b) Birkett, M. A.; Knight, D. W.; Little, P. B.; Mitchell, M. B. A new approach to dihydrobenzofurans and dihydrobenzopyrans (chromans) based on the intramolecular trapping by alcohols of benzynes generated from 7-substituted-1-aminobenzotriazoles *Tetrahedron* **2000**, *56*, 1013. (c) Perry, R. J.; Turner, S. R. Preparation of N-substituted phthalimides by the palladium-catalyzed carbonylation and coupling of o-dihalo aromatics and primary amines. *J. Org. Chem.* **1991**, *56*, 6573. (d) Rodríguez-Lojo, D.; Cobas, A.; Peña, D.; Pérez, D.; Guitián, E. Aryne Insertion into I–I σ-Bonds. *Org. Lett*. **2012**, *14*, 1363−1365. (e) For a related haloamination reaction see: Hendrick, C. E.; McDonald, S. L.; Wan, Q. Insertion of arynes into *N*-halo bonds: A direct approach to *o*-haloaminoarenes. *Org. Lett*. **2013**, *15*, 3444−3447.

96. (a) Rodebaugh, R.; Debenham, J. S.; Fraser-Reid, B.; Snyder, J. P. *J. Org. Chem.* **1999**, *64*, 1758−1761. (b) Uemura, S.; Sasaki, O.; Okano, M. *J. Chem. Soc. D* **1971**, 1064−1065. (c) Uemura, S.; Onoe, A.; Okano, M. Bull. *Chem. Soc. Jpn*. **1974**, *47*, 692−697. See also: (d) Kovacic, P.; Brace, N. O. *J. Am. Chem. Soc.* **1954**, *76*, 5491−5494. (e) Yang, L.; Lu, Z.; Stahl, S. S. *Chem. Commun*. **2009**, 6460−6462.

97. Yaroslavsky, S. Reaction of aryldiazonium salts with dimethylformamide. Tetrahedron Lett. 1965, 6, 1503.

98. Yoshida, H.; Watanabe, M.; Fukushima, H.; Ohshita, J.; Kunai, A. A 2:1 couling reaction of arynes with aldehydes via *o*-quinone methides Straightforward synthesis of 9-arylxanthenes. Org. Lett. 2004, 6, 4049

99. Yoshioka, E.; Kohtani, S.; Miyabe, H. Sequential reactions of arynes via insertion into the π-bond of amides and trapping reaction with dialkylzincs. Org. Lett. 2010, 12, 1956.

100. Yoshioka, E.; Kohtani, S.; Miyabe, H. A multicomponent coupling reaction induced by insertion of arynes into the C=O bond of formamide. Angew. Chem., Int. Ed. 2011, 50, 6638.

101. Crews, P.; Beard, J. Cycloadditions of benzyne with cyclic olefins. Competition between 2+ 4, ene, and 2+ 2 reaction pathways. *J. Org. Chem.* **2001**, *38*, 522–528.

102. Tabushi, I.; Okazaki, K.; Oda, R. Relative reactivities of substituted olefins toward benzyne. *Tetrahedron* **1969**, *25*, 4401–4407.

103. Karmakar, R.; Mamidipalli, P.; Yun, S. Y.; Lee, D. Alder-Ene Reactions of Arynes. *Org. Lett.* **2013**, *15*, 1938–1941.

104. a) Jones, M., Jr; Levin, R. H. Stereochemistry of the 2+ 2 and 2+ 4 cycloadditions of benzyne. *J. Am. Chem. Soc* **1969**, *91*, 6411–6415. b) Gassman, P. G.; Benecke, H. P. Evidence for the formation of diradical intermediates in the 2+2 addition of benzyne to olefins. *Tet. Lett.* **1969**, *14*, 1089–1092.

105. Hamura, T.; Ibusuki, Y.; Sato, K.; Matsumoto, T.; Osamura, Y.; Suzuki, K. Strain-induced regioselectivities in reactions of benzyne possessing a fused four-membered ring. *Org. Lett.* **2003**, *5*, 3551–3554.

106. Kraus, G. A.; Wu, T. A three-component reaction between benzynes, the enolate of acetaldehyde, and unsaturated esters and dihydroisoquinolines. *Tetrahedron* **2010**, *66*, 569–572.

107. Jayanth, T. T.; Jeganmohan, M.; Cheng, M.-J.; Chu, S.-Y.; Cheng, C.-H. Ene reaction of arynes with alkynes. *J. Am. Chem. Soc.* **2006**, *128*, 2232–2233.

108. Yoshida, H.; Asatsu, Y.; Mimura, Y.; Ito, Y.; Ohshita, J.; Takaki, K. Three-component coupling of arynes and organic bromides. *Angew. Chem. Int. Ed. Engl.* **2011**, *50*, 9676–9679.

109. a) Xie, C.; Liu, L.; Zhang, Y.; Xu, P. Copper-catalyzed alkyne−aryne and alkyne−alkene−aryne coupling reactions. *Org. Lett.* **2008**, *10*, 2393–2396. b) Yoshida, H.; Morishita, T.; Nakata, H.; Ohshita, J. Copper-catalyzed 2:1 coupling reaction of arynes with alkynes. *Org. Lett*. **2009**, *11*, 373–376. c) Berti, F.; Crotti, P.; Cassano, G.; Pineschi, M. Copper-catalyzed arylation of alkenyl aziridines via three-component coupling reaction involving alkynes and benzyne. *Synlett* **2012**, *23*, 2463–2468.

110. a) Yoshikawa, E.; Radhakrishnan, K. V.; Yamamoto, Y. Palladium-catalyzed controlled carbopalladation of benzyne. *J. Am. Chem. Soc.* **2000**, *122*, 7280–7286. b) Yoshikawa, E.; Yamamoto, Y. Palladium-catalyzed intermolecular controlled insertion of benzyne-benzyne-alkene and benzyne-alkyne-alkene-synthesis of phenanthrene and naphthalene derivatives. *Angew. Chem. Int. Ed. Engl.* **2000**, *39*, 173–175.

111. a) Bennett, M. A.; Wenger, E. Insertion reactions of benzyne-nickel (0) complexes with acetylenes. *Organometallics* **1995**, *14*, 1267–1277. b) Bennett, M. A.; Wenger, E. Further observations on the formation of naphthalenes by double insertion of acetylenes into benzyne-nickel(0) complexes. *Organometallics* **1996**, *15*, 5536–5541.

112. Deaton, K. R.; Gin, M. S. Regioselective [2 + 2 + 2] Cycloaddition of a Nickel−Benzyne Complex with 1,3-Diynes. *Org. Lett* **2003**, *5*, 2477–2480.

113. Yang, T.; Zhao, X.; Nagase, S. Cycloaddition of Benzyne to Armchair Single-Walled Carbon Nanotubes: [2 + 2] or [4 + 2]? *Org. Lett* **2013**, *15*, 5960–5963.

114. Van Tamelen, E. E.; Pappas, S. P.; Kirk, K. L. Valence bond isomers of aromatic systems. Bicyclo [2.2. 0] hexa-2, 5-dienes (Dewar benzenes). *J. Am. Chem. Soc.* **1971**, *93*, 6092–6101.

115. Miki, S.; Katayama, T.; Yoshida, Z. Novel naphthalene derivatives undergoing thermal valence isomerization to hemi-Dewar-naphthalene. *Chem Lett.* **1992**, 41–44.

116. Schottelius, M. J.; Chen, P. 9,10-Dehydroanthracene: p-Benzyne-type biradicals abstract hydrogen unusually slowly. *J. Am. Chem. Soc.* **1996**, *118*, 4896–4903.

117. Miki, S.; Ema, T.; Shimizu, R.; Nakatsuji, H.; Yoshida, Z.-I. Synthesis and photoreaction of 1, 2, 3, 4-tetra-t-butylnaphthalene: a highly crowded naphthalene derivative and its valenceisomers. *Tetrahedron Lett.* **1992**, *33*, 1619–1620.

118. (a) Juhl, M.; Tanner, D. Recent applications of intramolecular Diels–Alder reactions to natural product synthesis. *Chem. Soc. Rev.* **2009**, *38*, 2983–2992. (b) Takao, K.; Munakata, R.; Tadano, K. Recent advances in natural product synthesis by using intrmolecular Diels–Alder reactions. *Chem. Rev.* **2005**, *105*, 4779–4807. And references therein to numerous earlier reviews.

119. Martin, S. F.; Williamson, S. A.; Gist, R. P.; Smith, K. M. Aspects of the intramolecular Diels-Alder reactions of some 1,3,9-trienic amides, amines, and esters. An approach to the pentacyclic skeleton of the yohimboid alkaloids *J. Org. Chem.* **1983**, *48*, 5170-5180.

120. Jung, M. E.; Kiankarimi, M. Substituent Effects in the Intramolecular Diels−Alder Reaction of 6-Furylhexenoates. *J. Org. Chem.* 1998, *63*, 2968-2974.

121. Consumption of triyne to the extent of ca. 50% (^{1}H NMR analysis) was observed at 165 °C after 1 h for **5014a**, at 150 °C after 1 h for **5014b**, at 200 °C after 1 h for **5014c**.

122. To guide assignment of the structure of the products **5016** and **5017**, we also studied two close structural analogs of the ketotetrayne **5015** in which one of the two siloxyethyl substituents was replaced by a siloxypropyl group on the top and bottom diyne. As expected, each reacted with essentially the same rate to give essentially the same ratio of normal to abnormal products, now with one containing a benzopyran and the other a benzofuran ring in each instance. See Experimental Section for details.

123. When heated at 165 °C for one hour, only a few percent of **5018** remained, and no definitive evidence for any HDDA-derived product was observed by either ^{1}H

NMR or GC-MS analysis. From the ^{1}H NMR spectrum, the coloration, and the tlc behavior of the crude reaction mixture, we judged that a substantial amount of oligomerization of **5018** was occurring.

124. Allen, F. H.; Kennard, O.; Watson, D. G.; Brammer, L.; Orpen, A. G.; Taylor, R. Tables of bond lengths determined by X-ray and neutron diffraction. Part 1. Bond lengths in organic compounds. *J. Chem. Soc. Perkin Trans. II* **1987**, S1–S19.

125. K. C. Nicolaou, Y. Ogawa, G. Zuccarello, E. J. Schweiger, T. Kumazawa, Cyclic conjugated enediynes related to calicheamicins and esperamicins: calculations, synthesis, and properties. *J. Am. Chem. Soc.* **1988**, *110*, 4866–4868.

126. M. Prall, A. Kruger, P. R. Schreiner, H. Hopf, The cyclization of parent and cyclic hexa-1,3-dien-5-ynes–A combined theoretical and experimental study. *Chem.-Eur. J.* **2001**, *7*, 4386–4394.

127. Cheng, S. Y.; Tseng, J. M.; Lin, S. Y.; Gupta, J. P.; Shu, C. M. Runaway reaction on tert-butyl peroxybenzoate by DSC tests. *Journal of Thermal Analysis and Calorimetry* **2008**, *93*, 121–126.

128. Cambie, R. C.; Hirschberg, A.; Jones, E. R. H.; Lowe, G. Chemistry of the higher fungi. Part XVI. Polyacetylenic metabolites from Aleurodiscus roseus. *Journal of the Chemical Society (Resumed)* **1963**, 4120.

129. Eisler, S.; Slepkov, A. D.; Elliott, E.; Luu, T.; McDonald, R.; Hegmann, F. A.; Tykwinski, R. R. Polyynes as a Model for Carbyne: Synthesis, Physical Properties, and Nonlinear Optical Response. *J. Am. Chem. Soc.* **2005**, *127*, 2666–2676.

130. Chalifoux, W. A.; Tykwinski, R. R. Synthesis of polyynes to model the sp-carbon allotrope carbyne. *Nature Chemistry* **2010**, *2*, 967–971.

131. The onset temperatures discussed in this Chapter are determined by the program software.

132. J. B. Armitage, E. R. H. Jones, M. C. Whiting. Researches on acetylenic compounds. Part XXVIII. A new route to diacetylene and its symmetrical derivates. *J. Chem. Soc.* **1951**, 44–47.

133. (1) Eisler, S.; Slepkov, A. D.; Elliott, E.; Luu, T.; McDonald, R.; Hegmann, F. A.; Tykwinski, R. R. Polyynes as a model for carbyne: Synthesis, physical properties, and nonlinear optical response. *J. Am. Chem. Soc.* **2005**, *127*, 2666–2676.

134. Chalifoux, W. A.; Tykwinski, R. R. Synthesis of polyynes to model the sp-carbon allotrope carbyne. *Nature Chemistry* **2010**, *2*, 967–971.

135. A. T. Glen, S. A. Hutchinson, N. J. McCorkindale, Hexa-1,3,5-triyne: A metabolite of Fomes Annosus. *Tetrahedron Lett*. **1996**, *35*, 4223–1225.

136. A. Ajaz, A. Z. Bradley, R. C. Burrell, W. H. H. Li, K. J. Daoust, L. B. Bovee, K. J. DiRico, R. P. Johnson. Concerted vs stepwise mechanisms in dehydro-Diels–Alder reactions. *J. Org. Chem.* **2011**, *76,* 9320–9328.

137. Conjugated multi-ynes preorganized in the solid state can undergo facile, controlled oligomerization: cf. J. W. Lauher, F. W. Fowler, N. S. Goroff. Single-crystal-to-single-crystal topochemical polymerizations by design. *Acc. Chem. Res*. **2008**, *41*, 1215–1229.

138. Xu, R.; Gramlich, V.; Frauenrath, H. Alternating Diacetylene Copolymer Utilizing Perfluorophenyl−Phenyl Interactions. *J. Am. Chem. Soc* **2006**, *128*, 5541–5547.

139. Daniel, D.; Middleton, R.; Henry, H.; Okamura, W. Inhibitors of 25-hydroxyvitamin D-3-1 alpha-hydroxylase: A-ring oxa analogs of 25-hydroxyvitamin D-3. *J. Org. Chem* **1996**, *61*, 5617–5625.

140. R Hoye, T.; Chen, J.; Baire, B. Cycloaddition Reactions of Azide, Furan, and Pyrrole Units with Benzynes Generated by the Hexadehydro-Diels–Alder (HDDA) Reaction. *HETEROCYCLES* **2014**, *88*, 1191.

141. Bowling, N. P.; Burrmann, N. J.; Halter, R. J.; Hodges, J. A.; McMahon, R. J. Synthesis of simple diynals, diynones, their hydrazones, and diazo compounds: Precursors to a family of dialkynyl carbenes (R 1—C≡C—C̈—C≡C—R_2). *J. Org. Chem.* **2010**, *75*, 6382–6390.

142. Trost, B. M.; Rudd, M. T. Ruthenium-Catalyzed Cycloisomerizations of Diynols. *J. Am. Chem. Soc* **2005**, *127*, 2763–4776.

143. Auer, D.; Maywald, M.; Schmittel, M.; Steffen, J.-P. Ring strain effects in enyne-allene thermolysis: switch from the Myers-Saito reaction to the C2-C6 biradical cyclization. *Tetrahedron Lett.* **1997**, *38*, 6177–6180.

144. Wang, K.-P.; Cho, E. J.; Yun, S. Y.; Rhee, J. Y.; Lee, D. Regio- and steroselectivity in the concatenated enyne cross metathesis-metallotropic [1,3]-shift of terminal 1,3-diyne. *Tetrahedron*. **2013**, *69*, 9105–9110.

145. Peng, Y.; Yu, M.; Zhang, L. Au-Catalyzed synthesis of 5,6-dihydro-8*H*-indolizin-7-ones from *N*-(pent-2-en-4-ynyl)-β-lactams *Org. Lett.* **2008**, *10*, 5187–5190.

146. Delort, E.; Klotz, P.; Salem, B.; Suffert, J. Cyclocarbopalladation: 5-Exo-dig Cyclization versus direct Stille cross-coupling reaction. The influence of the α,β-propargylic substitution. *Org. Lett.* **2003**, *5*, 2307–2310.

147. Abbiati, G.; Dell;Acqua, M.; Facoetti, D.; Rossi. Selective base-promoted synthesis of dihydroisobenzofurans by domino addition/annulation reactions of *ortho*-alkynylbenzaldehydes *Synthesis* **2010**, *14*, 2367–2378.

148. Turlington, M.; Du, Y.; Ostrum, S. G.; Santosh, V.; Wren, K.; Lin, T.; Sabat, M.; Pu, L. From highly enantioselective catalytic reaction of 1,3-diynes with aldehydes to facile asymmetric synthesis of polycyclic compounds. *J. Am. Chem. Soc.* **2011**, *133*, 11780–11794.

149. Marino, J. P.; Nguyen, H. N. Bulky trialkylsilyl acetylenes in the Cadiot−Chodkiewicz cross-coupling reaction. *J. Org. Chem.* **2002**, *67*, 6841–6844.

150. Dunetz, J. R.; Danheiser, R. L. Synthesis of highly substituted indolines and indoles via intramolecular [4 + 2] cycloaddition of ynamides and conjugated enynes. *J. Am. Chem. Soc.* **2005**, *127*, 5776–5777.

151. Gaussian 09, Revision A.1, Frisch, M. J.; Trucks, G. W.; Schlegel, H. B.; Scuseria, G. E.; Robb, M. A.; Cheeseman, J. R.; Scalmani, G.; Barone, V.; Mennucci, B.; Petersson, G. A.; Nakatsuji, H.; Caricato, M.; Li, X.; Hratchian, H. P.; Izmaylov, A. F.; Bloino, J.; Zheng, G.; Sonnenberg, J. L.; Hada, M.; Ehara, M.; Toyota, K.; Fukuda, R.; Hasegawa, J.; Ishida, M.; Nakajima, T.; Honda, Y.; Kitao, O.; Nakai, H.; Vreven, T.; Montgomery, Jr., J. A.; Peralta, J. E.; Ogliaro, F.; Bearpark, M.; Heyd, J. J.; Brothers, E.; Kudin, K. N.; Staroverov, V. N.; Kobayashi, R.; Normand, J.; Raghavachari, K.; Rendell, A.; Burant, J. C.; Iyengar, S. S.; Tomasi, J.; Cossi, M.; Rega, N.; Millam, N. J.; Klene, M.; Knox, J. E.; Cross, J. B.; Bakken, V.; Adamo, C.; Jaramillo, J.; Gomperts, R.; Stratmann, R. E.; Yazyev, O.; Austin, A. J.; Cammi, R.; Pomelli, C.; Ochterski, J. W.; Martin, R. L.; Morokuma, K.; Zakrzewski, V. G.; Voth, G. A.; Salvador, P.; Dannenberg, J. J.; Dapprich, S.; Daniels, A. D.; Farkas, Ö.; Foresman, J. B.; Ortiz, J. V.; Cioslowski, J.; Fox, D. J. Gaussian, Inc., Wallingford CT, 2009.

152. Zhao, Y.; Truhlar, D. G. The M06 suite of density functionals for main group thermochemistry, thermochemical kinetics, noncovalent interactions, excited states, and transition elements: Two new functionals and systematic testing of four M06 functionals and twelve other functionals. *Theor. Chem. Acc.* **2008**, *120*, 215–241. (b) Zhao, Y.; Truhlar, D. G. Density functionals with broad applicability in chemistry. *Acc. Chem. Res.* **2008**, *41*, 157–167.

153. MacroModel, version 10.0, Schrödinger, LLC, New York, NY, 2013. (b) Chang, G.; Guida, W. C.; Still, W. C. An internal coordinate Monte Carlo method for searching conformational space. *J. Am. Chem. Soc.* **1989**, *111*, 4379–4386.

154. GaussView, Version 5, Dennington, R.; Keith, T.; Millam, J. Semichem Inc., Shawnee Mission KS, 2009.

Appendix A: Crystal Structure Data for 4055

CRYSTAL STRUCTURE REPORT

$C_{49}H_{50}Cl_2O_8$

REFERENCE NUMBER: 14095z

Figure 29 | Thermal ellipsoid plot of **4055** showing 50% probability ellipsoids.

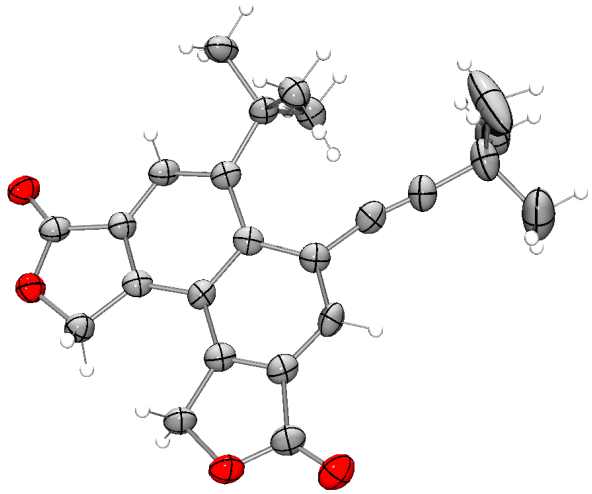

Report prepared for: Brian Woods

May 30, 2014

Laura J. Clouston
X-Ray Crystallographic Laboratory
Department of Chemistry
University of Minnesota
207 Pleasant St. S.E.

Minneapolis, MN 55455

Data collection:

A crystal (approximate dimensions 0.13 x 0.05 x 0.03 mm^3) was placed onto the tip of a 0.1 mm diameter glass capillary and mounted on a Bruker D8 Photon 100 CMOS diffractometer for a data collection at 173(2) K.[165] A preliminary set of cell constants was calculated from reflections harvested from three sets of 20 frames. These initial sets of frames were oriented such that orthogonal wedges of reciprocal space were surveyed. This produced initial orientation matrices determined from ?? reflections. The data collection was carried out using MoKα radiation (graphite monochromator) with a frame time of 120 seconds and a detector distance of 4.0 cm. A randomly oriented region of reciprocal space was surveyed to the extent of one sphere and to a resolution of 0.84 Å. The intensity data were corrected for absorption and decay (SADABS).[166] Final cell constants were calculated from the xyz centroids of 7557 strong reflections from the actual data collection after integration (SAINT).[167] Please refer to Table 1 for additional crystal and refinement information.

Structure solution and refinement:

The structure was solved using SHELXS-97 (Sheldrick, 2008) [168] and refined using SHELXL-97 (Sheldrick, 2008).[168] The space group P-1 was determined based on systematic absences and intensity statistics. A direct-methods solution was calculated which provided most non-hydrogen atoms from the E-map. Full-matrix least squares / difference Fourier cycles were performed which located the remaining non-hydrogen atoms. All non-hydrogen atoms were refined with anisotropic displacement parameters. All hydrogen atoms were placed in ideal positions and refined as riding atoms with relative isotropic displacement parameters. The final full matrix least squares refinement converged to $R1 = 0.0812$ and $wR2 = 0.2384$ (F^2, all data).

Structure description:

The structure is the one suggested. There are two unique molecules in the asymmetric unit, one of which required disorder modeling of the t-butyl group. The t-butyl group was found to be in a 63:37 ratio and was modeled using SAME restraints.

Data collection and structure solution were conducted at the X-Ray Crystallographic Laboratory, S146 Kolthoff Hall, Department of Chemistry, University of Minnesota. All calculations were performed using Pentium computers using the current SHELXTL suite of programs. All publications arising from this report MUST either 1)include Laura J Clouston as a coauthor or

---

[165] SMART V5.054, Bruker Analytical X-ray Systems, Madison, WI (2001).
[166] An empirical correction for absorption anisotropy, R. Blessing, *Acta Cryst.* **A51**, 33-38 (1995).
[167] SAINT+ V6.45, Bruker Analytical X-Ray Systems, Madison, WI (2003).
[168] SHELXTL V6.14, Bruker Analytical X-Ray Systems, Madison, WI (2000).

2)acknowledge Laura J. Clouston, Victor G. Young, Jr., and the X-Ray Crystallographic Laboratory.

Table 1. Crystal data and structure refinement for 14095Z.

Identification code	14095z	
Empirical formula	$C_{49}\,H_{50}\,Cl_2\,O_8$	
Formula weight	837.79	
Temperature	173(2) K	
Wavelength	1.54178 Å	
Crystal system	TRICLINIC	
Space group	P-1	
Unit cell dimensions	a = 10.1822(3) Å	α = 86.262(2)°
	b = 11.4248(4) Å	β = 88.850(2)°
	c = 20.2749(7) Å	γ = 65.461(2)°
Volume	2140.91(12) $Å^3$	
Z	2	
Density (calculated)	1.300 Mg/m^3	
Absorption coefficient	1.808 mm^{-1}	
F(000)	884	
Crystal color, morphology	COLORLESS, PLATE	
Crystal size	0.13 x 0.05 x 0.03 mm^3	
Theta range for data collection	4.26 to 67.04°	
Index ranges	$-12 \le h \le 12$, $-13 \le k \le 10$, $-24 \le l \le 24$	
Reflections collected	24076	
Independent reflections	7514 [R(int) = 0.0820]	
Observed reflections	4050	
Completeness to theta = 67.04°	98.4%	
Absorption correction	Multi-scan	
Max. and min. transmission	0.9478 and 0.8003	
Refinement method	Full-matrix least-squares on F^2	
Data / restraints / parameters	7514 / 18 / 560	
Goodness-of-fit on F^2	1.017	
Final R indices [I>2sigma(I)]	$R1$ = 0.0812, $wR2$ = 0.1991	
R indices (all data)	$R1$ = 0.1503, $wR2$ = 0.2384	
Largest diff. peak and hole	0.794 and -0.735 e.$Å^{-3}$	

Figure 30 | Thermal ellipsoid plot of **4055** showing 50% probability ellipsoids.

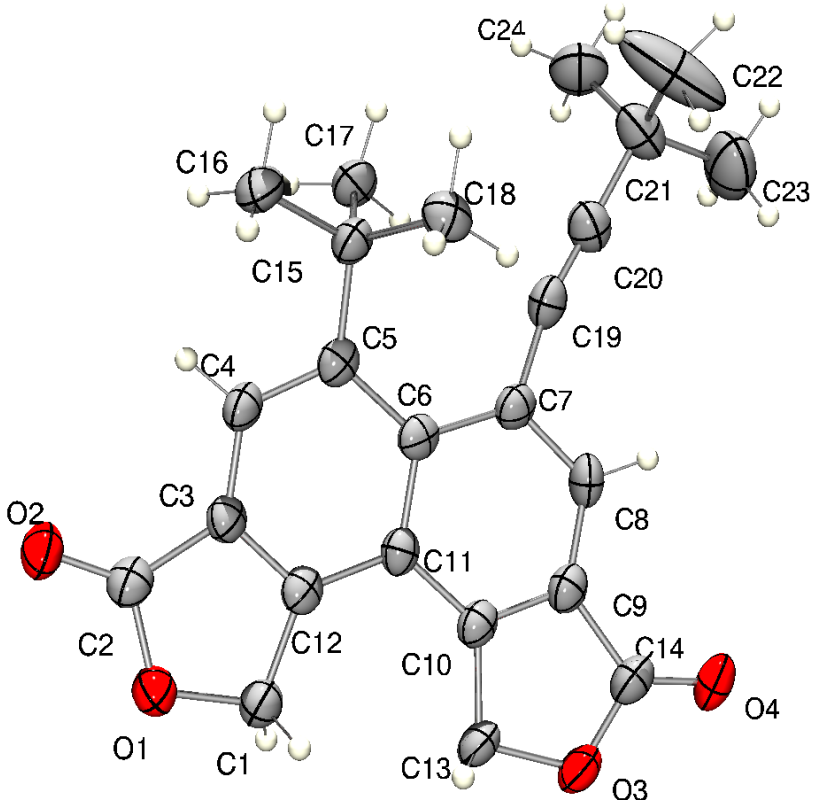

Table 2. Atomic coordinates (x 10^4) and equivalent isotropic displacement parameters ($Å^2$x 10^3) for 14095Z. U_{eq} is defined as one third of the trace of the orthogonalized U_{ij} tensor.

	x	y	z	U_{eq}
O1	3636(3)	3529(3)	10792(2)	42(1)
O2	4562(3)	1368(3)	10896(2)	47(1)
O3	-179(3)	7930(3)	9032(2)	43(1)
O4	-1538(4)	8370(3)	8117(2)	50(1)
C1	2726(5)	4540(4)	10333(2)	38(1)
C2	3799(5)	2358(4)	10597(2)	37(1)
C3	2889(4)	2593(4)	9998(2)	34(1)
C4	2577(4)	1708(4)	9662(2)	36(1)
C5	1617(4)	2094(4)	9132(2)	33(1)
C6	1054(4)	3466(4)	8888(2)	32(1)
C7	192(5)	4032(4)	8290(2)	35(1)
C8	-420(5)	5347(4)	8146(2)	38(1)
C9	-186(4)	6169(4)	8566(2)	36(1)
C10	691(4)	5693(4)	9101(2)	34(1)
C11	1343(4)	4356(4)	9276(2)	32(1)
C12	2262(4)	3870(4)	9841(2)	33(1)
C13	773(5)	6800(4)	9428(2)	38(1)
C14	-743(5)	7591(4)	8519(2)	41(1)
C15	1153(4)	1093(4)	8881(2)	35(1)
C16	1620(5)	-121(4)	9362(3)	47(1)
C17	1893(5)	610(4)	8218(2)	44(1)
C18	-515(5)	1605(5)	8866(2)	41(1)
C19	-117(5)	3354(4)	7779(2)	40(1)
C20	-531(5)	3016(5)	7313(2)	42(1)
C21	-1106(6)	2568(6)	6768(3)	53(1)
C22	-2263(9)	2189(11)	7042(4)	125(4)
C23	-1749(8)	3718(7)	6234(3)	83(2)
C24	88(7)	1477(6)	6440(3)	66(2)
O1'	6258(3)	1522(3)	9333(2)	42(1)
O2'	6016(4)	3349(3)	9768(2)	46(1)
O3'	4929(4)	-353(3)	6876(2)	51(1)

O4'	3627(4)	412(4)	5937(2)	66(1)
C1'	5890(5)	1134(4)	8725(2)	42(1)
C2'	5821(5)	2818(4)	9313(3)	40(1)
C3'	5099(5)	3348(4)	8667(2)	35(1)
C4'	4555(5)	4614(4)	8386(2)	41(1)
C5'	3935(5)	4934(4)	7764(2)	39(1)
C6'	3702(5)	3937(4)	7435(2)	38(1)
C7'	2801(5)	4131(4)	6856(3)	41(1)
C8'	2858(5)	3096(5)	6517(3)	46(1)
C9'	3777(5)	1839(5)	6737(3)	44(1)
C10'	4496(5)	1600(4)	7321(2)	39(1)
C11'	4458(4)	2607(4)	7694(2)	36(1)
C12'	5124(4)	2369(4)	8321(2)	38(1)
C13'	5315(5)	161(4)	7434(3)	45(1)
C14'	4042(5)	613(5)	6450(3)	50(1)
C15'	3663(5)	6290(4)	7447(3)	43(1)
C16'	4639(7)	6825(6)	7768(3)	68(2)
C17'	2106(6)	7267(5)	7565(3)	55(2)
C18'	4064(6)	6249(5)	6716(3)	58(2)
C19'	1672(5)	5336(5)	6613(3)	46(1)
C20'	702(6)	6193(5)	6339(3)	55(1)
C21'	-630(30)	7300(20)	6141(11)	54(3)
C22'	-580(50)	7120(50)	5398(13)	81(5)
C23'	-500(30)	8576(16)	6248(12)	93(4)
C24'	-2010(30)	7290(30)	6425(16)	146(12)
C21"	-382(16)	7321(12)	5927(5)	54(3)
C22"	-890(30)	6910(30)	5317(8)	81(5)
C23"	323(13)	8250(10)	5686(7)	93(4)
C24"	-1672(17)	7952(15)	6369(8)	146(12)
C25	4971(7)	-2067(6)	5105(3)	75(2)
Cl1	3433(3)	-1282(2)	4614(1)	132(1)
Cl2	5665(3)	-3725(2)	5038(1)	108(1)

Table 3. Bond lengths [Å] and angles [°] for 14095Z.

O(1)-C(2)	1.362(6)
O(1)-C(1)	1.437(5)
O(2)-C(2)	1.204(5)
O(3)-C(14)	1.351(6)
O(3)-C(13)	1.451(5)
O(4)-C(14)	1.201(6)
C(1)-C(12)	1.491(6)
C(1)-H(1A)	0.9900
C(1)-H(1B)	0.9900
C(2)-C(3)	1.484(6)
C(3)-C(12)	1.346(6)
C(3)-C(4)	1.398(6)
C(4)-C(5)	1.387(6)
C(4)-H(4A)	0.9500
C(5)-C(6)	1.482(6)
C(5)-C(15)	1.525(6)
C(6)-C(11)	1.450(6)
C(6)-C(7)	1.459(6)
C(7)-C(8)	1.380(6)
C(7)-C(19)	1.446(7)
C(8)-C(9)	1.400(7)
C(8)-H(8A)	0.9500
C(9)-C(10)	1.353(6)
C(9)-C(14)	1.479(6)
C(10)-C(11)	1.413(6)
C(10)-C(13)	1.498(6)
C(11)-C(12)	1.422(6)
C(13)-H(13A)	0.9900
C(13)-H(13B)	0.9900
C(15)-C(17)	1.546(6)
C(15)-C(16)	1.547(6)
C(15)-C(18)	1.550(6)
C(16)-H(16A)	0.9800
C(16)-H(16B)	0.9800

C(16)-H(16C)	0.9800
C(17)-H(17A)	0.9800
C(17)-H(17B)	0.9800
C(17)-H(17C)	0.9800
C(18)-H(18A)	0.9800
C(18)-H(18B)	0.9800
C(18)-H(18C)	0.9800
C(19)-C(20)	1.192(7)
C(20)-C(21)	1.475(7)
C(21)-C(22)	1.500(8)
C(21)-C(24)	1.513(7)
C(21)-C(23)	1.566(8)
C(22)-H(22A)	0.9800
C(22)-H(22B)	0.9800
C(22)-H(22C)	0.9800
C(23)-H(23A)	0.9800
C(23)-H(23B)	0.9800
C(23)-H(23C)	0.9800
C(24)-H(24A)	0.9800
C(24)-H(24B)	0.9800
C(24)-H(24C)	0.9800
O(1')-C(2')	1.355(6)
O(1')-C(1')	1.444(6)
O(2')-C(2')	1.200(6)
O(3')-C(14')	1.362(6)
O(3')-C(13')	1.440(6)
O(4')-C(14')	1.201(6)
C(1')-C(12')	1.494(6)
C(1')-H(1'A)	0.9900
C(1')-H(1'B)	0.9900
C(2')-C(3')	1.479(7)
C(3')-C(12')	1.349(7)
C(3')-C(4')	1.402(6)
C(4')-C(5')	1.379(7)
C(4')-H(4'A)	0.9500
C(5')-C(6')	1.459(7)

C(5')-C(15')	1.552(6)
C(6')-C(7')	1.452(7)
C(6')-C(11')	1.455(6)
C(7')-C(8')	1.387(7)
C(7')-C(19')	1.443(6)
C(8')-C(9')	1.398(7)
C(8')-H(8'A)	0.9500
C(9')-C(10')	1.356(7)
C(9')-C(14')	1.470(7)
C(10')-C(11')	1.405(7)
C(10')-C(13')	1.507(6)
C(11')-C(12')	1.410(7)
C(13')-H(13C)	0.9900
C(13')-H(13D)	0.9900
C(15')-C(18')	1.529(7)
C(15')-C(17')	1.538(7)
C(15')-C(16')	1.539(7)
C(16')-H(16D)	0.9800
C(16')-H(16E)	0.9800
C(16')-H(16F)	0.9800
C(17')-H(17D)	0.9800
C(17')-H(17E)	0.9800
C(17')-H(17F)	0.9800
C(18')-H(18D)	0.9800
C(18')-H(18E)	0.9800
C(18')-H(18F)	0.9800
C(19')-C(20')	1.179(7)
C(20')-C(21')	1.46(3)
C(20')-C(21")	1.514(15)
C(21')-C(24')	1.514(17)
C(21')-C(22')	1.530(15)
C(21')-C(23')	1.546(16)
C(22')-H(22D)	0.9800
C(22')-H(22E)	0.9800
C(22')-H(22F)	0.9800
C(23')-H(23D)	0.9800

C(23')-H(23E)	0.9800
C(23')-H(23F)	0.9800
C(24')-H(24D)	0.9800
C(24')-H(24E)	0.9800
C(24')-H(24F)	0.9800
C(21")-C(24")	1.516(13)
C(21")-C(22")	1.527(11)
C(21")-C(23")	1.560(12)
C(22")-H(22G)	0.9800
C(22")-H(22H)	0.9800
C(22")-H(22I)	0.9800
C(23")-H(23G)	0.9800
C(23")-H(23H)	0.9800
C(23")-H(23I)	0.9800
C(24")-H(24G)	0.9800
C(24")-H(24H)	0.9800
C(24")-H(24I)	0.9800
C(25)-Cl(2)	1.738(6)
C(25)-Cl(1)	1.741(6)
C(25)-H(25A)	0.9900
C(25)-H(25B)	0.9900

C(2)-O(1)-C(1)	110.3(4)
C(14)-O(3)-C(13)	111.0(3)
O(1)-C(1)-C(12)	104.9(4)
O(1)-C(1)-H(1A)	110.8
C(12)-C(1)-H(1A)	110.8
O(1)-C(1)-H(1B)	110.8
C(12)-C(1)-H(1B)	110.8
H(1A)-C(1)-H(1B)	108.8
O(2)-C(2)-O(1)	121.8(4)
O(2)-C(2)-C(3)	130.8(5)
O(1)-C(2)-C(3)	107.3(4)
C(12)-C(3)-C(4)	122.6(4)
C(12)-C(3)-C(2)	108.7(4)
C(4)-C(3)-C(2)	128.6(4)

C(5)-C(4)-C(3)	121.7(4)
C(5)-C(4)-H(4A)	119.1
C(3)-C(4)-H(4A)	119.1
C(4)-C(5)-C(6)	117.3(4)
C(4)-C(5)-C(15)	117.2(4)
C(6)-C(5)-C(15)	125.4(4)
C(11)-C(6)-C(7)	115.6(4)
C(11)-C(6)-C(5)	118.3(4)
C(7)-C(6)-C(5)	126.0(4)
C(8)-C(7)-C(19)	111.6(4)
C(8)-C(7)-C(6)	121.3(4)
C(19)-C(7)-C(6)	127.1(4)
C(7)-C(8)-C(9)	120.2(4)
C(7)-C(8)-H(8A)	119.9
C(9)-C(8)-H(8A)	119.9
C(10)-C(9)-C(8)	121.1(4)
C(10)-C(9)-C(14)	109.2(4)
C(8)-C(9)-C(14)	129.7(4)
C(9)-C(10)-C(11)	121.2(4)
C(9)-C(10)-C(13)	108.3(4)
C(11)-C(10)-C(13)	130.5(4)
C(10)-C(11)-C(12)	120.6(4)
C(10)-C(11)-C(6)	120.1(4)
C(12)-C(11)-C(6)	119.3(4)
C(3)-C(12)-C(11)	120.1(4)
C(3)-C(12)-C(1)	108.7(4)
C(11)-C(12)-C(1)	131.3(4)
O(3)-C(13)-C(10)	104.2(4)
O(3)-C(13)-H(13A)	110.9
C(10)-C(13)-H(13A)	110.9
O(3)-C(13)-H(13B)	110.9
C(10)-C(13)-H(13B)	110.9
H(13A)-C(13)-H(13B)	108.9
O(4)-C(14)-O(3)	122.5(4)
O(4)-C(14)-C(9)	130.2(5)
O(3)-C(14)-C(9)	107.3(4)

C(5)-C(15)-C(17)	110.7(4)
C(5)-C(15)-C(16)	111.7(4)
C(17)-C(15)-C(16)	105.5(4)
C(5)-C(15)-C(18)	110.9(4)
C(17)-C(15)-C(18)	114.5(4)
C(16)-C(15)-C(18)	103.2(4)
C(15)-C(16)-H(16A)	109.5
C(15)-C(16)-H(16B)	109.5
H(16A)-C(16)-H(16B)	109.5
C(15)-C(16)-H(16C)	109.5
H(16A)-C(16)-H(16C)	109.5
H(16B)-C(16)-H(16C)	109.5
C(15)-C(17)-H(17A)	109.5
C(15)-C(17)-H(17B)	109.5
H(17A)-C(17)-H(17B)	109.5
C(15)-C(17)-H(17C)	109.5
H(17A)-C(17)-H(17C)	109.5
H(17B)-C(17)-H(17C)	109.5
C(15)-C(18)-H(18A)	109.5
C(15)-C(18)-H(18B)	109.5
H(18A)-C(18)-H(18B)	109.5
C(15)-C(18)-H(18C)	109.5
H(18A)-C(18)-H(18C)	109.5
H(18B)-C(18)-H(18C)	109.5
C(20)-C(19)-C(7)	168.0(5)
C(19)-C(20)-C(21)	176.0(6)
C(20)-C(21)-C(22)	108.0(5)
C(20)-C(21)-C(24)	110.9(4)
C(22)-C(21)-C(24)	112.5(6)
C(20)-C(21)-C(23)	107.5(5)
C(22)-C(21)-C(23)	110.6(6)
C(24)-C(21)-C(23)	107.2(5)
C(21)-C(22)-H(22A)	109.5
C(21)-C(22)-H(22B)	109.5
H(22A)-C(22)-H(22B)	109.5
C(21)-C(22)-H(22C)	109.5

H(22A)-C(22)-H(22C)	109.5
H(22B)-C(22)-H(22C)	109.5
C(21)-C(23)-H(23A)	109.5
C(21)-C(23)-H(23B)	109.5
H(23A)-C(23)-H(23B)	109.5
C(21)-C(23)-H(23C)	109.5
H(23A)-C(23)-H(23C)	109.5
H(23B)-C(23)-H(23C)	109.5
C(21)-C(24)-H(24A)	109.5
C(21)-C(24)-H(24B)	109.5
H(24A)-C(24)-H(24B)	109.5
C(21)-C(24)-H(24C)	109.5
H(24A)-C(24)-H(24C)	109.5
H(24B)-C(24)-H(24C)	109.5
C(2')-O(1')-C(1')	110.8(4)
C(14')-O(3')-C(13')	111.0(4)
O(1')-C(1')-C(12')	104.4(4)
O(1')-C(1')-H(1'A)	110.9
C(12')-C(1')-H(1'A)	110.9
O(1')-C(1')-H(1'B)	110.9
C(12')-C(1')-H(1'B)	110.9
H(1'A)-C(1')-H(1'B)	108.9
O(2')-C(2')-O(1')	122.0(4)
O(2')-C(2')-C(3')	130.6(4)
O(1')-C(2')-C(3')	107.4(4)
C(12')-C(3')-C(4')	121.1(5)
C(12')-C(3')-C(2')	108.9(4)
C(4')-C(3')-C(2')	129.8(5)
C(5')-C(4')-C(3')	122.0(5)
C(5')-C(4')-H(4'A)	119.0
C(3')-C(4')-H(4'A)	119.0
C(4')-C(5')-C(6')	117.5(4)
C(4')-C(5')-C(15')	117.1(4)
C(6')-C(5')-C(15')	125.2(4)
C(7')-C(6')-C(11')	115.5(4)
C(7')-C(6')-C(5')	126.4(4)

C(11')-C(6')-C(5')	118.0(4)
C(8')-C(7')-C(19')	112.5(5)
C(8')-C(7')-C(6')	121.2(4)
C(19')-C(7')-C(6')	126.0(5)
C(7')-C(8')-C(9')	119.9(5)
C(7')-C(8')-H(8'A)	120.0
C(9')-C(8')-H(8'A)	120.0
C(10')-C(9')-C(8')	120.9(5)
C(10')-C(9')-C(14')	109.5(4)
C(8')-C(9')-C(14')	129.4(5)
C(9')-C(10')-C(11')	121.4(4)
C(9')-C(10')-C(13')	107.9(4)
C(11')-C(10')-C(13')	130.6(5)
C(10')-C(11')-C(12')	121.8(4)
C(10')-C(11')-C(6')	119.7(4)
C(12')-C(11')-C(6')	118.5(4)
C(3')-C(12')-C(11')	120.9(4)
C(3')-C(12')-C(1')	108.5(4)
C(11')-C(12')-C(1')	130.5(5)
O(3')-C(13')-C(10')	104.3(4)
O(3')-C(13')-H(13C)	110.9
C(10')-C(13')-H(13C)	110.9
O(3')-C(13')-H(13D)	110.9
C(10')-C(13')-H(13D)	110.9
H(13C)-C(13')-H(13D)	108.9
O(4')-C(14')-O(3')	122.7(5)
O(4')-C(14')-C(9')	130.0(5)
O(3')-C(14')-C(9')	107.3(5)
C(18')-C(15')-C(17')	112.4(4)
C(18')-C(15')-C(16')	104.5(5)
C(17')-C(15')-C(16')	105.6(5)
C(18')-C(15')-C(5')	112.0(4)
C(17')-C(15')-C(5')	111.2(4)
C(16')-C(15')-C(5')	110.8(4)
C(15')-C(16')-H(16D)	109.5
C(15')-C(16')-H(16E)	109.5

H(16D)-C(16')-H(16E)	109.5
C(15')-C(16')-H(16F)	109.5
H(16D)-C(16')-H(16F)	109.5
H(16E)-C(16')-H(16F)	109.5
C(15')-C(17')-H(17D)	109.5
C(15')-C(17')-H(17E)	109.5
H(17D)-C(17')-H(17E)	109.5
C(15')-C(17')-H(17F)	109.5
H(17D)-C(17')-H(17F)	109.5
H(17E)-C(17')-H(17F)	109.5
C(15')-C(18')-H(18D)	109.5
C(15')-C(18')-H(18E)	109.5
H(18D)-C(18')-H(18E)	109.5
C(15')-C(18')-H(18F)	109.5
H(18D)-C(18')-H(18F)	109.5
H(18E)-C(18')-H(18F)	109.5
C(20')-C(19')-C(7')	168.5(6)
C(19')-C(20')-C(21')	167.7(10)
C(19')-C(20')-C(21")	171.8(8)
C(21')-C(20')-C(21")	19.3(9)
C(20')-C(21')-C(24')	116.1(17)
C(20')-C(21')-C(22')	99(2)
C(24')-C(21')-C(22')	109.6(18)
C(20')-C(21')-C(23')	110.7(17)
C(24')-C(21')-C(23')	112.1(18)
C(22')-C(21')-C(23')	108.6(18)
C(20')-C(21")-C(24")	106.1(8)
C(20')-C(21")-C(22")	112.8(13)
C(24")-C(21")-C(22")	108.3(12)
C(20')-C(21")-C(23")	109.4(10)
C(24")-C(21")-C(23")	112.8(11)
C(22")-C(21")-C(23")	107.7(10)
C(21")-C(22")-H(22G)	109.5
C(21")-C(22")-H(22H)	109.5
H(22G)-C(22")-H(22H)	109.5
C(21")-C(22")-H(22I)	109.5

H(22G)-C(22")-H(22I)	109.5
H(22H)-C(22")-H(22I)	109.5
C(21")-C(23")-H(23G)	109.5
C(21")-C(23")-H(23H)	109.5
H(23G)-C(23")-H(23H)	109.5
C(21")-C(23")-H(23I)	109.5
H(23G)-C(23")-H(23I)	109.5
H(23H)-C(23")-H(23I)	109.5
C(21")-C(24")-H(24G)	109.5
C(21")-C(24")-H(24H)	109.5
H(24G)-C(24")-H(24H)	109.5
C(21")-C(24")-H(24I)	109.5
H(24G)-C(24")-H(24I)	109.5
H(24H)-C(24")-H(24I)	109.5
Cl(2)-C(25)-Cl(1)	110.7(4)
Cl(2)-C(25)-H(25A)	109.5
Cl(1)-C(25)-H(25A)	109.5
Cl(2)-C(25)-H(25B)	109.5
Cl(1)-C(25)-H(25B)	109.5
H(25A)-C(25)-H(25B)	108.1

Symmetry transformations used to generate equivalent atoms:

Table 4. Anisotropic displacement parameters ($Å^2 x\ 10^3$) for 14095Z. The anisotropic displacement factor exponent takes the form: $-2\pi^2[\ h^2\ a^{*2}U_{11} + ...\ + 2\ h\ k\ a^*\ b^*\ U_{12}\ ]$

	U_{11}	U_{22}	U_{33}	U_{23}	U_{13}	U_{12}
O1	41(2)	39(2)	49(2)	3(2)	-10(2)	-19(1)
O2	44(2)	37(2)	58(2)	13(2)	-14(2)	-17(2)
O3	42(2)	25(2)	55(2)	0(1)	0(2)	-8(1)
O4	44(2)	33(2)	59(2)	4(2)	-4(2)	-1(2)
C1	36(2)	33(2)	44(3)	-1(2)	-2(2)	-12(2)
C2	33(2)	35(3)	47(3)	3(2)	2(2)	-17(2)
C3	27(2)	33(2)	41(3)	1(2)	-2(2)	-13(2)
C4	26(2)	28(2)	50(3)	3(2)	-1(2)	-8(2)
C5	26(2)	32(2)	38(3)	-2(2)	7(2)	-10(2)
C6	22(2)	32(2)	41(3)	-5(2)	7(2)	-10(2)
C7	28(2)	31(2)	42(3)	-5(2)	4(2)	-8(2)
C8	31(2)	39(3)	35(3)	6(2)	-6(2)	-7(2)
C9	28(2)	32(2)	43(3)	0(2)	3(2)	-8(2)
C10	27(2)	30(2)	43(3)	0(2)	4(2)	-10(2)
C11	26(2)	32(2)	34(2)	0(2)	2(2)	-9(2)
C12	24(2)	33(2)	42(3)	-1(2)	4(2)	-12(2)
C13	38(2)	24(2)	47(3)	-1(2)	1(2)	-9(2)
C14	37(2)	29(2)	50(3)	-2(2)	4(2)	-7(2)
C15	31(2)	28(2)	41(3)	-1(2)	1(2)	-8(2)
C16	48(3)	31(3)	64(4)	3(2)	-8(3)	-19(2)
C17	37(2)	36(3)	50(3)	-13(2)	1(2)	-6(2)
C18	35(2)	47(3)	45(3)	-4(2)	4(2)	-21(2)
C19	32(2)	35(3)	44(3)	0(2)	1(2)	-5(2)
C20	37(2)	48(3)	38(3)	-6(2)	1(2)	-13(2)
C21	42(3)	73(4)	46(3)	-14(3)	-1(2)	-24(3)
C22	127(7)	254(12)	73(5)	-69(6)	35(5)	-150(8)
C23	82(5)	85(5)	65(4)	-9(4)	-24(4)	-14(4)
C24	75(4)	59(4)	64(4)	-20(3)	-2(3)	-24(3)
O1'	41(2)	31(2)	49(2)	5(1)	-3(2)	-9(1)
O2'	47(2)	43(2)	51(2)	0(2)	-3(2)	-20(2)
O3'	49(2)	32(2)	67(2)	-8(2)	-1(2)	-11(2)

O4'	68(3)	50(2)	74(3)	-15(2)	-13(2)	-16(2)
C1'	35(2)	35(3)	51(3)	1(2)	2(2)	-9(2)
C2'	30(2)	38(3)	49(3)	6(2)	3(2)	-14(2)
C3'	29(2)	28(2)	46(3)	0(2)	4(2)	-10(2)
C4'	41(3)	30(2)	49(3)	-3(2)	6(2)	-14(2)
C5'	30(2)	34(2)	46(3)	0(2)	7(2)	-7(2)
C6'	30(2)	30(2)	49(3)	-1(2)	6(2)	-9(2)
C7'	30(2)	34(3)	53(3)	1(2)	-1(2)	-7(2)
C8'	37(3)	43(3)	54(3)	-2(2)	-4(2)	-13(2)
C9'	36(2)	38(3)	52(3)	-5(2)	6(2)	-9(2)
C10'	25(2)	32(2)	56(3)	-3(2)	5(2)	-8(2)
C11'	25(2)	32(2)	48(3)	1(2)	2(2)	-9(2)
C12'	24(2)	34(3)	51(3)	2(2)	11(2)	-8(2)
C13'	40(3)	32(3)	57(3)	-3(2)	3(2)	-10(2)
C14'	40(3)	40(3)	67(4)	-13(3)	1(3)	-12(2)
C15'	47(3)	32(3)	49(3)	7(2)	-4(2)	-16(2)
C16'	86(4)	57(4)	75(4)	25(3)	-29(4)	-46(3)
C17'	60(3)	31(3)	60(4)	-4(2)	1(3)	-4(2)
C18'	44(3)	43(3)	79(4)	13(3)	9(3)	-13(2)
C19'	43(3)	39(3)	49(3)	-6(2)	-2(2)	-10(2)
C20'	55(3)	40(3)	57(4)	-3(3)	-15(3)	-7(3)
C21'	60(7)	44(3)	31(8)	3(5)	-6(6)	4(3)
C22'	73(12)	77(10)	70(6)	3(5)	-32(6)	-7(6)
C23'	109(9)	44(5)	110(9)	22(6)	-46(7)	-16(5)
C24'	114(11)	129(18)	54(6)	37(10)	17(7)	83(13)
C21"	60(7)	44(3)	31(8)	3(5)	-6(6)	4(3)
C22"	73(12)	77(10)	70(6)	3(5)	-32(6)	-7(6)
C23"	109(9)	44(5)	110(9)	22(6)	-46(7)	-16(5)
C24"	114(11)	129(18)	54(6)	37(10)	17(7)	83(13)
C25	83(5)	65(4)	70(4)	3(3)	-17(4)	-23(3)
Cl1	105(2)	115(2)	147(2)	-23(2)	-60(2)	-13(1)
Cl2	145(2)	64(1)	99(2)	-3(1)	23(1)	-29(1)

Table 5. Hydrogen coordinates (x 10^4) and isotropic displacement parameters ($Å^2$ x 10^3) for 14095Z.

	x	y	z	U(eq)
H1A	3267	5003	10115	46
H1B	1881	5166	10560	46
H4A	3033	819	9800	43
H8A	-1002	5697	7760	45
H13A	438	6828	9891	46
H13B	1773	6736	9424	46
H16A	2676	-566	9373	71
H16B	1215	-700	9211	71
H16C	1266	135	9806	71
H17A	1787	1351	7917	66
H17B	1441	107	8021	66
H17C	2921	67	8297	66
H18A	-927	2445	8619	62
H18B	-882	1698	9319	62
H18C	-791	996	8651	62
H22A	-1817	1342	7281	188
H22B	-2862	2149	6679	188
H22C	-2867	2829	7345	188
H23A	-2420	4487	6445	125
H23B	-2264	3494	5896	125
H23C	-965	3893	6028	125
H24A	514	735	6760	99
H24B	834	1759	6284	99
H24C	-309	1229	6064	99
H1'A	5254	682	8811	51
H1'B	6769	558	8498	51
H4'A	4616	5272	8630	49
H8'A	2273	3241	6134	55
H13C	6368	-85	7448	54
H13D	5021	-153	7853	54

H16D	4559	7617	7519	102
H16E	5644	6184	7764	102
H16F	4337	7016	8225	102
H17D	1428	6964	7382	83
H17E	1955	8105	7348	83
H17F	1944	7354	8041	83
H18D	3489	5906	6476	87
H18E	5092	5692	6669	87
H18F	3868	7122	6534	87
H22D	-780	6371	5319	122
H22E	376	6981	5230	122
H22F	-1313	7892	5171	122
H23D	-569	8720	6721	140
H23E	-1287	9291	6010	140
H23F	428	8524	6082	140
H24D	-2046	6461	6351	219
H24E	-2844	7990	6208	219
H24F	-2041	7403	6901	219
H22G	-1478	6438	5454	122
H22H	-54	6348	5070	122
H22I	-1475	7673	5035	122
H23G	623	8563	6069	140
H23H	-378	8984	5421	140
H23I	1168	7788	5416	140
H24G	-1954	7292	6576	219
H24H	-2480	8583	6104	219
H24I	-1417	8388	6712	219
H25A	5710	-1751	4967	91
H25B	4727	-1870	5572	91

Table 6. Torsion angles [°] for 14095Z.

C2-O1-C1-C12	3.1(5)
C1-O1-C2-O2	177.3(4)
C1-O1-C2-C3	-3.3(5)
O2-C2-C3-C12	-178.5(5)
O1-C2-C3-C12	2.2(5)
O2-C2-C3-C4	7.1(8)
O1-C2-C3-C4	-172.3(4)
C12-C3-C4-C5	1.5(7)
C2-C3-C4-C5	175.3(4)
C3-C4-C5-C6	6.5(6)
C3-C4-C5-C15	-169.4(4)
C4-C5-C6-C11	-9.9(6)
C15-C5-C6-C11	165.7(4)
C4-C5-C6-C7	171.6(4)
C15-C5-C6-C7	-12.8(7)
C11-C6-C7-C8	-6.2(6)
C5-C6-C7-C8	172.4(4)
C11-C6-C7-C19	172.6(4)
C5-C6-C7-C19	-8.9(7)
C19-C7-C8-C9	-177.0(4)
C6-C7-C8-C9	1.9(7)
C7-C8-C9-C10	3.1(7)
C7-C8-C9-C14	-178.9(5)
C8-C9-C10-C11	-3.3(7)
C14-C9-C10-C11	178.2(4)
C8-C9-C10-C13	177.3(4)
C14-C9-C10-C13	-1.1(5)
C9-C10-C11-C12	-180.0(4)
C13-C10-C11-C12	-0.8(7)
C9-C10-C11-C6	-1.3(6)
C13-C10-C11-C6	177.9(4)
C7-C6-C11-C10	5.8(6)
C5-C6-C11-C10	-172.8(4)
C7-C6-C11-C12	-175.5(4)

C5-C6-C11-C12	5.8(6)
C4-C3-C12-C11	-6.0(7)
C2-C3-C12-C11	179.1(4)
C4-C3-C12-C1	174.6(4)
C2-C3-C12-C1	-0.2(5)
C10-C11-C12-C3	-179.3(4)
C6-C11-C12-C3	2.1(6)
C10-C11-C12-C1	-0.1(7)
C6-C11-C12-C1	-178.7(4)
O1-C1-C12-C3	-1.7(5)
O1-C1-C12-C11	179.0(4)
C14-O3-C13-C10	-1.8(5)
C9-C10-C13-O3	1.8(5)
C11-C10-C13-O3	-177.5(4)
C13-O3-C14-O4	-178.3(4)
C13-O3-C14-C9	1.2(5)
C10-C9-C14-O4	179.5(5)
C8-C9-C14-O4	1.2(9)
C10-C9-C14-O3	0.0(5)
C8-C9-C14-O3	-178.3(4)
C4-C5-C15-C17	-105.9(4)
C6-C5-C15-C17	78.5(5)
C4-C5-C15-C16	11.3(5)
C6-C5-C15-C16	-164.3(4)
C4-C5-C15-C18	125.9(4)
C6-C5-C15-C18	-49.7(6)
C8-C7-C19-C20	-7(3)
C6-C7-C19-C20	174(2)
C7-C19-C20-C21	-106(8)
C19-C20-C21-C22	7(8)
C19-C20-C21-C24	-117(7)
C19-C20-C21-C23	126(7)
C2'-O1'-C1'-C12'	-1.4(5)
C1'-O1'-C2'-O2'	179.9(4)
C1'-O1'-C2'-C3'	1.0(5)
O2'-C2'-C3'-C12'	-178.9(5)

O1'-C2'-C3'-C12'	-0.1(5)
O2'-C2'-C3'-C4'	6.4(9)
O1'-C2'-C3'-C4'	-174.8(4)
C12'-C3'-C4'-C5'	4.4(7)
C2'-C3'-C4'-C5'	178.6(4)
C3'-C4'-C5'-C6'	7.2(7)
C3'-C4'-C5'-C15'	-167.7(4)
C4'-C5'-C6'-C7'	165.6(4)
C15'-C5'-C6'-C7'	-19.9(7)
C4'-C5'-C6'-C11'	-15.7(6)
C15'-C5'-C6'-C11'	158.7(4)
C11'-C6'-C7'-C8'	-10.3(7)
C5'-C6'-C7'-C8'	168.4(5)
C11'-C6'-C7'-C19'	162.6(5)
C5'-C6'-C7'-C19'	-18.6(8)
C19'-C7'-C8'-C9'	-172.7(5)
C6'-C7'-C8'-C9'	1.1(8)
C7'-C8'-C9'-C10'	7.6(8)
C7'-C8'-C9'-C14'	-178.3(5)
C8'-C9'-C10'-C11'	-6.3(7)
C14'-C9'-C10'-C11'	178.5(4)
C8'-C9'-C10'-C13'	176.6(4)
C14'-C9'-C10'-C13'	1.4(6)
C9'-C10'-C11'-C12'	175.8(4)
C13'-C10'-C11'-C12'	-7.9(8)
C9'-C10'-C11'-C6'	-3.6(7)
C13'-C10'-C11'-C6'	172.7(4)
C7'-C6'-C11'-C10'	11.4(6)
C5'-C6'-C11'-C10'	-167.4(4)
C7'-C6'-C11'-C12'	-167.9(4)
C5'-C6'-C11'-C12'	13.2(6)
C4'-C3'-C12'-C11'	-7.2(7)
C2'-C3'-C12'-C11'	177.6(4)
C4'-C3'-C12'-C1'	174.5(4)
C2'-C3'-C12'-C1'	-0.8(5)
C10'-C11'-C12'-C3'	178.7(4)

C6'-C11'-C12'-C3'	-1.9(6)
C10'-C11'-C12'-C1'	-3.3(7)
C6'-C11'-C12'-C1'	176.1(4)
O1'-C1'-C12'-C3'	1.3(5)
O1'-C1'-C12'-C11'	-176.8(4)
C14'-O3'-C13'-C10'	2.3(5)
C9'-C10'-C13'-O3'	-2.2(5)
C11'-C10'-C13'-O3'	-178.9(5)
C13'-O3'-C14'-O4'	177.1(5)
C13'-O3'-C14'-C9'	-1.5(6)
C10'-C9'-C14'-O4'	-178.5(6)
C8'-C9'-C14'-O4'	6.9(10)
C10'-C9'-C14'-O3'	0.0(6)
C8'-C9'-C14'-O3'	-174.7(5)
C4'-C5'-C15'-C18'	137.6(5)
C6'-C5'-C15'-C18'	-36.8(6)
C4'-C5'-C15'-C17'	-95.7(5)
C6'-C5'-C15'-C17'	89.9(6)
C4'-C5'-C15'-C16'	21.4(6)
C6'-C5'-C15'-C16'	-153.0(5)
C8'-C7'-C19'-C20'	0(3)
C6'-C7'-C19'-C20'	-173(3)
C7'-C19'-C20'-C21'	123(5)
C7'-C19'-C20'-C21"	-95(6)
C19'-C20'-C21'-C24'	-46(6)
C21"-C20'-C21'-C24'	149(4)
C19'-C20'-C21'-C22'	-163(4)
C21"-C20'-C21'-C22'	32(3)
C19'-C20'-C21'-C23'	83(5)
C21"-C20'-C21'-C23'	-82(3)
C19'-C20'-C21"-C24"	-152(5)
C21'-C20'-C21"-C24"	5(3)
C19'-C20'-C21"-C22"	90(5)
C21'-C20'-C21"-C22"	-113(4)
C19'-C20'-C21"-C23"	-30(5)
C21'-C20'-C21"-C23"	127(4)